frontiers | Research Topics

Exploring autoimmune diseases and endocrine crosstalk

Edited by
Alessandro Antonelli and Anette S. B. Wolff

Coordinated by
Deepika Watts

Published in
Frontiers in Immunology

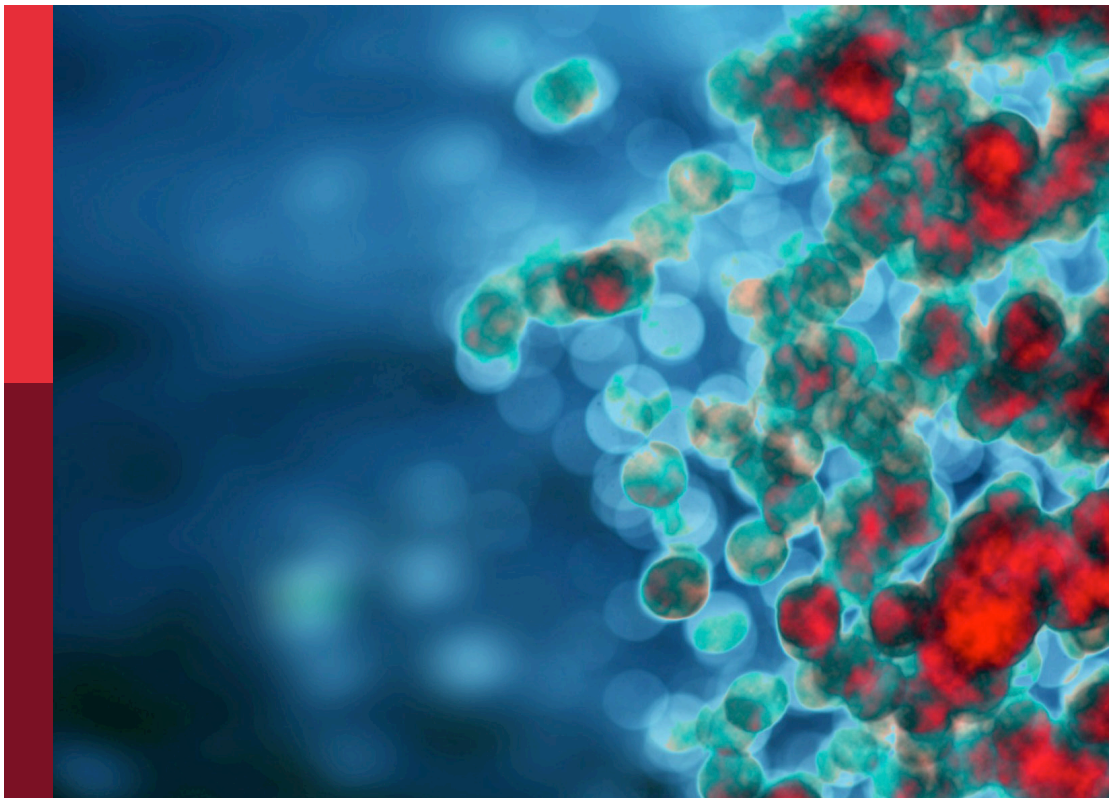

FRONTIERS EBOOK COPYRIGHT STATEMENT

The copyright in the text of individual articles in this ebook is the property of their respective authors or their respective institutions or funders. The copyright in graphics and images within each article may be subject to copyright of other parties. In both cases this is subject to a license granted to Frontiers.

The compilation of articles constituting this ebook is the property of Frontiers.

Each article within this ebook, and the ebook itself, are published under the most recent version of the Creative Commons CC-BY licence. The version current at the date of publication of this ebook is CC-BY 4.0. If the CC-BY licence is updated, the licence granted by Frontiers is automatically updated to the new version.

When exercising any right under the CC-BY licence, Frontiers must be attributed as the original publisher of the article or ebook, as applicable.

Authors have the responsibility of ensuring that any graphics or other materials which are the property of others may be included in the CC-BY licence, but this should be checked before relying on the CC-BY licence to reproduce those materials. Any copyright notices relating to those materials must be complied with.

Copyright and source acknowledgement notices may not be removed and must be displayed in any copy, derivative work or partial copy which includes the elements in question.

All copyright, and all rights therein, are protected by national and international copyright laws. The above represents a summary only. For further information please read Frontiers' Conditions for Website Use and Copyright Statement, and the applicable CC-BY licence.

ISSN 1664-8714
ISBN 978-2-8325-7027-2
DOI 10.3389/978-2-8325-7027-2

Generative AI statement
Any alternative text (Alt text) provided alongside figures in the articles in this ebook has been generated by Frontiers with the support of artificial intelligence and reasonable efforts have been made to ensure accuracy, including review by the authors wherever possible. If you identify any issues, please contact us.

About Frontiers

Frontiers is more than just an open access publisher of scholarly articles: it is a pioneering approach to the world of academia, radically improving the way scholarly research is managed. The grand vision of Frontiers is a world where all people have an equal opportunity to seek, share and generate knowledge. Frontiers provides immediate and permanent online open access to all its publications, but this alone is not enough to realize our grand goals.

Frontiers journal series

The Frontiers journal series is a multi-tier and interdisciplinary set of open-access, online journals, promising a paradigm shift from the current review, selection and dissemination processes in academic publishing. All Frontiers journals are driven by researchers for researchers; therefore, they constitute a service to the scholarly community. At the same time, the *Frontiers journal series* operates on a revolutionary invention, the tiered publishing system, initially addressing specific communities of scholars, and gradually climbing up to broader public understanding, thus serving the interests of the lay society, too.

Dedication to quality

Each Frontiers article is a landmark of the highest quality, thanks to genuinely collaborative interactions between authors and review editors, who include some of the world's best academicians. Research must be certified by peers before entering a stream of knowledge that may eventually reach the public - and shape society; therefore, Frontiers only applies the most rigorous and unbiased reviews. Frontiers revolutionizes research publishing by freely delivering the most outstanding research, evaluated with no bias from both the academic and social point of view. By applying the most advanced information technologies, Frontiers is catapulting scholarly publishing into a new generation.

What are Frontiers Research Topics?

Frontiers Research Topics are very popular trademarks of the *Frontiers journals series*: they are collections of at least ten articles, all centered on a particular subject. With their unique mix of varied contributions from Original Research to Review Articles, Frontiers Research Topics unify the most influential researchers, the latest key findings and historical advances in a hot research area.

Find out more on how to host your own Frontiers Research Topic or contribute to one as an author by contacting the Frontiers editorial office: frontiersin.org/about/contact

Exploring autoimmune diseases and endocrine crosstalk

Topic editors
Alessandro Antonelli — University of Pisa, Italy
Anette S. B. Wolff — University of Bergen, Norway

Topic coordinator
Deepika Watts — Technical University Dresden, Germany

Citation
Antonelli, A., Wolff, A. S. B., Watts, D., eds. (2025). *Exploring autoimmune diseases and endocrine crosstalk*. Lausanne: Frontiers Media SA.
doi: 10.3389/978-2-8325-7027-2

Table of contents

frontiers | Frontiers in Immunology

TYPE Editorial
PUBLISHED 09 October 2025
DOI 10.3389/fimmu.2025.1709567

Check for updates

OPEN ACCESS

EDITED AND REVIEWED BY
Betty Diamond,
Feinstein Institute for Medical Research,
United States

*CORRESPONDENCE
Anette S. B. Wolff
anette.boe@uib.no

RECEIVED 20 September 2025
ACCEPTED 29 September 2025
PUBLISHED 09 October 2025

CITATION
Wolff ASB and Antonelli A (2025) Editorial: Exploring autoimmune diseases and endocrine crosstalk. *Front. Immunol.* 16:1709567. doi: 10.3389/fimmu.2025.1709567

COPYRIGHT
© 2025 Wolff and Antonelli. This is an open-access article distributed under the terms of the Creative Commons Attribution License (CC BY). The use, distribution or reproduction in other forums is permitted, provided the original author(s) and the copyright owner(s) are credited and that the original publication in this journal is cited, in accordance with accepted academic practice. No use, distribution or reproduction is permitted which does not comply with these terms.

Editorial: Exploring autoimmune diseases and endocrine crosstalk

Anette S. B. Wolff[1,2]* and Alessandro Antonelli[3]

[1]Department of Medicine, Haukeland University Hospital, Bergen, Norway, [2]Department of Biomedicine, University of Bergen, Bergen, Norway, [3]Department of Surgery, Medical and Molecular Pathology and Critical Area, University of Pisa, Pisa, Italy

KEYWORDS

endocrine-immune interaction, complexity, autoimmune, immune-metabolic axis, biomarkers

Editorial on the Research Topic
Exploring autoimmune diseases and endocrine crosstalk

Autoimmune endocrine diseases are increasingly recognized as complex, multifactorial conditions that arise from a breakdown in immune tolerance caused by genetic susceptibility and uncharacterized environmental triggers, and result in targeted destruction of hormone-producing organs. These disorders, which include Hashimoto's thyroiditis, thyroid eye disease, autoimmune polyendocrine syndromes, and endocrine involvement in systemic autoimmune diseases, are not only clinically diverse but also mechanistically intricate. The crosstalk between the immune and endocrine systems plays a pivotal role in both maintaining physiological homeostasis and driving disease when dysregulated. This Research Topic brings together nine original and review articles that collectively explore the immunological, genetic, metabolic, and environmental dimensions of autoimmune endocrine diseases.

A central theme across several contributions was thyroid autoimmunity, which remains one of the most prevalent and studied forms of organ-specific autoimmunity. One novel study explored the role of tryptophan metabolism in the pathogenesis of Hashimoto's thyroiditis (HT), demonstrating that HT patients exhibit significantly reduced serum tryptophan levels. Supplementation with tryptophan alleviated thyroid inflammation and tissue damage, while pharmacological inhibition of tryptophan metabolism exacerbated disease severity. Mechanistically, tryptophan was shown to modulate T cell subset distribution and influence the PI3K-Akt signaling pathway, suggesting that metabolic pathways may serve as viable therapeutic targets in HT (Zhang et al.). This underscores the importance of metabolic-immune interactions in endocrine autoimmunity.

Oxidative stress has long been suspected as a contributing factor in thyroid eye disease (TED), but its molecular underpinnings have remained elusive. A bioinformatics-driven study identified 53 oxidative stress-related differentially expressed genes (OS-DEGs) in TED, with FOS, MCL1, and ANGPTL7 emerging as key candidates. These genes were validated through immunohistochemistry in orbital tissues, confirming their upregulation in TED patients. The findings implicate mitochondrial dysfunction and reactive oxygen species (ROS) metabolism in TED pathogenesis and propose these genes as potential biomarkers for early diagnosis and risk stratification (Hai et al.). In a complementary study, the therapeutic potential of Linsitinib, a small-molecule inhibitor of IGF-1R phosphorylation, was evaluated in cell lines expressing IGF-1R and TSH-R, both of which are implicated in TED. Linsitinib effectively inhibited cell proliferation and induced apoptosis (Luffy et al.). These results

suggest that dual targeting of IGF-1R and TSH-R signaling may offer a promising strategy for managing TED.

Mavridou and Pearce highlighted that the genetic basis of organ-specific autoimmunity is still not fully understood. The authors explained how polymorphisms in genes encoding endocrine-specific antigens, such as INS, TSHR, TPO, CYP21A2, and PIT-1, can impair central tolerance through mechanisms including altered thymic expression, alternative splicing, and post-translational modifications (Mavridou and Pearce). These insights are crucial for understanding why certain endocrine tissues are preferentially affected and may inform future strategies for disease prediction and prevention.

The clinical complexity of syndromes in which several endocrine conditions appear in concert was illustrated in a case report of autoimmune polyendocrine syndrome type 2 (APS-2), which involves Addison's disease, Hashimoto's thyroiditis, and type 1 diabetes mellitus (Yao et al.). The patient presented with an adrenal crisis after a nine-year delay in diagnosis, highlighting the challenges of recognizing asynchronous multi-glandular involvement. The case also raised concerns about the potential impact of exogenous substances on immune balance and hormone metabolism. This underscores the need for vigilant, multidisciplinary monitoring of patients with known autoimmune conditions.

Pregnancy introduces unique immunological and hormonal dynamics, and hypothyroidism during gestation poses significant risks to both maternal and fetal health. A metagenomic and proteomic study investigated the gut microbiota and immune profiles of pregnant women with hypothyroidism. The results revealed reduced microbial diversity and enrichment of *Phocaeicola vulgatus* and *Bacteroides fragilis*, alongside downregulation of DGKK and S10A8 proteins (Zhang et al.). These changes were found to be associated with a shift in the Th1/Th2 balance, suggesting that microbial and immune alterations may contribute to disease onset. This study adds to the growing body of evidence linking gut microbiota to endocrine and immune health.

Systemic autoimmune diseases may also manifest symptoms in endocrine organs. In primary Sjögren's syndrome (pSS), thyroid involvement is a common but often under-recognized complication. A retrospective study of 202 pSS patients resulted in the development of a predictive nomogram that incorporates clinical and serological variables such as high-sensitivity CRP, Ro52, AST, dryness symptoms, anxiety, and hyperuricemia. This tool can aid clinicians in identifying pSS patients at risk for thyroid dysfunction, enabling earlier intervention and more personalized care (Yang et al.). The systemic nature of autoimmune diseases was further exemplified in a study examining the risk of type 2 diabetes mellitus (T2D) in patients with rheumatoid arthritis (RA). Among 488 RA patients, those with comorbid T2D exhibited a longer disease duration, a higher BMI, and an increased prevalence of hypertension and a family history of diabetes. Immunologically, these patients had reduced Th2 and Treg cell populations, leading to elevated Th1/Th2 and Th17/Treg ratios. A multivariate analysis identified immune cell imbalance, systemic inflammation, and metabolic factors as key contributors to T2D risk in RA patients, highlighting the importance of immune-metabolic crosstalk in the development of comorbidities (Pei et al.). Another article in this Research Topic focused on SLE, with its findings on dyslipidemia and immune activation in SLE highly relevant to endocrine autoimmunity (Xuan et al.). Another article in this Research Topic focused on SLE, which may share immunometabolic pathways with endocrine autoimmune disorders; hormones influence lipid metabolism, patients with SLE often have secondary autoimmune endocrine disorders such as thyroid disease or type 1 diabetes and glucocorticoids are frequently used as therapy for systemic autoimmune disorders. Therefore, biomarkers of these disorders may be the same or influence each other. These studies underscore the importance of immune-metabolic crosstalk and shared inflammatory pathways, along with the need for the integrated management of autoimmune diseases that span both systemic and endocrine domains.

Together, the articles in this Research Topic provide a comprehensive and nuanced view of different areas of autoimmune endocrine diseases. They emphasize the importance of integrating immunological, genetic, metabolic, and clinical data to unravel the complexities of immune-endocrine interactions. From molecular mechanisms and biomarker discovery to predictive modeling and therapeutic innovation, these studies pave the way for improved diagnostics, personalized risk assessment, and targeted treatments.

As the prevalence and complexity of autoimmune endocrine diseases continue to rise, interdisciplinary collaboration will be essential to fostering the development of precision medicine approaches. We hope that this Research Topic will inspire further research and clinical innovation aimed at improving the lives of patients affected by these challenging disorders.

Author contributions

AW: Writing – original draft, Writing – review & editing. AA: Writing – original draft, Writing – review & editing.

Conflict of interest

The authors declare that the research was conducted in the absence of any commercial or financial relationships that could be construed as a potential conflict of interest.

The author(s) declared that they were an editorial board member of Frontiers, at the time of submission. This had no impact on the peer review process and the final decision.

Generative AI statement

The author(s) declare that Generative AI was used in the creation of this manuscript. Copilot (chat-gtp) was used as inspiration for generating this Editorial, but ideas from Copilot was re-written.

Any alternative text (alt text) provided alongside figures in this article has been generated by Frontiers with the support of artificial intelligence and reasonable efforts have been made to ensure accuracy, including review by the authors wherever possible. If you identify any issues, please contact us.

Publisher's note

All claims expressed in this article are solely those of the authors and do not necessarily represent those of their affiliated organizations, or those of the publisher, the editors and the reviewers. Any product that may be evaluated in this article, or claim that may be made by its manufacturer, is not guaranteed or endorsed by the publisher.

frontiers | Frontiers in Immunology

TYPE Original Research
PUBLISHED 04 October 2024
DOI 10.3389/fimmu.2024.1445639

Check for updates

OPEN ACCESS

EDITED BY
Alessandro Antonelli,
University of Pisa, Italy

REVIEWED BY
Saeed Mohammadi,
Golestan University of Medical Sciences, Iran
Piero Ruscitti,
University of L'Aquila, Italy

*CORRESPONDENCE
Peifeng He
hepeifeng2006@126.com

RECEIVED 07 June 2024
ACCEPTED 12 September 2024
PUBLISHED 04 October 2024

CITATION
Pei R, Wang J, He P, Yu Q, Zhang S, Shi G, Liu G and Li X (2024) Risk factors for type 2 diabetes mellitus in Chinese rheumatoid arthritis patients from 2018 to 2022: a real-world, single-center, retrospective study. *Front. Immunol.* 15:1445639. doi: 10.3389/fimmu.2024.1445639

COPYRIGHT
© 2024 Pei, Wang, He, Yu, Zhang, Shi, Liu and Li. This is an open-access article distributed under the terms of the Creative Commons Attribution License (CC BY). The use, distribution or reproduction in other forums is permitted, provided the original author(s) and the copyright owner(s) are credited and that the original publication in this journal is cited, in accordance with accepted academic practice. No use, distribution or reproduction is permitted which does not comply with these terms.

Risk factors for type 2 diabetes mellitus in Chinese rheumatoid arthritis patients from 2018 to 2022: a real-world, single-center, retrospective study

Ruomeng Pei[1,2,3,4], Jia Wang[5], Peifeng He[2,3,4,6]*, Qi Yu[2,3,4,6], Shengxiao Zhang[5], Gaoxiang Shi[1,3,4,7], Geliang Liu[2,3,4] and Xiaofeng Li[5]

[1]Third Hospital of Shanxi Medical University, Shanxi Bethune Hospital, Shanxi Academy of Medical Sciences, Tongji Shanxi Hospital, Taiyuan, China, [2]School of Management, Shanxi Medical University, Taiyuan, China, [3]Institute of Medical Data Science, Shanxi Medical University, Taiyuan, China, [4]Shanxi Key Laboratory of Big Data for Clinical Decision, Shanxi Medical University, Taiyuan, China, [5]Department of Rheumatology, The Second Hospital of Shanxi Medical University, Taiyuan, Shanxi, China, [6]Key Laboratory of Cellular Physiology, Ministry of Education, Shanxi Medical University, Taiyuan, China, [7]School of Basic Medical Sciences, Shanxi Medical University, Taiyuan, China

Introduction: In patients with rheumatoid arthritis (RA), the increased risk of concomitant type 2 diabetes mellitus (T2D) is an important contributor to increased mortality and decreased quality of life; however, the mechanisms and pathogenetic factors remain unknown.

Methods: In this study, we aimed to assess the risk factors for T2D in patients with RA. We recruited 206 healthy controls and 488 patients with RA, 160 of whom had comorbid T2D. General clinical information, disease characteristics, and circulating lymphocyte levels detected using modified flow cytometry were collected from all participants. Logistic regression models adjusted for confounders were fitted to estimate the risk factors of T2D in patients with RA.

Results: The incidence of RA in patients with T2D was 15.6%. Patients with RA and T2D had a longer disease duration, higher BMI, and a higher incidence of hypertension and a family history of diabetes than those with RA but no T2D. The absolute numbers of T helper 2 cell (Th2) and Regulatory T cells (Treg) decreased in patients with RA and T2D, which led to an increase in the ratios of Th1/Th2 and Th17/Treg cells. Multivariate logistic regression analysis showed that a family history of diabetes, a higher incidence of hypertension, higher neutrophil-lymphocyte ratio (NLR) levels, lower platelet-lymphocyte ratio (PLR) levels, and fewer circulating Th2 and Treg cells were associated with an increased risk of T2D in patients with RA.

Discussion: The levels of peripheral lymphocytes, especially Th2 and Treg cells, are closely related to the occurrence of T2D in patients with RA; however, the influence of body mass index (BMI), family history of diabetes, and systemic inflammation should not be ignored.

KEYWORDS

rheumatoid arthritis, type 2 diabetes mellitus, helper T cells, regulatory T cells, risk factors

1 Introduction

Rheumatoid arthritis (RA) is an autoimmune disease characterized by persistent synovial inflammation and bone damage; the diseases affects 1% of the global population (1). While several factors such as genetics, environment, and immunity, are undoubtedly involved in the occurrence and progression of RA, evidence for its pathogenesis confirm the crucial role of immune cells (2). Although the long-term prognosis of RA has improved to some extent owing to the emergence of multiple treatment modalities, the life expectancy of patients with RA is still significantly lower than that of the general population because of the emergence of extra-articular manifestations and various comorbidities, especially type 2 diabetes mellitus (T2D) (3, 4). Diabetes mellitus (DM) is a chronic systemic disease characterized by elevated blood sugar levels and ocular, renal, and vascular involvement, which can result in systemic inflammation, impaired glucose metabolism, and potentially life-threatening complications (5).

Although the relevant mechanisms remain elusive, increasing evidence indicates that patients with RA are more likely to develop DM, with a prevalence rate of approximately 6%-14%; this not only increases the long-term mortality of patients with RA but also aggravates the original metabolic disorders of DM (6–9). The abnormal immune response mediated by unbalanced lymphocyte subgroups such as $CD4^+$ T subpopulations during the occurrence and development of RA not only damages bones and joints but also affects metabolic organs, including the liver. This results in glucose metabolism disorders and participating in the development of DM (10). However, thus far, no reports have detailed the changes in circulating lymphocyte population levels in patients with RA and DM.

In this study, we collected data on patient demographics, disease characteristic, and the absolute numbers and proportions of peripheral lymphocytes, especially $CD4^+$ T subsets, of patients with RA and DM and those with RA but without DM (RA-T2D and RA-N-T2D, respectively), and analyzed the factors influencing the occurrence of DM in patients with RA. We hope our findings provide new ideas for early clinical prevention and treatment.

2 Methods

2.1 Study population

The study population was selected from 1025 patients with RA who were consecutively enrolled between January 2018 and June 2022, all of whom met the 1987 ARA criteria and the 2010 EULAR revised RA classification diagnostic criteria (11, 12). Patients with RA with other rheumatic diseases, malignant tumors, and acute and chronic infections were excluded, and 780 patients who met the inclusion criteria were enrolled. Among them, 719 patients did not take hormones, DMARDs, or other drugs that may have affected the number of peripheral blood lymphocytes for at least six months. Based on the diagnostic criteria for T2D published by the World Health Organization (WHO) in 1999 (13), 160 patients were included in the RA-DM group (108 females, 52 males). Among the remaining 559 patients with RA, 328 age- and sex-matched patients were randomly selected as the RA-N-DM group (223 females and 105 males). In addition, 206 healthy controls (136 females and 70 males) were enrolled from the rheumatology clinic or physical examination center of the Second Hospital of Shanxi Medical University (Figure 1).

2.2 Data collection

General clinical information of patients with RA and healthy controls was collected, including sex, age, disease duration, height,

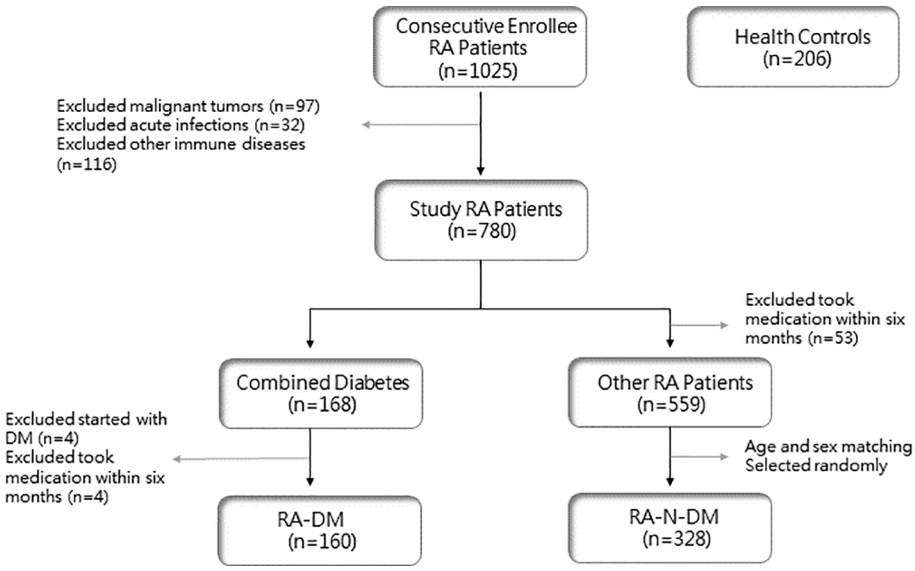

FIGURE 1
Flow chart of patient enrolment. RA, rheumatoid arthritis; DM, diabetes mellitus.

weight, calculated BMI, smoking status, alcohol consumption, hypertension, osteoporosis, history of nephropathy, and family history of diabetes. Indicators of disease activity, such as tender joint count (TJC), swollen joint count (SJC), and disease activity score in 28 joints (DAS28), were recorded for all patients. The general laboratory indicators included in the analysis were erythrocyte sedimentation rate (ESR), C-reactive protein (CPR), immunoglobulin G (IgG), immunoglobulin A (IgA), immunoglobulin M (IgM), white blood cell (WBC), red blood cell (RBC), platelet (PLT), lymphatic (LYM), monocytes (MO), neutrophilic granulocyte (NE), platelet-lymphocyte ratio (PLR), monocytes- lymphatic ratio (LMR), neutrophil-lymphocyte ratio (NLR), systemic immune-inflammation index (SII), blood urea nitrogen (BUN), serum creatinine (Cr), fasting blood glucose (FBG), albumin (ALB), globulin (GLB) and albumin/globulin ratio (A/G). Simultaneously, the absolute counts and proportions of T, B, $CD8^+$ T, natural killer (NK), and $CD4^+$ T cells and their subsets, such as T helper 1 (Th1), Th2, Th17, and regulatory T (Treg) cells, were recorded in detail for all recruiters.

2.3 Statistical analysis

IBM SPSS Statistics version 22 was used for all statistical analyses. The sample size of each group was analyzed by power analysis to ensure its validity. Percentages and mean values with standard deviations (SD) were used to describe the demographic information of all the subjects. Medians and quartiles were used to describe the disease characteristics of all patients. The chi-square test was used for categorical variables, whereas the t-test, Mann–Whitney U test, and Wilcoxon test were used for continuous variables. Factors associated with T2D in patients with RA were assessed using univariate and multivariate logistic regression analyses. $p<0.05$ indicated that the difference was statistically significant.

3 Results

3.1 Demographic features and general information

There was no significant difference in sex ($\chi^2 = 0.227$, $p>0.05$) and mean age (t = 3.242, $p>0.05$) between patients with RA (including 328 RA-N-DM patients and 160 RA-DM patients) and 206 healthy controls. Compared with RA-N-DM group, baseline demographics information including disease duration (Z=−4.571, $p<0.001$), body weight (Z=−7.736, $p<0.001$), BMI (Z=−6.8, $p<0.001$), the proportion of combined hypertensive (Z=9.434, $p<0.01$), history of nephropathy (Z=-2.078, $p<0.05$) and family history of diabetes (Z=5.541, $p<0.001$) in RA-DM group were increased (Table 1). This suggests that the combination of T2D may affect the vascular function, renal function, and nutritional status of patients with RA and increase their medical costs.

TABLE 1 A summary of baseline demographics of all enrolled patients.

	RA-N-DM	RA-DM	X^2/t/Z	*p*-value
N	328	160		
Sex (female/male)	223/105	108/52	0.227	0.893
Age (years), mean (SD)	61.02 ± 9.35	62.71 ± 9.24	3.242	0.072
Disease duration (years), mean (SD)	7.67 ± 7.67	11.64 ± 10.32	-4.571	**<0.001**
Height (cm), mean (SD)	161.2 ± 7.31	159.39 ± 7.25	-1.944	0.052
Weight (kg), mean (SD)	60.28 ± 9.82	65.07 ± 8.4	-7.736	**<0.001**
BMI, mean (SD)	21.76 ± 5.41	24.52 ± 6.74	-6.8	**<0.001**
DAS28	4.4 ± 0.5	4.5 ± 0.5	-1.928	0.054
Smoking, n (%)	51 (15.5)	33 (20.6%)	1.945	0.163
Alcohol consumption, n (%)	16 (4.9)	14 (8.8%)	2.794	0.095
Hypertension, n (%)	103 (31.4)	73 (45.6%)	9.434	**0.002**
Osteoporosis, n (%)	70 (21.3)	41 (25.6%)	1.123	0.289
Nephropathy, n (%)	19 (5.8)	19 (11.9)	5.541	**<0.001**
Family history of diabetes, n (%)	27 (8.2)	37 (23.1)	20.934	**<0.001**

Bold values in the summary indicate significant p values <0.05.
N, number of patients; SD, standard deviation; BMI, Body mass index; DAS28, disease activity score 28S.

3.2 Disease characteristics

Compared with RA-N-DM group, the levels of IgG (Z=−2.826, $p<0.05$), IgM (Z=−2.827, $p<0.01$), ALB (Z=−4.957, $p<0.001$) and A/G (Z=−3.095, $p<0.05$) in RA-DM group were significantly reduced, CRP (Z=−2.078, $p<0.05$), FBG (Z=−10.85, $p<0.001$) and GLB (Z=−2.349, $p<0.05$) were increased. There was no significant difference in ESR (Z=−1.412, $p>0.05$), IgA (Z=−0.091, $p>0.05$), WBC (Z=−1.39, $p>0.05$), RBC (Z=−1.123, $p>0.05$), PLT (Z=−1.942, $p>0.05$), LYM (Z=−1.38, $p>0.05$), MO (Z=−0.097, $p>0.05$), NE (Z=−1.861, $p>0.05$), PLR (Z=−0.372, $p>0.05$), LMR (Z=−1.496, $p>0.05$), NLR (Z=−1.928, $p>0.05$), SII (Z=−0.479, $p>0.05$), BUN (Z=−1.728, $p>0.05$) and Cr (Z=−1.278, $p>0.05$) between group RA-N-DM and RA-DM (Table 2). This suggests that patients with RA and T2D may have more severe systemic inflammatory reactions and immunoregulatory function disorders.

3.3 Peripheral lymphocyte subsets

Compared with healthy controls, the absolute numbers of B, $CD8^+$ T and NK cells in RA-N-DM patients (Z=−2.967, $p<0.01$; Z=−2.23, $p<0.05$; Z=−4.194, $p<0.001$) and RA-DM patients (Z=−3.705, $p<0.001$;

TABLE 2 A summary of disease characteristics of patients with RA, median (Q1, Q3).

	RA-N-DM	RA-DM	Z	*p*-value
ESR (mm/h)	46 (27, 83)	53.5 (27.75, 94)	−1.412	0.158
CRP (mg/L)	15.9 (5.63, 43.6)	18.9 (6.55, 68.1)	−2.078	**0.038**
IgG (g/L)	13 (10.4, 16.2)	11.8 (8.27, 14.95)	−2.826	**0.005**
IgA (g/L)	2.95 (2.06, 3.99)	2.86 (2.01, 4.09)	−0.091	0.927
IgM (g/L)	1.29 (0.91, 1.76)	1.06 (0.79, 1.59)	−2.827	**0.005**
WBC ($\times10^9$/L)	6.74 (5.38, 8.35)	7.37 (5.41, 8)	−1.39	0.165
RBC ($\times10^{12}$/L)	4.18 (3.9, 4.49)	4.17 (3.7, 4.57)	−1.123	0.261
PLT ($\times10^9$/L)	279 (221, 358.75)	263 (198.25, 340.75)	−1.942	0.052
LYM ($\times10^9$/L)	1.63 (1.33, 2.18)	1.55 (1.15, 2.22)	−1.38	0.167
MO ($\times10^9$/L)	0.5 (0.33, 0.64)	0.48 (0.35, 0.63)	−0.097	0.923
NE ($\times10^9$/L)	4.27 (3.27, 5.64)	4.88 (3.41, 6.19)	−1.861	0.063
PLR	159.64 (118.6, 228.95)	160.89 (109.24,235.04)	−0.372	0.71
LMR	3.56 (2.59, 5.06)	3.41 (2.46, 4.73)	−1.496	0.135
NLR	2.5 (1.85, 3.63)	2.8 (2.03, 4.32)	−1.928	0.054
SII	716.39 (461.65, 1125.16)	738.3 (464.47, 1291.05)	−0.479	0.632
BUN (mg/dL)	5.15 (4.2, 6.2)	5.5 (4.13, 7.1)	−1.728	0.084
Cr (mg/dL)	54.2 (47.25, 62)	53 (44, 63.75)	−1.278	0.201
FBG (mmol/L)	4.83 (4.33, 5.38)	6.71 (5.34, 8.82)	−10.85	**<0.001**
ALB (mg/L)	37.15 (33.9, 40.23)	34.25 (31.25, 38.2)	−4.957	**<0.001**
GLB (mg/L)	28.35 (19.33, 33.98)	29.4 (24.93, 35.48)	−2.349	**0.019**
A/G	1.21 (1.02, 1.44)	1.1 (0.91, 1.36)	−3.095	**0.002**

Bold values in the summary indicate significant p values <0.05.
Q1, Q3, Quartile 1, Quartile 3; ESR, erythrocyte sedimentation rate; CRP, C-reactive protein; IgG, immunoglobulin G; IgA, immunoglobulin A; IgM, immunoglobulin M; WBC, white blood cell; RBC, red blood cell; PLT, platelet; LYM, lymphatic; MO, monocytes; NE, neutrophilic granulocyte; PLR, platelet-lymphocyte ratio; LMR, monocytes- lymphatic ratio; NLR, neutrophil-lymphocyte ratio; SII, systemic immune-inflammation index; BUN, blood urea nitrogen; Cr, creatinine; FBG, fasting blood glucose; ALB, albumin; GLB, globulin; A/G, albumin-globulin ratio.

Z=−3.682, p<0.001; Z=−3.053, p<0.01) were significantly reduced, while the proportions of these did not differ significantly (p>0.05). This indicates that the proportions of immune cells were not completely parallel to their absolute numbers, and the absolute counts of T cells in RA-DM were significantly lower than those in healthy controls (Z=−3.705, p<0.001) and RA-N-DM (Z=−2.314, p<0.05) (Figure 2; Supplementary Figure S1). These results suggest that rheumatic diseases interfere with the balance of the immune system, which might be associated with the development of complications.

3.4 Peripheral CD4$^+$ T subsets

Compared with the healthy controls, the absolute numbers of Th2 cells in the RA-DM group (Z=−4.114, p<0.001) were significantly reduced, and the proportions of Th2 cells in the RA-N-DM (Z=−4.082, p<0.001) and RA-DM groups (Z=−5.987, p<0.001) were significantly decreased, resulting in a higher ratio of Th1/Th2 cells (Z=−2.672, p<0.01; Z=-4.465, p<0.001). Compared to healthy controls, the absolute numbers and proportions of Treg cells in the RA-N-DM (Z=−2.431, p<0.05; Z=−4.113, p<0.001) and RA-DM groups (Z=−6.041, p<0.001; Z=−6.395, p<0.001) were significantly reduced. Furthermore, compared to the RA-N-DM group, the absolute numbers of Th2 (Z=−4.323, <0.001) and Treg cells (Z=−3.704, p<0.001) and their proportions were significantly reduced in the RA-DM group, which led to an increase in the proportions of Th1/Th2 (Z=−2.479, p<0.05) and Th17/Treg (Z=−3.08, p <0.05) cells (Figure 3; Supplementary Figure S2). This suggests that a reduction in the absolute number and proportion of Th2 and Treg cells affects the activity and development of RA, and is closely related to the occurrence of T2D complications.

3.5 Factors associated with combined T2D in patients with RA (Univariable model)

To elucidate the factors associated with T2D in patients with RA, we first performed univariate logistic regression analyses with 21 variables chosen from the results of the previous independent-sample Kruskal-Wallis H test (Table 3). In the univariable regression analysis, the risk factors of combined hypertension (OR:1.833, 95% CI: 1.243–2.704, p<0.01), history of nephropathy (OR:2.191, 95% CI: 1.125–4.267, p<0.05), family history of diabetes (OR:3.354, 95% CI: 1.957–5.747, p<0.001), CRP (OR:1.008, 95% CI: 1.003–1.013, p<0.01), NLR (OR:1.119, 95% CI: 1.034–1.211, p<0.05), GLB (OR:1.023, 95% CI: 1.007–1.038, p<0.05) and Th17/Treg ratio (OR:3.419, 95% CI: 1.549–7.547, p<0.05) increased the chances of combined T2D in patients with RA. Oppositely, protective factors such as IgG (OR:0.956, 95% CI: 0.915–0.999, p<0.05), IgM (OR:0.739, 95% CI: 0.549–0.995, p<0.05), ALB (OR:0.9, 95% CI: 0.863–0.939, p<0.001), A/G ratio (OR:0.433, 95% CI: 0.236–0.794, p<0.01), the levels of Th2 (OR:0.913, 95% CI: 0.873–0.956, p<0.001) and Treg cells (OR:0.974, 95% CI: 0.962–0.987, p<0.001) reduced the probability of combined T2D in patients with RA.

3.6 Factors associated with combined T2D in patients with RA (multivariable model)

Based on the results of the univariate logistic regression analysis and, on this basis, through the analysis of previous research results

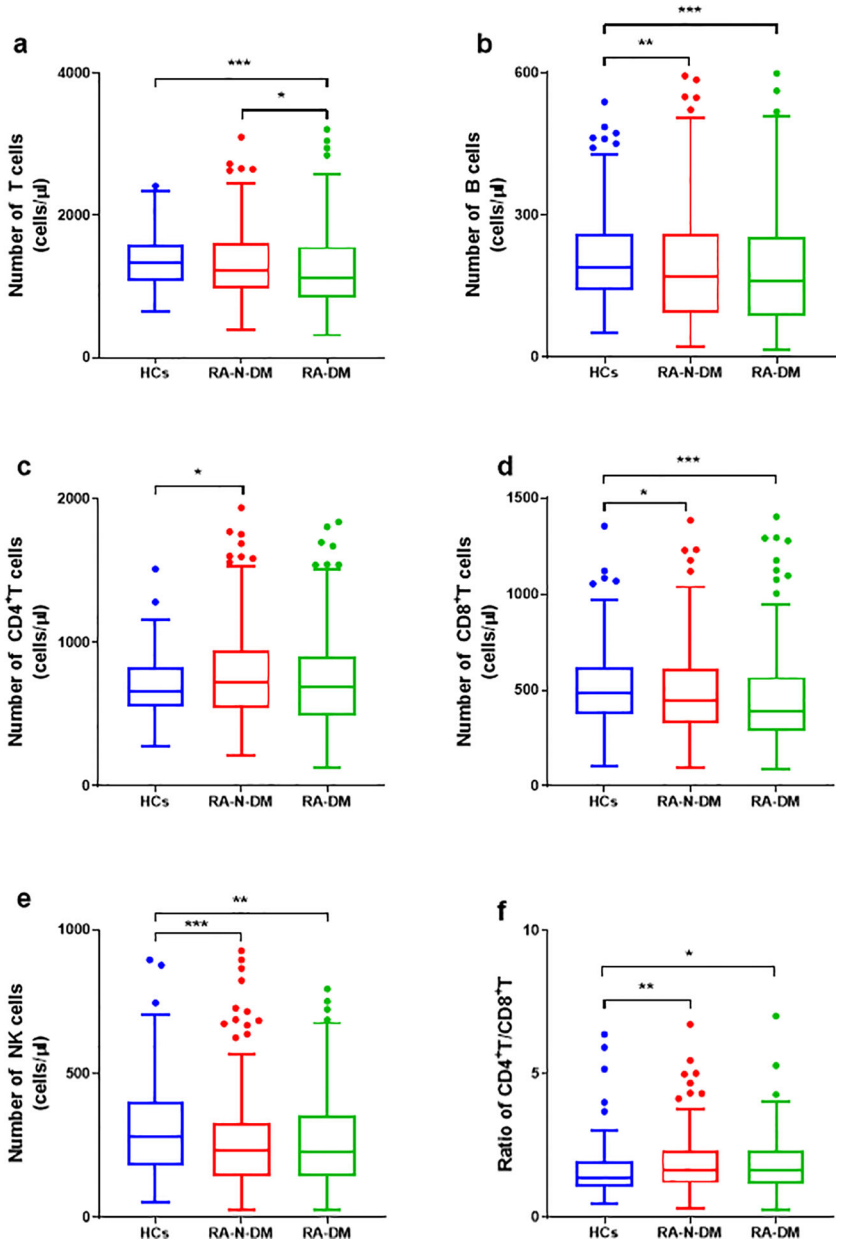

FIGURE 2
The differences of absolute numbers (cells/μL) of peripheral immune cells among health controls(HCs) and RA patients with and without DM. **(A)** The absolute numbers of T cells in RA-DM (n=160) were significantly lower than HCs (n= 206) and RA-N-DM (n=328). **(B, E)** Absolute numbers of B and NK cells were higher in HCs than both RA-N-DM and RA-DM patients. **(C, D, F)** The levels of $CD8^+$T cells were increased while that of $CD4^+$T cells reduced in RA patients, resulting in a higher ratio of $CD4^+$T / $CD8^+$T. Data are presented by median (range), and using the Independent-Samples Kruskal–Wallis H test for statistical analysis. *$p < 0.05$, **$p < 0.01$, ***$p < 0.001$.

and the summary of long-term clinical experience, after adjusting for confounding factors, a multivariate logistic regression analysis was conducted on 16 variables (Figure 4). The risk factors for RA with diabetes included decreased PLR levels (OR:0.997, 95% CI: 0.994–1, p<0.05), ALB (OR:0.881, 95% CI: 0.819–0.946, p<0.01), increased NLR levels (OR:1.139, 95% CI: 1.014–1.281, p<0.05), fewer Th2 (OR:0.902, 95% CI: 0.837–0.971, p<0.01) and Treg cells (OR:0.978, 95% CI: 0.957–0.999, p<0.05), increased combined hypertension (OR:1.984, 95% CI: 1.177–3.345, p<0.05), and family history of diabetes (OR:3.923, 95% CI: 1.989–7.736, p<0.001).

4 Discussion

This study identified that certain risk factors, especially immune dysfunction mediated by abnormal numbers of Th2 and Treg cells, may be conducive to the occurrence and development of T2D in patients with RA. A continuous longitudinal population study to explore complications and $CD4^+$ T cell subsets in patients with RA may provide new insights into the mechanism of RA complications and provide new ideas for early clinical prevention and treatment.

Among the patients with RA included in this study, the proportion of patients with T2D was approximately 15.6%, and

10.3389/fimmu.2024.1445639

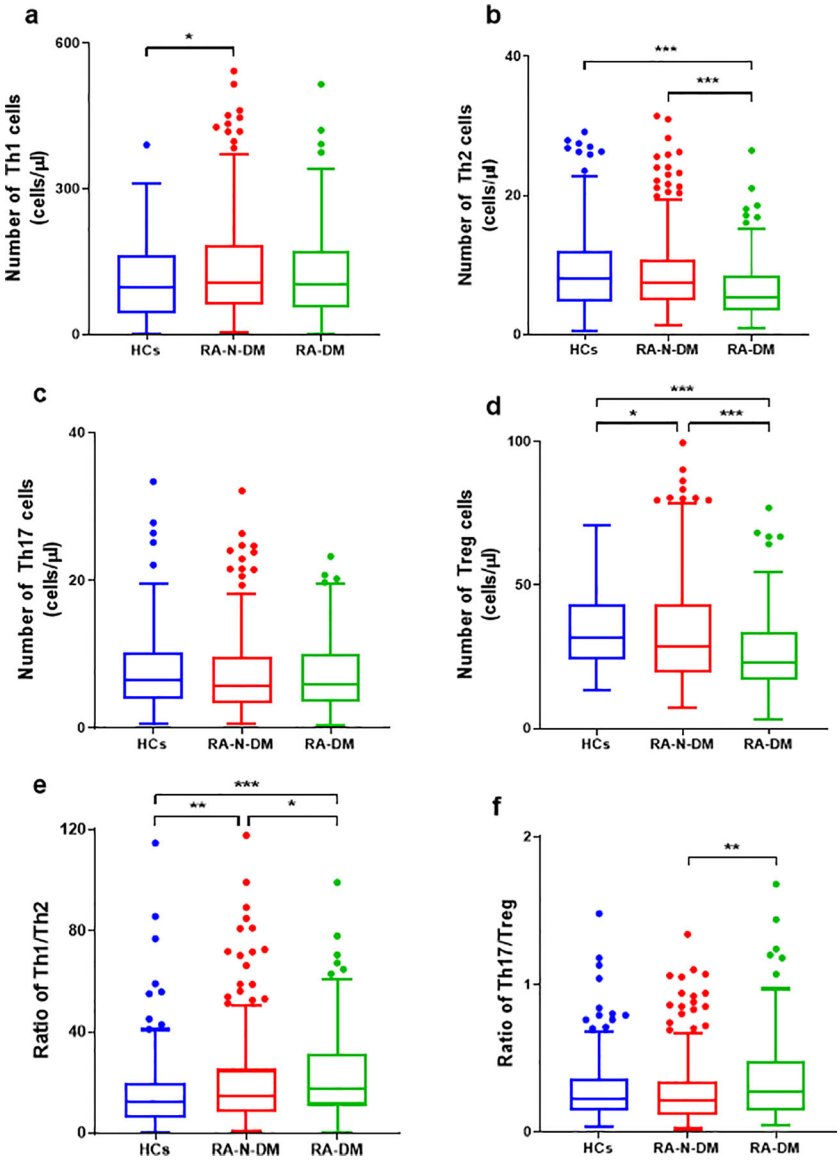

FIGURE 3
The differences of absolute numbers (cells/μL) of peripheral $CD4^+$T subgroups between RA patients (including combined diabetes and not) and healthy controls. **(A, B, D-F)** The absolute numbers of Th2 and Treg cells were significantly reduced in RA-DM patients (n=160), resulting in a higher ratio of Th1/Th2 Th17/Treg. The absolute numbers of Tregs and the ratio of Th1/Th2 in health controls (n=206) were lower than RA patients than, and the Th1 cells was lower than RA-N-DM patients (n=328). **(C)** No statistically significant difference in the Th17 cell numbers between the RA patients and healthy controls. Data are presented by median (range), and using the Independent-Samples Kruskal–Wallis H test for statistical analysis. *$p < 0.05$, **$p < 0.01$, ***$p < 0.001$.

this high prevalence is partly explained by the higher average age and duration of disease in the enrolled patients or the smaller sample size data bias. Studies have shown an increase in average age, BMI, duration of hospitalization, and incidence of hypertension and nephropathy in RA patient with concomitant T2D (14, 15), which is consistent with the findings of this study. Among them, the occurrence of obesity and the increase of BMI may be related to the insulin resistance of type 2 diabetes (16, 17). Notably, poor health, poor exercise capacity, secondary high body weight, and various metabolic organ dysfunctions, which eventually lead to insulin resistance, may be responsible for the increased incidence of T2D and cardiovascular complications in patients with RA (18). T2D has underlying genetic susceptibility (19); as observed in this study, RA patients with T2D also have a higher percentage of a family history of diabetes. Body weight, body mass index (BMI), long disease duration, and family history of diabetes were noteworthy risk factors for RA patients with T2D.

Elevated CRP has not only been observed in patients with RA, but may also be associated with the development of induced insulin resistance and T2D by inhibiting insulin signaling (20, 21). More precisely, CRP induces insulin resistance by activating the MAPK signaling pathways or interfering with the IRS/PI3K/AKT signaling pathway (insulin receptor substrate/phosphatidylinositol 3 kinase/AKT) (22, 23). Consistent with this mechanism, elevated CRP levels

10.3389/fimmu.2024.1445639

TABLE 3 A summary of associated factors of RA patients with combined diabetes (Univariable model).

	OR	95% CI	*p*-value
Gender (female/male)	0.98	0.653–1.465	0.914
Age (years)	1.02	0.999–1.041	0.062
Hypertension, n(%)	1.83	1.243–2.704	**0.002**
History of Nephropathy, n(%)	2.19	1.125–4.267	**0.021**
Family history of Diabetes, n(%)	3.35	1.957–5.747	**<0.001**
CRP (mg/L)	1.01	1.003–1.013	**0.001**
IgG (g/L)	0.96	0.915–0.999	**0.043**
IgM (g/L)	0.74	0.549–0.995	**0.046**
PLR	1.00	0.999–1.002	0.74
NLR	1.12	1.034–1.211	**0.005**
ALB (mg/L)	0.90	0.863–0.939	**<0.001**
GLB (mg/L)	1.02	1.007–1.038	**0.003**
A/G	0.43	0.236–0.794	**0.007**
T (cells/μL)	1.00	0.999–1.000	0.133
$CD4^+$ T (cells/μL)	1.00	0.999–1.000	0.226
Th2 (cells/μL)	0.91	0.873–0.956	**<0.001**
Th2%	0.56	0.381–0.831	**0.004**
Treg (cells/μL)	0.97	0.962–0.987	**<0.001**
Treg %	0.86	0.771–0.953	**0.004**
Th1/Th2	1.01	1.000–1.022	**0.05**
Th17/Treg	3.42	1.549–7.547	**0.002**

Bold values in the univariable model indicate significant p values <0.05.
CRP, C-reactive protein; PLR, platelet-lymphocyte ratio; NLR, neutrophil-lymphocyte ratio; ALB, albumin; GLB, globulin; A/G, albumin-globulin ratio; T, T lymphocyte; Th1, T helper 1 cells; Th2, T helper 2 cells; Treg, Regulatory cells.

have been observed in RA patients with T2D. IgG is deposited in the joints of patients with RA and induces arthritis via its effect on osteoclast production (24). Other studies have shown that a decrease in IgG and other immunoglobulins is associated with insulin resistance (25), which may explain the decrease in IgG and IgM levels observed in RA patients with T2D in this study. In addition, a decrease in immunoglobulin levels may also indicate immune impairment caused by hypoglycemia (26). PLR is an inflammatory index used to predict chronic complications of T2D, and an elevated PLR in patients with type 2 diabetes may reflect the underlying inflammatory burden of the disease (27, 28). In a recent study, remission of the disease and correction of immune disorders in RA patients reduced the incidence of HBP, T2D, and other comorbidities such as MetS and cardiovascular benefits (29). In addition, the underlying chronic low-grade inflammatory state is exacerbated by worsening glycated hemoglobin (HbA1c) levels as a result of poor diabetes control; therefore, inflammatory markers, including PLR, are increased. In the logistic regression analysis adjusted for covariates in this study, PLR was a risk factor for T2D in patients with RA. In this study, ALB, a risk factor for RA patients with T2D, and A/G were significantly lower and GLB was significantly higher in RA patients with T2D, suggesting that T2D plays a crucial role in maintaining glucose homeostasis, insulin clearance, and inflammatory cytokines (29). RA also causes progressive liver damage, which may be associated with vasculitis and hepatocyte amyloidosis caused by RA (30).

Multiple lymphocyte subsets, such as T and B cells are heavily involved in the development of joint dysfunction and systemic inflammation in RA (31). In patients with early RA, the number of T cells, $CD80^+$, memory B cells, and NK cells was significantly reduced compared to that in HC, and there was also a trend towards a decrease in the number of $CD8^+$ T cells (32, 33). Consistent results were also observed in our study; however, there was no statistical difference in the proportions of B and $CD8^+$ T cells between patients compared to HCs, suggesting that the absolute

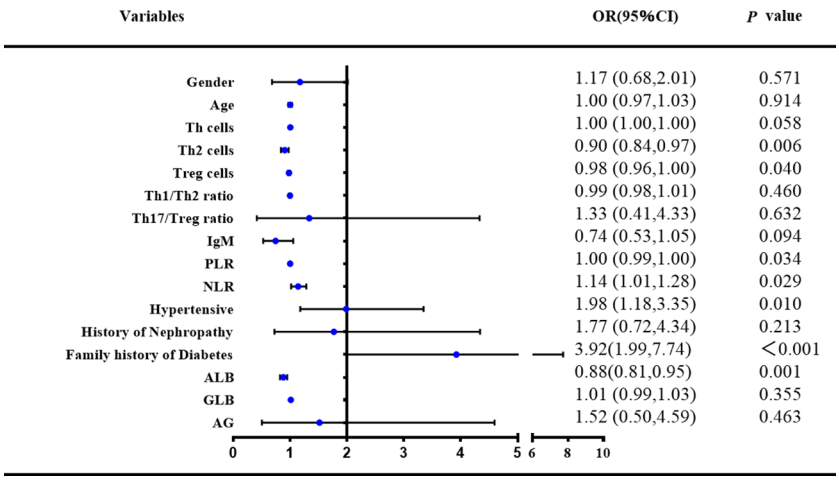

FIGURE 4
Associated factors of combined diabetes in RA patients (Multivariable model).

numbers and proportions may not be exactly parallel. Moreover, abnormal cellular immune function plays an indispensable role in the pathogenesis of T2D. T cells and their subsets, which play the most important roles in cellular immunity, are closely related to changes in blood sugar and immune functions (34, 35). Brooks-Worrell et al. demonstrated that T cells are involved in autoimmunity-mediated insulin resistance in a cross-sectional analysis of 322 patients with T2D (36). In this study, compared to RA patients without T2D, patients with T2D had a decreased absolute number of T cells and an increased proportion of $CD4^+$ T cells, suggesting that T cells, especially $CD4^+$ T subsets, are involved in the occurrence and development of T2D in patients with RA.

Naive $CD4^+$ T cells can differentiate into different cell types under the action of antigen-presenting cells (APC). An imbalance in the function and number of these cells leads to abnormalities in the cellular and humoral immunity (37, 38). Previous studies have suggested that the number of Th1 and Th17 cells increases, and the number of Th2 and Treg cells decreases in patients with RA during the active stage of the disease, resulting in an increase in the ratio of Th1/Th2 and Th17/Treg (39–41), which is consistent with our observations. Humoral immune disorders often lead to the overactivation of autoantigen T and B cells, resulting in the deposition of immune complexes in synovial tissue, persistent synovitis, and joint destruction (42).

In this study, the absolute numbers and proportions of Th2 and Treg cells were significantly lower in patients with T2D than in patients without T2D. Previous studies have shown that Th2 cells produce anti-inflammatory factors, such as IL-4, IL-5, IL-6, IL-9, IL-10, and IL-13 to alleviate the inflammatory response, whereas Treg cells inhibit the inflammatory response by inhibiting Th1 and Th17 cells (43). In fact, IL-1, as a common inflammatory pathway of RA, atherosclerotic heart disease, T2D and other systemic diseases, plays a special role in the pathological mechanism of RA combined with T2D (44). Studies have shown that IL-1 inhibition is beneficial for both RA patients and T2D patients, and may become a new targeted treatment option (45). Winer et al (46). detected the number and proportion of Th1, Th17, and Treg cells in the adipose tissue of obese mouse models induced by a high-fat diet, and found that the number of Th1 and Th17 cells in obese mice increased, whereas the number of Treg cells decreased, confirming that Th1 and Th17 cells induce insulin resistance, which can be reversed by Treg cells. Further examination of the $CD4^+$ T cell subset levels in the peripheral blood and adipose tissue of newly diagnosed T2D patients showed that $CD4^+$ T cells tended to be polarized into pro-inflammatory Th1 and Th17 cells in T2D patients, ultimately leading to inflammation and insulin resistance, underscoring the crucial role of $CD4^+$ T subpopulations in the pathogenesis of T2D (46). The results of this study suggest that secondary T2D in patients with RA may be related to reduced anti-insulin resistance caused by decreased Th2 and Treg cells, which was also confirmed in the logistic regression analysis with the multivariable model. This may provide a new possibility for predicting the risk factors for RA in patients with T2D and explain its pathological features.

This study was based on single-center and retrospective methods, with a small sample size and limited comprehensiveness in describing the risk factors for T2D in patients with RA. This should be further developed into a multicenter prospective study to facilitate a more objective and comprehensive research. In this study, patients taking hormones and DMARDs for six months were excluded from the enrollment phase to reduce the effect on peripheral blood lymphocyte levels. However, because these drugs are widely used in clinical treatments, further studies should be conducted to determine their effects on secondary T2D in patients with RA.

5 Conclusion

In patients with RA, BMI, cardiovascular comorbidities, systemic inflammatory status, liver function, and lymphocyte levels (particularly Th2 and Treg levels) influence the risk of developing T2D. Testing circulating lymphocyte populations should be a part of the routine management of RA.

Data availability statement

The original contributions presented in the study are included in the article/Supplementary Material. Further inquiries can be directed to the corresponding author.

Ethics statement

The studies involving humans were approved by The Ethics Committee of the Second Hospital of Shanxi Medical University. The studies were conducted in accordance with the local legislation and institutional requirements. The participants provided their written informed consent to participate in this study.

Author contributions

RP: Conceptualization, Data curation, Software, Visualization, Writing – original draft. JW: Data curation, Validation, Writing – original draft. PH: Conceptualization, Funding acquisition, Resources, Supervision, Writing – review & editing. QY: Resources, Supervision, Writing – review & editing. SZ: Resources, Supervision, Writing – review & editing. GS: Software, Visualization, Writing – original draft. GL: Software, Visualization, Writing – original draft. XL: Conceptualization, Supervision, Writing – review & editing.

Funding

The author(s) declare financial support was received for the research, authorship, and/or publication of this article. Funded by the Key Research and Development Projects of Shanxi Province (grant No. 202102130501003 to PH), the National Social Science Foundation of China (grant No. 21BTQ050 to PH), National Natural Science Foundation of China (grant No. 72474125).

Acknowledgments

We would like to thank Editage (www.editage.cn).

Conflict of interest

The authors declare that the research was conducted in the absence of any commercial or financial relationships that could be construed as a potential conflict of interest.

Publisher's note

All claims expressed in this article are solely those of the authors and do not necessarily represent those of their affiliated organizations, or those of the publisher, the editors and the reviewers. Any product that may be evaluated in this article, or claim that may be made by its manufacturer, is not guaranteed or endorsed by the publisher.

Supplementary material

The Supplementary Material for this article can be found online at: https://www.frontiersin.org/articles/10.3389/fimmu.2024.1445639/full#supplementary-material

References

1. Lee DM, Weinblatt ME. Rheumatoid arthritis. *Lancet*. (2001) 358:903–11. doi: 10.1016/S0140-6736(01)06075-5

2. Safiri S, Kolahi AA, Smith E, Hill C, Bettampadi D, Mansournia MA, et al. Global, regional and national burden of rheumatoid arthritis 1990-2017: a systematic analysis of the Global Burden of Disease study 2017. *Ann Rheum Dis*. (2019) 78:1463–71. doi: 10.1136/annrheumdis-2019-215920

3. Chiu YM, Lu YP, Lan JL, Chen DY, Wang JD. Lifetime risks, life expectancy, and health care expenditures for rheumatoid arthritis: A nationwide cohort followed up from 2003 to 2016. *Arthritis Rheumatol*. (2021) 73:750–8. doi: 10.1002/art.41597

4. Sakran N, Graham Y, Pintar T, Yang W, Kassir R, Willigendael EM, et al. The many faces of diabetes. Is there a need for re-classification? A narrative review. *BMC Endocr Disord*. (2022) 22:9. doi: 10.1186/s12902-021-00927-y

5. Malone JI, Hansen BC. Does obesity cause type 2 diabetes mellitus (T2DM)? Or is it the opposite? *Pediatr Diabetes*. (2019) 20:5–9. doi: 10.1111/pedi.12787

6. Radner H, Lesperance T, Accortt NA, Solomon DH. Incidence and prevalence of cardiovascular risk factors among patients with rheumatoid arthritis, psoriasis, or psoriatic arthritis. *Arthritis Care Res (Hoboken)*. (2017) 69:1510–8. doi: 10.1002/acr.v69.10

7. Semb AG, Rollefstad S, Ikdahl E, Wibetoe G, Sexton J, Crowson C, et al. Diabetes mellitus and cardiovascular risk management in patients with rheumatoid arthritis: an international audit. *RMD Open*. (2021) 7:e001724. doi: 10.1136/rmdopen-2021-001724corr1

8. Nikiphorou E, de Lusignan S, Mallen CD, Khavandi K, Bedarida G, Buckley CD, et al. Cardiovascular risk factors and outcomes in early rheumatoid arthritis: a population-based study. *Heart*. (2020) 106:1566–72. doi: 10.1136/heartjnl-2019-316193

9. Naranjo A, Sokka T, Descalzo MA, Calvo-Alén J, Hørslev-Petersen K, Luukkainen RK, et al. Cardiovascular disease in patients with rheumatoid arthritis: results from the QUEST-RA study. *Arthritis Res Ther*. (2008) 10:R30. doi: 10.1186/ar2383

10. Radovanović-Dinić B, Tešić-Rajković S, Zivkovic V, Grgov S. Clinical connection between rheumatoid arthritis and liver damage. *Rheumatol Int*. (2018) 38:715–24. doi: 10.1007/s00296-018-4021-5

11. Arnett FC, Edworthy SM, Bloch DA, McShane DJ, Fries JF, Cooper NS, et al. The American Rheumatism Association 1987 revised criteria for the classification of rheumatoid arthritis. *Arthritis Rheum*. (1988) 31:315–24. doi: 10.1002/art.1780310302

12. Aletaha D, Neogi T, Silman AJ, Funovits J, Felson DT, Bingham CO, et al. 2010 rheumatoid arthritis classification criteria: an American College of Rheumatology/European League Against Rheumatism collaborative initiative. *Ann Rheum Dis*. (2010) 69:1580–8. doi: 10.1136/ard.2010.138461

13. THE EXPERT COMMITTEE ON THE DIAGNOSIS AND CLASSIFICATION OF DIABETES MELLITUS. Report of the expert committee on the diagnosis and classification of diabetes mellitus. *Diabetes Care*. (1997) 20:1183–97. doi: 10.2337/diacare.20.7.1183

14. Ursini F, Angelo S, Russo E, Ammerata G, Abenavoli L, Mauro D, et al. Serum complement C3 and type 2 diabetes in rheumatoid arthritis: A case-control study. *Rev Recent Clin Trials*. (2018) 13:215–21. doi: 10.2174/1574887113666180314092757

15. Costello RE, Marsden A, Movahedi M, Lunt M, Humphreys JH, Emsley R, et al. The effect of glucocorticoid therapy on mortality in patients with rheumatoid arthritis and concomitant type II diabetes: a retrospective cohort study. *BMC Rheumatol*. (2020) 4:4. doi: 10.1186/s41927-019-0105-4

16. Gobato AO, Vasques AC, Zambon MP, Barros Filho Ade A, Hessel G. Metabolic syndrome and insulin resistance in obese adolescents. *Rev Paul Pediatr*. (2014) 32:55–62. doi: 10.1590/S0103-05822014000100010

17. Jung SH, Jung CH, Reaven GM, Kim SH. Adapting to insulin resistance in obesity: role of insulin secretion and clearance. *Diabetologia*. (2018) 61:681–7. doi: 10.1007/s00125-017-4511-0

18. Baghdadi LR, Woodman RJ, Shanahan EM, Mangoni AA. The impact of traditional cardiovascular risk factors on cardiovascular outcomes in patients with rheumatoid arthritis: a systematic review and meta-analysis. *PloS One*. (2015) 10: e0117952. doi: 10.1371/journal.pone.0117952

19. Harrison TA, Hindorff LA, Kim H, Wines RC, Bowen DJ, McGrath BB, et al. Family history of diabetes as a potential public health tool. *Am J Prev Med*. (2003) 24:152–9. doi: 10.1016/S0749-3797(02)00588-3

20. Shapiro SC. Biomarkers in rheumatoid arthritis. *Cureus*. (2021) 13:e15063. doi: 10.7759/cureus.15063

21. Pope JE, Choy EH. C-reactive protein and implications in rheumatoid arthritis and associated comorbidities. *Semin Arthritis Rheum*. (2021) 51:219–29. doi: 10.1016/j.semarthrit.2020.11.005

22. Neale EP, Batterham MJ, Tapsell LC. Consumption of a healthy dietary pattern results in significant reductions in C-reactive protein levels in adults: a meta-analysis. *Nutr Res*. (2016) 36:391–401. doi: 10.1016/j.nutres.2016.02.009

23. Xu JW, Morita I, Ikeda K, Miki T, Yamori Y. C-reactive protein suppresses insulin signaling in endothelial cells: role of spleen tyrosine kinase. *Mol Endocrinol*. (2007) 21:564–73. doi: 10.1210/me.2006-0354

24. Yu T, Qiu W, Deng GM. Regulatory effects of autoantibody IgG on osteoclastogenesis. *Clin Immunol*. (2023) 246:109200. doi: 10.1016/j.clim.2022.109200

25. Asare-Anane H, Botchey CPK, Ofori EK, Boamah I, Crabbe S, Asamoah-Kusi K. Altered immunoglobulins (A and G) in Ghanaian patients with type 2 diabetes. *SAGE Open Med*. (2018) 6:2050312118762042. doi: 10.1177/2050312118762042

26. Amiel SA. The consequences of hypoglycaemia. *Diabetologia*. (2021) 64:963–70. doi: 10.1007/s00125-020-05366-3

27. Liu N, Sheng J, Pan T, Wang Y. Neutrophil to lymphocyte ratio and platelet to lymphocyte ratio are associated with lower extremity vascular lesions in chinese patients with type 2 diabetes. *Clin Lab*. (2019) 65. doi: 10.7754/Clin.Lab.2018.180804

28. Atak B, Aktas G, Duman TT, Erkus E, Kocak MZ, Savli H. Diabetes control could through platelet-to-lymphocyte ratio in hemograms. *Rev Assoc Med Bras (1992)*. (2019) 65:38–42. doi: 10.1590/1806-9282.65.1.38

29. Kunutsor SK, Abbasi A, Apekey TA. Aspartate aminotransferase - risk marker for type-2 diabetes mellitus or red herring? *Front Endocrinol (Lausanne)*. (2014) 5:189. doi: 10.3389/fendo.2014.00189

30. Sen D, González-Mayda M, Brasington RD Jr. Cardiovascular disease in rheumatoid arthritis. *Rheum Dis Clin North Am*. (2014) 40:27–49. doi: 10.1016/j.rdc.2013.10.005

31. Wu X. Innate lymphocytes in inflammatory arthritis. *Front Immunol*. (2020) 11:565275. doi: 10.3389/fimmu.2020.565275

32. Chalan P, Bijzet J, Kroesen BJ, Boots AM, Brouwer E. Altered natural killer cell subsets in seropositive arthralgia and early rheumatoid arthritis are associated with autoantibody status. *J Rheumatol*. (2016) 43:1008–16. doi: 10.3899/jrheum.150644

33. Lübbers J, van Beers-Tas MH, Vosslamber S, Turk SA, de Ridder S, Mantel E, et al. Changes in peripheral blood lymphocyte subsets during arthritis development in arthralgia patients. *Arthritis Res Ther*. (2016) 18:205. doi: 10.1186/s13075-016-1102-2

34. Donath MY, Størling J, Maedler K, Mandrup-Poulsen T. Inflammatory mediators and islet beta-cell failure: a link between type 1 and type 2 diabetes. *J Mol Med (Berl)*. (2003) 81:455–70. doi: 10.1007/s00109-003-0450-y

35. Pereira FO, Frode TS, Medeiros YS. Evaluation of tumour necrosis factor alpha, interleukin-2 soluble receptor, nitric oxide metabolites, and lipids as inflammatory markers in type 2 diabetes mellitus. *Mediators Inflammation*. (2006) 2006:39062. doi: 10.1155/MI/2006/39062

36. Brooks-Worrell B, Hampe CS, Hattery EG, Palomino B, Zangeneh SZ, Utzschneider K, et al. Islet autoimmunity is highly prevalent and associated with

diminished β-cell function in patients with type 2 diabetes in the grade study. *Diabetes*. (2022) 71:1261–71. doi: 10.2337/db21-0590

37. Wu R, Li N, Zhao X, Ding T, Xue H, Gao C, et al. Low-dose Interleukin-2: Biology and therapeutic prospects in rheumatoid arthritis. *Autoimmun Rev*. (2020) 19:102645. doi: 10.1016/j.autrev.2020.102645

38. Rao DA, Gurish MF, Marshall JL, Slowikowski K, Fonseka CY, Liu Y, et al. Pathologically expanded peripheral T helper cell subset drives B cells in rheumatoid arthritis. *Nature*. (2017) 542:110–4. doi: 10.1038/nature20810

39. Wang T, Wang Z, Qi W, Jiang G, Wang G. The role, targets and mechanisms of traditional Chinese medicine in regulating the balance of T helper type 17/regulatory Tcells in rheumatoid arthritis. *Int J Rheum Dis*. (2023) 26:613–24. doi: 10.1111/1756-185X.14560

40. Yamaki K, Uchida H, Li X, Yanagisawa R, Takano H, Hayashi H, et al. Effect of varying types of anti-arthritic drugs on Th1 and Th2 immune responses in mice. *Int J Immunopathol Pharmacol*. (2005) 18:133–44. doi: 10.1177/039463200501800114

41. De A, Blotta HM, Mamoni RL, Louzada P, Bertolo MB, Foss NT, et al. Effects of dexamethasone on lymphocyte proliferation and cytokine production in rheumatoid arthritis. *J Rheumatol*. (2002) 29:46–51. doi: 10.1300/J094v10n01_21

42. Lee KH, Ahn BS, Cha D, Jang WW, Choi E, Park S, et al. Understanding the immunopathogenesis of autoimmune diseases by animal studies using gene modulation: A comprehensive review. *Autoimmun Rev*. (2020) 19:102469. doi: 10.1016/j.autrev.2020.102469

43. Kahn SE, Hull RL, Utzschneider KM. Mechanisms linking obesity to insulin resistance and type 2 diabetes. *Nature*. (2006) 444:840–6. doi: 10.1038/nature05482

44. Weber BN, Giles JT, Liao KP. Shared inflammatory pathways of rheumatoid arthritis and atherosclerotic cardiovascular disease. *Nat Rev Rheumatol*. (2023) 19:417–28. doi: 10.1038/s41584-023-00969-7

45. Ruscitti P, Cipriani P, Liakouli V, Iacono D, Pantano I, Margiotta DPE, et al. Anti-interleukin-1 treatment in patients with rheumatoid arthritis and type 2 diabetes (TRACK): A multicentre, open-label, randomised controlled trial. *PloS Med*. (2019) 16: e1002901. doi: 10.1371/journal.pmed.1002901

46. Winer S, Chan Y, Paltser G, Truong D, Tsui H, Bahrami J, et al. Normalization of obesity-associated insulin resistance through immunotherapy. *Nat Med*. (2009) 15:921–9. doi: 10.1038/nm.2001

frontiers | Frontiers in Immunology

TYPE Original Research
PUBLISHED 12 November 2024
DOI 10.3389/fimmu.2024.1445916

Check for updates

OPEN ACCESS

EDITED BY
Anette S. B. Wolff,
University of Bergen, Norway

REVIEWED BY
Jing Luo,
Second Hospital of Shanxi Medical University, China
Muhammad Shahnawaz Soyfoo,
Université libre de Bruxelles, Belgium

*CORRESPONDENCE
Bingnan Cui
cbn1998@163.com

†These authors have contributed equally to this work and share first authorship

RECEIVED 08 June 2024
ACCEPTED 28 October 2024
PUBLISHED 12 November 2024

CITATION
Yang Y, Du Y, Ren Z, Mei Q, Jiang M, Liu W, Zhang H and Cui B (2024) Predicting thyroid involvement in primary Sjögren's syndrome: development and validation of a predictive nomogram.
Front. Immunol. 15:1445916.
doi: 10.3389/fimmu.2024.1445916

COPYRIGHT
© 2024 Yang, Du, Ren, Mei, Jiang, Liu, Zhang and Cui. This is an open-access article distributed under the terms of the Creative Commons Attribution License (CC BY). The use, distribution or reproduction in other forums is permitted, provided the original author(s) and the copyright owner(s) are credited and that the original publication in this journal is cited, in accordance with accepted academic practice. No use, distribution or reproduction is permitted which does not comply with these terms.

Predicting thyroid involvement in primary Sjögren's syndrome: development and validation of a predictive nomogram

Yixuan Yang[1†], Yanyuan Du[2†], Zhaoyang Ren[3], Qingqing Mei[3], Mengyao Jiang[3], Wenjing Liu[3], Huadong Zhang[3] and Bingnan Cui[1*]

[1]Department of Dermatology, Guang'anmen Hospital, China Academy of Chinese Medical Sciences, Beijing, China, [2]Department of Oncology, Guang'anmen Hospital, China Academy of Chinese Medical Sciences, Beijing, China, [3]Department of Rheumatology, Guang'anmen Hospital, China Academy of Chinese Medical Sciences, Beijing, China

Introduction: Patients with Primary Sjögren's syndrome (pSS) are at a higher risk of thyroid disorders than the general population. This retrospective analysis of 202 patients with pSS was conducted to uncover risk factors associated with thyroid involvement and to create a predictive model for this condition.

Methods: We analyzed 202 patients with pSS from Guang'anmen Hospital, China Academy of Chinese Medical Sciences, with 105 cases of thyroid involvement and 97 without. The Least Absolute Shrinkage and Selection Operator method was used to identify key variables for our risk model. These variables were then subjected to multivariate logistic regression to develop the model. The accuracy of the model was assessed through the C-index, receiver operating characteristic curves, calibration plots, and decision curve analysis, with internal validation via bootstrapping.

Results: High-sensitivity C-reactive protein (HCRP), pulmonary disease, pharyngeal dryness, forgetfulness, night sweats, hyperuricemia, nasal dryness, anxiety, Ro52, and aspartate aminotransferase (AST) were incorporated into the nomogram. The model showed robust discrimination and calibration abilities. Decision curve analysis indicated the clinical utility of our nomogram in intervening on the probability thresholds of thyroid disease.

Conclusion: By integrating HCRP, pulmonary disease, pharyngeal dryness, forgetfulness, night sweats, hyperuricemia, nasal dryness, anxiety, Ro52, and AST, our thyroid risk nomogram can predict the risk of thyroid involvement in patients with pSS, aiding in more informed treatment strategies.

KEYWORDS

thyroid events, nomogram, predictive model, primary Sjögren's syndrome, risk

1 Introduction

Primary Sjögren's syndrome (pSS) is a chronic autoimmune disease marked by the infiltration of lymphocytes into the salivary and lacrimal glands. This leads to symptoms such as dry mouth (xerostomia) and dry eye (keratoconjunctivitis sicca), along with the production of autoantibodies (1). The occurrence of pSS varies widely among studies and ethnic groups, from 0.1% to 4.8% (2). While the exact cause of pSS is not fully understood, factors like genetics, hormones, and the environment are believed to be significant in its development. The pathogenesis of pSS involves a complex mix of elements, with environmental triggers possibly initiating the disease in genetically susceptible individuals. Central to pSS are autoimmune reactions and chronic inflammation, which involve the disrupted activation of both innate and adaptive immune responses (3). pSS is not limited to exocrine glands; it can also affect various systemic organs, including the skin, joints, lungs, gastrointestinal tract, kidneys, hematopoietic system, and nervous system (4).

It is important to note that patients with pSS have a significantly higher incidence of thyroid disease compared to the general population, especially for autoimmune thyroiditis (AITD) and subclinical hypothyroidism (5). The occurrence of AITD in patients with pSS is nine times that of the general population (5). Studies have indicated that hypothyroidism is the most common autoimmune disorder in patients with pSS over a 10.5-year follow-up period (6). The association between pSS and thyroid disease suggests shared genetic or environmental factors and similar pathological mechanisms. Thyroid dysfunction in patients with pSS can present as hyperthyroidism, hypothyroidism, or chronic AITD. Moreover, the coexistence of Sjögren's syndrome (SS) and AITD is relatively common, suggesting a special link between these two diseases in the context of autoimmune disease overlap. For instance, patients with pSS and thyroid disease are often women who test positive for anti-thyroglobulin, anti-follicular cells, and anti-thyroid peroxidase antibodies (7). These thyroid diseases may further influence the clinical presentation and therapeutic decisions for patients with pSS.

Studies have shown varying degrees of thyroid disease prevalence in patients with pSS. Kelly et al. (8) found that 14% of 100 patients with SS had thyroid disorders, with 11% having hypothyroidism and 3% hyperthyroidism. Perez et al. (9) identified thyroid diseases in 45% of 33 patients with SS, including 24% with AITD, 33% with hypothyroidism, and 6% with hyperthyroidism. A study of 160 patients with pSS reported thyroid disease signs in 36%, with 20% diagnosed with AITD and 16% with non-AITD thyroid disorders. Notably, over half of the patients with pSS showed signs of subclinical hypothyroidism (5). Warfvinge et al. (10) examined 63 patients with AITD, with 19 also evaluated for salivary gland morphology and function; 11 had abnormalities in salivary glands, and 31.5% showed clinical and histological features of pSS. Rojas et al. (11), in their analysis of 1083 patients across four autoimmune disease cohorts, found that AITD and SS are the most common co-occurring autoimmune diseases. Several non-controlled studies have reported AITD in SS, with frequencies from 10% to 30% (12). In Lazarus et al.'s study (6), 16% of SS patients developed AITD. The most common clinical manifestation of AITD in SS is hypothyroidism, though subclinical AITD may be even more prevalent. Zeher et al. (13) surveyed 479 patients with pSS for various thyroid diseases, finding thyroid dysfunction in 95 cases (21.25%). The high prevalence of thyroid disease in patients with pSS underscores the importance of screening for thyroid function in this group.

The connection between thyroid disorders and pSS is supported by several theoretical perspectives. Both conditions show similar histological features, such as cellular infiltration dominated by $CD4^+$ T cells, forming structures similar to lymphoid follicles without B-cell activation (12). Genetically, they share common HLA class II molecules, including HLA-B8 and HLA-DR3, expressed in thyroid and epithelial cells (12). The combination of HLA-B8 and HLA-DR3 is more prevalent in patients with pSS and AITD, and CTLA-4 gene variations are more common in AITD and other autoimmune diseases like rheumatoid arthritis (14).

Another point strengthening the pathogenic connection between AITD and SS is the pivotal role of chemokines and cytokines in autoimmune inflammatory diseases. Thyroid follicular cells produce CXCL10, which particularly promotes the migration of Th1 cells to the thyroid, triggering the secretion of IFN-γ and TNF-α (15). These cytokines, in turn, stimulate the production of CXCL10, creating a positive feedback loop that intensifies the autoimmune response (16). In Graves' disease, a subtype of AITD, Th1 cells may play a significant role in the early stages, despite the disease typically being Th2-dominant (17). The expression of CXCL10/IP-10 in thyroid and vascular endothelial cells, along with elevated serum levels of CXCL10, is closely related to the disease activity (18). Similarly, in a mouse model of SS, Th1-associated chemokines are significantly increased in the submandibular gland, whereas Th2-associated chemokines are not detected, suggesting that CXCL10 antagonists might have therapeutic potential by reducing the infiltration of $CXCR3^+$ Th1 cells and the production of IFN-γ (19). These findings not only reveal the central role of chemokines in autoimmune inflammatory diseases but also provide molecular evidence for the pathological link between AITD and SS.

Given the multitude of risk factors associated with pSS, predicting the risk of thyroid involvement could prevent thyroid events and improve patient outcomes. Currently, there is no predictive model for thyroid involvement risk in patients with pSS. This study aims to retrospectively identify potential risk factors for thyroid involvement in patients with pSS and to develop a thyroid risk nomogram. The goal is to provide clinicians with a new tool to more accurately identify patients at higher risk of thyroid involvement, allowing for earlier interventions and potentially better patient outcomes.

2 Methods

2.1 Participants

From January 2022 to December 2022, patients with pSS were diagnosed and followed up in the Department of Rheumatology at Guang'anmen Hospital, China Academy of Chinese Medical

Sciences. Inclusion Criteria: All patients met the ACR/EULAR 2016 classification criteria, which are as follows. Patients must have at least one of the symptoms of dry eyes or dry mouth, and must not meet any exclusion criteria. A diagnosis of pSS can be made if the total score of the following five items is ≥4: ①Focal lymphocytic sialadenitis in labial salivary gland biopsy with a focus score of ≥1 focus/4 mm^2, 3 points. ②Positive anti-SSA/Ro antibodies, 1 point. ③Ocular staining score (OSS) of ≥5 in at least one eye or a van Bijsterveld score of ≥4, 1 point. ④Schirmer's test result of ≤5 mm/5 min in at least one eye, 1 point. ⑤Unstimulated whole saliva flow rate of ≤0.1 ml/min as measured by the Navazesh and Kumar method, 1 point. (American College of Rheumatology/European League Against Rheumatism classification criteria for pSS: a consensus and data-driven methodology involving three international patient cohorts). Exclusion Criteria: Patients were excluded if they lacked essential data, such as thyroid involvement.

This study was approved by the Ethics Committee of Guang'anmen Hospital, China Academy of Chinese Medical Sciences (Approval No.2022-132-KY) and adhered to the principles of the Declaration of Helsinki. Informed consent was obtained verbally from all patients at the time of their clinical visits. After confirming the research protocol, we conducted a brief telephone follow-up with the participants. Initially, we verified the participants' identities and provided a concise explanation of the clinical trial, including its design and the approval from the ethics committee. We then obtained verbal informed consent. Upon receiving informed consent, we collected the participants' information and proceeded with the relevant research. Participants who declined to participate were excluded from the study, and no information was collected from them.

2.2 Characteristics

As a retrospective observational study, the sociodemographic and clinical characteristics of our patients were obtained through interviews and physical examinations. Information collected from medical histories included age at initial diagnosis, gender, symptoms, involved systems, and other comorbidities at the first visit. The data were collected by trained clinicians and medical staff to ensure accuracy. Symptoms primarily included dry nose, dry throat, anxiety and irritability, night sweats, forgetfulness and so on. In our study, dry nose is defined as dryness of the nasal mucosa with reduced secretion. Dry throat is defined as reduced salivary secretion and dryness of the pharyngeal mucosa.Anxiety and irritability are defined as encompassing feelings of fear, worry, and restlessness, possibly escalating to panic and a sense of impending doom, as well as an intolerance for waiting, a propensity for excitability, and an exaggerated reaction to setbacks and delays. Night sweats is defined as excessive sweating after falling asleep, which stops upon waking. Forgetfulness is defined as an inability to remember new events or recall one or more past memories. Pulmonary diseases are defined as various conditions affecting lung function, impacting respiratory function, including but not limited to chronic obstructive pulmonary disease, asthma, and interstitial lung disease. Hyperuricemia is defined as serum uric acid levels above 420 μmol/L on a regular diet. The laboratory data for these patients were obtained from standardized tests conducted at the clinical laboratory of Guang'anmen Hospital, China Academy of Chinese Medical Sciences, all of which have been validated. The laboratory information included complete blood count, blood biochemistry, liver and kidney function tests, antibody profiles, and urinalysis. During the follow-up period, thyroid events such as hyperthyroidism, hypothyroidism, thyroiditis, and goiter were recorded. The laboratory tests were conducted under controlled conditions to ensure consistency and reliability. In this study, the complete blood count (CBC) was performed using the Sysmex XN-3000 analyzer (Sysmex Corporation, Kobe, Japan), which combines flow cytometry and impedance technology for accurate measurement of red blood cells, white blood cells, and platelets. Flow cytometry was used for fluorescence labeling and classification of white blood cells, while impedance technology measured cell volume. Blood samples were collected in EDTA tubes and analyzed within one hour of collection to ensure stability and accuracy. Blood biochemistry analysis was conducted using the Beckman AU5800 automated biochemical analyzer (Beckman Coulter, Brea, CA, USA). The AU5800 uses spectrophotometric methods to quantify biochemical parameters, including liver and kidney function, glucose, lipids, and electrolytes. Blood samples were centrifuged at 3,000 rpm for 10 minutes to separate serum for analysis. Antibody profiling was performed using the Freedom EVOlyzer automated ELISA analyzer (Tecan Group Ltd., Männedorf, Switzerland) with validated commercial ELISA kits. Venous blood samples were collected, centrifuged, and analyzed with automated pipetting, incubation, washing, and optical detection at 450 nm. Urinalysis was carried out using the Sysmex UN-2000 system, consisting of the UF-3000 flow cytometry analyzer and the UC-3500 chemical module (Sysmex Corporation, Kobe, Japan). The UF-3000 used fluorescence flow cytometry to analyze urine particles, while the UC-3500 used dry chemistry for biochemical parameters such as glucose, protein, and pH. Urine samples were collected in sterile containers and analyzed within two hours to ensure integrity.

2.3 Classification of patients with pSS

Our previous analysis of patients with pSS revealed that the incidence of structural or functional thyroid abnormalities is higher in patients with pSS compared to the healthy population. Consequently, we defined hyperthyroidism, hypothyroidism, thyroiditis, and goiter as thyroid events. Based on the occurrence of subsequent thyroid events during the follow-up period, we categorized the patients into two groups: the thyroid disease group (TD) and the non-thyroid disease group (NTD). Hyperthyroidism is an endocrine disorder characterized by excessive secretion of thyroid hormones, including triiodothyronine (T3) and thyroxine (T4), from the thyroid gland. This condition is typically accompanied by a decrease in serum thyroid-stimulating hormone (TSH) levels. Clinically, hyperthyroidism presents with symptoms such as palpitations, weight loss, excessive sweating, irritability, and other systemic manifestations associated with increased thyroid activity. TSH levels are usually significantly below the normal range, often less than 0.1 mIU/L. Elevated serum free T4 (FT4) and free T3 (FT3) levels indicate excessive secretion of thyroid hormones, confirming the diagnosis of hyperthyroidism (20).

Hypothyroidism is a condition characterized by a decreased secretion of thyroid hormones or a reduction in their physiological action, leading to a slowdown in metabolic processes. The disease can be classified into overt hypothyroidism and subclinical hypothyroidism. Overt hypothyroidism is marked by significantly elevated levels of TSH, typically greater than 10 mIU/L, accompanied by decreased levels of FT4. Subclinical hypothyroidism, on the other hand, presents with mildly elevated TSH levels, usually ranging between 4.5 and 10 mIU/L, while FT4 levels remain within the normal range (21). Thyroiditis refers to a group of disorders involving inflammation of the thyroid gland, commonly associated with thyroid dysfunction. Depending on the underlying pathophysiological mechanisms, thyroiditis can be classified into various types, including autoimmune thyroiditis (e.g., Hashimoto's thyroiditis), subacute thyroiditis, and painless thyroiditis. Hashimoto's thyroiditis is the most prevalent form of autoimmune thyroiditis, typically presenting with hypothyroidism. Clinically, it is characterized by diffuse thyroid enlargement (goiter). Laboratory findings include elevated serum TSH levels and decreased FT4 levels. Autoimmune markers, such as thyroid peroxidase antibodies (TPOAb) or thyroglobulin antibodies (TgAb), are usually positive. On thyroid ultrasound, the thyroid gland often exhibits an irregular structure and reduced echogenicity, indicative of chronic inflammation (22). Subacute thyroiditis, often caused by viral infections, presents clinically with thyroid pain and tenderness, frequently accompanied by systemic symptoms such as fever, palpitations, weight loss, and sweating, which are indicative of transient hyperthyroidism. Laboratory tests show decreased TSH levels and elevated levels of FT4 and FT3. The erythrocyte sedimentation rate (ESR) is typically elevated. A thyroid radionuclide scan usually demonstrates reduced radioactive iodine uptake, reflective of diminished thyroid function (23). Painless thyroiditis presents similarly to subacute thyroiditis but without pain. It may initially cause transient hyperthyroidism, followed by hypothyroidism. Thyroid function tests reveal a brief period of hyperthyroidism, similar to subacute thyroiditis. Autoimmune markers (TPOAb or TgAb) may be positive, and a thyroid radionuclide scan typically shows decreased radioactive iodine uptake (24).

2.4 Data management

All collected data, including laboratory results and clinical observations, were securely stored in an electronic database. Data entry was double-checked to avoid transcription errors. This data management process ensures both the reliability and traceability of the collected information. Only authorized personnel had access to the database, ensuring the protection of patient confidentiality.

2.5 Statistical analysis

The sociodemographic and clinical characteristics of our patients are presented as mean (SD), median (interquartile range), or count (percentage) and were analyzed using R software (version 4.3.3; https://www.R-project.org). Comparisons between the two groups were performed using the t-test, Mann-Whitney U test, or chi-squared test as appropriate. The Mann-Whitney U test was used for continuous variables, while Fisher's exact test was used for categorical variables. Odds ratios (OR) with 95% confidence intervals (CI) and p-values (two-tailed) were used to evaluate these characteristics. We used the Least Absolute Shrinkage and Selection Operator (LASSO) regression model to select the most predictive non-zero features for thyroid events in patients with pSS. Subsequently, we performed multivariate logistic regression on these features and developed a predictive model. This model included all sociodemographic and clinical characteristics with p-values less than 0.05. Additionally, other potential predictive factors were incorporated into the thyroid risk prediction model. Receiver operating characteristic (ROC) curves and calibration curves were used to evaluate the thyroid risk nomogram. Harrell's C-index was measured to quantify the discrimination ability of the thyroid risk model. Bootstrapping validation (1000 bootstrap resamples) was used to obtain a relatively calibrated model C-index. Calibration curve analysis was performed to assess the clinical applicability of the thyroid risk model by quantifying the net benefit (the proportion of true positive patients minus the proportion of false positive patients, balancing the relative harm of not intervening with the negative impact of unnecessary intervention) across different threshold probabilities in the pSS cohort.

3 Results

3.1 Characteristics of patients

This study involved the diagnosis and follow-up of 202 patients with primary pSS at Guang'anmen Hospital, China Academy of Chinese Medical Sciences, conducted from January 2022 to December 2022. The study included 8 male and 194 female patients, aged between 21 and 92 years. Based on the occurrence of thyroid events after diagnosis, 97 patients were categorized into TD group, and 105 patients were categorized into the non-thyroid disease NTD group. The characteristics of all study patients (TD and NTD groups) are shown in (Table 1). Compared to the TD group, the NTD group had a higher prevalence of pulmonary diseases (87.62% vs 73.20%, p=0.009), and significantly higher levels of high-sensitivity C-reactive protein (HCRP) (89.52% vs 59.79%, p<0.001). Additionally, the TD group was more prone to hyperuricemia than the NTD group (98.97% vs 93.33%, p=0.04). Furthermore, the NTD group exhibited a higher prevalence of dry throat (45.36% vs 31.43%, p=0.042), anxiety and irritability (25.77% vs 11.43%, p=0.008), forgetfulness (10.31% vs 21.90%, p=0.026), and elevated aspartate aminotransferase (AST) levels (88.66% vs 96.19%, p=0.041). There were no significant differences between the two groups in other characteristics.

3.2 Feature selection

Based on a cohort of 202 patients, we employed a LASSO regression model with the following parameters: cross-validation

TABLE 1 Clinical characteristics of patients with primary Sjögren's syndrome.

Characteristics	TD (n=105)	NTD (n=97)	χ^2	p
Pulmonary disease,n (%)	92 (87.619)	71 (73.196)	6.733	0.009
	13 (12.381)	26 (26.804)		
Hyperuricemia,n (%)	98 (93.333)	96 (98.969)	4.21	0.04
	7 (6.667)	1 (1.031)		
Dry nose,n (%)	78 (74.286)	81 (83.505)	2.558	0.11
	27 (25.714)	16 (16.495)		
Dry throat,n (%)	33 (31.429)	44 (45.361)	4.149	0.042
	72 (68.571)	53 (54.639)		
Anxiety and irritability, n (%)	12 (11.429)	25 (25.773)	6.934	0.008
	93 (88.571)	72 (74.227)		
Night sweats,n (%)	46 (43.810)	54 (55.670)	2.837	0.092
	59 (56.190)	43 (44.330)		
Forgetfulness,n (%)	23 (21.905)	10 (10.309)	4.96	0.026
	82 (78.095)	87 (89.691)		
AST,n (%)	101 (96.190)	86 (88.660)	4.16	0.041
	4 (3.810)	11 (11.340)		
Ro52,n (%)	16 (15.238)	10 (10.309)	1.092	0.296
	89 (84.762)	87 (89.691)		
HCRP,n (%)	94 (89.524)	58 (59.794)	23.927	<0.001
	11 (10.476)	39 (40.206)		

TD, Thyroid Disease; NTD, non-thyroid disease; AST, Aspartate Aminotransferase; HCRP, High-sensitivity C-Reactive Protein.

folds (cv) set to 5, maximum iterations (max_iter) set to 1000, tolerance (tol) set to 0.0001, and L1 regularization coefficient (alpha) set to 0.01. Upon fitting the model, the regression coefficients for each feature were extracted. The absolute value of these coefficients indicates the contribution of each feature to the model's prediction, with larger absolute values signifying greater importance. The importance of features was then ranked by sorting the absolute values of all coefficients (Figure 1). This process reduced the 62 sociodemographic and clinical features to 10 potential predictive factors with non-zero coefficients, representing a reduction ratio of approximately 6:1 (Figure 2). These features include HCRP, pulmonary disease, hyperuricemia, Ro52, AST, dry nose, dry throat, anxiety and irritability, night sweats, and forgetfulness. HCRP serves as an inflammatory marker that typically escalates in the presence of acute inflammation or infection. Ro-52 antibodies, commonly referred to as anti-Ro-52 antibodies, are a nonspecific indicator often observed in autoimmune diseases. AST is a biomarker for liver function that tends to increase in the blood when liver damage is present.

3.3 Identification of significant risk factors for TD

We established a logistic regression model incorporating HCRP, pulmonary disease, hyperuricemia, Ro52, AST, dry nose, dry throat, anxiety and irritability, night sweats, and forgetfulness (Table 2). The odds ratios (OR) and 95% confidence intervals (CI) for each factor were expressed using a forest plot (Figure 3). Patients with pulmonary disease were more likely to develop TD compared to those without pulmonary disease (OR: 2.437, 95% CI: 1.081–5.705, p=0.035). The relationships between hyperuricemia (OR: 0.124, 95% CI: 0.006–0.909, p=0.078), dry nose (OR: 0.531, 95% CI: 0.229–1.197, p=0.131),

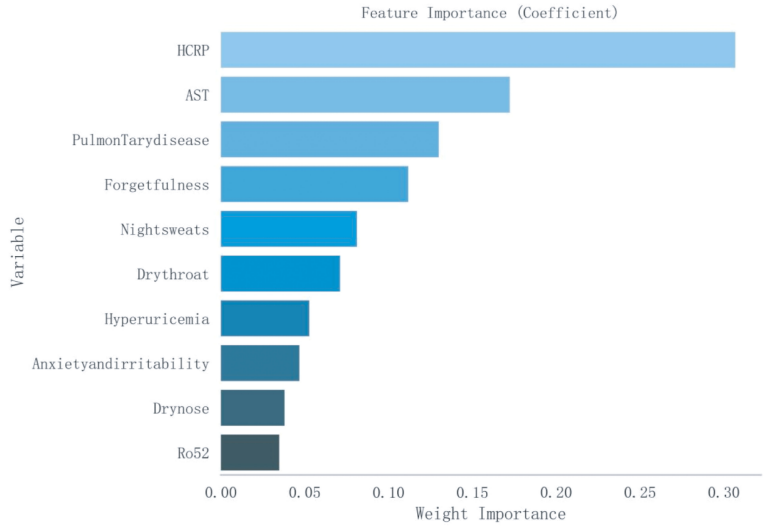

FIGURE 1
Ranking of Importance of Ten Features. AST, Aspartate Aminotransferase; HCRP, High-sensitivity C-Reactive Protein.

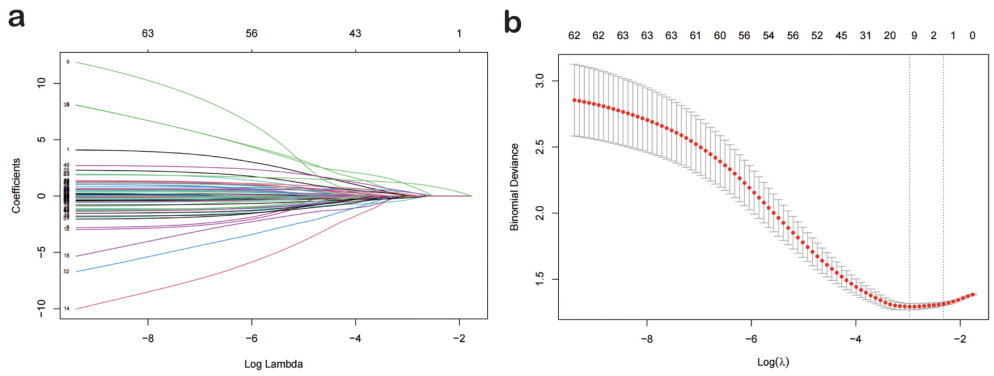

FIGURE 2
Lasso Logistic Regression for Feature Selection. **(A)** The optimal parameter (lambda) in the lasso model was selected using the minimum criterion via five-fold cross-validation. The partial likelihood deviance (binomial deviance) curve was plotted against the logarithm of lambda. Dashed lines were drawn at the optimal values using the minimum criterion and the 1-SE criterion. **(B)** Lasso coefficient profiles for 77 features. A coefficient profile plot was generated against the logarithm of lambda sequence. A vertical line was drawn at the value selected by five-fold cross-validation, where the optimal analysis resulted in five features with non-zero coefficients. Lasso, Least Absolute Shrinkage and Selection Operator; SE, Standard Error.

dry throat (OR: 0.521, 95% CI: 0.265–1.011, p=0.055), anxiety and irritability (OR: 0.759, 95% CI: 0.308–1.82, p=0.539), and TD were not significant. Additionally, patients with night sweats had a significantly lower risk of developing TD (OR: 0.446, 95% CI: 0.224–0.868, p=0.019). Forgetfulness was near significance (OR: 2.356, 95% CI: 0.944–6.205, p=0.072). Elevated AST levels significantly increased the risk of TD (OR: 5.437, 95% CI: 1.572–22.42, p=0.011). Elevated HCRP levels also significantly increased the risk of TD (OR: 5.544, 95% CI: 2.521–13.145, p<0.001). Although the presence of Ro52 antibodies did not reach significance (OR: 2.081, 95% CI: 0.78–5.886, p=0.152), it indicated a potential correlation. In summary, pulmonary disease, night sweats, AST, and HCRP are important predictive factors for TD. Particularly, high levels of HCRP and AST significantly increase the risk of TD, while night sweats are associated with a lower risk of TD.

TABLE 2 Predictive factors for thyroid risk in patients with primary Sjögren's syndrome.

Intercept and variable	Prediction model		p
	β	OR	
(Intercept)	-0.907	0.404	0.231
Pulmonarydisease	0.891	2.437	0.035
Hyperuricemia	-2.088	0.124	0.078
Drynose	-0.634	0.531	0.131
Drythroat	-0.652	0.521	0.055
Anxiety and irritability	-0.276	0.759	0.539
Nightsweats	-0.807	0.446	0.019
Forgetfulness	0.857	2.356	0.072
AST	1.693	5.437	0.011
HCRP	1.713	5.544	<0.001
Ro52	0.733	2.081	0.152

AST, Aspartate Aminotransferase; HCRP, High-sensitivity C-Reactive Protein.

3.4 Establishment of the thyroid risk nomogram

To facilitate clinical assessment, we developed a nomogram based on 10 significant risk factors, displayed in image form (Figure 4). The nomogram model demonstrated satisfactory predictive accuracy with a concordance index of 0.788 (95% CI: 0.726–0.85). The points for each risk factor range from 0 to 100, with a total score ranging from 0 to 450.

3.5 Assessment of the thyroid risk nomogram

The area under the ROC curve (AUC) for the thyroid risk nomogram is 0.788, indicating a relatively good predictive capability (Figure 5A). The calibration curve of the nomogram used to predict thyroid risk in patients with pSS demonstrated good concordance (Figure 5B). The Brier Score of the calibration curve was 0.187, indicating that the model has relatively good predictive performance. The decision curve analysis demonstrates that the thyroid risk nomogram provides more benefit than the intervention strategy when the threshold probability for a patient and a clinician is greater than 10% and less than 82%, respectively (Figure 5C). The net benefit of the thyroid risk nomogram is comparable to that of several overlapping sections within this range.

4 Discussion

In this study, a retrospective analysis was conducted on 202 patients with pSS, leading to the identification of ten key risk factors associated with thyroid involvement: HCRP, pulmonary disease, pharyngeal dryness, forgetfulness, night sweats, hyperuricemia, nasal dryness, anxiety, Ro52 antibodies, and AST. Based on these characteristics, we developed and validated an individualized nomogram to predict the risk of thyroid involvement in patients

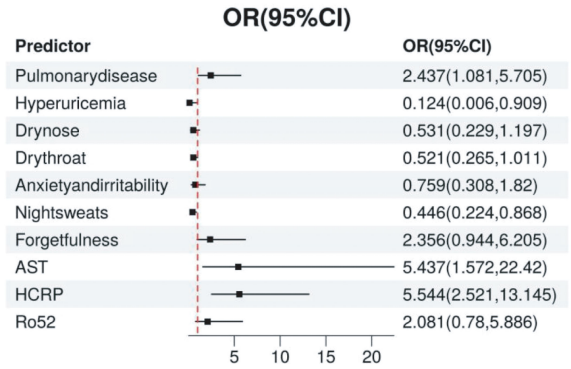

FIGURE 3
The Relationship Between Various Predictive Variables and TD. The point estimates (odds ratios, OR) and their 95% confidence intervals (CI) for each variable are displayed in the figure. Each point represents the odds ratio for the respective variable, and the horizontal line denotes the 95% confidence interval. TD, Thyroid Disease.

with pSS. The nomogram demonstrated good discrimination and calibration, with a C-index of 0.788, indicating high predictive accuracy. Decision curve analysis further confirmed the potential clinical utility of the nomogram in guiding intervention strategies. The findings suggest that this predictive tool can assist in early identification of high-risk patients, enabling timely clinical intervention and potentially improving patient outcomes.

In patients with pSS, elevated levels of AST may be associated with an increased risk of thyroid involvement. AST serves as a marker for liver function, with levels typically elevated in the blood in response to liver damage. However, AST is also present in other tissues, including the heart and skeletal muscle, where injury can similarly increase AST levels. In autoimmune conditions such as pSS, chronic inflammation and immune-mediated tissue damage may lead to increased AST levels. Abnormal levels can be observed in Graves' disease patients, with studies indicating that 29% of 146 Graves' patients had at least one instance of abnormal AST (25). In Graves' disease, liver enzyme abnormalities are commonly seen with GGT, followed by ALT, ALP, and then AST. While elevated serum ALP is most frequently observed in hyperthyroid patients, increases in AST and ALT are also common (26). In hypothyroid patients, serum liver enzymes, including AST, often exhibit abnormalities. Hypothyroidism may lead to a slight increase in serum ALT and GGT concentrations, potentially associated with impaired lipid metabolism and hepatic steatosis reported in hypothyroidism (27). Furthermore, increases in AST and LDH may be related to myopathy induced by hypothyroidism (28). However, our study did not identify ALT as a potential risk factor, a discrepancy that might be attributed to the small sample

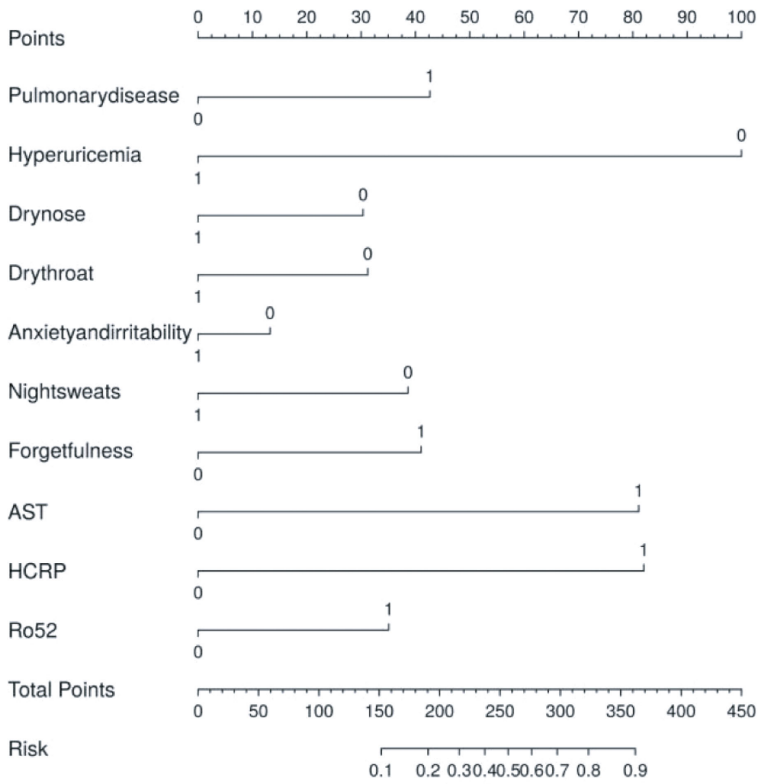

FIGURE 4
Model establishment and the nomogram. The thyroid risk nomogram was developed within the cohort, incorporating HCRP, pulmonary disease, dry throat, forgetfulness, night sweats, hyperuricemia, dry nose, anxiety and irritability, Ro52, and AST. AST, Aspartate Aminotransferase; HCRP, High-sensitivity C-Reactive Protein.

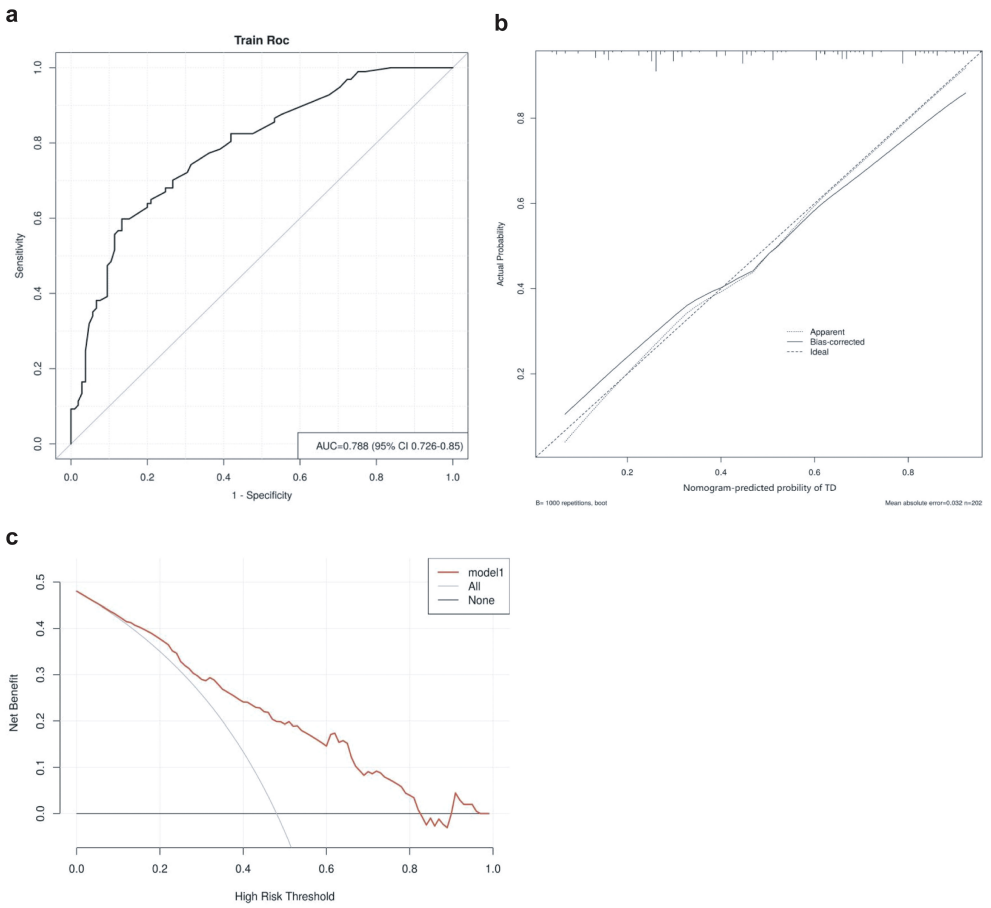

FIGURE 5
(A) Receiver operating characteristics curve for the thyroid risk nomogram in the Cohort. The area under the curve (AUC) is 0.788 (95% confidence interval: 0.726–0.85). **(B)** Calibration curve for the thyroid risk nomogram prediction in the cohort. The x-axis represents the predicted thyroid risk, while the y-axis represents the actual diagnosed thyroid involvement. The diagonal dashed line represents the perfect prediction of an ideal model. The solid line indicates the performance of the nomogram, with a closer proximity to the diagonal dashed line signifying better predictive accuracy. **(C)** Decision curve analysis for the thyroid risk nomogram. The y-axis represents net benefit.

size and variability in disease activity. In patients with pSS, the heightened risk of thyroid events may be associated with systemic inflammation and immune-mediated injury. It could be hypothesized that AST levels in the blood may indirectly reflect this state of systemic inflammation, potentially linking to the risk of thyroid events. However, there is currently no direct evidence implicating AST as a key independent risk factor for thyroid events in patients with pSS. Further research is required to delineate the relationship between AST and thyroid disease in patients with pSS. Future studies should consider large-scale prospective cohort studies to identify potential connections between AST levels and thyroid events in patients with pSS and explore the possible biological mechanisms involved.

In patients with pSS, the positivity of anti-Ro52 antibodies may be associated with an increased risk of thyroid involvement. Ro52, also known as TRIM21, is an E3 ubiquitin ligase that primarily functions in the cytoplasm but can translocate to the nucleus in inflammatory environments and participate in the regulation of type I interferon production (29). Ro52 and anti-Ro52 antibodies are involved in many autoimmune diseases, particularly rheumatic diseases such as pSS and systemic lupus erythematosus (30). The presence of Ro52 antibodies is one of the key indicators for the diagnosis of pSS (31). Anti-Ro52 antibodies may be associated with an increased risk of AITD in patients with pSS. For instance, the expression of HLA class II molecules such as HLA-DR3, HLA-DQ, and HLA-B8 is higher in AITD (32), and they are also susceptibility genes for SS, with HLA-DR3 being particularly associated with the positivity of anti-Ro52 antibodies (33). Although the mechanisms underlying the development of autoimmune diseases including pSS and the formation of thyroid abnormality-related diseases remain elusive, two important characteristics shared by these two diseases are chronic inflammatory states and metabolic dysfunction. The association of anti-Ro52 antibody positivity with thyroid involvement in our model may underscore the potential role of autoimmune responses in thyroid dysfunction in patients with pSS. This finding may suggest that modulation of autoimmune responses could be key in managing thyroid involvement in patients with pSS. Future research should further explore the mechanism by which Ro52 is involved in thyroid involvement in

patients with pSS and how this biomarker can be utilized to optimize treatment strategies. For example, studying how the expression of Ro52 in thyroid cells affects the synthesis and secretion of thyroid hormones, and how anti-Ro52 antibodies affect the function of thyroid cells. Additionally, investigating the interaction between anti-Ro52 antibodies and other thyroid autoantibodies (such as anti-TPO and anti-TG antibodies), and how they collectively affect thyroid function, is also an important direction for future research.

HCRP, a biomarker of inflammation, typically increases in response to inflammation or infection. In autoimmune diseases, including pSS, chronic inflammation may result in sustained elevation of HCRP levels. As an inflammatory biomarker, HCRP may reflect the immune-mediated inflammatory processes, and its elevated levels in patients with pSS may correlate with an increased risk of thyroid disease. Research by Manisha Panchal et al. has shown an increased prevalence of elevated levels of HCRP in patients with subclinical hypothyroidism (34), suggesting a potential association between HCRP and the risk of thyroid disease. The inflammatory signs observed in patients with hypothyroidism are thought to be related to the interplay between IL-6, TNF-α, and IL-1, which may be linked to elevated levels of HCRP during hypothyroidism. During this condition, the absence of thyroid hormones leads to a decreased metabolic rate, potentially affecting the clearance rate of HCRP. Hyperthyroidism may be associated with rapid metabolic processes, which could lead to enhanced adrenergic nervous system activity, stimulation of the immune system, and increased peripheral blood flow, all of which may contribute to increased concentrations of HCRP (35). However, despite these associations, it remains unclear whether HCRP is a direct cause of thyroid events in patients with pSS or if it merely serves as a marker of the inflammatory process. Further research is needed to clarify the exact relationship between HCRP and thyroid disease in patients with pSS, including prospective and interventional studies. Such studies would determine whether elevated levels of HCRP predict an increased risk of future thyroid events in pSS and assess whether interventions to reduce levels of HCRP (such as anti-inflammatory therapy) could reduce the risk of thyroid events in the patients. Should HCRP prove to be a reliable predictor of thyroid involvement in pSS, its clinical monitoring could facilitate early detection of patients at risk and inform preemptive therapeutic strategies.

Lung involvement is common in pSS, with a prevalence of interstitial lung disease (ILD) associated with pSS ranging from 3% to 11% (36, 37). Studies have indicated that patients with pSS with lung involvement may exhibit elevated levels of inflammatory markers, such as erythrocyte sedimentation rate (ESR) and CRP, potentially linking to an increased risk of thyroid disease (38). Obstructive disease in patients with dysfunctional thyroid disorders may arise from the direct impact of hormones on pulmonary function (39). Hypothyroidism can lead to a spectrum of respiratory consequences, from mild dyspnea to overt respiratory failure (40), which may alternatively elucidate symptoms of dry throat and nose in patients. Dryness of the throat and nose in patients with pSS primarily results from impaired glands responsible for saliva and nasal mucus production. Thyroid hormones modulate glandular function, and thus, thyroid dysfunction may exacerbate symptoms of dryness indirectly by affecting glandular secretion. Both pSS and thyroid disease encompass autoimmune and inflammatory processes. Systemic inflammation can lead to widespread tissue damage and dysfunction, including effects on thyroid and pulmonary function. Integrated management for patients with pSS with concurrent thyroid involvement and pulmonary abnormalities may be necessary, including thyroid hormone adjustments and autoimmune response control. For symptoms of dry throat and nose, artificial lubricants and immunomodulatory treatments may be required. Future research should further explore the precise mechanisms linking lung involvement, dry throat and nose, and thyroid involvement in patients with pSS, as well as how these symptoms impact quality of life and disease management. Additionally, the efficacy of targeted treatment strategies, such as immunomodulatory therapy and thyroid hormone replacement therapy in patients with pSS, particularly in improving glandular function, alleviating inflammation, and improving prognosis, should be assessed.

Thyroid hormones exert crucial influence on brain metabolism and function, encompassing the regulation of memory and cognitive faculties. Abnormalities in thyroid function, whether hyperthyroidism or hypothyroidism, have the potential to impair memory and cognitive functions (41), leading to forgetfulness. Thyroid hormones and retinoids are now recognized as key signals in modulating neuronal plasticity associated with learning, with variations in the expression of transthyretin protein—a blood carrier for these biomodulatory factors—being characteristically associated with the consolidation of memory traces (42). In patients with pSS, cognitive dysfunction is frequently reported and may be related to systemic inflammation, immune-mediated damage, and other comorbidities (43). Approximately 20% of SS patients exhibit involvement of the central nervous system (CNS). Cognitive and behavioral symptoms of CNS SS include forgetfulness and mental sluggishness, progressing monthly (44, 45). However, a longitudinal study on cognitive decline in SS patients found no significant cognitive deterioration over a 7-year follow-up period (46). Hypothyroidism is not only a potential factor for mood and behavioral changes but also associated with a decline in cognitive function. Its clinical manifestations feature a slowing and inhibition of higher neural activities, sluggish and sustained thinking and speech, and a reduction in memory, sometimes resembling coma, accompanied by symptoms of weakness syndrome and organic dementia (47). Furthermore, hypothyroidism may accelerate the progression of neurodegenerative diseases, increasing the risk of dementia, including Alzheimer's disease (48, 49). Patients with overt hypothyroidism often exhibit anxiety, inattention, disorientation, impaired learning and perception, and a general decline in intellectual, linguistic, psychomotor, and executive functions (50–52). However, forgetfulness, as a nonspecific symptom, has not yet established a direct link with thyroid events in patients with pSS. Neurological involvement in patients with pSS is diverse, including peripheral, autonomic, and central nervous systems. Future research is needed to investigate the molecular pathways linking thyroid dysfunction with cognitive impairment in pSS and identify potential early interventions to prevent or slow cognitive decline.

Patients with pSS have a significantly higher prevalence of psychiatric disorders compared to the general population (53). Anxiety, the most prevalent subjective symptom, substantially impacts their health, increasing the risk of cardiovascular diseases (53), linking with various psychological disorders (54), impairing work performance (55), and potentially worsening the disease. Reduced salivary secretion raises the risk of dental caries and oral candidiasis in patients with pSS, who also suffer from tooth loss and severe periodontal damage, causing painful chewing (12, 56, 57). This may lead to avoidance of chewing, further deteriorating dental health. Moreover, dry throat and mouth in patients with pSS can impair functions such as chewing, speaking, or swallowing, and cause a sensation of choking, thereby inducing anxiety (58). As the disease progresses, anxiety or depressive moods can intensify dysphagia. Dysphagia not only affects eating but may also cause patients to avoid public eating due to the fear of choking or aspiration pneumonia, reducing quality of life and increasing anxiety. Thyroid hormones play a crucial role in mood regulation, and thyroid dysfunction, particularly hyperthyroidism, often presents with anxiety and irritability. However, no association was found between anti-thyroid antibodies and anxiety or depression in a population-based study. Night sweats, a nonspecific symptom, are associated with mood disorders and hyperthyroidism and may be influenced by physical conditions or anxiety states (59). Lack of understanding of pSS can exacerbate anxiety and depression. Therefore, disease education for patients with pSS is crucial for alleviating these emotional disorders, which may help reduce the occurrence of thyroid events. Education helps patients understand their condition, learn coping strategies, and reduce social and psychological burdens. However, whether anxiety and irritability in patients with pSS directly increase the risk of thyroid events or merely reflect the psychological burden of the disease requires further research for clarification.

While there is currently no direct evidence to suggest that hyperuricemia is an independent risk factor for thyroid events in patients with pSS, several studies have proposed potential links. Uric acid (UA), the end product of purine metabolism, has serum levels that reflect the balance between purine nucleotide catabolism and UA excretion (60). Thyroid hormones can modulate levels of UA, as hyperuricemia is more common in individuals with subclinical thyroid dysfunction than in those with normal thyroid function (61). Giordano et al. (61) reported a significantly higher incidence of hyperuricemia in patients with both hyperthyroidism and hypothyroidism compared to the general population. It has been suggested that hyperthyroidism might precipitate hyperuricemia by enhancing UA synthesis or diminishing renal clearance, potentially due to accelerated purine nucleotide metabolism during the production of UA (62–64). pSS, an autoimmune disease, is characterized by chronic inflammation and immune cell activation. This inflammatory milieu could promote the production of UA, and the thyroid, being a potential target of immune responses, might be influenced by inflammatory mediators. There might be molecular similarities between thyroid and salivary gland cells, allowing the autoimmune response to target not only salivary glands but also the thyroid, resulting in thyroid dysfunction. Hyperuricemia could serve as a biomarker for autoimmune response activation. Further research is warranted to elucidate these mechanisms and to clarify the link between hyperuricemia and thyroid disease in patients with pSS, which could inform clinical management strategies.

This study introduces the first nomogram designed to predict thyroid involvement in patients with pSS. The tool demonstrated good discrimination and calibration in internal validation, signifying its potential accuracy in risk prediction. Additionally, decision curve analysis substantiated the clinical application value of the nomogram, particularly for guiding decisions on thyroid intervention. Despite these promising findings, the study has limitations. Firstly, this study was conducted in a single medical center, and there may be a delay in the diagnosis of thyroid disease in patients with pSS. Future multicenter studies with larger cohorts could enhance and validate the model. Secondly, while we endeavored to include relevant factors, it is still inevitable that some variables influencing thyroid risk were overlooked. Thirdly, patient demographics of our study, predominantly female, reflect the typical gender distribution in pSS and may not be generalizable. Additionally, the exclusion of patients with incomplete data could introduce bias. Lastly, while internal validation has been performed, the robustness of the nomogram has not been verified in external cohorts and should be evaluated in a broader pSS population. At the same time, the applicability of this model in pSS populations in other regions and countries remains to be determined, which requires further validation through prospective studies in larger samples to ascertain its clinical relevance.

In summary, this study identified key factors—HCRP, pulmonary disease, throat dryness, cognitive issues, night sweats, hyperuricemia, nasal dryness, anxiety, Ro52, and AST—that correlate with thyroid involvement in patients with pSS. We developed a personalized nomogram with proven clinical validity for predicting such risks. This tool allows clinicians and patients to make informed decisions on interventions, including lifestyle modifications and medical treatments. Future research should assess the generalizability of the nomogram across diverse populations and refine it with additional risk factors for enhanced predictive accuracy. Additionally, external validation in other pSS cohorts is necessary to confirm its potential to mitigate thyroid risks and influence clinical management strategies.

Data availability statement

The raw data supporting the conclusions of this article will be made available by the authors, without undue reservation.

Ethics statement

The studies involving humans were approved by Ethics Committee of Guang'anmen Hospital, China Academy of Chinese Medical Sciences (Approval No.2022-132-KY). The studies were conducted in accordance with the local legislation and institutional requirements. The participants provided their written informed consent to participate in this study.

Author contributions

YY: Visualization, Writing – original draft. YD: Visualization, Writing – original draft. ZR: Data curation, Writing – original draft. QM: Data curation, Writing – original draft. MJ: Data curation, Writing – original draft. WL: Data curation, Writing – original draft. HZ: Supervision, Writing – review & editing. BC: Supervision, Writing – review & editing.

Funding

The author(s) declare that no financial support was received for the research, authorship, and/or publication of this article.

Conflict of interest

The authors declare the research was conducted in the absence of any commercial or financial relationships that could be construed as a potential conflict of interest.

Publisher's note

All claims expressed in this article are solely those of the authors and do not necessarily represent those of their affiliated organizations, or those of the publisher, the editors and the reviewers. Any product that may be evaluated in this article, or claim that may be made by its manufacturer, is not guaranteed or endorsed by the publisher.

References

1. Brito-Zerón P, Baldini C, Bootsma H, Bowman SJ, Jonsson R, Mariette X, et al. Sjögren syndrome, Nature reviews. *Dis Primers*. (2016) 2:16047. doi: 10.1038/nrdp.2016.47

2. Mavragani CP, Moutsopoulos HM. The geoepidemiology of Sjögren's syndrome. *Autoimmun Rev*. (2010) 9:A305–10. doi: 10.1016/j.autrev.2009.11.004

3. Nocturne G, Mariette X. Advances in understanding the pathogenesis of primary Sjögren's syndrome, Nature reviews. *Rheumatology*. (2013) 9:544–56. doi: 10.1038/nrrheum.2013.110

4. Ritter J, Chen Y, Stefanski AL, Dörner T. Current and future treatment in primary Sjögren's syndrome - A still challenging development. *Joint Bone Spine*. (2022) 89:105406. doi: 10.1016/j.jbspin.2022.105406

5. Jara LJ, Navarro C, Brito-Zerón Mdel P, García-Carrasco M, Escárcega RO, Ramos-Casals M. Thyroid disease in Sjögren's syndrome. *Clin Rheumatol*. (2007) 26:1601–6. doi: 10.1007/s10067-007-0638-6

6. Lazarus MN, Isenberg DA. Development of additional autoimmune diseases in a population of patients with primary Sjögren's syndrome. *Ann rheumatic Dis*. (2005) 64:1062–4. doi: 10.1136/ard.2004.029066

7. Ramos-Casals M, García-Carrasco M, Cervera R, Gaya J, Halperin I, Ubieto I, et al. Thyroid disease in primary Sjögren syndrome. Study in a series of 160 patients. *Medicine*. (2000) 79:103–8. doi: 10.1097/00005792-200003000-00004

8. Kelly CA, Foster H, Pal B, Gardiner P, Malcolm AJ, Charles P, et al. Primary Sjögren's syndrome in north east England–a longitudinal study. *Br J Rheumatol*. (1991) 30:437–42. doi: 10.1093/rheumatology/30.6.437

9. Pérez B, Kraus A, López G, Cifuentes M, Alarcón-Segovia D. Autoimmune thyroid disease in primary Sjögren's syndrome. *Am J Med*. (1995) 99:480–4. doi: 10.1016/s0002-9343(99)80223-x

10. Warfvinge G, Larsson A, Henricsson V, Ericsson UB, Hansen B, Manthorpe R. Salivary gland involvement in autoimmune thyroiditis, with special reference to the degree of association with Sjögren's syndrome. *Oral surgery Oral medicine Oral Pathol*. (1992) 74:288–93. doi: 10.1016/0030-4220(92)90061-t

11. Rojas-Villarraga A, Amaya-Amaya J, Rodriguez-Rodriguez A, Mantilla RD, Anaya JM. Introducing polyautoimmunity: secondary autoimmune diseases no longer exist. *Autoimmune Dis*. (2012) 2012:254319. doi: 10.1155/2012/254319

12. Amador-Patarroyo MJ, Arbelaez JG, Mantilla RD, Rodriguez-Rodriguez A, Cárdenas-Roldán J, Pineda-Tamayo R, et al. Sjögren's syndrome at the crossroad of polyautoimmunity. *J Autoimmun*. (2012) 39:199–205. doi: 10.1016/j.jaut.2012.05.008

13. Zeher M, Horvath IF, Szanto A, Szodoray P. Autoimmune thyroid diseases in a large group of Hungarian patients with primary Sjögren's syndrome. *Thyroid: Off J Am Thyroid Assoc*. (2009) 19:39–45. doi: 10.1089/thy.2007.0398

14. Lazúrová I, Benhatchi K, Rovenský J, Kozáková D, Wagnerová H, Tajtáková M, et al. Autoimmune thyroid disease and autoimmune rheumatic disorders: a two-sided analysis. *Ann New York Acad Sci*. (2009) 1173:211–6. doi: 10.1111/j.1749-6632.2009.04809.x

15. Antonelli A, Ferrari SM, Giuggioli D, Ferrannini E, Ferri C, Fallahi P. Chemokine (C-X-C motif) ligand (CXCL)10 in autoimmune diseases. *Autoimmun Rev*. (2014) 13:272–80. doi: 10.1016/j.autrev.2013.10.010

16. Antonelli A, Ferrari SM, Fallahi P, Frascerra S, Santini E, Franceschini SS, et al. Monokine induced by interferon gamma (IFNgamma) (CXCL9) and IFNgamma inducible T-cell alpha-chemoattractant (CXCL11) involvement in Graves' disease and ophthalmopathy: modulation by peroxisome proliferator-activated receptor-gamma agonists. *J Clin Endocrinol Metab*. (2009) 94:1803–9. doi: 10.1210/jc.2008-2450

17. Mariotti S, del Prete GF, Mastromauro C, de Carli M, Romagnani S, Ricci M, et al. The autoimmune infiltrate of Basedow's disease: analysis of clonal level and comparison with Hashimoto's thyroiditis. *Exp Clin Endocrinol*. (1991) 97:139–46. doi: 10.1055/s-0029-1211053

18. García-López MA, Sancho D, Sánchez-Madrid F, Marazuela M. Thyrocytes from autoimmune thyroid disorders produce the chemokines IP-10 and Mig and attract CXCR3+ lymphocytes. *J Clin Endocrinol Metab*. (2001) 86:5008–16. doi: 10.1210/jcem.86.10.7953

19. Hasegawa H, Inoue A, Kohno M, Muraoka M, Miyazaki T, Terada M, et al. Antagonist of interferon-inducible protein 10/CXCL10 ameliorates the progression of autoimmune sialadenitis in MRL/lpr mice. *Arthritis rheumatism*. (2006) 54:1174–83. doi: 10.1002/art.21745

20. Mendez CE, Shiffermiller JF, Razzeto A, Hannoush Z. Endocrine care for the surgical patient: diabetes mellitus, thyroid and adrenal conditions. *Med Clinics North America*. (2024) 108:1185–200. doi: 10.1016/j.mcna.2024.04.007

21. Aidoo ED, Ababio GK, Arko-Boham B, Tagoe EA, Aryee NA. Thyroid dysfunction among patients assessed by thyroid function tests at a tertiary care hospital: a retrospective study. *Pan Afr Med J*. (2024) 49:7. doi: 10.11604/pamj.2024.49.7.44173

22. Klobučar S, Kenđel Jovanović G, Kryczyk-Kozioł J, Cigrovski Berković M, Vučak Lončar J, Morić N, et al. Association of dietary inflammatory index and thyroid function in patients with hashimoto's thyroiditis: an observational cross-sectional multicenter study. *Medicina (Kaunas Lithuania)*. (2024) 60(9):1454. doi: 10.3390/medicina60091454

23. Majety P, Hennessey JV. Acute and subacute, and riedel's thyroiditis. In: Feingold KR, Anawalt B, Blackman MR, Boyce A, Chrousos G, Corpas E, de Herder WW, Dhatariya K, Dungan K, Hofland J, Kalra S, Kaltsas G, Kapoor N, Koch C, Kopp P, Korbonits M, Kovacs CS, Kuohung W, Laferrère B, Levy M, McGee EA, McLachlan R, New M, Purnell J, Sahay R, Shah AS, Singer F, Sperling MA, Stratakis CA, Trence DL, Wilson DP, editors. *Endotext*. MDText.com, Inc, South Dartmouth (MA (2000).

24. Yamaguchi Y, Okajima F, Sugihara H, Iwabu M, Emoto N. Atypical clinical courses of graves' Disease confound differential diagnosis of hyperthyroidism. *J Nippon Med School = Nippon Ika Daigaku zasshi*. (2024) 91:48–58. doi: 10.1272/jnms.JNMS.2024_91-104

25. Hsieh A, Adelstein S, McLennan SV, Williams PF, Chua EL, Twigg SM. Liver enzyme profile and progression in association with thyroid autoimmunity in Graves' disease. *Endocrinology Diabetes Metab*. (2019) 2:e00086. doi: 10.1002/edm2.86

26. Piantanida E, Ippolito S, Gallo D, Masiello E, Premoli P, Cusini C, et al. The interplay between thyroid and liver: implications for clinical practice. *J endocrinological Invest*. (2020) 43:885–99. doi: 10.1007/s40618-020-01208-6

27. Targher G, Montagnana M, Salvagno G, Moghetti P, Zoppini G, Muggeo M, et al. Association between serum TSH, free T4 and serum liver enzyme activities in a large cohort of unselected outpatients. *Clin Endocrinol*. (2008) 68:481–4. doi: 10.1111/j.1365-2265.2007.03068.x

28. Laycock MA, Pascuzzi RM. The neuromuscular effects of hypothyroidism. *Semin Neurol*. (1991) 11:288–94. doi: 10.1055/s-2008-1041234

29. Kong HJ, Anderson DE, Lee CH, Jang MK, Tamura T, Tailor P, et al. Cutting edge: autoantigen Ro52 is an interferon inducible E3 ligase that ubiquitinates IRF-8 and enhances cytokine expression in macrophages. *J Immunol (Baltimore Md.: 1950)*. (2007) 179:26–30. doi: 10.4049/jimmunol.179.1.26

30. Yoshimi R, Ishigatsubo Y, Ozato K. Autoantigen TRIM21/Ro52 as a possible target for treatment of systemic lupus erythematosus. *Int J Rheumatol*. (2012) 2012:718237. doi: 10.1155/2012/718237

31. Shiboski CH, Shiboski SC, Seror R, Criswell LA, Labetoulle M, Lietman TM, et al. 2016 American college of rheumatology/European league against rheumatism classification criteria for primary Sjögren's syndrome: A consensus and data-Driven methodology involving three international patient cohorts. *Arthritis Rheumatol (Hoboken N.J.)*. (2017) 69:35–45. doi: 10.1002/art.39859

32. Effraimidis G, Wiersinga WM. Mechanisms in endocrinology: autoimmune thyroid disease: old and new players. *Eur J Endocrinol*. (2014) 170:R241–52. doi: 10.1530/eje-14-0047

33. Cruz-Tapias P, Rojas-Villarraga A, Maier-Moore S, Anaya JM. HLA and Sjögren's syndrome susceptibility. A meta-analysis of worldwide studies. *Autoimmun Rev*. (2012) 11:281–7. doi: 10.1016/j.autrev.2011.10.002

34. Panchal M, Gondaliya UB. A study of high sensitive C reactive protein in subclinical hypothyroidism. *Int J Contemp Med, Surg Radiol*. (2019) 4(1):A85–7. doi: 10.21276/ijcmsr.2019.4.1.21

35. Czarnywojtek A, Owecki M, Zgorzalewicz-Stachowiak M, Woliński K, Szczepanek-Parulska E, Budny B, et al. The role of serum C-reactive protein measured by high-sensitive method in thyroid disease. *Archivum immunologiae therapiae experimentalis*. (2014) 62:501–9. doi: 10.1007/s00005-014-0282-1

36. Luppi F, Sebastiani M, Sverzellati N, Cavazza A, Salvarani C, Manfredi A. Lung complications of Sjogren syndrome. *Eur Respir review: an Off J Eur Respir Soc*. (2020) 29(157):200021. doi: 10.1183/16000617.0021-2020

37. Sambataro G, Ferro F, Orlandi M, Sambataro D, Torrisi SE, Quartuccio L, et al. Clinical, morphological features and prognostic factors associated with interstitial lung disease in primary Sjögren's syndrome: A systematic review from the Italian Society of Rheumatology. *Autoimmun Rev*. (2020) 19:102447. doi: 10.1016/j.autrev.2019.102447

38. Wang Y, Jia Y, Qin Y, Feng M, Liang Z, Zhao X, et al. Predicting the risk of interstitial lung disease in patients with primary Sjögren's syndrome: Novel nomogram and elevated Th2 cells. *Mol Immunol*. (2024) 168:25–37. doi: 10.1016/j.molimm.2024.02.008

39. Valjevac S, Hadzovic-Dzuvo A, Valjevac A, Kucukalic-Selimovic E, Lepara O. Assessment of lung dysfunction with spirometry in patients with thyroid disorders. *Acta Inform Med*. (2011) 19(1):16. J.A.I.M.

40. McQuade C, Skugor M, Brennan DM, Hoar B, Stevenson C, Hoogwerf BJ. Hypothyroidism and moderate subclinical hypothyroidism are associated with increased all-cause mortality independent of coronary heart disease risk factors: a PreCIS database study. *Thyroid: Off J Am Thyroid Assoc*. (2011) 21:837–43. doi: 10.1089/thy.2010.0298

41. Churilov LP, Sobolevskaia PA, Stroev YI. Thyroid gland and brain: Enigma of Hashimoto's encephalopathy, Best practice & research. *Clin Endocrinol Metab*. (2019) 33:101364. doi: 10.1016/j.beem.2019.101364

42. Monopoli MP, Raghnaill MN, Loscher JS, O'Sullivan NC, Pangalos MN, Ring RH, et al. Temporal proteomic profile of memory consolidation in the rat hippocampal dentate gyrus. *Proteomics*. (2011) 11:4189–201. doi: 10.1002/pmic.201100072

43. Yoshikawa K, Hatate J, Toratani N, Sugiura S, Shimizu Y, Takahash T, et al. Prevalence of Sjögren's syndrome with dementia in a memory clinic. *J neurological Sci*. (2012) 322:217–21. doi: 10.1016/j.jns.2012.07.060

44. Caselli RJ, Scheithauer BW, Bowles CA, Trenerry MR, Meyer FB, Smigielski JS, et al. The treatable dementia of Sjögren's syndrome. *Ann Neurol*. (1991) 30:98–101. doi: 10.1002/ana.410300117

45. Kawashima N, Shindo R, Kohno M. Primary Sjögren's syndrome with subcortical dementia. *Internal Med (Tokyo Japan)*. (1993) 32:561–4. doi: 10.2169/internalmedicine.32.561

46. Martínez S, Cáceres C, Mataró M, Escudero D, Latorre P, Dávalos A. Is there progressive cognitive dysfunction in Sjögren Syndrome? A preliminary study. *Acta neurologica Scandinavica*. (2010) 122:182–8. doi: 10.1111/j.1600-0404.2009.01293.x

47. Heinrich TW, Grahm G. Hypothyroidism presenting as psychosis: myxedema madness revisited. *Primary Care companion to J Clin Psychiatry*. (2003) 5:260–6. doi: 10.4088/pcc.v05n0603

48. Tan ZS, Beiser A, Vasan RS, Au R, Auerbach S, Kiel DP, et al. Thyroid function and the risk of Alzheimer disease: the Framingham Study. *Arch Internal Med*. (2008) 168:1514–20. doi: 10.1001/archinte.168.14.1514

49. Yoshimasu F, Kokmen E, Hay ID, Beard CM, Offord KP, Kurland LT. The association between Alzheimer's disease and thyroid disease in Rochester, Minnesota. *Neurology*. (1991) 41:1745–7. doi: 10.1212/wnl.41.11.1745

50. Davis JD, Tremont G. Neuropsychiatric aspects of hypothyroidism and treatment reversibility. *Minerva endocrinologica*. (2007) 32:49–65.

51. Joffe RT, Pearce EN, Hennessey JV, Ryan JJ, Stern RA. Subclinical hypothyroidism, mood, and cognition in older adults: a review. *Int J geriatric Psychiatry*. (2013) 28:111–8. doi: 10.1002/gps.3796

52. Samuels MH. Cognitive function in subclinical hypothyroidism. *J Clin Endocrinol Metab*. (2010) 95:3611–3. doi: 10.1210/jc.2010-1242

53. Anyfanti P, Pyrpasopoulou A, Triantafyllou A, Triantafyllou G, Gavriilaki E, Chatzimichailidou S, et al. Association between mental health disorders and sexual dysfunction in patients suffering from rheumatic diseases. *J sexual Med*. (2014) 11:2653–60. doi: 10.1111/jsm.12672

54. Lendrem D, Mitchell S, McMeekin P, Bowman S, Price E, Pease CT, et al. Health-related utility values of patients with primary Sjögren's syndrome and its predictors. *Ann rheumatic Dis*. (2014) 73:1362–8. doi: 10.1136/annrheumdis-2012-202863

55. Westhoff G, Dörner T, Zink A. Fatigue and depression predict physician visits and work disability in women with primary Sjögren's syndrome: results from a cohort study. *Rheumatol (Oxford England)*. (2012) 51:262–9. doi: 10.1093/rheumatology/ker208

56. Lu MC, Jheng CH, Tsai TY, Koo M, Lai NS. Increased dental visits in patients prior to diagnosis of primary Sjögren's syndrome: a population-based study in Taiwan. *Rheumatol Int*. (2014) 34:1555–61. doi: 10.1007/s00296-014-3003-5

57. Olate S, Muñoz D, Neumann S, Pozzer L, Cavalieri-Pereira L, de Moraes M. A descriptive study of the oral status in subjects with Sjögren's syndrome. *Int J Clin Exp Med*. (2014) 7:1140–4.

58. Rostron J, Rogers S, Longman L, Kaney S, Field EA. Health-related quality of life in patients with primary Sjögren's syndrome and xerostomia: a comparative study. *Gerodontology*. (2002) 19:53–9. doi: 10.1111/j.1741-2358.2002.00053.x

59. Bryce C. Persistent night sweats: diagnostic evaluation. *Am Family physician*. (2020) 102:427–33.

60. Maiuolo J, Oppedisano F, Gratteri S, Muscoli C, Mollace V. Regulation of uric acid metabolism and excretion. *Int J Cardiol*. (2016) 213:8–14. doi: 10.1016/j.ijcard.2015.08.109

61. Xing Y, Yang L, Liu J, Ma H. The association with subclinical thyroid dysfunction and uric acid. *Int J Endocrinol*. (2021) 2021:9720618. doi: 10.1155/2021/9720618

62. Ford HC, Lim WC, Chisnall WN, Pearce JM. Renal function and electrolyte levels in hyperthyroidism: urinary protein excretion and the plasma concentrations of urea, creatinine, uric acid, hydrogen ion and electrolytes. *Clin Endocrinol*. (1989) 30:293–301. doi: 10.1111/j.1365-2265.1989.tb02238.x

63. Fukui H, Taniguchi S, Ueta Y, Yoshida A, Ohtahara A, Hisatome I, et al. Enhanced activity of the purine nucleotide cycle of the exercising muscle in patients with hyperthyroidism. *J Clin Endocrinol Metab*. (2001) 86:2205–10. doi: 10.1210/jcem.86.5.7516

64. Yazar A, Döven O, Atis S, Gen R, Pata C, Yazar EE, et al. Systolic pulmonary artery pressure and serum uric acid levels in patients with hyperthyroidism. *Arch Med Res*. (2003) 34:35–40. doi: 10.1016/s0188-4409(02)00457-5

frontiers | Frontiers in Immunology

TYPE Original Research
PUBLISHED 11 December 2024
DOI 10.3389/fimmu.2024.1488220

Check for updates

OPEN ACCESS

EDITED BY
Alessandro Antonelli,
University of Pisa, Italy

REVIEWED BY
Rosario Le Moli,
University of Catania, Italy
Silvia Martina Ferrari,
University of Pisa, Italy
Poupak Fallahi,
University of Pisa, Italy
Sandra Incerpi,
Roma Tre University, Italy

*CORRESPONDENCE
George J. Kahaly
George.kahaly@unimedizin-mainz.de

†These authors share senior authorship

RECEIVED 29 August 2024
ACCEPTED 25 November 2024
PUBLISHED 11 December 2024

CITATION
Luffy M, Ganz A-L, Wagner S, Wolf J, Ropertz J, Zeidan R, Kent JD, Douglas RS and Kahaly GJ (2024) Linsitinib inhibits proliferation and induces apoptosis of both IGF-1R and TSH-R expressing cells. *Front. Immunol.* 15:1488220. doi: 10.3389/fimmu.2024.1488220

COPYRIGHT
© 2024 Luffy, Ganz, Wagner, Wolf, Ropertz, Zeidan, Kent, Douglas and Kahaly. This is an open-access article distributed under the terms of the Creative Commons Attribution License (CC BY). The use, distribution or reproduction in other forums is permitted, provided the original author(s) and the copyright owner(s) are credited and that the original publication in this journal is cited, in accordance with accepted academic practice. No use, distribution or reproduction is permitted which does not comply with these terms.

Linsitinib inhibits proliferation and induces apoptosis of both IGF-1R and TSH-R expressing cells

Maximilian Luffy[1], Anna-Lena Ganz[1], Stefanie Wagner[1], Jan Wolf[1], Julian Ropertz[1], Ryan Zeidan[2], Jeffrey D. Kent[2], Raymond S. Douglas[2†] and George J. Kahaly[1*†]

[1]Molecular Thyroid Research Laboratory, Department of Medicine I, Johannes Gutenberg-University (JGU) Medical Center, Mainz, Germany, [2]Sling Therapeutics, Ann Arbor, MI, United States

Background: The insulin-like growth factor 1 receptor (IGF-1R) and the thyrotropin receptor (TSH-R) are expressed on orbital cells and thyrocytes. These receptors are targeted in autoimmune-induced thyroid eye disease (TED). Effective therapeutic treatment of TED inhibits activation of the IGF-1R/TSH-R complex.

Methods: The inhibitory effect on cell proliferation of a small molecule targeting IGF-1R phosphorylation (Linsitinib) was investigated in an IGF-1R expressing cell line and a Chinese Hamster Ovary (CHO) cell line overexpressing TSH-R. An IGF-1R monoclonal antibody antagonist, Teprotumumab served as control. Both cell lines were plated in a 96-well format and treated with both compounds for 24 hours. After addition of tetrazolium, absorbance was measured. The apoptosis marker caspase-3/7 activity was measured. The half-maximal inhibitory concentration (IC_{50}) of TSH-R-Ab induced stimulation (stimulatory monoclonal antibody, mAb, M22) of the TSH-R cell line was evaluated with a cell-based bioassay for blocking TSH-R-Ab. Cells were treated with ten rising concentrations of either Linsitinib, Linsitinib + Metformin, Teprotumumab, or a blocking TSH-R mAb (K1-70).

Results: Linsitinib strongly inhibited the proliferation of both cell lines at several concentrations: 31,612.5 ng/mL (IGF-1R cell line -78%, P=0.0031, TSH-R cell line -75%, P=0.0059), and at 63,225 ng/mL (IGF-1R cell line -73%, P=0.0073, TSH-R cell line -73%, P=0.0108). Linsitinib induced apoptosis of both cell lines, both morphologically confirmed and with an increased caspase-3/7 activity at concentrations of 31,612.5 ng/mL (IGF-1R cell line P=0.0158, TSH-R cell line P=0.0048) and 63,225 ng/mL (IGF-1R cell line P=0.0005, TSH-R cell line P=0.0020). Linsitinib markedly inhibited proliferation of the IGF-1R cell line at all concentrations compared to Teprotumumab (P=0.0286). Teprotumumab inhibition was significant only at 15,806.25 ng/mL with the TSH-R cell line (-15%, P=0.0396). In addition, in the TSH-R-Ab blocking bioassay, Linsitinib and the tested compounds demonstrated strong inhibition across all ten dilutions (100%).

Conclusions: Linsitinib effectively induces apoptosis and inhibits proliferation of both IGF-1R and TSH-R expressing target cells, therefore demonstrating its therapeutic potential to block the reported crosstalk of the two mediators in autoimmune TED.

KEYWORDS

Linsitinib, small molecule kinase inhibitor, insulin-like growth factor 1 receptor, thyrotropin receptor, thyroid eye disease, apoptosis, cell proliferation, cell-based bioassays

1 Introduction

The Graves' disease (GD) specific autoantigen thyrotropin receptor (TSH-R) and the insulin-like growth factor 1 receptor (IGF-1R) are molecular targets on both thyrocytes and orbital fibroblasts (1, 2) playing pivotal roles in the pathogenesis of GD and thyroid eye disease (TED) (3, 4). Both the TSH-R and IGF-1R form a physical and functional signaling complex in orbital fibroblasts upon binding of TSH-R autoantibodies to the TSH-R, facilitating receptor crosstalk (5–7). Signaling through this protein complex leads to subsequent expansion of orbital fat and muscle (8), illustrating its role in TED (9, 10). Importantly, pathogenic signaling at either receptor relies on IGF-1R activity, supporting receptor crosstalk and potential TSH-R transactivation of IGF-1R (7). Several therapeutic compounds were investigated to block crosstalk in TED, with IGF-1R being a key target for managing the disease (11, 12).

The IGF-1R functions as an integral membrane receptor and belongs to the tyrosine kinase family (12, 13). Structurally, IGF-1R is a heterotetramer consisting of two α and β subunits linked by disulfide bonds (12). The extracellular ligand-binding domains are located in the α subunits, while the β subunits contain the tyrosine kinase domain, which is crucial for signaling (7). Binding of ligands IGF-1 and IGF-2 to the receptor stimulates intrinsic tyrosine kinase activity, leading to auto phosphorylation and activation of signaling cascades that enhance cell growth, proliferation, and apoptosis modulation through protein kinase B (AKT) and extracellular-signal regulated kinase (ERK) pathways (14–17).

Linsitinib, also known as OSI-906, is a selective small molecule inhibitor of IGF-1R and to a lesser extent insulin receptor (IR) (18). Its selectivity derives from its unique binding mode to both receptors (18), showing over a 100-fold selectivity compared to more than 100 other kinases (19). Linsitinib demonstrates potent activity and favorable pharmacokinetic properties, with bioavailability exceeding 60% in various pre-clinical species, including mouse, rat, dog, and monkey (16). This small molecule, administered orally, has been tested within a phase 2b randomized, double-masked study in patients with clinically active and severe TED (NCT05276063).

In the present pre-clinical study, for the first time the inhibitory effects of Linsitinib on cell proliferation and apoptosis were investigated in both IGF-1R and TSH-R expressing cell lines. Teprotumumab, a fully human monoclonal antibody (mAb) targeting the IGF-1R, served as control. In addition, the half-maximal inhibitory concentration (IC_{50}) of TSH-R-Ab induced stimulation in the TSH-R cell line was evaluated using a cell-based bioassay for blocking TSH-R-Ab, comparing the IC_{50} of Linsitinib to Linsitinib + Metformin, Teprotumumab, and a blocking TSH-R mAb (K1-70). Combined treatment Linsitinib + Metformin was included to evaluate potential synergistic effects, as Metformin modulates key signaling pathways targeted by Linsitinib.

Abbreviations: Ab, Antibody; AKT, Protein kinase B; ATP, Adenosine triphosphate; CHO, Chinese hamster ovary; EC_{80}, 80% effective concentration; ERK, Extracellular-signal regulated kinase; IC_{50}, Half-maximal inhibitory concentration; IGF-1, Insulin-like growth factor 1; IGF-1R, Insulin-like growth factor 1 receptor; IGF-2, Insulin-like growth factor 2; MAb, Monoclonal Antibody; Mdm2, Mouse double minute 2 homolog; MTOR, Mammalian target of rapamycin; RB, Reaction buffer; RLU, Relative light units; Rpm, Rounds per minute; SRR%, Specimen to reference ratio %; TBI, Thyroid blocking immunoglobulins; TED, Thyroid eye disease; TSH, Thyrotropin; TSH-R, Thyrotropin receptor; TSH-R-Ab, Thyrotropin receptor antibodies; TSI, Thyroid stimulating immunoglobulins.

2 Materials and methods

2.1 Cell proliferation assay

2.1.1 Cell lines and cell culture

The human IGF-1R expressing tumor cell line NCI-H295R (ATCC, Manassas, VA, USA), isolated from the adrenal gland of a patient with adrenal cancer, grows primarily adherent as a monolayer and in suspension. This cell line was continuously cultured in 75 cm^2 flasks containing 25 mL DMEM: F12 base medium from ATCC under aseptic conditions. This growth medium was supplemented with 0.00625 mg/mL insulin, 0.00625 mg/mL transferrin, 6.25 ng/mL selenium, 1.25 mg/mL bovine serum albumin and 0.00535 mg/mL linoleic acid in the form of ITS+ Premix from Corning (Corning, NY, USA), along with a final

concentration of 2.5% Nu-Serum (Corning) containing newborn calf serum, epidermal growth factor, endothelial cell growth supplement, insulin and transferrin. The medium was changed three times per week to maintain high cell quality. The medium from the culture flask was dispensed into two 15 mL falcon tubes and 25 mL of fresh DMEM: F12 medium was added to the culture flask. The falcon tubes were centrifuged at 700 rpm for 5 minutes to obtain a cell pellet, allowing the retrieval of cells in suspension. After resuspension of the cell pellet in 1 mL of fresh DMEM: F12 medium, the cells were transferred back into the culture flask. Cultivation was continued in an incubator at 37°C with 5% CO_2.

The Chinese Hamster Ovary (CHO) cell line overexpressing the TSH-R (QuidelOrtho, San Diego, CA, USA), was thawed immediately before seeding for the proliferation assay and subsequently incubated in the DMEM: F12 medium under the same conditions as the IGF-1R expressing cell line.

2.1.2 Assay protocol

The Cell Proliferation Assay (Promega, Madison, WI, USA) is a colorimetric method using a tetrazolium compound (MTS) for determining the number of viable cells. The assay procedure (Supplementary Figure 1) extends over three days and was conducted under aseptic conditions. Upon reaching a minimum of 80% confluence, the IGF-1R expressing cell line was detached from the culture flask using 3 mL of Trypsin-EDTA (PAN Biotech, Aidenbach, Germany) solution for 10 minutes. The resulting cell suspension, supplemented with 8 mL of complete growth medium, was transferred to a falcon tube and spun at 700 rpm for 5 minutes to obtain a cell pellet. Following resuspension of the cell pellet in 1 mL of fresh DMEM: F12 medium, cell counting was performed using Acridine Orange (Logos Biosystems, Anyang-si, South Korea) to prepare a cell suspension containing 200,000 cells. Subsequently, 100 µL of the cell suspension containing the IGF-1R cell line was pipetted into each of the 20 inner wells in quadruplicate of a 96-well test plate (10,000 cells/well). Similarly, the TSH-R cell line was thawed using a 37°C water bath, mixed with 5 mL of DMEM: F12 medium and 100 µL of the resulting cell suspension was pipetted into each of the 20 inner wells in quadruplicate of the test plate (10,000 cells/well) alongside the IGF-1R cell line (Supplementary Figure 2). For the blank control, 100 µL of DMEM: F12 medium was pipetted in quadruplicate into the wells. The test plate was cultivated for 24 hours in an incubator at 37°C with 5% CO_2.

On the second day, a dilution series with four (n=4) rising concentrations (7,903.125 ng/mL, 15,806.25 ng/mL, 31,612.5 ng/mL and 63,225 ng/mL) of Linsitinib (Sling Therapeutics, Ann Arbor, MI, USA) or Teprotumumab (BioVision, Milpitas, CA, USA), as well as a 1:11 dilution in complete DMEM: F12 medium, was prepared for cell treatment. These concentrations were selected based on pre-experimental data, which demonstrated the most significant inhibition. Subsequently, the contents of the test plate were discarded and 100 µL of fresh DMEM: F12 medium was transferred to each well. Afterward, 100 µL of each Linsitinib or Teprotumumab sample were transferred into the wells according to the pipetting scheme (Supplementary Figure 2). The incubation of the test plate was continued for an additional 24 hours in an incubator at 37°C with 5% CO_2.

Morphological changes were microscopically examined in each well on the third day at a magnification of 100x. Subsequently, a tetrazolium compound from Promega was thawed in a 37°C water bath for 10 minutes. Afterward, 40 µL of the tetrazolium reagent was added to each well of the test plate containing the samples in 200 µL of medium. The test plate was incubated for 4 hours in an incubator at 37°C with 5% CO_2, after which the absorbance of each sample was recorded at 490 nm (GloMax luminometer, Promega).

2.2 Caspase-Glo® 3/7 Assay (apoptosis)

2.2.1 Assay protocol

The Caspase-Glo® 3/7 Assay (Madison, WI, USA) measures activities of caspase-3 and -7 as apoptosis marker. The assay was conducted under the same conditions and followed the same general procedure as the proliferation assay. The main differences are outlined below.

Day 2: After discarding the contents of the test plate, 50 µL (instead of 100 µL) of each Linsitinib or Teprotumumab sample was transferred to 50 µL (instead of 100 µL) of fresh DMEM: F12 medium in the wells according to the pipetting scheme (Supplementary Figure 2).

Day 3: Morphological changes were microscopically examined in each well at a magnification of 100x. Subsequently, the caspase buffer was thawed in a 37°C water bath for 10 minutes and the caspase substrate was stored until use at room temperature. The thawed buffer was transferred to the bottle containing substrate and mixed. Afterward, 100 µL of the mixed caspase reagent was added to each well of the test plate containing the samples in 100 µL of medium. Following this, the contents of the wells were mixed using a plate shaker at 300 rpm for 30 seconds. The test plate was incubated for 30 minutes at room temperature protected from light, after which the luminescence of each sample was recorded (GloMax luminometer, Promega).

2.3 TSH-R-Ab bioassays

2.3.1 Testing of M22

The 80% effective concentration (EC_{80}) of the stimulatory mAb M22 (RSR, Cardiff, UK) was determined using a FDA-cleared cell-based stimulating TSH-R-Ab (TSI) bioassay (Thyretain, QuidelOrtho). The bioassay was performed as previously described (20, 21).

In detail, on the first day, the TSH-R cell line was thawed using a 37°C water bath and mixed with 5 mL of growth medium. Subsequently, 100 µL of the cell suspension was pipetted into each of the 48 inner wells of a 96-well plate (10,000 cells/well) pre-coated with Cell Attachment Solution under laminar flow conditions. The cells were grown for 15 to 18 hours to a confluent monolayer in an incubator at 37°C with 5% CO_2.

On the second day, a dilution series of M22, testing ten (n=10) rising concentrations (0.1420 – 18.1818 ng/mL), as well as a 1:11 dilution in Reaction Buffer (RB), was prepared in test tubes for subsequent cell treatment. In addition, TSI positive, reference and normal controls were diluted 1:11 in RB. For the 1:11 dilutions, 40 µL of the sample/control was mixed with 400 µL of RB. Subsequently, 100 µL of each M22 and control sample was pipetted in duplicate into the test plate according to the pipetting scheme (Supplementary Figure 3). The test plate was then incubated for 3 hours at 37°C with 5% CO_2. After incubation, the contents of the wells were discarded and 75 µL of luciferase solution was added to each well. The test plate was incubated protected from light for 10 minutes, following which luciferase levels in each well were measured using a luminometer (Tecan, Männedorf, Zürich, Switzerland). The recorded relative light units (RLU) were converted to percentage of specimen-to-reference ratio (SRR %) with a cut-off of ≥ 140 SRR percentage (22, 23).

2.3.2 Compound testing

Next, the IC_{50} of TSH-R-Ab induced stimulation by M22 of the TSH-R cell line was evaluated with a FDA-cleared cell-based blocking TSH-R-Ab (TBI) bioassay (Thyretain, QuidelOrtho). IC_{50} values for Linsitinib, Linsitinib + Metformin, Teprotumumab and a blocking TSH-R mAb (K1-70, RSR, Cardiff, Wales, UK) were determined using this blocking bioassay (24–26).

On the first day, the TSH-R cell line was thawed using a 37°C water bath and mixed with 5 mL of growth medium. Afterward, 100 µL of the cell suspension containing 10,000 cells per well was pipetted into each of the 48 inner wells of a 96-well plate pre-coated with Cell Attachment Solution under laminar flow conditions. The cells were incubated at 37°C with 5% CO_2 for 15 to 18 hours until confluent growth.

On the second day, a dilution series encompassing ten (n=10) rising concentrations of each compound, along with a 1:11 dilution in RB, was prepared for cell treatment. In addition, TBI positive, reference and negative controls were diluted 1:11 in RB and included in each test plate. For the 1:11 dilutions, 30 µL of the sample/control were mixed with 300 µL of RB. Subsequently, the TSH-R cells were initially treated with 100 µL of each compound and control sample in duplicate (Supplementary Figure 4) for 1 hour, followed by 2 hours of stimulation with the previously determined double EC_{80} concentration of M22. Afterward, the contents of the wells were discarded and 75 µL of luciferase solution were transferred to each well. The test plate was incubated protected from light for 10 minutes, after which luciferase levels in each well were recorded using the Tecan luminometer. The measured RLU were reported as percent inhibition of luciferase expression relative to induction with bovine TSH alone, with a cut-off of ≥ 34%.

2.4 Statistical analysis

Statistical analysis was carried out using GraphPad Prism software version 9.5.1 (GraphPad Software, Boston, Massachusetts, USA) and/or the GraphPad QuickCalcs Web site: https://www.graphpad.com/quickcalcs/Ecanything1.cfm. P-values for statistical comparisons of each concentration relative to the control in the Cell Proliferation Assay as well as in the Caspase-Glo® 3/7 Assay were calculated using Kruskal-Wallis test followed by Dunnett's multiple comparisons test. The data are expressed as the fold change relative to the control.

P-values for statistical comparisons of Linsitinib versus Teprotumumab in the Cell Proliferation Assay of the IGF-1R expressing cell line were calculated using the two-tailed Mann-Whitney test. The statistical significance was defined as $p < 0.05$.

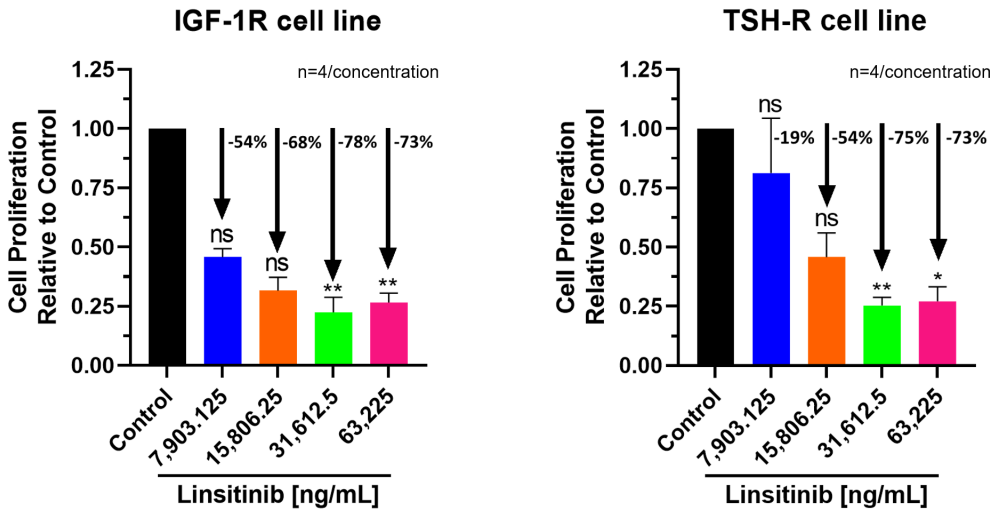

FIGURE 1
Cell Proliferation Assay of Linsitinib in both IGF-1R and TSH-R cell lines. In the IGF-1R cell line, inhibition ranged from 54 to 78% compared to control, while in the TSH-R cell line, inhibition ranged from 19 to 75%. Significant inhibition was observed at concentrations of 31,612.5 ng/mL (IGF-1R cell line -78%, P=0.0031, TSH-R cell line -75%, P=0.0059), and 63,225 ng/mL (IGF-1R cells -73%, P=0.0073, TSH-R cells -73%, P=0.0108). At lower concentrations (7,903.125 ng/mL or 15,806.25 ng/mL), milder inhibition was noted in both cell lines. Each concentration of Linsitinib was tested in quadruplicate (n=4). ns means P > 0.05. * means P ≤ 0.05, ** means P ≤ 0.01.

10.3389/fimmu.2024.1488220

Data of the TSH-R-Ab assays were visualized in dose-response curves to determine EC/IC.

3 Results

3.1 Cell proliferation assay

Similar, highly significant and marked inhibitory effects of Linsitinib were noted for both IGF-1R and TSH-R expressing cell lines. In the IGF-1R cell line, inhibition ranged from 54 to 78% compared to control, while in the TSH-R cell line, inhibition ranged from 19 to 75% (Figure 1). Specifically, substantial inhibition of proliferation was observed at the following Linsitinib concentrations: 31,612.5 ng/mL (IGF-1R cell line -78%, P=0.0031, TSH-R cell line -75%, P=0.0059), and 63,225 ng/mL (IGF-1R cells -73%, P=0.0073, TSH-R cells -73%, P=0.0108). At lower concentrations (7,903.125 ng/mL or 15,806.25 ng/mL), milder inhibition was noted in both cell lines.

Linsitinib induced a microscopically and morphologically confirmed decrease in proliferation across all concentrations,

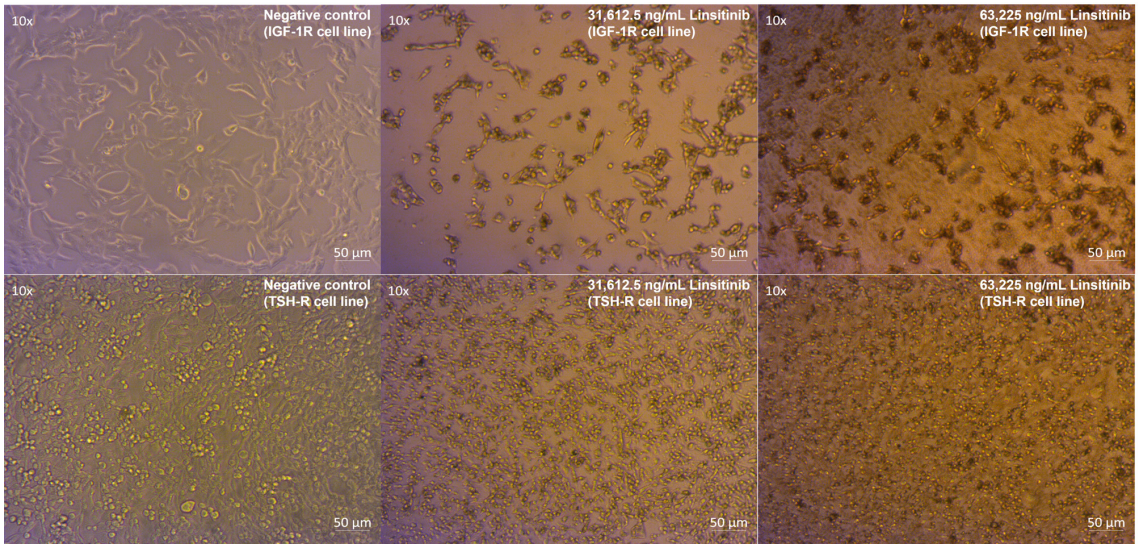

FIGURE 2
Linsitinib markedly decreases proliferation and induces apoptosis in both IGF-1R and TSH-R cell lines.

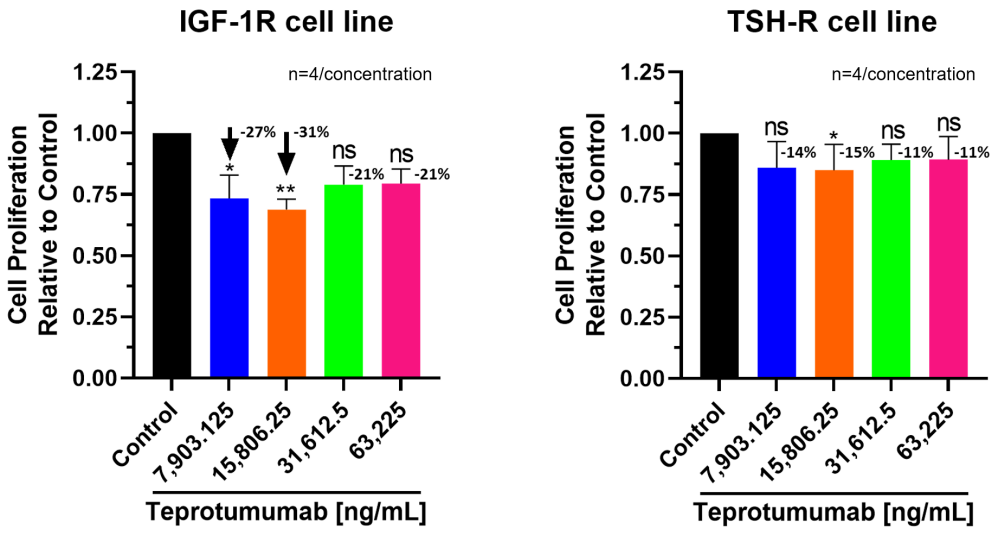

FIGURE 3
Cell Proliferation Assay of Teprotumumab in both IGF-1R and TSH-R cell lines. In the IGF-1R cell line, inhibition ranged from 21 to 31% compared to control, while in the TSH-R cell line, inhibition ranged from 11 to 15%. Teprotumumab demonstrated significant inhibition of proliferation at 7,903.125 ng/mL (-27%, P=0.0278) and 15,806.25 ng/mL (-31%, P=0.0059) of the IGF-1R cell line, while it was significant only at 15,806.25 ng/mL with the TSH-R cell line (-15%, P=0.0396). Each concentration of Teprotumumab was tested in quadruplicate (n=4). ns means P > 0.05. * means P ≤ 0.05, ** means P ≤ 0.01.

occurring at low (7,903.125 ng/mL) and moderate (15,806.25 ng/mL) concentrations over 24-hour treatment of both cell lines (Zeiss Microscopy, Göttingen, Germany). This inhibitory effect was increased at higher concentrations (31,612.5 ng/mL and 63,225 ng/mL) in both cell lines compared to control (Figure 2).

Compared to control, inhibition of proliferation by Teprotumumab ranged from 21 to 31% in the IGF-1R and from 11 to 15% in the TSH-R cell line (Figure 3). Teprotumumab demonstrated significant inhibition of proliferation at 7,903.125 ng/mL (-27%, P=0.0278) and 15,806.25 ng/mL (-31%, P=0.0059) of the IGF-1R cell line, while it was significant only at 15,806.25 ng/mL with the TSH-R cell line (-15%, P=0.0396). No morphological changes in proliferation were observed with Teprotumumab across all tested concentrations in both cell lines (Figure 4). Compared to Teprotumumab, Linsitinib inhibited the proliferation of the IGF-1R cell line markedly more at all concentrations (Linsitinib versus Teprotumumab, P=0.0286, Figure 5).

3.2 Caspase-Glo® 3/7 Assay (apoptosis)

Linsitinib significantly increased caspase-3/7 activity in both IGF-1R and TSH-R cell lines. The caspase-3/7 activity ranged from +2.75 to +6.68 relative to control in the IGF-1R cell line and from +2.75 to +5.75 relative to control in the TSH-R cell line (Figure 6). Specifically, Linsitinib markedly increased caspase-3/7 activity at concentrations of 31,612.5 ng/mL (IGF-1R cell line +6.24 relative to control, P=0.0158, TSH-R cell line +5.53 relative to control, P=0.0048) and 63,225 ng/mL (IGF-1R cell line +6.68 relative to control, P=0.0005, TSH-R cell line +5.75 relative to control,

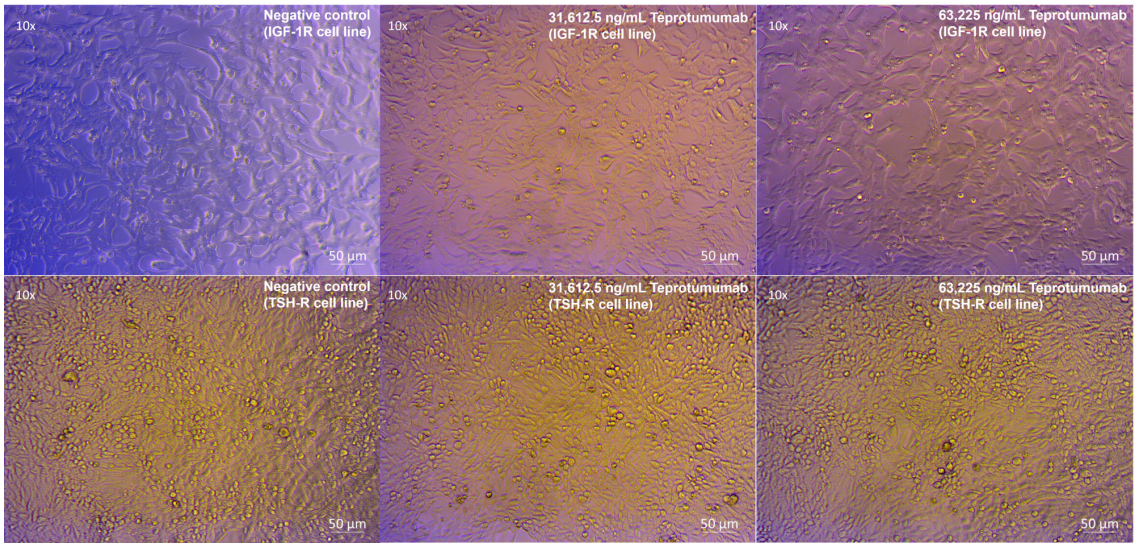

FIGURE 4
No morphological changes in IGF-1R and TSH-R cell lines following incubation with Teprotumumab, compared to control.

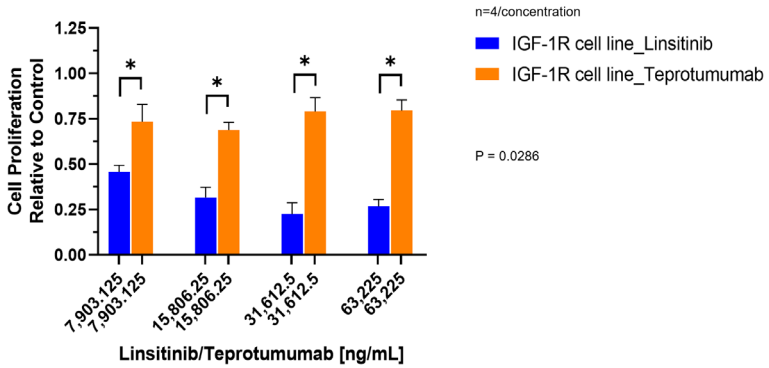

FIGURE 5
Comparison of Linsitinib and Teprotumumab effects on Cell Proliferation in the IGF-1R cell line. Compared to Teprotumumab, Linsitinib inhibited the proliferation of the IGF-1R cell line markedly more at all concentrations (Linsitinib versus Teprotumumab, P=0.0286). Each concentration of Linsitinib and Teprotumumab was tested in quadruplicate (n=4). * means $P \leq 0.05$.

10.3389/fimmu.2024.1488220

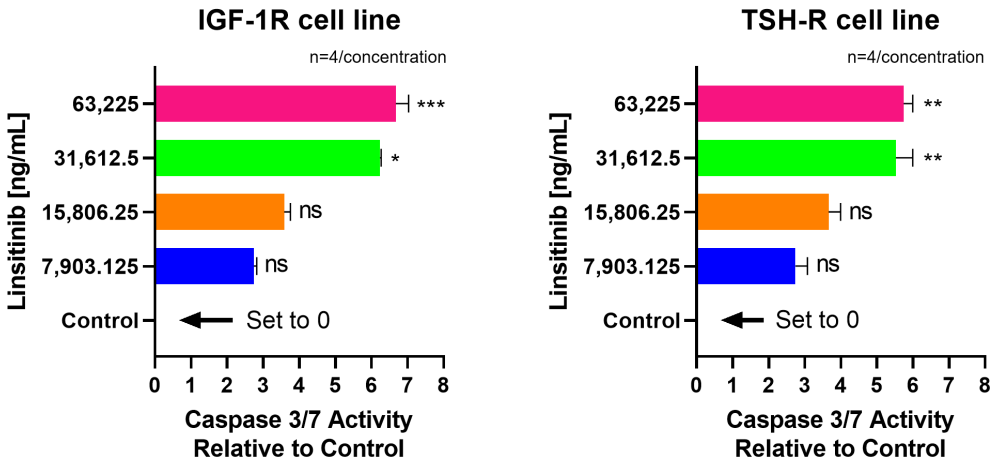

FIGURE 6
Effect of Linsitinib on Caspase-3/7 Activity in IGF-1R and TSH-R cell lines. In the IGF-1R cell line, caspase-3/7 activity ranged from +2.75 to +6.68 relative to control, while in the TSH-R cell line, caspase-3/7 activity ranged from +2.75 to +5.75 relative to control. Specifically, Linsitinib markedly increased caspase-3/7 activity at concentrations of 31,612.5 ng/mL (IGF-1R cell line +6.24 relative to control, P=0.0158, TSH-R cell line +5.53 relative to control, P=0.0048) and 63,225 ng/mL (IGF-1R cell line +6.68 relative to control, P=0.0005, TSH-R cell line +5.75 relative to control, P=0.0020). At lower concentrations (7,903.125 ng/mL and 15,806.25 ng/mL), no significant increase in caspase-3/7 activity was observed in either cell line. Each concentration of Linsitinib was tested in quadruplicate (n=4). ns means P > 0.05. * means P ≤ 0.05, ** means P ≤ 0.01, *** means P ≤ 0.001.

P=0.0020). At lower concentrations (7,903.125 ng/mL and 15,806.25 ng/mL), no significant increase in caspase-3/7 activity was observed in either cell line. In contrast, Teprotumumab did not significantly increase caspase-3/7 activity across all tested concentrations in both cell lines. Caspase-3/7 activity ranged from -0.03 to +0.01 relative to control in the IGF-1R cell line and from -0.05 to +0.01 relative to control in the TSH-R cell line (Figure 7).

3.3 TSH-R-Ab bioassays

In the cell-based TSI bioassay testing M22, seven out of 10 (70%) samples are positive, with their SRR percentage ranging from 158 to 238% (Figure 8). An EC_{80} of 1.82 ng/mL of M22 was observed. In the TBI blocking bioassay, all tested compounds demonstrated strong inhibition (100%) across all ten dilutions after induced stimulation by the previously determined double EC_{80} concentration of M22 (3.64 ng/mL). Linsitinib inhibition ranged from 74 to 94%, showing potent effects already at low concentrations (Figure 9), with an IC_{50} of 147.1 ng/mL. Notably, five out of 10 (50%) samples demonstrated inhibition ≥ 90%. Addition of Metformin to Linsitinib did not lower the IC_{50}. Teprotumumab showed an IC_{50} of 160.6 ng/mL, with inhibition ranging from 69 to 94% (Figure 10). Highest positivity was registered at high concentrations of 181.81 ng/mL (93%) and 363.63 ng/mL (94%), respectively. As anticipated, the TSH-R

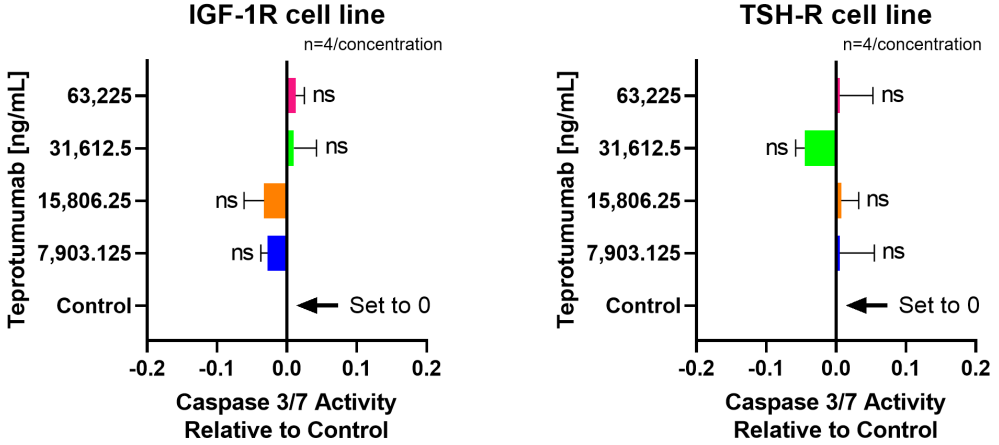

FIGURE 7
No effect of Teprotumumab on Caspase-3/7 Activity across all tested concentrations in IGF-1R and TSH-R cell lines. Caspase-3/7 activity ranged from -0.03 to +0.01 relative to control in the IGF-1R cell line and from -0.05 to +0.01 relative to control in the TSH-R cell line. Each concentration of Teprotumumab was tested in quadruplicate (n=4). ns means P > 0.05.

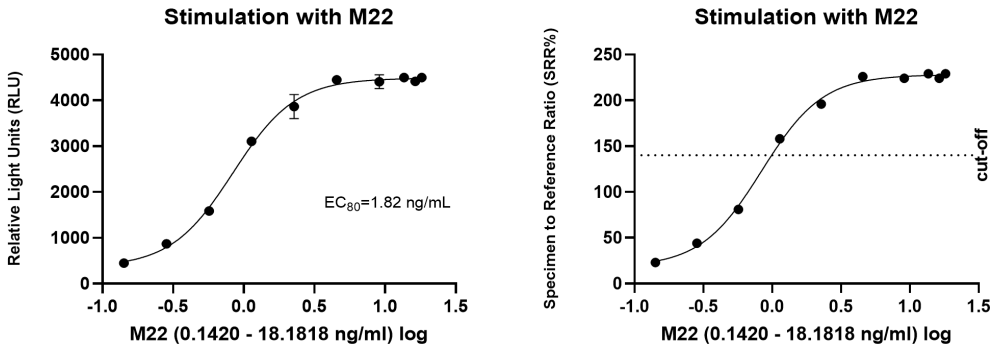

FIGURE 8
Dose-response curves for M22 in cell-based Thyretain TSH-R-Ab Stimulating (TSI) bioassay. An EC_{80} of 1.82 ng/mL of M22 was observed. Ten (n=10) rising concentrations of M22 were tested. The recorded relative light units (RLU) were converted to percentage of specimen-to-reference ratio (SRR %) with a cut-off of ≥ 140 SRR percentage.

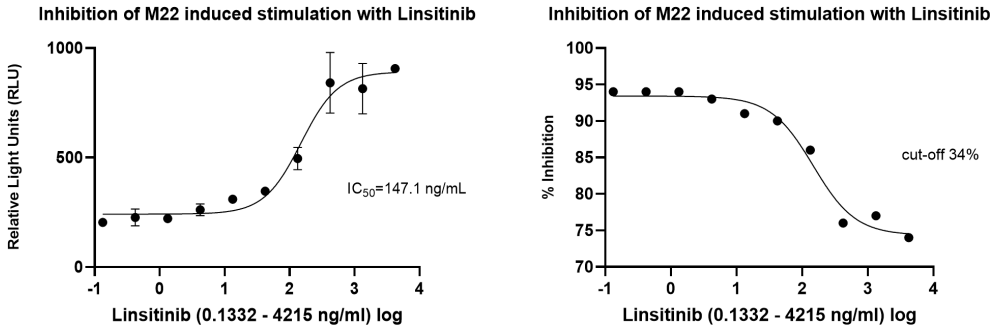

FIGURE 9
Dose-response curves for Linsitinib in cell-based Thyretain TSH-R-Ab Blocking (TBI) bioassay. An IC_{50} of 147.1 ng/mL of Linsitinib was observed. Ten (n=10) rising concentrations of Linsitinib were tested. The recorded relative light units (RLU) were reported as percent inhibition with a cut-off of ≥ 34%.

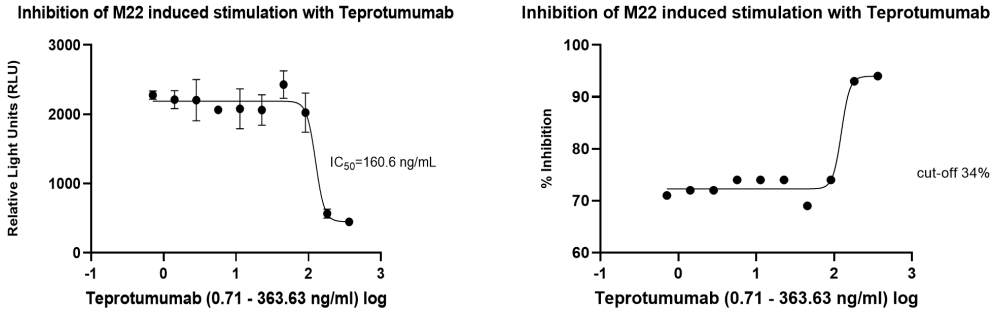

FIGURE 10
Dose-response curves for Teprotumumab in the cell-based TSH-R-Ab Blocking (TBI) bioassay. Teprotumumab showed an IC_{50} of 160.6 ng/mL. Ten (n=10) rising concentrations of Teprotumumab were tested. The recorded relative light units (RLU) were reported as percent inhibition with a cut-off of ≥ 34%.

blocking mAb K1-70 had the lowest IC_{50} of 20.57 ng/mL and demonstrated strong inhibition (98%) at high concentrations. In addition, four out of 10 (40%) samples showed inhibition ≥ 90% (Supplementary Figure 5).

4 Discussion

This pre-clinical study demonstrated for the first time, the potent inhibitory effect of the small molecule IGF-1R inhibitor

Linsitinib on both IGF-1R and TSH-R expressing cell lines. Both qualitative morphological relevant changes of the cultured cells were registered as well as a quantitatively marked and highly significant inhibition of cell proliferation. In addition, Linsitinib strongly induced apoptosis of both IGF-1R and TSH-R expressing cells. Furthermore, potent inhibition of M22-induced stimulation with Linsitinib was observed in a cell-based blocking TBI bioassay, with an IC_{50} comparable to that of Teprotumumab. Beta arrestin 1 may also mediate the dual inhibitory effect of Linsitinib on both cell lines, which scaffolds the reported crosstalk between the two major receptors in TED. Subsequent to binding of the small molecule Linsitinib to the ß subunit (ATP-binding domain) of the IGF-1 tyrosine kinase receptor, ß-arrestin 1 is recruited. Beta arrestin promotes binding of the E3 ubiquitin ligase Mouse double minute 2 homolog (Mdm2) to the IGF-1R. Subsequently, ubiquitination induces proteosomal degradation of the IGF-1R. Beta arrestin 1 also modulates the ERK signaling pathway. In comparison, monoclonal antibodies e.g. Teprotumumab particularly inhibit the PI3K/AKT signaling pathway. Overall, the pivotal role of ß-arrestin in mediating the reported crosstalk between both key receptors requires further investigation to assess its contribution to the dual inhibitory effect of Linsitinib.

In other words, these findings suggest that Linsitinib inhibits not only IGF-1R and TSH-R but also the crosstalk between these two key players. In line with our data, Linsitinib strongly inhibited TSH-R/IGF-1R crosstalk in TED fibroblasts, evidenced by the suppression of M22 mAb-stimulated hyaluronic acid secretion (27), hence highlighting its potential as a promising treatment for TED.

Linsitinib is a potent dual ATP-competitive kinase inhibitor of IGF-1R as well as IR (16, 19) and binds to the intracellular ATP-binding site of the kinase domain in an ATP-competitive fashion (18). This inhibition prevents the auto phosphorylation of the activation loop in the kinase domain, thereby blocking ligand-dependent activation of IGF-1R by IGF-1 and IGF-2 (16). Linsitinib has demonstrated antitumor activity, showing therapeutically efficacy across multiple pre-clinical tumor models (18, 28). Specifically, OSI-906-treated colorectal cancer xenografts exhibited decreased tumor growth and increased apoptosis in both *in vivo* and *in vitro* studies (29). Linsitinib's inhibitory effects on cell growth were also highlighted in the human H295R cell line, which overexpresses the IGF-1R, and in the genetically identical HAC15 cell line, alone and in combination with mammalian target of rapamycin (mTOR) inhibitors (28). In addition, Linsitinib inhibited the proliferation of human adrenocortical carcinoma cell lines *in vitro* at lower concentrations than *in vivo* in humans (28). In hepatocellular carcinoma cell lines, OSI-906 reduced proliferation by at least 40% (30). Of note, Linsitinib has already reached clinical investigation and was tested in a phase III clinical trial (NCT00924989) for both patients with locally advanced adrenocortical carcinoma (31) as well as with advanced cell lung cancer (32).

Pertaining to its potential role in autoimmune endocrine and/or thyroidal disease, Linsitinib effectively prevented autoimmune hyperthyroidism in its early stages in an animal model and demonstrated a dose-dependent reduction in orbital adipogenesis (15). Furthermore, Linsitinib blocked bone marrow activation, inhibiting progression of TED, by reducing proinflammatory cytokines and inflammation in a mouse model (33).

Compared to Linsitinib, anti-IGF-1R monoclonal antibodies, such as Teprotumumab, target the cysteine-rich region of the IGF-1R extracellular domain with high-affinity and specificity (34). By binding to this extracellular region, Teprotumumab effectively blocks the binding pocket of the receptor, thereby preventing ligand-induced activation of downstream signaling pathways including AKT and ERK (16, 34). As previously mentioned, the anti-IGF-1R small molecules e.g. Linsitinib and monoclonal antibodies i.e. Teprotumumab use different blocking mechanisms: Linsitinib targets the intracellular while Teprotumumab targets the extracellular domain of the IGF-1R. Further experiments are of course warranted and foreseen to explore and confirm the novel and challenging findings of a markedly stronger inhibition of cell proliferation and an exclusive Linsitinib-induced apoptosis of both IGF-1R and TSH-R expressing cells. Noteworthy, the relevant function of β-arrestin 1, which can be modulated by other small molecules (35), should also be looked at.

Several current limitations of this pre-clinical study should be discussed. The experiments were conducted on cell lines, only. A larger sample size is being tested to confirm the robustness and reproducibility of the presented results. In addition, experiments with cultured primary human cells, e.g. orbital target cells (fibroblasts, pre-adipocytes, etc.) are ongoing to enhance the relevance of the results. Furthermore, ongoing experiments are assessing the toxicity of Linsitinib and Teprotumumab in both IGF-1R and TSH-R-expressing cells as well as in human orbital fibroblasts.

In the cell-based blocking TSHR-Ab bioassay, combined treatment with Linsitinib + Metformin was included to evaluate potential synergistic effects. Metformin is known to modulate IGF-1R downstream signaling pathways also targeted by Linsitinib. In this bioassay, we used a cell line overexpressing TSH-R, with much lower expression of IGF-1R, which may explain the lack of Metformin's effect in this study. Additionally, the response to Metformin is highly dependent on glucose conditions. Metformin shows stronger inhibitory effects under low or physiological glucose levels. Future experiments will test Linsitinib + Metformin combination in low-glucose medium to evaluate Metformin's additive effects.

In conclusion, Linsitinib's potent induction of apoptosis and inhibition of proliferation in IGF-1R and TSH-R expressing cells highlights its promising therapeutic potential for effectively managing TED.

Author's note

The cell lines present in this study were obtained from [ATCC, American Type Culture Collection, Manassas, VA, USA] for the IGF-1R cell line, and from [QuidelOrtho, San Diego, CA, USA] for the TSH-R cell line.

Data availability statement

The original contributions presented in the study are included in the article/Supplementary Material. Further inquiries can be directed to the corresponding author.

Ethics statement

Ethical approval was not required for the studies on humans in accordance with the local legislation and institutional requirements because only commercially available established cell lines were used. Ethical approval was not required for the studies on animals in accordance with the local legislation and institutional requirements because only commercially available established cell lines were used.

Author contributions

ML: Conceptualization, Data curation, Formal analysis, Investigation, Methodology, Visualization, Writing – original draft, Writing – review & editing. A-LG: Investigation, Methodology, Writing – review & editing. SW: Investigation, Methodology, Writing – review & editing. JW: Conceptualization, Data curation, Formal analysis, Validation, Writing – review & editing. JR: Investigation, Methodology, Writing – review & editing. RZ: Writing – review & editing, Funding acquisition, Resources. JK: Writing – review & editing, Funding acquisition, Resources. RD: Writing – review & editing, Data curation, Formal analysis, Funding acquisition, Resources. GK: Conceptualization, Data curation, Formal analysis, Funding acquisition, Project administration, Resources, Supervision, Validation, Writing – original draft, Writing – review & editing, Investigation.

Funding

The author(s) declare financial support was received for the research, authorship, and/or publication of this article. The JGU Medical Center receives research-associated funding from and GJK consults for Sling Therapeutics, Ann Arbor, MI, USA. The authors declare that this study received funding from Sling Therapeutics, Ann Arbor, MI, USA. The funder was not involved in the study design, collection, analysis, interpretation of data, the writing of this article, or the decision to submit it for publication.

Conflict of interest

RZ, JK & RD are employees of Sling Therapeutics.

The remaining authors declare that the research was conducted in the absence of any commercial or financial relationships that could be construed as a potential conflict of interest.

Publisher's note

All claims expressed in this article are solely those of the authors and do not necessarily represent those of their affiliated organizations, or those of the publisher, the editors and the reviewers. Any product that may be evaluated in this article, or claim that may be made by its manufacturer, is not guaranteed or endorsed by the publisher.

Supplementary material

The Supplementary Material for this article can be found online at: https://www.frontiersin.org/articles/10.3389/fimmu.2024.1488220/full#supplementary-material

SUPPLEMENTARY FIGURE 1
Procedure of the cell proliferation assay.

SUPPLEMENTARY FIGURE 2
Pipetting scheme for cell proliferation and caspase-Glo® 3/7 Assay.

SUPPLEMENTARY FIGURE 3
Pipetting scheme for M22 testing in cell-based TSH-R-Ab Stimulating (TSI) bioassay.

SUPPLEMENTARY FIGURE 4
Pipetting scheme for testing IGF-1R and TSH-R inhibitors in cell-based TSH-R-Ab Blocking (TBI) bioassay.

SUPPLEMENTARY FIGURE 5
Dose-response curves for K1-70 in cell-based Thyretain TSH-R-Ab Blocking (TBI) bioassay.

References

1. Davies TF, Andersen S, Latif R, Nagayama Y, Barbesino G, Brito M, et al. Graves' disease. *Nat Rev Dis Primers*. (2020) 6:52. doi: 10.1038/s41572-020-0184-y

2. Kahaly GJ. Management of graves thyroidal and extrathyroidal disease: an update. *J Clin Endocrinol Metab*. (2020) 105:3704–20. doi: 10.1210/clinem/dgaa646

3. Bartalena L, Kahaly GJ, Baldeschi L, Dayan CM, Eckstein A, Marcocci C, et al. The 2021 European Group on Graves' orbitopathy (EUGOGO) clinical practice guidelines for the medical management of Graves' orbitopathy. *Eur J Endocrinol*. (2021) 185:G43–67. doi: 10.1530/EJE-21-0479

4. Kahaly GJ, Douglas RS, Holt RJ, Sile S, Smith TJ. Teprotumumab for patients with active thyroid eye disease: a pooled data analysis, subgroup analyses, and off-treatment follow-up results from two randomised, double-masked, placebo-controlled, multicentre trials. *Lancet Diabetes Endocrinol*. (2021) 9:360–72. doi: 10.1016/S2213-8587(21)00056-5

5. Krieger CC, Perry JD, Morgan SJ, Kahaly GJ, Gershengorn MC. TSH/IGF-1 receptor cross-talk rapidly activates extracellular signal-regulated kinases in multiple cell types. *Endocrinology*. (2017) 158:3676–83. doi: 10.1210/en.2017-00528

6. Smith TJ, Janssen J. Insulin-like growth factor-I receptor and thyroid-associated ophthalmopathy. *Endocr Rev*. (2019) 40:236–67. doi: 10.1210/er.2018-00066

7. Tsui S, Naik V, Hoa N, Hwang CJ, Afifiyan NF, Sinha Hikim A, et al. Evidence for an association between thyroid-stimulating hormone and insulin-like growth factor 1 receptors: a tale of two antigens implicated in Graves' disease. *J Immunol*. (2008) 181:4397–405. doi: 10.4049/jimmunol.181.6.4397

8. Smith TJ, Hoa N. Immunoglobulins from patients with Graves' disease induce hyaluronan synthesis in their orbital fibroblasts through the self-antigen, insulin-like

growth factor-I receptor. *J Clin Endocrinol Metab*. (2004) 89:5076–80. doi: 10.1210/jc.2004-0716

9. Buonfiglio F, Ponto KA, Pfeiffer N, Kahaly GJ, Gericke A. Redox mechanisms in autoimmune thyroid eye disease. *Autoimmun Rev*. (2024) 23:103534. doi: 10.1016/j.autrev.2024.103534

10. Lee ACH, Kahaly GJ. Pathophysiology of thyroid-associated orbitopathy. *Best Pract Res Clin Endocrinol Metab*. (2023) 37:101620. doi: 10.1016/j.beem.2022.101620

11. Krieger CC, Sui X, Kahaly GJ, Neumann S, Gershengorn MC. Inhibition of TSH/IGF-1 receptor crosstalk by teprotumumab as a treatment modality of thyroid eye disease. *J Clin Endocrinol Metab*. (2022) 107:e1653–e60. doi: 10.1210/clinem/dgab824

12. Smith TJ. Insulin-like growth factor pathway and the thyroid. *Front Endocrinol (Lausanne)*. (2021) 12:653627. doi: 10.3389/fendo.2021.653627

13. Lerario AM, Worden FP, Ramm CA, Hesseltine EA, Stadler WM, Else T, et al. The combination of insulin-like growth factor receptor 1 (IGF1R) antibody cixutumumab and mitotane as a first-line therapy for patients with recurrent/metastatic adrenocortical carcinoma: a multi-institutional NCI-sponsored trial. *Horm Cancer*. (2014) 5:232–9. doi: 10.1007/s12672-014-0182-1

14. Dupont J, Fernandez AM, Glackin CA, Helman L, LeRoith D. Insulin-like growth factor 1 (IGF-1)-induced twist expression is involved in the anti-apoptotic effects of the IGF-1 receptor. *J Biol Chem*. (2001) 276:26699–707. doi: 10.1074/jbc.M102664200

15. Gulbins A, Horstmann M, Daser A, Flogel U, Oeverhaus M, Bechrakis NE, et al. Linsitinib, an IGF-1R inhibitor, attenuates disease development and progression in a model of thyroid eye disease. *Front Endocrinol (Lausanne)*. (2023) 14:1211473. doi: 10.3389/fendo.2023.1211473

16. Mulvihill MJ, Cooke A, Rosenfeld-Franklin M, Buck E, Foreman K, Landfair D, et al. Discovery of OSI-906: a selective and orally efficacious dual inhibitor of the IGF-1 receptor and insulin receptor. *Future Med Chem*. (2009) 1:1153–71. doi: 10.4155/fmc.09.89

17. Penny MK, Finco I, Hammer GD. Cell signaling pathways in the adrenal cortex: Links to stem/progenitor biology and neoplasia. *Mol Cell Endocrinol*. (2017) 445:42–54. doi: 10.1016/j.mce.2016.12.005

18. Jin M, Wang J, Buck E, Mulvihill MJ. Small-molecule ATP-competitive dual IGF-1R and insulin receptor inhibitors: structural insights, chemical diversity and molecular evolution. *Future Med Chem*. (2012) 4:315–28. doi: 10.4155/fmc.11.180

19. Buck E, Mulvihill M. Small molecule inhibitors of the IGF-1R/IR axis for the treatment of cancer. *Expert Opin Investig Drugs*. (2011) 20:605–21. doi: 10.1517/13543784.2011.558501

20. Diana T, Kanitz M, Lehmann M, Li Y, Olivo PD, Kahaly GJ. Standardization of a bioassay for thyrotropin receptor stimulating autoantibodies. *Thyroid*. (2015) 25:169–75. doi: 10.1089/thy.2014.0346

21. Diana T, Wuster C, Olivo PD, Unterrainer A, Konig J, Kanitz M, et al. Performance and specificity of 6 immunoassays for TSH receptor antibodies: A multicenter study. *Eur Thyroid J*. (2017) 6:243–9. doi: 10.1159/000478522

22. Diana T, Holthoff HP, Fassbender J, Wuster C, Kanitz M, Kahaly GJ, et al. A novel long-term graves' Disease animal model confirmed by functional thyrotropin receptor antibodies. *Eur Thyroid J*. (2020) 9:51–8. doi: 10.1159/000508790

23. Diana T, Olivo PD, Chang YH, Wuster C, Kanitz M, Kahaly GJ. Comparison of a novel homogeneous cyclic amp assay and a luciferase assay for measuring stimulating thyrotropin-receptor autoantibodies. *Eur Thyroid J*. (2020) 9:67–72. doi: 10.1159/000504509

24. Diana T, Krause J, Olivo PD, Konig J, Kanitz M, Decallonne B, et al. Prevalence and clinical relevance of thyroid stimulating hormone receptor-blocking antibodies in autoimmune thyroid disease. *Clin Exp Immunol*. (2017) 189:304–9. doi: 10.1111/cei.12980

25. Diana T, Li Y, Olivo PD, Lackner KJ, Kim H, Kanitz M, et al. Analytical performance and validation of a bioassay for thyroid-blocking antibodies. *Thyroid*. (2016) 26:734–40. doi: 10.1089/thy.2015.0447

26. Diana T, Olivo PD, Kahaly GJ. Thyrotropin receptor blocking antibodies. *Horm Metab Res*. (2018) 50:853–62. doi: 10.1055/a-0723-9023

27. Krieger CC, Neumann S, Place RF, Marcus-Samuels B, Gershengorn MC. Bidirectional TSH and IGF-1 receptor cross talk mediates stimulation of hyaluronan secretion by Graves' disease immunoglobins. *J Clin Endocrinol Metab*. (2015) 100:1071–7. doi: 10.1210/jc.2014-3566

28. De Martino MC, van Koetsveld PM, Feelders RA, de Herder WW, Dogan F, Janssen J, et al. IGF and mTOR pathway expression and *in vitro* effects of linsitinib and mTOR inhibitors in adrenocortical cancer. *Endocrine*. (2019) 64:673–84. doi: 10.1007/s12020-019-01869-1

29. Leiphrakpam PD, Agarwal E, Mathiesen M, Haferbier KL, Brattain MG, Chowdhury S. *In vivo* analysis of insulin-like growth factor type 1 receptor humanized monoclonal antibody MK-0646 and small molecule kinase inhibitor OSI-906 in colorectal cancer. *Oncol Rep*. (2014) 31:87–94. doi: 10.3892/or.2013.2819

30. Fuentes-Baile M, Ventero MP, Encinar JA, Garcia-Morales P, Poveda-Deltell M, Perez-Valenciano E, et al. Differential effects of IGF-1R small molecule tyrosine kinase inhibitors BMS-754807 and OSI-906 on human cancer cell lines. *Cancers (Basel)*. (2020) 12. doi: 10.3390/cancers12123717

31. Fassnacht M, Berruti A, Baudin E, Demeure MJ, Gilbert J, Haak H, et al. Linsitinib (OSI-906) versus placebo for patients with locally advanced or metastatic adrenocortical carcinoma: a double-blind, randomised, phase 3 study. *Lancet Oncol*. (2015) 16:426–35. doi: 10.1016/S1470-2045(15)70081-1

32. Ciuleanu TE, Ahmed S, Kim JH, Mezger J, Park K, Thomas M, et al. Randomised Phase 2 study of maintenance linsitinib (OSI-906) in combination with erlotinib compared with placebo plus erlotinib after platinum-based chemotherapy in patients with advanced non-small cell lung cancer. *Br J Cancer*. (2017) 117:757–66. doi: 10.1038/bjc.2017.226

33. Gulbins A, Horstmann M, Keitsch S, Soddemann M, Wilker B, Wilson GC, et al. Potential involvement of the bone marrow in experimental Graves' disease and thyroid eye disease. *Front Endocrinol (Lausanne)*. (2023) 14:1252727. doi: 10.3389/fendo.2023.1252727

34. Smith TJ. Challenges in orphan drug development: identification of effective therapy for thyroid-associated ophthalmopathy. *Annu Rev Pharmacol toxicology*. (2019) 59:129–48. doi: 10.1146/annurev-pharmtox-010617-052509

35. Kahaly GJ, Steiner L, van der Lee MMC, van Achterberg TAE, Arends RJ, Karstens WFJ, et al. Thyrotropin receptor antagonism by a novel small molecule: preclinical *in vitro* observations. *Thyroid*. (2023) 33:732–42. doi: 10.1089/thy.2022.0694

frontiers | Frontiers in Immunology

TYPE Original Research
PUBLISHED 14 January 2025
DOI 10.3389/fimmu.2024.1503434

Check for updates

OPEN ACCESS

EDITED BY
Anette S. B. Wolff,
University of Bergen, Norway

REVIEWED BY
Faxi Wang,
Renmin Hospital of Wuhan University, China
Brian Skaggs,
University of California, Los Angeles,
United States

*CORRESPONDENCE
Yuan Liu
liuyuan@xmu.edu.cn
Shiju Chen
shiju@xmu.edu.cn

†These authors have equally contributed to this work

RECEIVED 29 September 2024
ACCEPTED 23 December 2024
PUBLISHED 14 January 2025

CITATION
Xuan J, Deng C, Lu H, He Y, Zhang J, Zeng X, Sun Y, Chen S and Liu Y (2025) Serum lipid profile in systemic lupus erythematosus. *Front. Immunol.* 15:1503434. doi: 10.3389/fimmu.2024.1503434

COPYRIGHT
© 2025 Xuan, Deng, Lu, He, Zhang, Zeng, Sun, Chen and Liu. This is an open-access article distributed under the terms of the Creative Commons Attribution License (CC BY). The use, distribution or reproduction in other forums is permitted, provided the original author(s) and the copyright owner(s) are credited and that the original publication in this journal is cited, in accordance with accepted academic practice. No use, distribution or reproduction is permitted which does not comply with these terms.

Serum lipid profile in systemic lupus erythematosus

Jingxiu Xuan[1,2,3†], Chaoqiong Deng[1†], Huiqin Lu[1†], Yan He[1,2,3], Jimin Zhang[1], Xiaoli Zeng[1,3], Yuechi Sun[1,2,3], Shiju Chen[1,2,3*] and Yuan Liu[1,2,3*]

[1]Department of Rheumatology and Clinical Immunology, the First Affiliated Hospital of Xiamen University, School of Medicine, Xiamen University, Xiamen, Fujian, China, [2]Xiamen Municipal Clinical Research Center for Immune Diseases, Xiamen, China, [3]Xiamen Key Laboratory of Rheumatology and Clinical Immunology, Xiamen, Fujian, China

Background: Dyslipidemia presents in various autoimmune diseases, and the serum lipid profile in systemic lupus erythematosus (SLE) has not yet been clearly defined. This study aims to evaluate the level of serum lipids in patients with SLE.

Methods: A case–control study evaluated four conventional sera lipids—total cholesterol (TC), triglyceride (TG), high-density lipoprotein (HDL), and low-density lipoprotein (LDL)—in patients with SLE compared to healthy controls (HCs). Correlations between serum lipids and clinical characteristics were analyzed in patients with SLE. A systematic review and meta-analysis were conducted to assess the epidemiology of lipid profiles in patients with SLE, and a random-effects meta-analysis was performed for data synthesis.

Results: TC and TG were elevated significantly, and HDL decreased in patients with SLE compared to HCs. Elevated lipids were associated with progressive disease activity. TC, TG, and HDL were elevated in patients with SLE and were associated with decreased IgG, increased 24-h proteinuria, white blood cells (WBCs), and neutrophils. Decreased HDL and increased TG were associated with an increase in the Systemic Lupus Erythematosus Disease Activity Index (SLEDAI). Patients with SLE who took glucocorticoids (GCs) may have experienced increases in TC and TG, while those who took hydroxychloroquine (HCQ) may have experienced increases in TC and HDL. Eleven eligible studies including the present study on associations between serum lipids and SLE were reviewed by the meta-analysis. The results demonstrated elevated TC (MD = 0.85, 95% CI 0.82 to 0.89, $p < 0.00001$) and TG (MD = 0.96, 95% CI 0.94 to 0.99, $p < 0.00001$) levels in SLE, while HDL decreased (MD = −0.19, 95% CI −0.20 to −0.17, $p < 0.00001$).

Conclusions: Dyslipidemia is present in SLE. There was a significant association between SLE disease activity and TC, TG, and HDL. The exact pathogenesis of metabolic disorders in SLE needs to be further addressed.

KEYWORDS

serum lipids, systemic lupus erythematosus, disease activity, meta-analysis, systemic review

1 Introduction

Systemic lupus erythematosus (SLE) is an autoimmune disease involving multiple organs that occurs primarily in young women (1). The clinical manifestations of SLE are diverse and may involve multiple systems, including the circulatory, renal, and hematologic systems (2). When the kidney is involved, its clinical manifestations include nephritis or nephrotic syndrome. Notably, proteinuria is present in nephritis, and hyperlipidemia may be present in nephrotic syndrome (3). Involvements of the hematologic system include anemia, leukopenia, and thrombocytopenia (4). Cardiovascular involvement is a significant cause contributing to mortality in patients with SLE (5, 6). Moreover, it is well known that the risk factors of CVDs (cardiovascular diseases) grew with long-term corticosteroid use, such as hypertension, obesity, hyperlipidemia, and atherosclerosis (7–10). To date, the exact pathogenesis of SLE is unknown. Furthermore, it has been shown that metabolic disorders contribute to SLE due to abnormal intestinal flora, mainly including abnormalities of glucose tolerance and dyslipidemia, ultimately eliciting an increasing incidence of cardiovascular events (11, 12).

Assessment of serum lipid profile mainly includes total cholesterol (TC), triglyceride (TG), high-density lipoprotein (HDL), and low-density lipoprotein (LDL) in the clinic. Dyslipidemia embedding hyperlipidemia has also been extensively studied in the pathogenesis of CVDs (13). Dyslipidemia is also present in various autoimmune diseases. There are many investigations on the association between lipids and rheumatoid arthritis (RA). Cardiovascular events top the list of causes of death in RA (14). Patients with active RA at an early stage had obvious lipid metabolic disorders, manifested as elevated TG, LDL, and reduced HDL in the presence of comorbid inflammation, along with an increasing incidence of cardiovascular events (15, 16).

Previous studies have also investigated the association between serum lipid profile and SLE (17). The mechanisms underlying the abnormalities of lipid metabolism in patients with SLE are complicated. The possible mechanism included the formation of autoantibodies to lipoprotein lipases (LPLs), which disturbed homeostasis between pro-atherogenic lipoprotein and anti-atherogenic lipoprotein (18). The levels of TC and TG were significantly higher in patients with SLE than in healthy controls (HCs), while the level of HDL was reduced. This elevated TG and decreased HDL pattern in patients with SLE has been referred to in the literature as the "lupus pattern", which is more pronounced in patients with higher disease activity (19, 20). Other studies have described inconsistent results for TC. A study showed that TC was decreased in patients with SLE compared to HCs (21). Studies on LDL are also controversial, with some suggesting no significant difference in LDL, while others indicated that LDL was increased in patients with SLE compared to HCs (12, 19). Thus, the serologic evidence for the association between serum lipids and SLE has not been well evaluated. The relevance of dyslipidemia for the risk of CVD development in SLE has not been consistently recognized.

To better understand the serum lipid profile of patients with SLE and the impact of serum lipids on the development of CVDs in SLE, the present study retrospectively investigated the serum lipid profile of patients with SLE. Furthermore, it explored the association between serum lipids and disease activity. A systematic review and meta-analysis, including previous studies and the present study, were also performed to assess the epidemiology of lipid profiles in patients with SLE.

2 Materials and methods

2.1 Participants

A case–control seroepidemiological study was conducted to analyze the serum lipid profile in SLE. A total of 203 patients with SLE admitted to the First Affiliated Hospital of Xiamen University from February 2018 to December 2019 were included. SLE was diagnosed based on the 2019 classification criteria of the American College of Rheumatology (ACR) and the European League Against Rheumatism (EULAR) (22). The control group of 100 individuals is a normal population from the physical examination center of the hospital who had no autoimmune diseases, infectious diseases, or CVDs and has taken no medications recently, including lipid-lowering agents. The medical examination reports of the selected controls, including laboratory items and imagological examinations, were shown to be normal, their serum lipid concentrations were within the reference intervals, and their age and gender matched SLE patients. The mean age of patients with SLE was (37.05 ± 14.38) years, and the mean age of the HC group was (35.5 ± 11.8) years. There were 179 female patients with SLE (88.2%) and 90 women among HCs (90%). There were no statistical differences in age and gender between the SLE and HC groups (p_{age} = 0.55 and p_{gender} = 0.70). This study was approved by the Medical Ethics Committee of the First Affiliated Hospital of Xiamen University (approval number KY-2019-022). Written informed consent was obtained from all participants in the study.

2.2 Clinical assessment

The disease activity of patients with SLE was assessed using the EULAR Systemic Lupus Erythematosus Disease Activity Index (SLEDAI) (23) score: 0–4 means inactive (n = 110), 5–9 means mild (n = 41), 10–14 means moderate (n = 23), and ≥15 means severe (n = 14). The SLEDAI scores for the 203 patients with SLE were 5.9 ± 5.3. Clinical data were collected, including patients' age, gender, medical history, clinical manifestations, medications, complications, durations of illness, and clinical laboratory results. The medication treatments of patients with SLE are detailed in Table 1. Sera derived from patients with SLE were stored at −80°C for antibody to dsDNA quantitation assay. IgG anti-dsDNA was detected by enzyme-linked immunosorbent assay (ELISA) according to the introduction of the kit (AESKU, Germany). Negative values: <12 IU/mL; cutoff values: 12–18 IU/mL; positive values: >18 IU/mL. IgG anti-C1q was also detected by ELISA according to the introduction of the kit (IMTEC, Germany). Positive was judged as >20 U/mL.

10.3389/fimmu.2024.1503434

TABLE 1 Drug treatments of patients with SLE.

Categories of drugs	Drugs	Patients with SLE (n = 203)
GCs	Prednisone, n (%)	82 (40.39%)
	Methylprednisolone, n (%)	68 (33.49%)
	Dexamethasone, n (%)	4 (1.97%)
csDMARDs	Hydroxychloroquine, n (%)	137 (67.48%)
	Mycophenolate mofetil, n (%)	40 (19.70%)
	Methotrexate, n (%)	14 (6.89%)
	Leflunomide, n (%)	12 (5.91%)
	Tacrolimus, n (%)	10 (4.92%)
	Cyclophosphamide, n (%)	8 (3.94%)
	Ciclosporin, n (%)	6 (2.95%)
	Thalidomide, n (%)	2 (0.98%)
	Azathioprim, n (%)	1 (0.49%)
bDMARDs	Belimumab, n (%)	1 (0.49%)
NSAIDs	Aspirin, n (%)	27 (12.32%)
	Celecoxib, n (%)	11 (5.41%)
	Etoricoxib, n (%)	2 (0.98%)
	Imrecoxib, n (%)	1 (0.49%)
LLDs	Atorvastatin, n (%)	5 (2.46%)
	Pitavastatin, n (%)	1 (0.49%)

GCs, glucocorticoids; csDMARDs, conventional synthetic disease-modifying anti-rheumatic drugs; bDMARDs, biological disease-modifying anti-rheumatic drugs; NSAIDs, nonsteroidal anti-inflammatory drugs; LLDs, lipid-lowering drugs.

2.3 Detection of serum lipids

TC, TG, HDL, and LDL of all patients with SLE and HCs have been measured routinely by commercial reagents according to the instructions of the kits in the clinical laboratories of the hospitals where the serum lipid results were obtained. The reference interval for TC was 3.1–5.2 mmol/L; that for TG was 0.4–1.82 mmol/L; that for HDL was 1.04–1.55 mmol/L; and that for LDL was 0–3.1 mmol/L.

2.4 Statistical analysis

The raw data were organized, and outliers were verified or excluded within an interpretable range. Continuous variables in comparing serum lipid profiles between patients with SLE and HCs were expressed as mean ± standard deviation (mean ± SD). Normality tests were conducted for continuous variables. The Mann–Whitney U test was used for between-group comparisons because the data did not meet normal distribution. Since the serum lipid profiles had a non-normal distribution, Spearman or Spearman rank correlation was used to analyze whether serum lipids and clinical characteristics of patients with SLE were correlated and the magnitude of the correlation. Data analysis and plotting were performed using GraphPad software (Version 8.0, GraphPad Software, California, USA). Binary logistic regression analysis was conducted to assess the independence of serum lipid profile differences between patients with SLE and HCs after adjusting for gender and age. Regression coefficients β, odds ratios (ORs), and adjusted p-values were displayed. Through natural logarithm transformation of non-normal distribution data, multiple linear regression analysis was performed to assess the independent relationship between serum lipid profile and gender, age, disease durations, and drugs in patients with SLE, including regression coefficients β and adjusted p-values. Regression analysis was performed using IBM SPSS Statistics (Version 26.0, IBM Corp., Armonk, NY, USA). All tests were two-tailed, and $p < 0.05$ was considered statistically significant.

2.5 Systematic review and meta-analysis

A systematic review and meta-analysis were conducted to evaluate the relationship between lipid profile and patients with SLE. PubMed, Embase, and Cochrane electronic databases were searched for studies published before 10 April 2023. Reference citations of included studies were also searched to identify additional relevant articles. The following search terms were used: ("Systemic Lupus Erythematosus" OR "Lupus Erythematosus Disseminatus" OR "Libman-Sacks Disease" OR "Disease, Libman-Sacks" OR "Libman Sacks Disease" OR "Lupus Erythematosus, Systemic") AND ("Metabolism, Lipid" OR "Lipid Metabolism") without language restrictions. The inclusion criteria for studies in this meta-analysis were as follows: (1) cohort studies, cross-sectional studies, or case–control studies; (2) adult patients; and (3) at least 10 patients in the SLE group. The exclusion criteria were as follows: (1) letters, reviews, abstracts, case reports, or comments; (2) not HCs; (3) overlapping data, unavailable or insufficient data; and (4) patients receiving statin or fibrate drugs. A random-effect or fixed-effect model was performed to pool the mean difference (MD) with 95% CI on the association between lipid profile and patients with SLE. Heterogeneity across studies was performed by I^2 test, and an I^2 over 50% suggested high heterogeneity (24). All analyses were performed by RevMan software (Version 5.4; Cochrane Collaboration, London, UK). $p < 0.05$ was considered statistically significant.

3 Results

3.1 Case–control study

3.1.1 Serum lipid profile in patients with SLE

In the case–control study, the concentrations of 50 cases (24.63%) of TC, 55 cases (27.09%) of TG, and 31 cases (15.27%) of LDL were higher than the reference intervals. In 48 cases (23.65%), HDL was lower than the reference intervals. TC and TG concentration increased significantly in patients with SLE compared to HCs. However, HDL was markedly decreased in the SLE group compared to the HC group. Interestingly, there was no

significant difference in LDL between the two groups. Therefore, LDL may not be included in later correlation analyses (Table 2; Figure 1).

To assess the independence of serum lipid profile differences between patients with SLE and HCs, binary logistic regression analysis was conducted, controlling for confounding factors such as age and gender. The results indicated significant differences in all serum lipids between the patients with SLE and HCs. Four indicators were the independent risks for SLE. TC (OR = 103.830, $p < 0.0001$) and TG (OR = 19.444, $p < 0.0001$) were increased in SLE. However, HDL (OR = 0.004, $p < 0.0001$) and LDL (OR = 0.004, $p < 0.0001$) decreased (Table 2).

Approximately 90% of female patients were seen in SLE; gender may influence the serum lipid profiles during illness. Therefore, a comparison of TC, TG, HDL, and LDL concentrations between women and men in both groups of patients with SLE and HCs was conducted. The results showed that only LDL exhibited a significant difference between male and female patients in the SLE group, with male patients having higher LDL levels than female patients. However, in the HC group, the TC and LDL levels were higher in female than in male patients, while no significant difference was observed in other lipids (Figure 2).

3.1.2 Correlation of serum lipids with clinical characteristics in patients with SLE

The data showed that the serum lipid profile and clinical characteristics of patients with SLE were extremely strongly correlated. Serum IgG was especially reversely associated with the levels of TC, TG, and HDL. Elevated TC, TG, and HDL were associated with increased 24-h urinary protein quantities, white blood cells (WBCs), and neutrophils (Table 3; Figure 3).

Not only were TC, TG, and HDL associated with the above four clinical indicators, but each of the three serum lipids was also associated with some other indicators. When the level of TC rose, UA, Urea, PRO, ACR, and PLTs increased, and TGAb, IgA, CRP, and AST decreased. A significant increase in TC was shown in patients treated with hydroxychloroquine (HCQ) and/or glucocorticoids (GCs). At the same time, TC is not different between patients with and without medications. When TG was elevated, UA, Cr, Urea, PRO, ESR, ANA, HGB and SLEDAI increased. Patients with SLE who have taken GCs also showed an increase in TG. When HDL was decreased, C3, C4, HGB, lymphocyte, disease duration, and PLTs were also decreased, whereas CRP, ESR, IgA, AST, SLEDAI, disease durations, and autoantibodies, including ANA, anti-dsDNA, and anti-C1q, were increased. Furthermore, HDL increased dramatically in both the medication and HCQ groups (Table 3). Overall, the disease activity got aggressive with increased TC and TG and decreased HDL. Thus, analyzing the connection between serum lipids and multiorgan damages, HDL was reversely associated with multiorgan injuries including lupus nephritis ($r = -0.166$, $p = 0.0184$), interstitial lung disease ($r = -0.207$, $p = 0.003$), gastrointestinal diseases ($r = -0.159$, $p = 0.024$), osteoarthritis ($r = -0.198$, $p = 0.005$), hematological diseases ($r = -0.253$, $p < 0.001$), and dermatological impairment ($r = -0.217$, $p = 0.002$). The remaining lipids were not significantly linked to multiorgan damage.

The correlations between dyslipidemia and clinical features were further analyzed in patients with SLE who had higher levels of TC and TG, and lower levels of HDL than reference intervals. Hypercholesterolemia was associated with elevated 24-h PRO, PRO WBCs, and neutrophils. SLEDAI scores were also increased. Disease progression got worse in patients with SLE with dyslipidemia. Hypercholesterolemia is inversely correlated with IgG, AST, ALT, and antibodies to the thyrotropin receptor (TRAbs). Hypertriglyceridemia was accompanied by elevated CRP. The negative correlation between HDL and IgG and anti-C1q antibodies became more pronounced. Similarly, TNFα increased, accompanied by decreased HDL. These results suggested that dyslipidemia development is associated with severe disease course and progressive inflammatory state in SLE (Table 4).

The above data indicated a multifactorial effect on the lipid profile in patients with SLE. A multiple linear regression analysis was conducted to analyze the independence of each factor on the lipid profile. Traditional factors such as gender and age, disease duration, and medications of high-frequency use, including HCQ and GCs, which are picked out to influence the lipid profile, were conducted. The results showed that the use of GCs in patients with SLE significantly increased TC (β = 0.214, 95% CI 0.043 to 0.215, $p = 0.004$) and LDL (β = 0.253, 95% CI 0.088 to 0.313, $p = 0.001$), while the use of HCQ increased HDL (β = 0.213, 95% CI 0.046 to 0.248, $p = 0.004$). Additionally, male patients with SLE had higher LDL levels (β = 0.160, 95% CI 0.026 to 0.336, $p = 0.022$); gender difference seems to affect the lipids in SLE. However, age and disease duration did not significantly impact the lipid profile in our study (Table 5).

TABLE 2 Serum lipid profiles of patients with SLE and HCs in the case–control study.

Serum lipids	SLE (n = 203)	HCs (n = 100)	p-values	Regression coefficient β	OR	Adjusted p-values*
TC (mmol/L)	4.60 ± 1.35	4.21 ± 0.53	**0.0171**	4.643	103.830	**<0.0001**
TG (mmol/L)	1.52 ± 0.74	0.88 ± 0.30	**<0.0001**	2.968	19.444	**<0.0001**
HDL (mmol/L)	1.31 ± 0.43	1.37 ± 0.14	**<0.001**	−5.569	0.004	**<0.0001**
LDL (mmol/L)	2.32 ± 0.88	2.27 ± 0.45	0.5754	−5.438	0.004	**<0.0001**

Bold values suggest statistically significant findings. *adjusted for age and gender.

10.3389/fimmu.2024.1503434

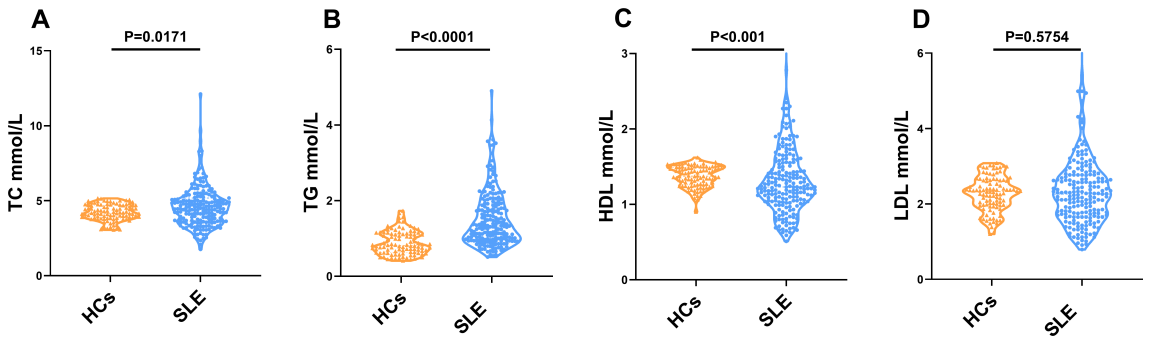

FIGURE 1
Comparison of TC, TG, HDL, and LDL concentrations between patients with SLE and HCs. **(A)** The differences in the concentration of TC between patients with SLE and HCs. **(B)** The differences in the concentration of TG between patients with SLE and HCs. **(C)** The differences in the concentration of HDL between patients with SLE and HCs. **(D)** The differences in the concentration of LDL between patients with SLE and HCs.

3.2 Systematic review and meta-analysis

A total of 1,363 articles were retrieved through searching in PubMed (n = 413), Cochrane (n = 29), Embase (n = 917), and other sources (n = 4). After an initial evaluation of titles and abstracts, 1,272 articles were excluded. Full texts of the remaining 91 studies were assessed, and finally, 10 studies were identified according to the inclusion and exclusion criteria. The characteristics of the included studies are presented in Table 6. Together with the present case–control study, 11 studies were analyzed in the meta-analysis, which contained 911 patients with SLE and 730 HCs. After 11 studies pooled into the meta-analysis, serum TC levels were elevated in SLE (MD = 0.85, 95% CI 0.82 to 0.89, $p < 0.00001$). As a significant heterogeneity was observed (I^2 = 98%), the subgroup analysis was performed based on whether CVD was excluded or unclear in the SLE group. It showed that serum TC levels were decreased significantly in SLE without CVD in six studies (MD = −0.34, 95% CI −0.47 to −0.21, $p < 0.00001$), but elevated considerably in SLE with unclear in other 4 studies (MD

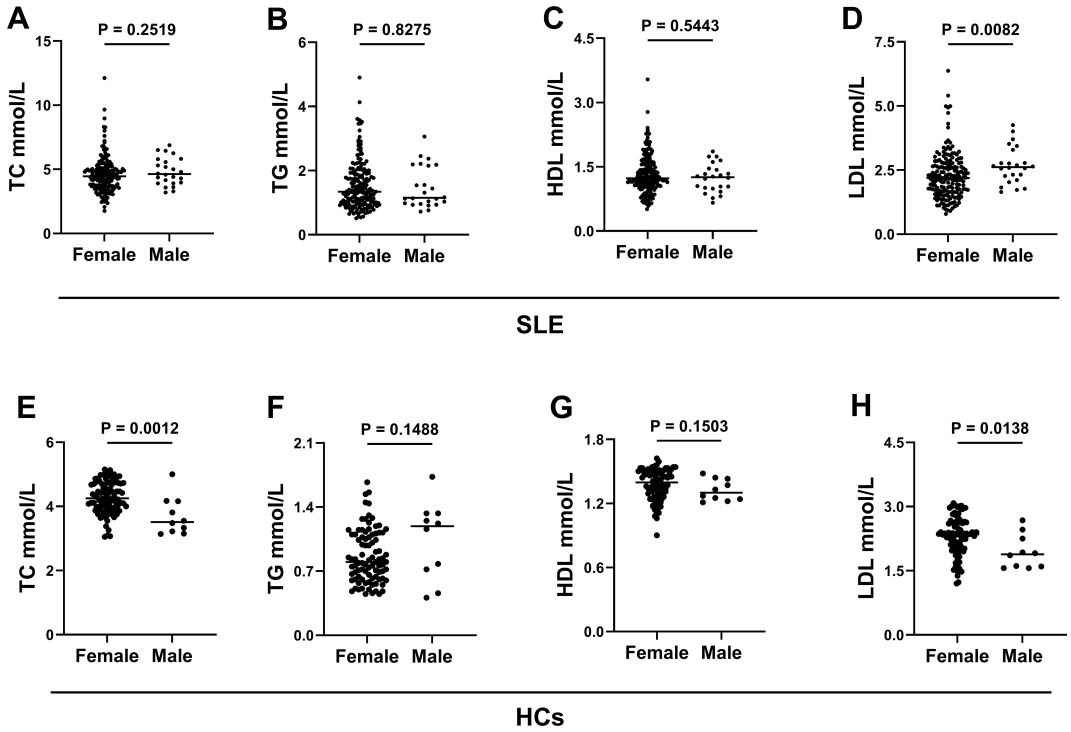

FIGURE 2
Comparison of the TC, TG, HDL, and LDL levels between women and men in patients with SLE and HCs. **(A)** The concentration differences of TC between women and men in patients with SLE. **(B)** The concentration differences of TG between women and men in patients with SLE. **(C)** The concentration differences of HDL between women and men in patients with SLE. **(D)** The concentration differences of LDL between women and men in patients with SLE. **(E)** The concentration differences of TC between women and men in HCs. **(F)** The concentration differences of TG between women and men in HCs. **(G)** The concentration differences of HDL between women and men in HCs. **(H)** The concentration differences of LDL between women and men in HCs.

10.3389/fimmu.2024.1503434

TABLE 3 Serum lipid and clinical characteristic correlations in patients with SLE.

	TC		TG		HDL	
	r	*p*	*r*	*p*	*r*	*p*
WBCs	0.235	**<0.001***	0.207	**0.003***	0.206	**0.003***
Neutrophils	0.240	**<0.001***	0.257	**<0.001***	0.141	**0.047***
Lymphocytes	0.048	0.495	−0.104	0.142	0.250	**<0.0001***
PLTs	0.225	**0.001***	−0.002	0.974	0.200	**0.004***
HGB	0.076	0.283	0.146	**0.039***	0.284	**<0.0001***
IgG	−0.470	**<0.0001***	−0.180	**0.021***	−0.406	**<0.0001***
IgA	−0.210	**0.013***	−0.060	0.487	−0.207	**0.015***
C3	0.118	0.096	−0.103	0.144	0.263	**<0.0001***
C4	0.128	0.069	−0.093	0.187	0.222	**0.002***
AST	−0.159	**0.023***	−0.063	0.371	−0.202	**0.004***
UA	0.189	**0.008***	0.230	**0.001***	−0.080	0.266
Urea	0.184	**0.010***	0.222	**0.002***	0.022	0.763
Cr	0.096	0.180	0.255	**<0.001***	0.029	0.689
24-h PRO	0.485	**<0.0001***	0.397	**<0.001***	0.294	**0.009***
PRO	0.303	**<0.0001***	0.380	**<0.0001***	0.060	0.406
ACR	0.537	**<0.0001***	0.256	0.098	0.142	0.363
CRP	−0.174	**0.030***	0.021	0.798	−0.334	**<0.0001***
ESR	−0.107	0.207	0.217	**0.009***	−0.360	**<0.0001***
ANA	−0.079	0.296	0.168	**0.026***	−0.287	**<0.001***
Anti-dsDNA	−0.050	0.476	0.070	0.322	−0.144	**0.042***
Anti-C1q	−0.247	0.189	0.223	0.235	−0.574	**<0.001***
TGAb	−0.281	**0.044***	−0.102	0.471	−0.198	0.159
SLEDAI	−0.022	0.759	0.167	**0.020***	−0.295	**<0.0001***
Disease duration	0.095	0.183	−0.022	0.753	0.159	**0.025***
Drugs	0.130	0.065	0.039	0.576	0.164	**0.020***
HCQ	0.138	**0.049***	−0.028	0.695	0.224	**0.001***
GCs	0.237	**0.001***	0.141	**0.045***	0.107	0.129

*Bold values suggest statistically significant findings. 24-h PRO, 24-h proteinuria quantitation; PRO, proteinuria quality; ACR, Umalb/Ucr; ANA, antinuclear antibody; Anti-dsDNA, type IgG anti-double-stranded DNA antibody; Anti-C1q, anti-complement 1q antibody; TGAb, antibody to thyroglobulin; "Drugs" means untreated with medications vs. treated with medications; HCQ, hydroxychloroquine; GCs, glucocorticoids.

= 0.94, 95% CI 0.90 to 0.97, $p < 0.00001$). As for serum TG, eight studies were pooled into a meta-analysis. TG was elevated in SLE (MD = 0.96, 95% CI 0.94 to 0.99, $p < 0.00001$). Subgroup analysis also showed elevated TG levels in SLE either without CVD (MD = 0.20, 95% CI 0.11 to 0.28, $p < 0.00001$) or with unclear (MD = 1.02, 95% CI 1.00 to 1.04, $p < 0.00001$). After 11 studies were pooled into the meta-analysis, HDL levels showed reduced HDL levels in SLE (MD = −0.19, 95% CI −0.20 to −0.17, $p < 0.00001$). Subgroup analysis showed lower HDL levels in SLE either without CVD (MD = −0.11, 95% CI −0.17 to −0.05, $p < 0.00001$) or with unclear (MD = −0.19, 95% CI −0.20 to −0.18, $p < 0.00001$). However, significant heterogeneity was still observed (Figure 4).

4 Discussion

The association between metabolic disorders and autoimmune diseases has received growing attention recently (34), while the association between dyslipidemia and SLE is not yet well defined. To better understand it, the serum lipid profile was first performed in patients with SLE. The results showed that the concentrations of TC and TG increased significantly in patients with SLE compared to HCs, while HDL decreased. LDL did not show a statistical difference in patients with SLE compared to HCs. The subsequent meta-analysis also displayed the same results. Considering the effects of traditional factors (e.g., age and sex) on lipid profile, the adjusted

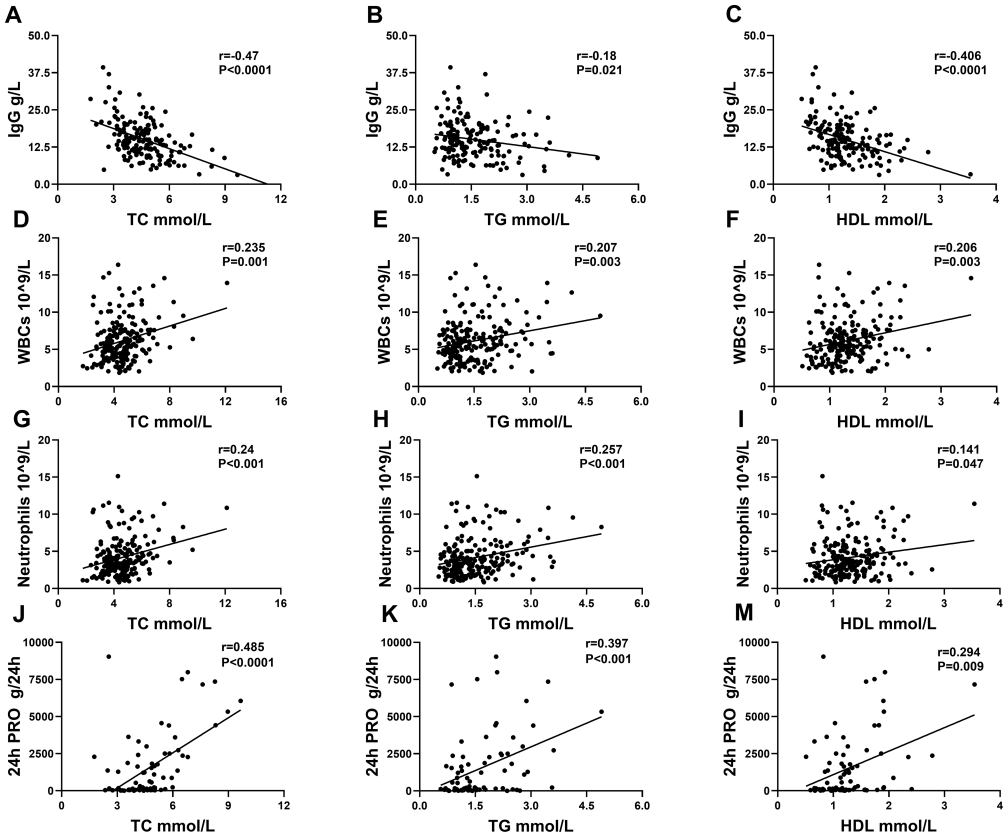

FIGURE 3
Correlation analysis between serum lipids and IgG, WBCs, neutrophils, and 24-h PRO in patients with SLE. **(A–C)** displayed a correlation between IgG and TC, TG, and HDL. **(D–F)** displayed a correlation between WBCs and TC, TG, and HDL. **(G–I)** displayed a correlation between neutrophils and TC, TG, and HDL. **(J–M)** displayed a correlation between 24-h PRO and TC, TG, and HDL.

TABLE 4 Correlation analysis between serum lipids and clinical characteristics in patients with SLE with dyslipidemia.

	TC ≥ 5.2 mmol/L		TG ≥ 1.82 mmol/L		HDL ≤ 1.04 mmol/L	
	r	*p*	*r*	*p*	*r*	*p*
WBCs	**0.279**	**0.049***	0.192	0.160	0.132	0.378
Neutrophils	**0.304**	**0.032***	0.259	0.054	0.122	0.414
HGB	−0.119	0.412	−0.055	0.689	**0.336**	**0.021***
AST	**−0.344**	**0.014***	−0.152	0.263	0.065	0.661
ALT	**−0.279**	**0.049***	−0.104	0.444	0.188	0.202
IgG	**−0.357**	**0.019***	−0.183	0.209	**−0.497**	**<0.001***
24-h PRO	**0.614**	**0.003***	−0.002	0.993	0.037	0.864
PRO	**0.578**	**<0.0001***	0.237	0.084	−0.028	0.853
CRP	−0.292	0.064	**0.329**	**0.031***	−0.159	0.308
TNFα	0.373	0.323	0.357	0.432	**−0.569**	**0.042***
Anti-C1q	0.071	0.879	−0.165	0.648	**−0.781**	**0.002***
TRAb	**−0.867**	**0.012***	−0.164	0.651	0.161	0.567
SLEDAI	**0.378**	**0.007***	−0.097	0.489	0.112	0.465

*Bold values suggest statistically significant findings. TRAb, antibody to thyrotropin receptor.

10.3389/fimmu.2024.1503434

TABLE 5 Multiple linear regression analysis of the independent relationship between serum lipid profile and gender, age, disease duration, and medications in patients with SLE.

Lipids profile	Factors	Regression coefficient β	95% CI	Adjusted *p*-values
TC	Gender (Male)	0.077	−0.053,0.185	0.273
	Age (Y)	−0.040	−0.004,0.002	0.569
	Disease duration (Mo)	0.076	−0.0003,0.001	0.286
	Drugs			
	HCQ	0.088	−0.034,0.140	0.234
	GCs	0.214	0.043,0.215	**0.004***
TG	Gender (Male)	−0.043	−0.252,0.135	0.553
	Age (Y)	0.017	−0.004,0.005	0.819
	Disease duration (Mo)	−0.025	−0.001,0.001	0.727
	Drugs			
	HCQ	−0.082	−0.219,0.065	0.284
	GCs	0.146	−0.001,0.280	0.052
HDL	Gender (Male)	−0.022	−0.160,0.116	0.756
	Age (Y)	−0.018	−0.004,0.003	0.804
	Disease duration (Mo)	0.101	−0.0002,0.001	0.155
	Drugs			
	HCQ	0.213	0.046,0.248	**0.004***
	GCs	0.073	−0.049,0.151	0.318
LDL	Gender (Male)	0.160	0.026,0.336	**0.022***
	Age (Y)	−0.012	−0.004,0.003	0.861
	Disease duration (Mo)	0.094	−0.0003,0.002	0.179
	Drugs			
	HCQ	−0.032	−0.139,0.088	0.664
	GCs	0.253	0.088,0.313	**0.001***

*Bold values suggest statistically significant findings. Y, year; Mo, month.

results showed that LDL was also increased significantly in patients with SLE.

Probably, LDL is easily oxidized to oxLDL, which plays a key role in the metabolic disorders in patients with SLE. One study indicated no significant difference in the LDL level of patients with SLE with metabolic syndrome compared to HCs, but the oxLDL level was significantly increased (12). Paraoxonase1 (PON1) activity was evaluated in patients with SLE because it protects LDL from oxidation, its activity was compromised, and the antioxidant capacity of LDL was sequentially impaired. This resulted in an increasing possibility of atherosclerosis. oxLDL accumulation is mainly attributed to HDL dysfunction, reduced PON1 activity, and increased susceptibility of LDL to oxidation (30). Multiple factors such as corticosteroid usage, overweight, and age are responsible for increasing LDL oxidative susceptibility (20). One study reported that HCQ reduced LDL levels and promoted the conversion of TC to HDL (35). However, changes in LDL in patients with SLE need to be further confirmed in the future.

SLE is nine times more common in young women than in men. Patients with SLE have a risk of atherosclerosis almost twice as high as HCs compared by age and sex (36). Patients with SLE had a 27% higher risk of non-fatal CV events compared with age- and sex-matched patients with diabetes (37). Hence, the effect of sex differences on lipids was analyzed in the SLE group and HC group. The results present heterogeneity. Male individuals had higher LDL levels than female individuals in the SLE group. In support, multiple studies showed that being male was associated with higher mortality in SLE (38, 39). A multicenter study found that approximately 25% of 10,000 deaths with SLE were caused by CVDs (40). It was reported that patients with SLE had a 50-fold higher risk of CVDs than matched controls (41). The sex hormone changes may also be associated with increased cardiovascular risk in menopausal women (42). In addition, age-specific metabolomic profiles were identified in patients with SLE vs. HCs, reduced HDL, and elevated GlycA levels associated with disease activity, atherosclerosis, and myocardial infarction at all ages. Glycolysis

TABLE 6 Eligible study characteristics in the meta-analysis.

Study	Country	Participants (SLE/Control)	Female/Male (SLE, Control)	Serum lipid profile	CVD exclusion	Disease activity (scores)	Disease duration (years)
Formiga F 2001 (25)	Sweden	53/45	Unclear	TC, TG, HDL, and LDL	Unclear	SLEDAI: 4 ± 2	10.5 ± 5.5
Svenungsson E 2001 (26)	Spain	52/26	Unclear	TC, TG, HDL, and LDL	Yes	SLAM: 5.5	19.25 ± 9.7
Delgado Alves J 2002 (27)	Britain	32/20	28/4, 17/3	TC and HDL	Yes	BILAG: 6.7 ± 4.5	5.8(1-12.3)
Santos M J 2010 (28)	Portugal	100/102	Unclear	TC, TG, HDL, and LDL	Yes	SLEDAI-2K: 2 ± 4	6.6 ± 6.8
Parra S 2014 (29)	Spain	60/34	Unclear	TC, TG, HDL, and LDL	Yes	SLEDAI <4	Unclear
Gaál K 2016 (21)	Korea	51/49	44/7, 41/8	TC, HDL, and LDL	Unclear	SLEDAI: 4.0 (2.0–6.0)	6.59 ± 5.26
Park J K 2016 (30)	Germany	35/15	34/1, 13/2	TC, TG, HDL, and LDL	Unclear	SLEDAI-2K: 4.26 ± 4.24	12.1 ± 7.6
Sánchez-Pérez H 2020 (31)	Spain	195/223	185/10, 155/68	TC, TG, HDL, and LDL	Yes	SLEDAI: 2.0 (0.0–5.0)	17 ± 10
Diószegi A 2023 (32)	Hungary	51/41	44/7, 36/5	TC, HDL, and LDL	Yes	SLEDAI: 5.96 (2–10)	Unclear
Huang S S 2023 (33)	China	105/75	94/11, Unclear	TC, TG, HDL, and LDL	Unclear	SLEDAI: 10.70 ± 0.57	6.10 ± 0.62
Present study	China	203/100	179/24, 90/10	TC, TG, HDL, and LDL	Unclear	SLEDAI: 5.9 ± 5.3	Unclear

pathway metabolites uniquely increased with age in SLE, significantly influenced by prednisolone and HCQ treatment (43). Genetic factors are one cofactor of SLE etiopathogenesis and the risk factor of dyslipidemia. Apart from the sex and age of the patients, autosomal mutations of the LDL receptors cause familial hypercholesterolemia (44). Another study reported that CC homozygosity of the GCKR gene and plasma TG concentrations are independently associated with subclinical carotid atherosclerosis in women with SLE (45).

HCQ and GCs are frequently used in the clinic in SLE pharmaceutical therapy. In this study, HDL was increased in patients with SLE with medications and HCQ compared to others without medications. TC was also elevated in patients with SLE with HCQ and or GCs. Moreover, an increase in TG was accompanied by GC use. Multiple linear regression analysis was performed to explore medications' effects on lipid profile in SLE, combined with other factors (age, sex, and disease duration). The results showed that GC use was an independent risk factor of elevated TC and LDL, and HCQ use was an independent risk factor of increased HDL. They are consistent with other published reports. HCQ is the milestone of SLE therapy for its multiple beneficial effects, including anti-inflammatory and lipid-lowering properties and controlling the glycemic profile. HCQ has the following atheroprotective effects: (i) NO (nitric oxide) availability increases; (ii) improvement in the function of endothelium by reduction of ROS; (iii) reduction of type I IFN production by pDCs; (iv) an impediment to NET formation; and (v) inhibition of platelet activation and aggregation (46). Current evidence and previous studies have provided promising therapy for HCQ on CVD burden in SLE. GCs are anti-inflammatory drugs widely used in many autoimmune inflammatory diseases, including SLE and RA. GCs are essential in relieving pain and reducing the risk of joint injuries. Long-term GC administration increases the risk of dyslipidemia and premature CVDs (47). GCs impact multiple aspects of lipid metabolism, including (i) promotion of insulin resistance, (ii) increase in VLDL from hepatic synthesis, (iii) reduction in LPL, (iv) increase in the conversion of VLDL to LDL, (v) downregulation of the LDL, and (vi) increase in the activity of 3-hydroxy-3-methylglutaryl coenzyme A. These effects on GCs develop hypertriglyceridemia (48).

The present study shows a strong correlation between serum lipids and active SLE. Increased TG and decreased HDL were related to SLEDAI. Decreased HDL was particularly associated with disease progression indicators such as decreased WBC, C3, and C4 consumptions and increased IgG, IgA, CRP, ESR, ANA titers, anti-dsDNA, and anti-C1q. TG significantly correlates with WBCs, lymphocytes, neutrophils, and monocytes. Similar results were seen in our study. However, the hypothesis that serum lipids are the causal pathway for leukocytogenesis is not yet tenable because leukocyte development is influenced by multiple factors (49). Increased TC was associated with kidney damage 24-h PRO, PRO, ACR, and the inflammatory marker CRP. 24-h PRO was also positively correlated to TG and HDL. There is evidence that hyperlipidemia in patients with SLE may be involved in their

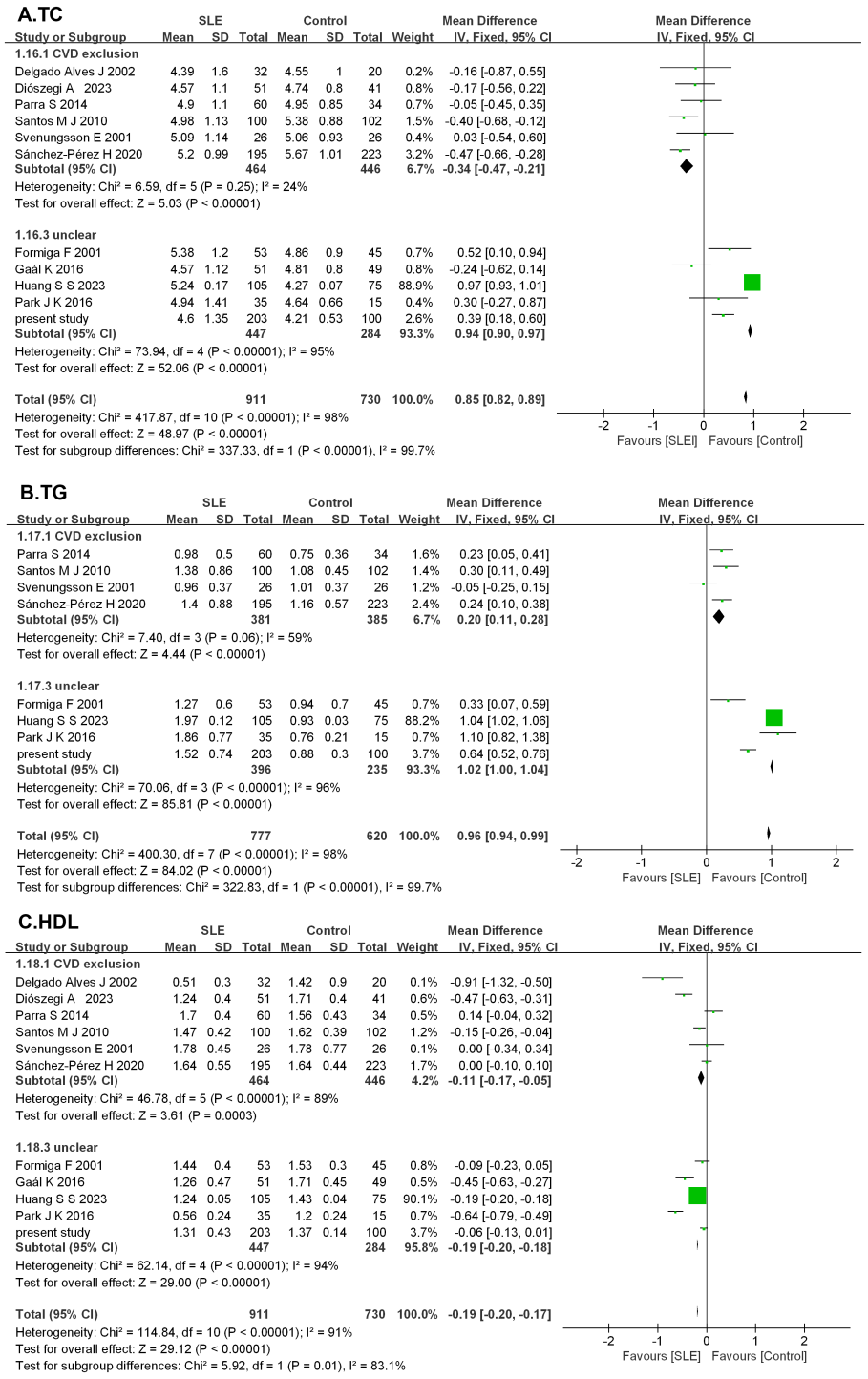

FIGURE 4
Forest plots in the meta-analysis of serum lipid profile in SLE. **(A)** Forest plots in the meta-analysis of TC in SLE. **(B)** Forest plots in the meta-analysis of TG in SLE. **(C)** Forest plots in the meta-analysis of HDL in SLE.

kidney injury through TNFSF1A and TNFSF1B (33). Hence, abnormality of serum lipids could serve as an indicator reflecting renal injury.

Further analyzing the association between serum lipids and clinical features in the dyslipidemia of patients with SLE proved that dyslipidemia is linked to disease progression. Notably, increased TC was correlated with elevated SLEDAI scores and serious renal damage in patients with dyslipidemia. In contrast, decreased HDL was associated with elevated TNFα, and increased TG was accompanied by elevated CRP. The exact mechanism by which inflammation reduces HDL levels is yet unclear. Nonetheless, TNFα was increased in patients with SLE with CVDs two to three times higher than those without CVDs (50). Patients with SLE have a high prevalence of metabolic syndrome; 56% of patients over 55 years old

exhibited hypercholesterolemia, which is directly attributed to the inflammatory status and increased oxidative stress (20, 51). The systemic inflammatory state of lupus disrupted cholesterol homeostasis and increased the susceptibility of arterial wall cells (including macrophages and endothelial cells) to cholesterol accumulation (52). Cholesterol accumulation may exacerbate T- and B-cell responses to facilitate autoantibody production in patients with SLE (53). Reduced HDL may cause cholesterol accumulation through impaired cholesterol efflux capacity (CEC) (54). HDL displays many biological functions, including cholesterol mobilization, antioxidants, anti-inflammatory, anti-thrombotic, and anti-apoptotic effects (55). Meanwhile, lipid-related CV risk in autoimmune diseases has been attributed to inflammation-induced HDL dysfunction. HDL dysfunction leads to anti-inflammatory HDL converting to the phenotype of proinflammatory HDL (56–61). The pro-inflammatory HDL in female patients with SLE has been associated with carotid artery atherosclerosis and increased carotid intima-media thickness (59). Increases in proinflammatory HDL were correlated with increases in oxLDL in SLE. They formed a vicious cycle including inflammation, the formation of proinflammatory HDL, and increased oxLDL (61). In our study, decreased HDL was associated with increasing risks of kidney, lung, digestive, joint, and blood disorders and skin damage. The evidence showed that increased CRP was linked to LPL, the rate-limiting enzyme in TG metabolism. This activity might correlate with autoantibodies in SLE (52). It sequentially reduces the ability to remove chylomicrons from plasma, accumulating chylomicrons and VLDL and ultimately elevating TG level (62). Elevated TG levels may affect vascular function and contribute to vascular inflammation in patients with SLE (32). Inflammation damages and impairs organ function if it is excessive and dysregulated (63, 64). In the cardiovascular system, atherosclerosis is the prominent impact of inflammation (65, 66). Endothelial dysfunction is the beginning of atherosclerosis development in SLE. The mechanism of the endothelial lesion is the disruption of local microenvironmental homeostasis through multifactorial oxidative stress, pro-inflammatory cytokines, NETs, the activation of B cells and autoantibodies, and abnormal T cells. Mitochondrial dysfunction, energy metabolism, and telomere alterations contribute at a molecular level to the increased oxidative stress in SLE. oxLDLs can stimulate endothelial activation. High levels of oxLDL and proinflammatory HDL reduced LDL uptake capacity in SLE and coronary or peripheral arterial disease, and carotid plaque was found (67, 68).

The atherosclerotic plaque was formed via at least three events. Endothelial dysfunction may be primarily present in endothelial lesions, caused by an imbalance between vasoconstrictive (endothelin) and vasodilating (NO) substances and the formation of ROS in the damaged endothelial cells. Inadequate NO synthesis triggers the production of proinflammatory cytokines, including TNFα, IL6, and IL1β, and reduces the production of antithrombotic agents in the endothelium. Thereby, LDL accumulates in the vascular wall. Subsequently, the accumulated LDL in the arterial intima is modified (aggregation, oxidation, and/or glycosylation) and converted into oxLDL; the release of chemokines is necessary for the recruitment of monocytes (CCL2 and CCL5) and T lymphocytes from the bloodstream to the intima. The inflammatory process further accelerates the recruitment and activation of neutrophils, monocytes, and T and B lymphocytes towards the lesion. Finally, the atherosclerotic plaque formed, including rupture, thrombosis, or bleeding. Additionally, platelets, which tend to stick to the intima, contribute to the growth of the atheromatous plaque (69).

One apparent phenotype of SLE is various autoantibody productions such as anti-dsDNA, anti-C1q and anti-Sm, anti-neutrophil cytoplasmic antibodies (ANCA), and antiphospholipid antibodies. Consequently, the immune complexes binding with C1q interrupted cholesterol homeostasis in the arterial wall by inhibiting the expression of two reverse cholesterol transport proteins (CYP27A1 and ABCA1) involved with cholesterol efflux in macrophages for the formation of foam cells (70). Additionally, HDL regulates cholesterol reverse transport. The above explained the phenomenon that decreased HDL was associated with elevated anti-dsDNA and anti-C1q antibodies.

In metabolism studies in patients with SLE, the often-mentioned antibodies to cardiolipin (aCLs) and β2 glycoprotein1 (β2-GP1) are correlated with decreased HDL and ApoA1 (71). A large complex is formed by autoantibodies to β2-GP1 binding to oxLDLs, and the complexes can be taken up by macrophages with the scavenger receptors, by which macrophages are eventually converted to foam cells (72). However, there is no correlation between serum lipids and aCL or anti-β2-GP1 in our study. The possible reason is that total aCL and anti-β2-GP1were measured instead of IgG and IgM aCL and anti-β2-GP1.

The association between serum lipids and SLE cannot directly elucidate the mechanisms causing the metabolic disorder. This should be addressed. Furthermore, apparent heterogeneity was observed in the studies evaluated. Disease duration, CVD exclusion, and the use of lipid-altering drugs showed differences across included studies, which may contribute to this heterogeneity. Meanwhile, there are inherent differences in the study populations, including demographics, gender, ethnicity, and geographic location, and variations in the criteria for inclusion may also contribute to heterogeneity and weaken the strength of the meta-analysis. Based on the above, subgroup analyses were performed to determine whether the included studies combined CVD or not, and the final results were consistent with the results of this study.

In conclusion, this study provided strong evidence for the association between serum lipids and disease activity in patients with SLE. Additionally, dyslipidemia may be a cause of disease aggravation in SLE. Serum lipids in SLE pathogenesis and their implications for clinical diagnosis and treatment require further investigation and confirmative evidence.

Data availability statement

The original contributions presented in the study are included in the article/supplementary material. Further inquiries can be directed to the corresponding authors.

Ethics statement

The studies involving humans were approved by The medical ethics committee of The First Affiliated Hospital of Xiamen University. The studies were conducted in accordance with the local legislation and institutional requirements. The participants provided their written informed consent to participate in this study.

Author contributions

JX: Writing – original draft, Writing – review & editing, Supervision. CD: Data curation, Formal analysis, Methodology, Writing – original draft, Writing – review & editing. HL: Formal analysis, Software, Writing – original draft. YH: Writing – review & editing, Resources. JZ: Resources, Writing – review & editing. XZ: Resources, Writing – review & editing. YS: Funding acquisition, Writing – review & editing. SC: Formal analysis, Methodology, Software, Supervision, Validation, Writing – review & editing. YL: Conceptualization, Funding acquisition, Project administration, Validation, Writing – review & editing.

Funding

The author(s) declare financial support was received for the research, authorship, and/or publication of this article. This work was supported by grants from the National Natural Science Foundation of China (Grant No. 81971496) and the Nature Science Foundation of Fujian Province (Grant No. 2021CXB021) to YL, and the Natural Science Foundation of Fujian Province, China (Grant No. 2022J011381) to YS.

Acknowledgments

All authors would like to thank the researchers for the data used in the meta-analysis of this work. They would also like to express their special thanks to Prof. Zhibin Li (Epidemiology Research Unit, Center of Translational Medical Research, The First Affiliated Hospital of Xiamen University, Xiamen University, Medical School) for his help in reviewing this paper and statistical analysis. The authors thank AiMi Academic Services (www.aimieditor.com) for English language editing and review services.

Conflict of interest

The authors declare that the research was conducted in the absence of any commercial or financial relationships that could be construed as a potential conflict of interest.

Generative AI statement

The author(s) declare that no Generative AI was used in the creation of this manuscript.

Publisher's note

All claims expressed in this article are solely those of the authors and do not necessarily represent those of their affiliated organizations, or those of the publisher, the editors and the reviewers. Any product that may be evaluated in this article, or claim that may be made by its manufacturer, is not guaranteed or endorsed by the publisher.

References

1. Lou H, Ling GS, Cao X. Autoantibodies in systemic lupus erythematosus: From immunopathology to therapeutic target. *J Autoimmun*. (2022) 132:102861. doi: 10.1016/j.jaut.2022.102861

2. Durcan L, O'Dwyer T, Petri M. Management strategies and future directions for systemic lupus erythematosus in adults. *Lancet*. (2019) 393:2332–43. doi: 10.1016/S0140-6736(19)30237-5

3. Shi X, Wang Z, Tang R, Chen W. Podocyte injury and death: New insights into lupus nephritis pathogenesis and therapy. *Rheumatol Autoimmun*. (2023) 3:193–204. doi: 10.1002/rai2.12103

4. Mak A, Isenberg DA, Lau C-S. Global trends, potential mechanisms and early detection of organ damage in SLE. *Nat Rev Rheumatol*. (2013) 9:301–10. doi: 10.1038/nrrheum.2012.208

5. Harden OC, Hammad SM. Sphingolipids and diagnosis, prognosis, and organ damage in systemic lupus erythematosus. *Front Immunol*. (2020) 11:586737. doi: 10.3389/fimmu.2020.586737

6. Accapezzato D, Caccavale R, Paroli MP, Gioia C, Nguyen BL, Spadea L, et al. Advances in the pathogenesis and treatment of systemic lupus erythematosus. *Int J Mol Sci*. (2023) 24(7):6578. doi: 10.3390/ijms24076578

7. Dos Santos M, Veronese FV, Moresco RN. Uric acid and kidney damage in systemic lupus erythematosus. *Clin Chim Acta*. (2020) 508:197–205. doi: 10.1016/j.cca.2020.05.034

8. Ganjali S, Shirmohammadi L, Read MI, Sahebkar A. High-density lipoprotein functionality in systemic lupus erythematosus. *Semin Arthritis Rheumatol*. (2020) 50:769–75. doi: 10.1016/j.semarthrit.2020.05.011

9. Fayyaz A, Igoe A, Kurien BT, Danda D, James JA, Stafford HA, et al. Haematological manifestations of lupus. *Lupus Sci Med*. (2015) 2:e000078. doi: 10.1136/lupus-2014-000078

10. Chen J, Tang Y, Zhu M, Xu A. Heart involvement in systemic lupus erythematosus: a systemic review and meta-analysis. *Clin Rheumatol*. (2016) 35:2437–48. doi: 10.1007/s10067-016-3373-z

11. Parker B, Bruce I. SLE and metabolic syndrome. *Lupus*. (2013) 22:1259–66. doi: 10.1177/0961203313502570

12. El Magadmi M, Ahmad Y, Turkie W, Yates AP, Sheikh N, Bernstein RM, et al. Hyperinsulinemia, insulin resistance, and circulating oxidized low density lipoprotein in women with systemic lupus erythematosus. *J Rheumatol*. (2006) 33:50–6.

13. Lai M, Peng H, Wu X, Chen X, Wang B, Su X. IL-38 in modulating hyperlipidemia and its related cardiovascular diseases. *Int Immunopharmacol*. (2022) 108:108876. doi: 10.1016/j.intimp.2022.108876

14. Bag-Ozbek A, Giles JT. Inflammation, adiposity, and atherogenic dyslipidemia in rheumatoid arthritis: is there a paradoxical relationship? *Curr Allergy Asthma Rep*. (2015) 15:497. doi: 10.1007/s11882-014-0497-6

15. Situnayake RD, Kitas G. Dyslipidemia and rheumatoid arthritis. *Ann Rheum Dis*. (1997) 56:341–2. doi: 10.1136/ard.56.6.341

16. Robertson J, Peters MJ, McInnes IB, Sattar N. Changes in lipid levels with inflammation and therapy in RA: a maturing paradigm. *Nat Rev Rheumatol*. (2013) 9:513–23. doi: 10.1038/nrrheum.2013.91

17. Sun W, Li P, Cai J, Ma J, Zhang X, Song Y, et al. Lipid metabolism: immune regulation and therapeutic prospectives in systemic lupus erythematosus. *Front Immunol*. (2022) 13:860586. doi: 10.3389/fimmu.2022.860586

18. Frostegård J. Systemic lupus erythematosus and cardiovascular disease. *J Intern Med*. (2023) 293:48–62. doi: 10.1111/joim.v293.1

19. Campos-López B, Meza-Meza MR, Parra-Rojas I, Ruiz-Ballesteros AI, Vizmanos-Lamotte B, Muñoz-Valle JF, et al. Association of cardiometabolic risk status with clinical activity and damage in systemic lupus erythematosus patients: A cross-sectional study. *Clin Immunol*. (2021) 222:108637. doi: 10.1016/j.clim.2020.108637

20. Borba EF, Bonfá E. Dyslipoproteinemias in systemic lupus erythematosus: influence of disease, activity, and anticardiolipin antibodies. *Lupus*. (1997) 6:533–9. doi: 10.1177/096120339700600610

21. Gaál K, Tarr T, Lőrincz H, Borbás V, Seres I, Harangi M, et al. High-density lipopoprotein antioxidant capacity, subpopulation distribution and paraoxonase-1 activity in patients with systemic lupus erythematosus. *Lipids Health Dis*. (2016) 15:60. doi: 10.1186/s12944-016-0229-0

22. Aringer M, Costenbader K, Daikh D, Brinks R, Mosca M, Ramsey-Goldman R, et al. 2019 European League Against Rheumatism/American College of Rheumatology classification criteria for systemic lupus erythematosus. *Ann Rheum Dis*. (2019) 78:1151–9. doi: 10.1136/annrheumdis-2018-214819

23. Gladman DD, Ibañez D, Urowitz MB. Systemic lupus erythematosus disease activity index 2000. *J Rheumatol*. (2002) 29:288–91.

24. Higgins JPT, Thompson SG, Deeks JJ, Altman DG. Measuring inconsistency in meta-analyses. *BMJ*. (2003) 327:557–60. doi: 10.1136/bmj.327.7414.557

25. Formiga F, Meco JF, Pinto X, Jacob J, Moga I, Pujol R. Lipid and lipoprotein levels in premenopausal systemic lupus erythematosus patients. *Lupus*. (2001) 10:359–63. doi: 10.1191/096120301669070811

26. Svenungsson E, Jensen-Urstad K, Heimbürger M, Silveira A, Hamsten A, de Faire U, et al. Risk factors for cardiovascular disease in systemic lupus erythematosus. *Circulation*. (2001) 104:1887–93. doi: 10.1161/hc4101.097518

27. Delgado Alves J, Ames PRJ, Donohue S, Stanyer L, Nourooz-Zadeh J, Ravirajan C, et al. Antibodies to high-density lipoprotein and beta2-glycoprotein I are inversely correlated with paraoxonase activity in systemic lupus erythematosus and primary antiphospholipid syndrome. *Arthritis Rheumatol*. (2002) 46:2686–94. doi: 10.1002/art.v46:10

28. Santos MJ, Vinagre F, Silva JJ, Gil V, Fonseca JE. Cardiovascular risk profile in systemic lupus erythematosus and rheumatoid arthritis: a comparative study of female patients. *Acta Reumatol Port*. (2010) 35:325–32.

29. Parra S, Cabré A, Marimon F, Ferré R, Ribalta J, Gonzàlez M, et al. Circulating FABP4 is a marker of metabolic and cardiovascular risk in SLE patients. *Lupus*. (2014) 23:245–54. doi: 10.1177/0961203313517405

30. Park JK, Kim J-Y, Moon JY, Ahn EY, Lee EY, Lee EB, et al. Altered lipoproteins in patients with systemic lupus erythematosus are associated with augmented oxidative stress: a potential role in atherosclerosis. *Arthritis Res Ther*. (2016) 18:306. doi: 10.1186/s13075-016-1204-x

31. Sánchez-Pérez H, Quevedo-Abeledo JC, de Armas-Rillo L, Rua-Figueroa Í, Tejera-Segura B, Armas-González E, et al. Impaired HDL cholesterol efflux capacity in systemic lupus erythematosus patients is related to subclinical carotid atherosclerosis. *Rheumatol (Oxford)*. (2020) 59:2847–56. doi: 10.1093/rheumatology/keaa038

32. Diószegi Á, Lőrincz H, Kaáli E, Soltész P, Perge B, Varga É, et al. Role of altered metabolism of triglyceride-rich lipoprotein particles in the development of vascular dysfunction in systemic lupus erythematosus. *Biomolecules*. (2023) 13(3):401. doi: 10.3390/biom13030401

33. Huang S, Zhang Z, Cui Y, Yao G, Ma X, Zhang H, et al. Dyslipidemia is associated with inflammation and organ involvement in systemic lupus erythematosus. *Clin Rheumatol*. (2023) 42(6):1565–72. doi: 10.1007/s10067-023-06539-2

34. Medina G, Vera-Lastra O, Peralta-Amaro AL, Jiménez-Arellano MP, Saavedra MA, Cruz-Domínguez MP, et al. Metabolic syndrome, autoimmunity and rheumatic diseases. *Pharmacol Res*. (2018) 133:277–88. doi: 10.1016/j.phrs.2018.01.009

35. Lang MG, Vinagre CG, Bonfa E, Freitas FR, Pasoto SG, Brito TS, et al. Hydroxychloroquine increased cholesterol transfer to high-density lipoprotein in systemic lupus erythematosus: A possible mechanism for the reversal of atherosclerosis in the disease. *Lupus*. (2022) 31:659–65. doi: 10.1177/09612033221090127

36. Colom C, Rull A, Sanchez-Quesada JL, Pérez A. Cardiovascular disease in type 1 diabetes mellitus: epidemiology and management of cardiovascular risk. *J Clin Med*. (2021) 10(8):1798. doi: 10.3390/jcm10081798

37. Barbhaiya M, Feldman CH, Chen SK, Guan H, Fischer MA, Everett BM, et al. Comparative risks of cardiovascular disease in patients with systemic lupus erythematosus, diabetes mellitus, and in general medicaid recipients. *Arthritis Care Res (Hoboken)*. (2020) 72:1431–9. doi: 10.1002/acr.v72.10

38. Yurkovich M, Vostretsova K, Chen W, Aviña-Zubieta JA. Overall and cause-specific mortality in patients with systemic lupus erythematosus: a meta-analysis of observational studies. *Arthritis Care Res (Hoboken)*. (2014) 66:608–16. doi: 10.1002/acr.22173

39. Thomas G, Mancini J, Jourde-Chiche N, Sarlon G, Amoura Z, Harlé J-R, et al. Mortality associated with systemic lupus erythematosus in France assessed by multiple-cause-of-death analysis. *Arthritis Rheumatol*. (2014) 66:2503–11. doi: 10.1002/art.38731

40. Croca S, Rahman A. Atherosclerosis in systemic lupus erythematosus. *Best Pract Res Clin Rheumatol*. (2017) 31:364–72. doi: 10.1016/j.berh.2017.09.012

41. Ward MM. Premature morbidity from cardiovascular and cerebrovascular diseases in women with systemic lupus erythematosus. *Arthritis Rheumatol*. (1999) 42:338–46. doi: 10.1002/1529-0131(199902)42:2<338::AID-ANR17>3.0.CO;2-U

42. Ogdie A, Maliha S, Shin D, Love TJ, Baker J, Jiang Y, et al. Cause-specific mortality in patients with psoriatic arthritis and rheumatoid arthritis. *Rheumatol (Oxford)*. (2017) 56:907–11. doi: 10.1093/rheumatology/kew502

43. Jury EC, Peng J, Van Vijfeijken A, Martin Gutierrez L, Woodridge L, Wincup C, et al. Systemic lupus erythematosus patients have unique changes in serum metabolic profiles across age associated with cardiometabolic risk. *Rheumatol (Oxford)*. (2024) 63:2741–53. doi: 10.1093/rheumatology/kead646

44. Kowynia E, Grygiel-Górniak B, Samborski W. Risk factors for lipid disorders in systemic lupus erythematosus. *Rheumatol Forum*. (2023) 9:14–22. doi: 10.5603/RF.2023.0004

45. Fanlo-Maresma M, Esteve-Luque V, Pintó X, Padró-Miquel A, Corbella E, Candás-Estébanez B. Study of common hypertriglyceridaemia genetic variants and subclinical atherosclerosis in a group of women with SLE and a control group. *Lupus Sci Med*. (2022) 9(1):e000774. doi: 10.1136/lupus-2022-000774

46. Kostopoulou M, Nikolopoulos D, Parodis I, Bertsias G. Cardiovascular disease in systemic lupus erythematosus: recent data on epidemiology, risk factors and prevention. *Curr Vasc Pharmacol*. (2020) 18:549–65. doi: 10.2174/1570161118666191227101636

47. Petta I, Peene I, Elewaut D, Vereecke L, De Bosscher K. Risks and benefits of corticosteroids in arthritic diseases in the clinic. *Biochem Pharmacol*. (2019) 165:112–25. doi: 10.1016/j.bcp.2019.04.009

48. Wilkinson MJ, Shapiro MD. Immune-mediated inflammatory diseases, dyslipidemia, and cardiovascular risk: A complex interplay. *Arterioscler Thromb Vasc Biol*. (2024) 44:2396–406. doi: 10.1161/ATVBAHA.124.319983

49. Lai YC, Woollard KJ, McClelland RL, Allison MA, Rye K-A, Ong KL, et al. The association of plasma lipids with white blood cell counts: Results from the Multi-Ethnic Study of Atherosclerosis. *J Clin Lipidol*. (2019) 13:812–20. doi: 10.1016/j.jacl.2019.07.003

50. Svenungsson E, Fei GZ, Jensen-Urstad K, de Faire U, Hamsten A, Frostegard J. TNF-alpha: a link between hypertriglyceridaemia and inflammation in SLE patients with cardiovascular disease. *Lupus*. (2003) 12:454–61. doi: 10.1191/0961203303lu412oa

51. Lozovoy MAB, Simão ANC, Hohmann MSN, Simão TNC, Barbosa DS, Morimoto HK, et al. Inflammatory biomarkers and oxidative stress measurements in patients with systemic lupus erythematosus with or without metabolic syndrome. *Lupus*. (2011) 20:1356–64. doi: 10.1177/0961203311411348

52. Reiss AB. Effects of inflammation on cholesterol metabolism: impact on systemic lupus erythematosus. *Curr Rheumatol Rep*. (2009) 11:255–60. doi: 10.1007/s11926-009-0036-y

53. Andersen CJ. Impact of dietary cholesterol on the pathophysiology of infectious and autoimmune disease. *Nutrients*. (2018) 10(6):764. doi: 10.3390/nu10060764

54. Ronda N, Favari E, Borghi MO, Ingegnoli F, Gerosa M, Chighizola C, et al. Impaired serum cholesterol efflux capacity in rheumatoid arthritis and systemic lupus erythematosus. *Ann Rheum Dis*. (2014) 73:609–15. doi: 10.1136/annrheumdis-2012-202914

55. Rössner S. Further studies on serum lipoproteins in connective tissue diseases. *Atherosclerosis*. (1978) 31:93–9. doi: 10.1016/0021-9150(78)90041-2

56. Robinson G, Pineda-Torra I, Ciurtin C, Jury EC. Lipid metabolism in autoimmune rheumatic disease: implications for modern and conventional therapies. *J Clin Invest*. (2022) 132(2):e148552. doi: 10.1172/JCI148552

57. Gómez Rosso L, Lhomme M, Meroño T, Sorroche P, Catoggio L, Soriano E, et al. Altered lipidome and antioxidative activity of small, dense HDL in normolipidemic rheumatoid arthritis: relevance of inflammation. *Atherosclerosis*. (2014) 237:652–60. doi: 10.1016/j.atherosclerosis.2014.09.034

58. Watanabe J, Charles-Schoeman C, Miao Y, Elashoff D, Lee YY, Katselis G, et al. Proteomic profiling following immunoaffinity capture of high-density lipoprotein: association of acute-phase proteins and complement factors with proinflammatory high-density lipoprotein in rheumatoid arthritis. *Arthritis Rheumatol*. (2012) 64:1828–37. doi: 10.1002/art.34363

59. McMahon M, Grossman J, Skaggs B, Fitzgerald J, Sahakian L, Ragavendra N, et al. Dysfunctional proinflammatory high-density lipoproteins confer increased risk of atherosclerosis in women with systemic lupus erythematosus. *Arthritis Rheumatol*. (2009) 60:2428–37. doi: 10.1002/art.24677

60. Charles-Schoeman C, Watanabe J, Lee YY, Furst DE, Amjadi S, Elashoff D, et al. Abnormal function of high-density lipoprotein is associated with poor disease control and an altered protein cargo in rheumatoid arthritis. *Arthritis Rheumatol*. (2009) 60:2870–9. doi: 10.1002/art.24802

61. McMahon M, Grossman J, FitzGerald J, Dahlin-Lee E, Wallace DJ, Thong BY, et al. Proinflammatory high-density lipoprotein as a biomarker for atherosclerosis in patients with systemic lupus erythematosus and rheumatoid arthritis. *Arthritis Rheumatol*. (2006) 54:2541–9. doi: 10.1002/art.21976

62. Borba EF, Bonfá E, Vinagre CG, Ramires JA, Maranhão RC. Chylomicron metabolism is markedly altered in systemic lupus erythematosus. *Arthritis Rheumatol*. (2000) 43:1033–40. doi: 10.1002/1529-0131(200005)43:5<1033::AID-ANR11>3.0.CO;2-B

63. Chen L, Deng H, Cui H, Fang J, Zuo Z, Deng J, et al. Inflammatory responses and inflammation-associated diseases in organs. *Oncotarget*. (2018) 9:7204–18. doi: 10.18632/oncotarget.23208

64. Medzhitov R. The spectrum of inflammatory responses. *Science*. (2021) 374:1070–5. doi: 10.1126/science.abi5200

65. Soehnlein O, Libby P. Targeting inflammation in atherosclerosis - from experimental insights to the clinic. *Nat Rev Drug Discovery*. (2021) 20:589–610. doi: 10.1038/s41573-021-00198-1

66. Saba PS, Parodi G, Ganau A. From risk factors to clinical disease: new opportunities and challenges for cardiovascular risk prediction. *J Am Coll Cardiol*. (2021) 77:1436–8. doi: 10.1016/j.jacc.2021.01.040

67. Frostegård JSLE. atherosclerosis and cardiovascular disease. *J Intern Med*. (2005) 257:485–95. doi: 10.1111/j.1365-2796.2005.01502.x

68. Ahmad HM, Sarhan EM, Komber U. Higher circulating levels of OxLDL % of LDL are associated with subclinical atherosclerosis in female patients with systemic lupus erythematosus. *Rheumatol Int*. (2014) 34:617–23. doi: 10.1007/s00296-013-2875-0

69. Sircana MC, Erre GL, Castagna F, Manetti R. Crosstalk between inflammation and atherosclerosis in rheumatoid arthritis and systemic lupus erythematosus: is there a common basis? *Life (Basel)*. (2024) 14(6):716. doi: 10.3390/life14060716

70. Reiss AB, Awadallah NW, Malhotra S, Montesinos MC, Chan ES, Javitt NB, et al. Immune complexes and IFN-gamma decrease cholesterol 27-hydroxylase in human arterial endothelium and macrophages. *J Lipid Res*. (2001) 42:1913–22. doi: 10.1016/S0022-2275(20)31518-2

71. Lahita RG, Rivkin E, Cavanagh I, Romano P. Low levels of total cholesterol, high-density lipoprotein, and apolipoprotein A1 in association with anticardiolipin antibodies in patients with systemic lupus erythematosus. *Arthritis Rheumatol*. (1993) 36:1566–74. doi: 10.1002/art.1780361111

72. de Carvalho JF, Bonfá E, Borba EF. Systemic lupus erythematosus and "lupus dyslipoproteinemia." *Autoimmun Rev*. (2008) 7:246–50. doi: 10.1016/j.autrev.2007.11.016

frontiers | Frontiers in Immunology

TYPE Review
PUBLISHED 28 February 2025
DOI 10.3389/fimmu.2025.1561455

Check for updates

OPEN ACCESS

EDITED BY
Anette S. B. Wolff,
University of Bergen, Norway

REVIEWED BY
Kai Kisand,
University of Tartu, Estonia
Christopher Pohlmeyer,
Horizon Therapeutics, United States

*CORRESPONDENCE
Simon H. Pearce
simon.pearce@ncl.ac.uk

RECEIVED 15 January 2025
ACCEPTED 07 February 2025
PUBLISHED 28 February 2025

CITATION
Mavridou M and Pearce SH (2025) Exploring antigenic variation in autoimmune endocrinopathy. *Front. Immunol.* 16:1561455. doi: 10.3389/fimmu.2025.1561455

COPYRIGHT
© 2025 Mavridou and Pearce. This is an open-access article distributed under the terms of the Creative Commons Attribution License (CC BY). The use, distribution or reproduction in other forums is permitted, provided the original author(s) and the copyright owner(s) are credited and that the original publication in this journal is cited, in accordance with accepted academic practice. No use, distribution or reproduction is permitted which does not comply with these terms.

Exploring antigenic variation in autoimmune endocrinopathy

Maria Mavridou[1] and Simon H. Pearce[1,2]*

[1]Translational and Clinical Research Institute, Newcastle University, BioMedicine West, Newcastle-upon-Tyne, United Kingdom, [2]Endocrine Unit, Royal Victoria Infirmary, Newcastle-upon-Tyne, United Kingdom

Autoimmune disorders develop owing to a misdirected immune response against self-antigen. Genetic studies have revealed that numerous variants in genes encoding immune system proteins are associated with the development of autoimmunity. Indeed, many of these genetic variants in key immune receptors or transcription factors are common in the pathogenesis of several different autoimmune conditions. In contrast, the proclivity to develop autoimmunity to any specific target organ or tissue is under-researched. This has particular relevance to autoimmune endocrine conditions, where organ-specific involvement is the rule. Genetic polymorphisms in the genes encoding the targets of autoimmune responses have been shown to be associated with predisposition to several autoimmune diseases, including type 1 diabetes, autoimmune thyroid disease and Addison's disease. Mechanistically, variations leading to decreased intrathymic expression, overexpression, different localisation, alternative splicing or post-translational modifications can interfere in the tolerance induction process. This review will summarise the different ways genetic variations in certain genes encoding endocrine-specific antigens (INS, TSHR, TPO, CYP21A2, PIT-1) may predispose to different autoimmune endocrine conditions.

KEYWORDS

immunogenetics, autoimmune thyroid disease, thymus, central tolerance, Graves' disease, Addison's disease, type 1 diabetes

Introduction

Autoimmune endocrinopathies are, almost by definition, organ-specific autoimmune diseases whereby one specific hormone-secreting gland or tissue becomes the target of the immune response leading to immune-mediated destruction and, over time, clinical hormonal deficiency (1–3). Only Graves' disease (GD) deviates from this paradigm with stimulatory antibodies rather than a destructive immune response leading to organ hyperactivity and frequent clinical manifestations outside the primary organ of involvement (i.e. Graves' orbitopathy). These disorders are mostly inherited as complex genetic traits with a multigenic basis, that is variations in numerous genes (typically 50 or more identified to date) each contribute a small degree towards the proclivity to clinical autoimmune disease (2, 4). Perhaps unsurprisingly, it has been more straightforward to identify genetic variations in immune-related genes that contribute to multiple autoimmune disorders, than to identify

those disease or organ-specific variations. Many of these immune-related variants contribute to the susceptibility to more than one autoimmune condition, including both endocrine conditions and additional non-endocrine, organ-specific disorders (1–4). Some of the variants involved in several conditions are briefly reviewed in the next section.

Whilst the common autoimmune endocrinopathies are inherited as complex multigenic traits, there are two Mendelian conditions which provide relevant insights into mechanisms of immune tolerance. The first condition is the APECED (Autoimmune polyendocrinopathy, candidiasis and ectodermal dystrophy)/APS1 (autoimmune polyglandular type 1) syndrome, which is most frequently owing to loss of function mutations in both alleles of the AutoImmune REgulator (AIRE) gene (5). AIRE is expressed in thymic epithelial cells where it controls expression of transcripts relevant in thymic T cell selection. Defective AIRE function abrogates expression of certain self-peptides in antigen-presenting cells which is essential for educating the developing thymic T cell repertoire and leads to failure to delete T cells expressing potentially autoreactive T cell receptors. APS1 is characterised by high penetrance (70-90%) of autoimmune Addison's disease (AAD, autoimmune primary adrenal insufficiency) and autoimmune hypoparathyroidism (5). Both of these conditions are rare outside the context of APS1, with a prevalence of one in 8,000 in the sporadic population for AAD, showing the critical role of central thymic tolerance in this condition.

More recent findings have also highlighted the contribution of common genetic variants in the *AIRE* gene to the susceptibility of AAD in a Swedish cohort. The minor alleles of four intronic strongly linked SNPs, rs9983695, rs2075875, rs2075876, and rs6220374, have been shown to have significantly lower frequency in Swedish AAD patients (approximately 4%) compared to healthy controls (ranging from 10% to 11%) (6). Although none of these variants overlap with known transcription factor binding sites, their strong linkage suggests they may play a regulatory role in AIRE's function. This suggests that thymic antigen presentation is not just important in Addison's disease associated with APS1, but perhaps unsurprisingly with sporadic AAD as well (6).

The role of AIRE gene variants in APS1 contrasts to the IPEX (Immune dysregulation, polyendocrinopathy, enteropathy, X-linked) syndrome, caused by defects in the *FOXP3* gene, encoding the critical transcription factor for development of regulatory T cells (7). IPEX is X-linked, giving rise to autoimmune diabetes before the age of 1yr in around 50% of affected boys, and signalling failure of peripheral tolerance as the primary mechanism. Thus, these 2 monogenic disorders demonstrate that genetic variants can impact the establishment and maintenance of immune tolerance via different mechanisms including on central T cell selection or by influencing peripheral regulatory lymphocyte function (5, 7).

Brief review of immune system genetic variation in endocrine autoimmunity

Genome-wide association studies (GWAS) on patient cohorts with autoimmune endocrine disorders have revealed that most of the gene variants currently associated with autoimmunity encode proteins that have a role in the antigen recognition, and lymphocyte activation and inactivation pathways (3, 8). Whilst the focus of this review concerns gene variants that confer organ-specificity to the disease, that is the antigen or target-organ specific gene variants, we first make a brief review of the variants in immune system genes that have well-established roles in endocrine autoimmunity, with many of these variants contributing to disease risk in multiple different conditions (Table 1).

The locus that has the strongest effect in the predisposition to most autoimmune disorders is the MHC, encoding the human leukocyte antigen (HLA) molecules. This locus spans a large interval on the short arm of chromosome 6, with numerous different HLA genes, each with many different alleles which may either confer risk or protection from autoimmunity. Most studies have identified associations of HLA class II alleles and certain HLA-DRB1-DQA1-DQB1 haplotypes with autoimmune endocrine disorders, implying the essential role of binding and presentation of endocrine antigens to CD4+ T cells in the pathogenesis of particular diseases. It is thought that variants in DR and DQ genes encode proteins that might bind self-peptides with lower affinity, potentially inadequate for the central elimination of autoreactive T cells resulting in impaired tolerance (8, 9). An alternative scenario suggests that certain DR and DQ proteins communicate inefficiently with the TCRs on Tregs leading to the generation of a Treg population that is unable to control autoreactive T cells. Additionally, variations in HLA class I genes have been also linked with susceptibility to autoimmunity. However, the strong Linkage Disequilibrium (LD), a term used to describe the non-random association between alleles of two or more genetic loci, between HLA class I and class II loci and the abundance of alleles often poses a difficulty in the identification of linked alleles having independent association with a phenotype (9, 10).

The PTPN22 gene encodes the Lymphoid-tyrosine phosphatase (LYP) which is implicated not only in T and B cell signalling cascades, but also in natural killer (NK) cell and myeloid cell pathways. LYP acts by blocking T cell activation as it dephosphorylates CSK kinase and stops the downstream signal transduction. The rs2476601*T allele which leads to the Arg620*Trp substitution has been associated with autoimmune disorders including T1D and GD, with the variant having also been linked with relapse of GD after antithyroid treatment (11, 12). The Arg620*Trp variant is located in a highly conserved point in the

TABLE 1 Immune system genes linked to autoimmune endocrinopathies.

Locus	Gene	Disease
6p21	HLA class II	T1D, GD, HT, AAD
1p13	PTPN22	T1D, GD
2q33	CTLA4	T1D, GD, AAD
6q15	BACH2	T1D, GD, AAD,
10p15	IL2RA	T1D, GD, AAD

Genes involved in the immune system regulation with a role in the development of endocrine autoimmune disorders and their loci. T1D, Type 1 Diabetes; GD, Graves' Disease; HT, Hashimoto's Thyroiditis; AAD, Autoimmune Addison's Disease.

P1 motif of the catalytic domain of LYP, suggesting the potential to directly affect phosphatase activity (13). The exact underlying mechanism is unclear as some studies have shown that this variant results in an LYP with loss of function that cannot inhibit T cell activation, whilst others suggest that the variant produces an LYP with gain of function and elevated inhibitory effect on T cell signalling pathway. The relevance of these investigations might be limited, though, as several of these functional studies have been conducted on the ortholog of LYP in mice, which shares 90% similarity in the catalytic and 60% similarity in the non-catalytic domains with the human homolog (1, 3, 8, 10, 14–17). More recent studies, however, suggest that the role of the substitution might be different depending on the cellular context in which the protein is expressed, or the location of the protein, implying that LYP might have a multifunctional role in the autoimmunity development (18). In particular, the variant might have a gain of function effect leading to an even stronger blocking of TCR signalling, and a subsequent diminished negative selection of autoreactive T cells in the thymus, and a reduced response to the BCR signal, and consequently hyper-responsive B cell populations. However, Zhang *et al.* have shown that in Jurkat T cells transduced with plasmids carrying the mutated LYP, and in PBMC obtained from rheumatoid arthritis (RA) patients homozygous for the risk allele, the Arg620*Trp substitution makes the protein more susceptible to intracellular degradation and therefore the variant leads to weaker inhibitory effects (19). Additionally, the variant leads to an LYP with loss of function in myeloid cells as it exhibits reduced interaction with TRAF3 and reduced amounts of TLR-induced type I IFNs (16–18, 20–22). These results suggest that there are pleiotropic effects with a gain of function phenotype centrally, along with loss of function effect in peripheral immune cells and, even more interestingly, different regulatory effects in lymphocytes than in myeloid cells (16, 17, 19, 23–25).

The Cytotoxic T-Lymphocyte Associated Protein 4 (CTLA4) is encoded by the *CTLA4* gene and is an inhibitory co-stimulatory receptor which binds to B7 molecules on the surface of antigen presenting cells, and consequently, downregulates their activation. Amongst the polymorphisms which have been associated with autoimmune disorders, the variant rs231775*G on the exon 1, and an $(AT)_n$ repeat in the 3'-untranslated region (UTR) of the *CTLA4* gene have been linked to T1D and AAD. Both variants are associated with decreased expression of *CTLA4*, reducing levels of inhibitory signalling and, therefore, unchecked T cell activation. In addition, the frequency of rs3087243*G allele on the 3'-UTR of *CTLA4* gene is higher in GD and Hashimoto's thyroiditis (HT) patients than in healthy controls, with the allele also being associated with a reduction on the beneficial effects of anti-thyroid treatment in a Polish cohort with GD (26–29). The importance of the molecule can be understood by the fact that people with null *CTLA4* alleles develop immunodeficiency as a form of an autosomal dominant immune dysregulation syndrome, characterised by hypogammaglobulinemia and recurrent infections with several tissues being affected, whilst *CTLA4*-Knockout (*CTLA4*-KO) mice develop fatal lymphoproliferative disease in the first weeks of life (30).

BACH2 transcription factor (BTB and CNC Homology 1, Basic Leucine Zipper Transcription factor 2) is expressed predominantly in B lymphocytes and plays a vital role in regulating CD4+ T-cell differentiation. Its functions include repressing effector CD T-cell lineages (Th1, Th2, and Th17), and it is crucial for the formation of regulatory T cells. The intronic BACH2 variant rs3757247*T has been associated with susceptibility to AAD as the frequency of the risk T allele is significantly higher in UK AAD patients compared to controls (31). The frequency of the risk allele has been also found higher in Polish patients with autoimmune polyendocrine syndromes (APS) (*and in 6 Japanese T1D patients* (32)) compared to healthy individuals (33). Additionally, a recent study revealed a correlation between the risk T allele and the existence of circulating autoantibodies against thyroid peroxidase (TPO) in first-degree relatives of (Polish) AAD patients (34).

rs3757247 is in complete LD with the intronic rs11755527, rs72928017 and rs72928038 variants, with rs11755527 having been linked to susceptibility to T1D in northern European (35) and Pakistani populations (36), however no association was found in a Brazilian population (37). rs3757247 and rs11755527, along with another intronic SNP, rs2474619, have been associated with GD in a Chinese Han population with rs2474619 determined as the most disease-associated variant (11, 38). rs72928038*A allele has been associated with risk of development of T1D as the variant leads to lower expression of *BACH2* in multiple cell types, but mainly in T cells (39). The risk allele has been shown to impede the binding of the ETS1 transcription factor leading to decreased enhancer activity (39, 40). rs72928038*A has been also correlated with GD and HT in a UK cohort (11, 41). Thus, the exact molecular mechanisms by which the genetic variants affect gene regulation and the unravelling of the causative variant remain unidentified and require further investigation.

Interleukin-2 (IL-2) is a key driver of T cell maintenance, proliferation, and development. Polymorphisms on the gene encoding the alpha subunit of the IL-2 receptor (CD25) have been associated with T1D, GD *(and AAD although with contradictory results in different populations: UK-Norway)*. Amongst those, T1D patients carrying the intronic rs2104286*C allele have lower *CD25* expression on their naïve CD4+ T cells, but higher levels of soluble CD25. Thus, the variant could lead to an impaired IL-2 signalling transduction and lower responsiveness of T cells to IL-2 effects. Such a decrease in IL-2 signalling might have a sequential impact on *FOXP3* expression and Tregs activity, with the protective minor allele of the variant rs12722495 probably acting in an opposite way (10, 14, 42–44).

Identification of susceptibility loci is a complex process as the genes involved in disease pathogenesis are often in LD. Furthermore, power is frequently limited by cohort size, meaning that reproducibility is a key issue. Furthermore, genetic heterogeneity between affected patients of different ethnicities is not unexpected, complicating the interpretation of some studies (3, 8, 10, 14, 15). A deep understanding of the genetic – epigenetic interactions in

combination with environmental triggering events (viral or bacterial infections, alteration of gut and oral microbiome) that might have additional effects is required for an accurate unravelling of the multiple pathogenesis mechanisms of autoimmunity (45).

Role of target-organ genes in endocrine autoimmunity

Insulin gene variation in Type 1 Diabetes

Type 1 Diabetes Mellitus (T1D) is a chronic disease which is characterised by the autoimmune destruction of the insulin secreting β cells in the pancreatic islets by T lymphocytes (CTLs), leading to insulin deficiency. Similar to other autoimmune disorders, it is believed that a combination of numerous genetic variants, each with a small effect, along with environmental factors are implicated in the pathogenesis (46). These various susceptibility loci have been labelled as *IDDM1, IDDM2* etc. in chronological order of discovery, with *IDDM1* residing in the MHC on chromosome 6p21. As well as being the hormone that is deficient in T1D, insulin autoantibodies and T cell responses against insulin peptides are also central to its pathogenesis (46, 47). However, autoantibodies to other islet cell protein targets including glutamic acid decarboxylase (GAD) and insulinoma-associated 2 (IA-2) are highly prevalent and may predate the onset of T1D by many years.

One of the non-HLA loci involved in the disease susceptibility is a variable number of tandem repeats (VNTR) region upstream of the start codon of the insulin gene, *INS*, on chromosome 11. The region, which has also been known as the *IDDM2* locus, is a minisatellite as it consists of repeats of a 14bp sequence with variable length; alleles have been distinguished by repeat number with class I alleles having a shorter length, whilst classes II and III have more repeats of the sequence (47–54). Studies in T1D patients and healthy controls have shown that *IDDM2* class I alleles are associated with the disease susceptibility, with class I homozygosity increasing the risk for the disease development by 2-5 times (53). On the contrary, class III alleles, even in heterozygosity, have been shown to be dominantly protective.

Studies on the mRNA levels of insulin have shown that class I alleles are associated with increased *INS* mRNA levels in the pancreas compared to class III alleles (47, 50, 52). However, the opposite effect has been observed in human thymus, where class I alleles have been linked to decreased *INS* expression compared to class III alleles. Therefore, it is believed that the mechanism by which *IDDM2* class I and III alleles can regulate the predisposition to T1D is by controlling the thymic expression levels of the insulin gene and its subsequent epitope presentation by HLA molecules to maturing T cells (50). With lower thymic expression of insulin peptides in VNTR class I carriers, some INS-reactive TCR-carrying T cells escape clonal deletion leading to autoreactivity and ultimately T1D. Experiments in which insulin gene copy numbers were manipulated in knockout (KO) mice, confirm that thymic *INS* expression is strongly genetically determined and that animals with low or absent thymic insulin mRNA had autoreactive peripheral T cell clones against insulin. Conversely, mice with high thymic insulin expression were protected from insulin autoreactivity (55).

A genetic study involving detailed phenotyping of German families with children at risk of developing T1D confirmed that the short, class I VNTR was associated with early onset diabetes. Interestingly, individuals with the dominantly protective class III VNTR had a lower risk of developing insulin autoantibodies, but had similar rates of GAD and IA2 antibodies, supporting that this variation at the *INS* locus was acting directly to determine the prevalence of insulin autoreactivity (56).

Although it might not be intuitively obvious that variations leading to high expression of an autoantigen might protect against autoimmune disease, these experiments in both human and rodent demonstrated for the first time that thymic gene expression forms a critical tolerogenic mechanism that may be affected by naturally occurring human genetic variation.

Graves' disease

Graves' disease (GD) is a common autoimmune disorder of the thyroid gland characterised by the continuous activation of the thyroid stimulating hormone receptor (TSHR) by autoantibodies, leading to hyperthyroidism. Although the reason why these TSH receptor stimulating antibodies, known as TRAb, occur is unknown, it is believed that, again, an interaction of environmental and genetic factors might trigger their appearance (57–60). TRAb are central to disease pathogenesis and circulating TRAb concentrations correlate tightly with disease severity and clinical outcome (61). Unlike T1D which has an approximately equal gender distribution, GD affects 5-8 times more women than men. The TSHR is a G protein-coupled receptor, consisting of an extracellular A subunit, bound to a transmembrane domain (B) subunit by a flexible hinge region. The immunodominant T cell and B cell epitopes reside within the extracellular A-subunit. Soluble, circulating A subunits are shed from the cell membrane and found in the circulation, where they may consist of several homo-oligomeric forms (62).

Amongst the genetic loci associated with GD susceptibility, HLA-*DRB1*, *PTPN22*, *CTLA-4*, there is also the *TSHR* gene which encodes the main autoantigen. Studies on the non-coding regions of the *TSHR*, showed that the A allele in the intronic rs179247 SNP is strongly associated with disease susceptibility, whilst it is also linked to the earlier onset of the disease (57, 59, 60, 63). Analysis of the *TSHR* expression revealed that although the polymorphism does not have any effect on the expression levels in the thyroid gland, it can influence the mRNA levels in the thymus. More specifically, individuals homozygous for the high-risk A allele have been shown to have lower *TSHR* expression levels in their thymus compared to people carrying the protective G allele, with G/G homozygous showing the higher *TSHR* expression (57, 59). Thus, it has been suggested that, with similarities to the *INS* situation for T1D, a gene variant that regulates (mRNA or protein) expression quantitatively in the thymus, can lead to the disease development through inadequate recognition of 'autoreactive' T cells and breakdown of negative T cell selection.

An alternative mechanism which has also been suggested, though, links the high-risk rs179247*A allele with alternative splicing of the *TSHR* gene. Studies have shown that people carrying the rs179247*A allele have lower levels of the full-length *TSHR* mRNA, and increased levels of two alternative shorter truncated transcripts in the thyroid gland. These alternative forms lack the transmembrane and the hinge region and therefore lead to the production of soluble TSHR isoforms, similar to the A-subunit part of the receptor (59, 63–72). These secreted TSHR forms can be presented and contribute to the loss of peripheral tolerance (57, 59). Additionally, elevated levels of these soluble isoforms compared to the full-length receptor might result in increased production of autoantibodies against TSHR, as it has been shown that the A-subunit of the receptor is the main target of the autoantibodies and also promotes the affinity maturation of the B cells producing thyroid-stimulating antibodies (68, 72).

However, a more recent study measuring the expression levels of the different isoforms has shown that the disease-associated genotype was associated with higher levels of the alternative splice variants in the thymus, and not in the thyroid, implying that these might have a role in the induction of the central tolerance in the thymus instead (57). In contrast to the case of *INS*, it has been proposed that expression of non-immunodominant TSHR epitopes in thymus could have a role in inducing tolerance (57).

rs12101255, another SNP linked to the disease susceptibility, in intron 1 of the *TSHR* gene, is in complete LD with its adjacent rs12101261. The two polymorphisms were found to overlap with a region of monomethylated histone 3 lysine 4 (H3K4me1), a chromatin modification induced by IFN-α, during a viral infection (59, 60, 63). The region has been shown to be critical for the *TSHR* expression as it is the binding site of the promyelocytic leukaemia zinc finger (PLZF) transcription factor. PLZF binds with a stronger affinity in individuals homozygous for the high-risk rs12101261*T allele, and is correlated with lower intrathymic expression of *TSHR*, compared to people homozygous for the protective allele C (Figure 1) (59, 60, 63). Thus, an environmental event, such as a viral infection, might influence the expression of an autoantigen gene in individuals carrying the high-risk allele of this variant. Decreased expression of the *TSHR* in the thymus, induced by IFN-α production, in a susceptible individual could trigger autoimmunity development through failure to delete autoreactive T cells (59, 60, 63, 73–76).

The first SNP which has been associated with the disease susceptibility in Caucasians (UK and Polish populations), rs2268458 (77), is located in the same 40-kb region of intron 1 of *TSHR* gene together with rs179247, rs12101255 and rs12101261, and all of them are in moderate LD posing additional difficulty in the dissection of the causative SNP. However, logistic regression analysis on the most highly associated SNPs, rs179247 and rs12101255, performed by a group studying the association of their minor alleles with elevated expression of the truncated isoforms of the receptor in UK and Polish Caucasians, revealed that the rs12101255 might drive the association of the nearby variants (64, 78, 79), although rs179247 had previously been shown as the variant with the strongest association with the disease in UK GD patients (64).

Meta-analysis of different studies showed that there is a level of consistency in the results amongst Caucasian and Asian populations. Although the high-risk alleles in intron 1 were confirmed in a Spanish GD cohort (63), interestingly, a study in Japanese GD patients in 2005 revealed the existence of SNPs in introns 7 and 8 of *TSHR* that were also associated with the disease, and this association was confirmed when these variants were tested in a UK GD cohort (64, 79, 80). More recent studies performed by the China Consortium for the Genetics of Autoimmune Thyroid Disease confirmed the association of the intron 1 variants (rs12101261) with the disease susceptibility in Chinese patients, but did not show significant association of the intron 7 variants that had been previously detected in a Japanese cohort (76). These results indicate that although there may be complex LD patterns that vary between ethnicities, variants on intron 1 of the *TSHR* play an important role on the disease susceptibility in Caucasian and Asian populations (64, 78–80).

Hashimoto's thyroiditis

Hashimoto's thyroiditis (HT), the most common autoimmune disorder, causes destruction of the thyroid gland by lymphocytic infiltration and leads to hypothyroidism. The presence of circulating autoantibodies against the main thyroid antigens, thyroid peroxidase (TPO) and thyroglobulin (Tg) is crucial for the diagnosis, but the mechanism behind their occurrence is not yet known. Twin studies have shown that genetic susceptibility plays a role in the disease development, but environmental events, such as stress and iodine consumption, also contribute to disease onset (81–83).

TPO is an enzyme involved in the biosynthesis of the thyroid hormones T4 and T3 and is encoded by the *TPO* gene located on chromosome 2. It is uniquely expressed in thyroid. Polymorphisms in the *TPO* gene have been associated with both the development of the disease and the levels of circulating autoantibodies. The rs2071400 SNP in the promoter of *TPO* has been shown to have a potential role in the disease pathogenesis. Studies have shown that the prevalence of the rs2071400*T allele is significantly higher in people with hypothyroidism than in healthy controls. In addition, homozygosity for the rs2071400*T variant is significantly more frequent in individuals with hypothyroidism compared to healthy people (81, 84–88). These findings suggest that the rs2071400*T allele is a risk factor for the development of hypothyroidism. Another variant which has been linked with disease predisposition (in an Indian population) is the missense variant, rs732609, in exon 12 of the *TPO gene*, with rs732609*C occurring more frequently in patients with hypothyroidism than in controls, and therefore conferring risk for the disease onset. Substitution of the A allele with C, leads to the change of Threonine725 to Proline, which is predicted to be a structurally tolerated substitution. However, this may still alter expression of *TPO* or its enzymatic activity (85, 88–90).

The large extracellular domain of TPO is structurally homologous to the enzyme myeloperoxidase (MPO) and the threonine 725 (Thr725) residue is located within this MPO-like domain of TPO (Figure 2). This domain is crucial for the activity

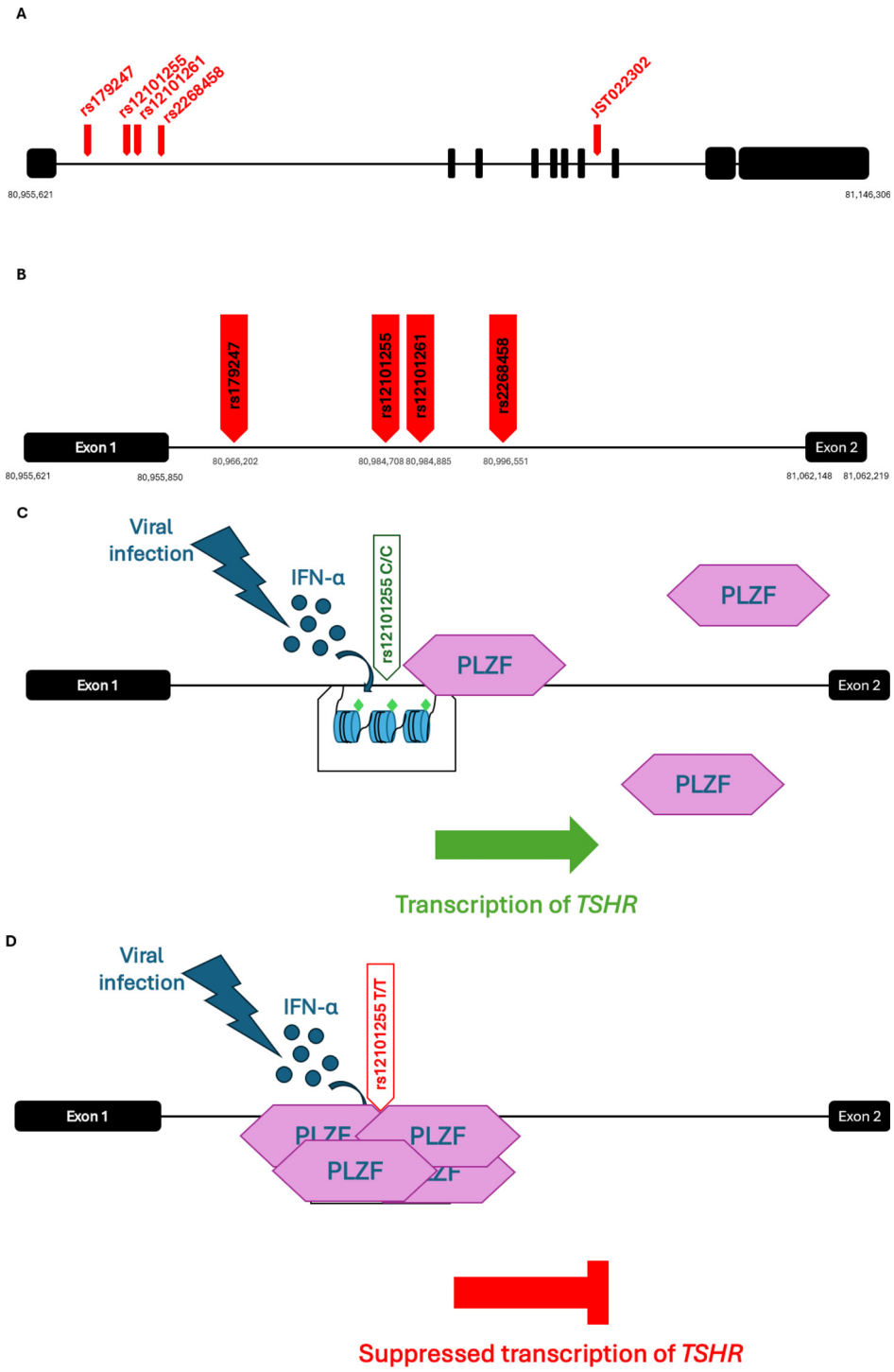

FIGURE 1
(A) Schematic representation of the GD-associated SNPs on the *TSHR* gene. The 10 exons are represented as black squares and SNPs as red arrows. The minor allele of the polymorphism JST022302 in intron 7 has been associated with the disease in a Japanese cohort (64, 79, 80) **(B)** Schematic representation of the GD-associated SNPs in intron 1 of the *TSHR* gene. **(C, D)** Effects of environmental events on individuals with genetic predisposition to GD; IFN-α is secreted in response to a viral infection event and induces monomethylation at the Lysine 4 of Histone 3 (H3K4me1) (represented as green diamond shapes) in the intronic region of TSHR containing the disease-associated variants. The transcription repressor PLZF binds with a stronger affinity in people homozygous for the high-risk rs12101261*T allele **(D)**, than in individuals homozygous for the protective C allele **(C)**. Thus, a viral infection can cause a reduction in the expression of *TSHR* in the thymus of people carrying the high-risk allele of the variant **(D)**, and therefore lead to a decreased presentation of the protein epitopes to T cells. GD, Graves' Disease; TSHR, thyroid stimulating hormone receptor; IFN-α, Interferon alfa; PLZF, promyelocytic leukemia zinc finger transcription factor. [Image created in PowerPoint and adapted from (59, 73, 130)].

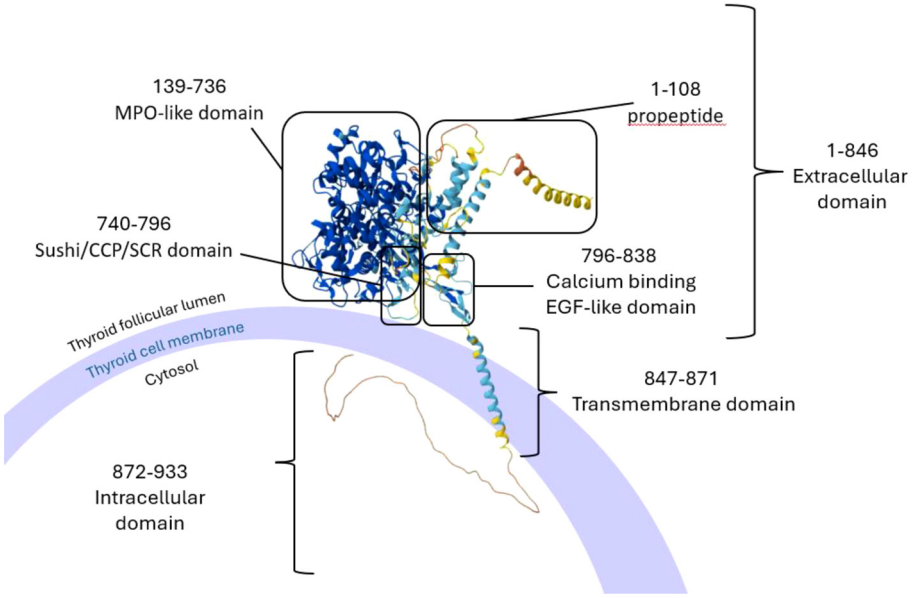

FIGURE 2
Schematic representation of the structure of TPO with its domains as it is bound on the membrane of thyroid cells. Image created in PowerPoint with the structure of the protein created by AlphaFold and the domains analysed by InterPro (result/InterProScan/iprscan5-R20241108-164444-0398-33458951-p1m/Overview). AlphaFold produces a per-residue model confidence score (pLDDT) between 0 and 100. Some regions below 50 pLDDT may be unstructured in isolation. Very high (pLDDT > 90) is shown in dark blue, high (90 > pLDDT > 70) in cyan blue, low (70 > pLDDT > 50) in yellow and very low (pLDDT < 50) in orange. TPO, thyroid peroxidase, MPO; myeloperoxidase; CCP, complement control protein; SCR, short consensus repeat; EGF, epidermal growth factor. Image adapted from (91, 92, 131).

of the enzyme, and therefore substitution of Threonine with Proline might have an impact on the enzyme's peroxidase activity. The residue is also close to an immunodominant B cell epitope of TPO, consisting of nine amino acids, and is recognised by the well-characterised monoclonal TPO antibody, MAb-47. Studies have shown that the MAb-47 recognises the native structure of human TPO, and thus there is a possibility that the nearby residues play a crucial role in the maintenance of the conformational structure of the epitope (91–94).

Similar to sodium iodide symporter (*NIS*), and *TSHR*, expression of *TPO* has been detected in the Hassall's corpuscles of human thymus tissue, although it was found to be expressed at lower levels compared to other thyroid antigens like Tg and TSHR by a Korean study. The same study showed a correlation between the expression levels of TPO and age, as TPO expression in the thymus was shown to be increased with increasing age (95). Another study by Misharin *et al.* on *AIRE*-KO mice, which investigated the correlation between AIRE and the expression of thyroid antigens in the thymus, revealed that intrathymic *TPO* expression was absent in AIRE deficient animals, whereas *Tg* and *TSHR* were still expressed, albeit at reduced levels (96, 97).

Thyroglobulin (Tg), the precursor molecule of T3 and T4 hormones, is encoded by the *Tg* gene which is located on chromosome 8. Although association studies have linked this locus with predisposition to autoimmune thyroid disorders in general, studies on HT patients have shown that the rs180195*G allele in the promoter region of the *Tg* gene is significantly more frequent in HT patients than in healthy individuals (75, 87, 98, 99). Substitution of the wild-type A allele with G, leads to an increase in the activity of the *Tg* promoter through the modification of the transcriptional activator interferon regulatory factor 1 (IRF-1) binding site. IRF-1 is activated in response to IFNAR signalling pathway and controls the expression of IFN-induced genes (75). It is possible, then, that an increase in IFN levels/activity as a protective mechanism against a potential infection could cause an increased expression of the *Tg* gene and therefore elevated presentation of the Tg epitopes. This finding can possibly explain the development of thyroid autoimmunity in people who have previously received IFN-α treatment and poses another example of genetic-epigenetic and environmental factors interaction for the induction of autoimmunity (75, 82, 87).

The rare splice site variant, c.1076-1G > C, which leads to the deletion of the whole of exon 9 of the *Tg* gene, has been found in all affected members of a family with early HT onset (100, 101). The shorter transcript, produced by the variant, might lead to the synthesis of a misfolded protein. Misfolding would either lead to an immunogenic isoform or expose different epitopes of the peptide sequence compared to the wild-type Tg (Figure 3). If the misfolded isoform is bound to MHC class II molecules, these alternative epitopes would not be recognised as 'self' by T cells, as they are not presented under normal conditions, and therefore activate an immune response; whilst if they manage to avoid intracellular degradation, they might also modify the level of post-translational modifications of the Tg, such as iodination (100–103). Although we cannot be sure about the mechanism causing this phenotype, the presence of autoantibodies against the Tg and the TPO in these patients implies that there is ongoing immunogenicity. Additionally, it is worth considering that any condition leading to

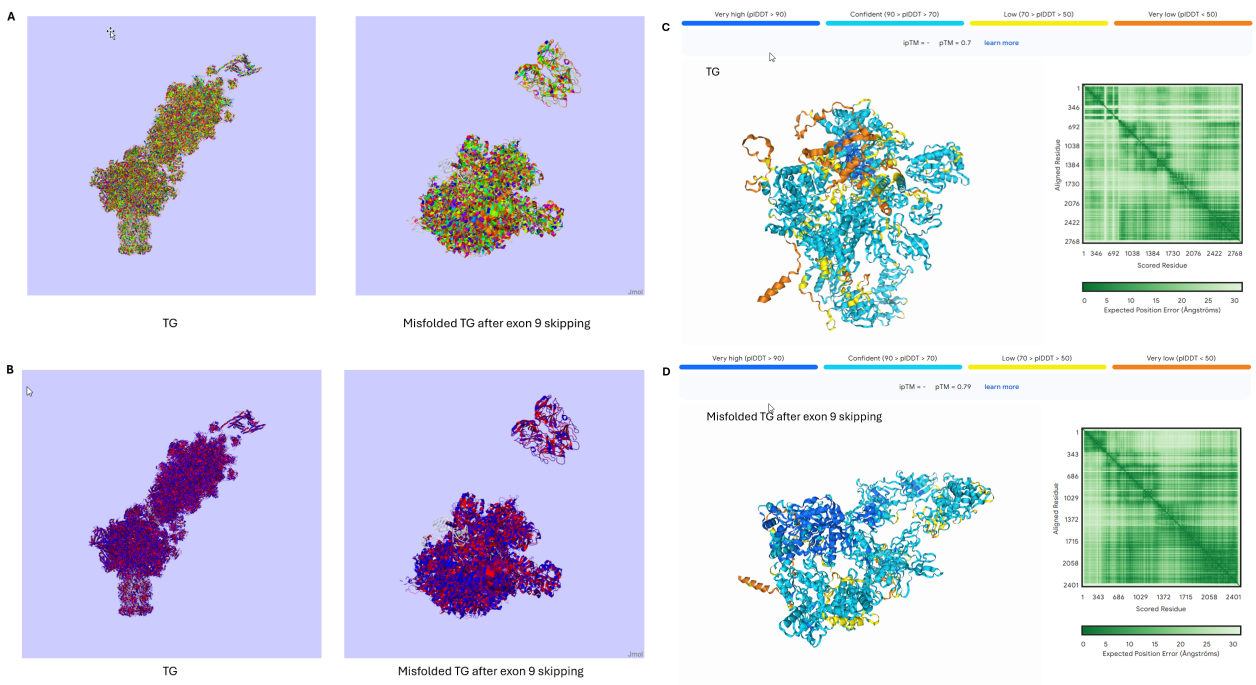

FIGURE 3
3D structures of the normal TG and the misfolded TG after the skipping of exon 9 (introduced by the rare variant c.1076-1G > C). **(A)** Taylor colour schemes highlighting the amino acids based on their physicochemical properties. Figures created in Jalview 2.11.4.1. **(B)** Hydrophobicity colour schemes highlighting the amino acids based on their hydrophobicity. Figures created in Jalview 2.11.4.1. **(C, D)** Prediction of the 3D structures of the normal TG **(C)** and the misfolded TG protein **(D)** based on their amino acid sequences. Figures created in Alphafold server. AlphaFold produces a per-residue model confidence score (pLDDT) between 0 and 100. Some regions below 50 pLDDT may be unstructured in isolation. Very high (pLDDT > 90) is shown in dark blue, high (90 > pLDDT > 70) in cyan blue, low (70 > pLDDT > 50) in yellow and very low (pLDDT < 50) in orange. TG, Thyroglobulin.

increased thyroid cell turnover might predispose to autoimmunity. Co-existing autoimmune thyroiditis has been well-documented in conditions such as resistance to thyroid hormone beta (RTHβ) and Pendred's syndrome, both of which are associated with goiter through distinct mechanisms. In RTHβ, mutations in the thyroid hormone receptor beta gene lead to impaired feedback regulation of the hypothalamic-pituitary-thyroid axis and persistent TSH stimulation of the thyroid with higher cell turnover and goiter, which may expose cryptic antigens and increase susceptibility to autoimmune thyroid diseases such as HT and GD (104–106). Similarly, Pendred's syndrome is characterised by mutations in the *SLC26A4* gene and causes thyroid dyshormonogenesis and deafness. Chronic TSH stimulation therefore leads to thyroid enlargement (goitre) and potentially in susceptible individuals increased thyroid antigen expression (106–109). Thus, loss of function Tg variants are known to impair thyroid hormone synthesis leading to congenital dyshormonogenetic goiter, and hypothyroidism. Genetic variants leading to less profoundly reduced Tg function (e.g. c.1076-1G > C), might be associated with inefficient rather than absent thyroid hormone synthesis and could lead to autoimmunity by means of increased TSH and thyrocyte turnover, goiter and higher thyroid antigen expression.

Studies on mice with experimental autoimmune thyroiditis (EAT), a murine model of HT, have proposed the co-existence of two T cell populations; the Tg-reactive T cells and the natural CD4 +CD25+ nTregs that are specific for the Tg (110). These studies have shown that continued Tg epitope presentation is essential in order to maintain a population of nTregs which are critical for the

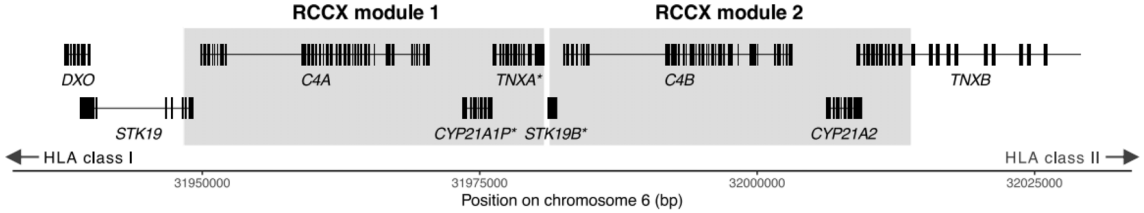

FIGURE 4
Schematic representation of the most common form of the RCCX cassette in healthy individuals, with pseudogenes noted with an asterisk. Figure adapted by Figure 1A of Lundtoft *et al.* (122).

control of Tg-reactive T cells in the periphery. Decreased levels of Tg in the circulation or presentation of alternative epitopes might disturb the balance required for the nTregs maintenance, and therefore lead to 'escaped' Tg-reactive T cells (81, 110, 111). This mechanism of peripheral tolerance contrasts to that demonstrated for insulin gene expression in the thymus.

Autoimmune Addison's disease

Autoimmune Addison's disease (AAD) is a rare autoimmune endocrine condition characterised by the destruction of the adrenal cortex. Autoantibodies against the steroid 21-hydroxylase (21-OHase) enzyme are detected in most patients, with the underlying mechanism for their production, though, remaining unclear (1, 8, 112). Given the fact that 21-OHase is an intracellular enzyme and unlikely to be accessible to circulating autoantibodies, their direct pathogenic role has never been demonstrated. However, the existence of antigen-specific T cells in the blood of AAD patients has been demonstrated and the presence of CD4+ and CD8+ T cells bearing 21-OHase-specific TCRs against two immunodominant 21-OHase epitopes has been confirmed, demonstrating the central contribution of Cytotoxic T cells to disease progression (8, 113, 114). Like in other autoimmune endocrine disorders, studies on twins and family members of AAD patients have shown that genetics play an essential role in the disease development. However, the rise in cases the recent years implies that environmental events, such as viral infections and stress, might also be involved (1, 5, 8, 115).

21-OHase is encoded by the *CYP21A2* gene, which is located in the MHC class III region on chromosome 6, and mutations on this gene are the commonest cause for Congenital Adrenal Hyperplasia (CAH) (1, 116, 117). The MHC class III region is located in the middle of the MHC gene cluster, flanked by the MHC class II (*HLA-DR, DQ*) genes on one side and MHC class I (HLA-A -C) on the other. Very near the CYP21A2 locus, there is an adjacent highly homologous pseudogene, *CYP21A1P*, which cannot produce a functional enzyme due to an 8-bp deletion in the exon 3 which results in a truncated protein (1, 118). Both the location and the high sequence identity of the two genes contribute to recombination events which are considered the main reason for the deleterious mutations accumulating in the *CYP21A2* gene that lead to CAH (118). The two genes, *CYP21A2* and *CYP21A1P*, belong to a repeated genomic cassette, called the RCCX module. Apart from the two CYP21 genes, in its most frequent form in Caucasians, the locus contains the serine/threonine kinase 19 (*STK19*) gene, the tenascin-X (*TNX*) gene, the complement 4 A (*C4A*) and B(*C4B*) genes, and the pseudogenes *STK19B* and *TNXA*. Non-allelic homologous recombination (NAHR) events in the locus alter the module structure and cause gene conversions and deletions increasing the complexity of the region (118) (Figure 4). Sequencing of the *CYP21A2* gene from AAD patients and healthy individuals showed five SNPs that occur more often in heterozygosity in AAD patients compared to controls (119). Three of them, rs61338903, rs6474 and rs6473, are located in the exonic sequence, whilst the other two, rs6467 and rs76565726, are intronic variants (119). The minor allele of variant rs6473 has been shown to regulate the transcriptional repressor CTCF binding site and has been associated with downregulation of *HLA-C* and *HLA-DRB1* expression (120). In addition, AAD patients with 21-OHase antibodies were more likely to carry these variants in a heterozygous state. However, regression analysis revealed that all variants were in LD with HLA-DRB1*03:01, *04:01 and *04:04 alleles which are associated with high-risk for AAD (119, 121). In contrast, the rs6472*C allele was found to be protective against the disease, and independent from the HLA-DRB1 locus, with a significantly lower frequency in AAD patients compared to controls (119). Thus, it remains unclear whether the primary association at this locus is with HLA-DR alleles or whether variants in *CYP21A2* itself could contribute to AAD susceptibility.

Analysis of the copy number variation of the CYP21 genes showed different patterns for the functional *CYP21A2* and the pseudogene *CYP21A1P* between healthy controls and AAD patients. Copy numbers of *CYP21A2* were similar between AAD patients and healthy people, with 95% of the individuals carrying 2 copies of the gene. Interestingly, the *CYP21A1P* showed larger variation ranging from 0 to 5 copies, with AAD patients revealed as more likely to have lower copy numbers than the healthy controls, with each 'lost' copy being associated with a 3.4-fold odds ratio for disease (122). Examination of the copy number variation of the Complement-4 A (*C4A*) and B (*C4B*) genes, which are located in the same RCCX cassette, showed that there is a stronger correlation of *CYP21A1P* variation with *C4A* than with *C4B*, however lower copy numbers of the C4A gene were slightly more associated with AAD compared to those of *CYP21A1P* (122). Nevertheless, lower copies of both *CYP21A1P* and *C4A* are in close LD with the high risk HLA-DRB1*03:01 allele, as the SNPs described above, and therefore it remains unclear whether they might have an independent effect (119, 122, 123). It is not immediately obvious why copy number or expression of *CYP21A1P*, a pseudogene, should be relevant for disease pathogenesis. However, we speculate that AAD patients have reduced copy number or absence of *CYP21A1P*, because thymic expression of this pseudogene could underly central tolerance, in a similar way to that found for insulin gene variation.

Anti–pituitary-specific transcriptional factor-1 syndrome (Anti-PIT-1 hypophysitis)

Immune-mediated pituitary dysfunction is a rare condition, either involving the cells of the anterior pituitary alone, or involving the posterior pituitary to produce an associated vasopressin deficiency, known as infundibulohypophysitis. Anti-PIT-1 hypophysitis is a rare but recently recognised autoimmune pituitary disease, which is characterised by growth hormone (GH), prolactin (PRL), and thyroid stimulating hormone (TSH) deficiency (124–127). PIT-1 is an important transcription factor for the control of GH, PRL and TSH expression in the somatotroph, lactotroph and thyrotroph cells of the anterior pituitary gland

respectively, and mutations on the *PIT-1* gene cause congenital GH, PRL, and TSH deficiency. The presence of not only circulating anti-PIT-1 antibodies, but also CD8+ T cells in the pituitary gland of patients with anti-PIT-1 hypophysitis, indicate another example of a tissue-specific autoimmune disorder where CTLs are implicated in organ-specific cell damage (124, 125, 127–129). Thus far, the disease has only been found in the presence of thymoma or other types of neoplasms that have ectopic expression of the *PIT-1* gene (124). Although it is currently unclear what types of malignancies coexist with the disease, and in which proportion, the underlying mechanism involves ectopic expression and presentation of PIT-1. Thus, somatic mutations leading to ectopic expression of *PIT-1* in thymoma(s), or other malignancies, represents another mechanism by which dysregulation of antigenic gene expression can precipitate an organ-specific autoimmune endocrine disease.

Perspective for other autoimmune conditions

Autoimmune endocrine disorders may be considered relatively unique amongst autoimmune conditions in that the clinical manifestations occur largely after a hormone-secreting cell-type is irreversibly damaged leading to hormonal deficiency. This contrasts to a disease such as systemic lupus erythematosus (SLE), where the nuclear antigens are ubiquitous in all cell types and damage causing some of the clinical presentations is mediated by immune-complex deposition. Thus, there are some striking differences in antigen distribution and it is easy to envisage how peripheral immune tolerance may have a more important role in systemic autoimmune diseases with less restricted antigen distribution/expression than for organ-specific ones. Even within the spectrum of autoimmune thyroid disease, it is notable that patients with APS1, a 'pure thymic defect' in tolerance (5), very rarely develop GD, but quite frequently develop HT. This may reflect that TSH receptor A-subunit is shed from the thyrocyte membrane (68) leading to degree of peripheral tolerance, whereas thyroid peroxidase has an apical (internal) membrane localisation and perhaps restricted access from ongoing immune surveillance. As mentioned above, role of antigen itself in autoimmunity is relatively neglected and further studies could cast important light on this subject.

Conclusion

Genetic variation in organ-specific antigens remain understudied in autoimmunity in general. However, because of the discrete involvement of endocrine glands/tissues in autoimmune endocrinopathy, we are starting to glimpse potential antigen-specific mechanisms that underly disease proclivity for these conditions. Ectopic expression of many antigens in thymus may be a critical stage in T lymphocyte selection and under-expression may lead to failure to delete auto-reactive TCR-bearing T cell populations. Importantly, thymic gene/antigen expression may be regulated differently to that of the native tissue, leading to complexity in understanding the pathophysiological link. In contrast, continuous exposure of the peripheral immune system to endogenous antigen, such as Tg, may also provide an important mechanism for tolerance. We have much to learn in this area, but a fuller understanding of the antigenic stimulus and the detail of how this is involved in pathogenesis holds the promise of a tissue-specific solution rather than a general 'immunosuppressive' approach to therapy for autoimmunity.

Author contributions

MM: Investigation, Software, Writing – original draft, Writing – review & editing. SP: conceptualization, Supervision, Writing – review & editing.

Funding

The author(s) declare that financial support was received for the research, authorship, and/or publication of this article. Work in this laboratory was funded by UKRI/MRC grants MR/S001611/1, MR/V005898/1 and a generous endowment from the Robotham family (Anthony Robotham PhD studentship).

Conflict of interest

The authors declare that the research was conducted in the absence of any commercial or financial relationships that could be construed as a potential conflict of interest.

Generative AI statement

The author(s) declare that no Generative AI was used in the creation of this manuscript.

Publisher's note

All claims expressed in this article are solely those of the authors and do not necessarily represent those of their affiliated organizations, or those of the publisher, the editors and the reviewers. Any product that may be evaluated in this article, or claim that may be made by its manufacturer, is not guaranteed or endorsed by the publisher.

References

1. Mitchell AL, Pearce SH. Autoimmune Addison disease: pathophysiology and genetic complexity. *Nat Rev Endocrinol*. (2012) 8:306–16. doi: 10.1038/nrendo.2011.245

2. Todd JA. Etiology of type 1 diabetes. *Immunity*. (2010) 32:457–67. doi: 10.1016/j.immuni.2010.04.001

3. Zenewicz LA, Abraham C, Flavell RA, Cho JH. Unraveling the genetics of autoimmunity. *Cell*. (2010) 140:791–7. doi: 10.1016/j.cell.2010.03.003

4. Saevarsdottir S, Olafsdottir TA, Ivarsdottir EV, Halldorsson GH, Gunnarsdottir K, Sigurdsson A, et al. FLT3 stop mutation increases FLT3 ligand level and risk of autoimmune thyroid disease. *Nature*. (2020) 584:619–23. doi: 10.1038/s41586-020-2436-0

5. Husebye ES, Pearce SH, Krone NP, Kämpe O. Adrenal insufficiency. *Lancet*. (2021) 397:613–29. doi: 10.1016/S0140-6736(21)00136-7

6. Eriksson D, Bianchi M, Landegren N, Dalin F, Skov J, Hultin-Rosenberg L, et al. Common genetic variation in the autoimmune regulator (AIRE) locus is associated with autoimmune Addison's disease in Sweden. *Sci Rep*. (2018) 8:8395. doi: 10.1038/s41598-018-26842-2

7. Chatila Ta, Blaeser F, Ho N, Lederman Hm, Voulgaropoulos C, Helms C, et al. JM2, encoding a fork head-related protein, is mutated in X-linked autoimmunity-allergic disregulation syndrome. *J Clin Invest*. (2000) 106:R75–81. doi: 10.1172/JCI11679

8. Pazderska A, Pearce SH, Mitchell AL. *Adrenal Disorders: Physiology, Pathophysiology and Treatment*. Levine AC, editor. Cham, Switzerland: S.I. Publishing (2018) p. 85–108. doi: 10.1007/978-3-319-62470-9

9. Gough SCL, Simmonds MJ. The HLA region and autoimmune disease: associations and mechanisms of action. *Curr Genomics*. (2007) 8:453–65. doi: 10.2174/138920207783591690

10. Hocking AM, Buckner JH. Genetic basis of defects in immune tolerance underlying the development of autoimmunity. *Front Immunol*. (2022) 13. doi: 10.3389/fimmu.2022.972121

11. Grixti L, Lane LC, Pearce SH. The genetics of Graves' disease. *Rev Endocrine Metab Disord*. (2023) 25:203–14. doi: 10.1007/s11154-023-09848-8

12. Vos XG, Endert E, Zwinderman AH, Tijssen JGP, Wiersinga WM. Predicting the risk of recurrence before the start of antithyroid drug therapy in patients with Graves' Hyperthyroidism. *J Clin Endocrinol Metab*. (2016) 101:1381–9. doi: 10.1210/jc.2015-3644

13. Tautz L, Critton DA, Grotegut S. Protein tyrosine phosphatases: structure, function, and implication in human disease. *Methods Mol Biol*. (2013) 1053:179–221. doi: 10.1007/978-1-62703-562-0_13

14. Gootjes C, Zwaginga JJ, Roep BO, Nikolic T. Functional impact of risk gene variants on the autoimmune responses in type 1 diabetes. *Front Immunol*. (2022) 13. doi: 10.3389/fimmu.2022.886736

15. Stephan K. Genetic modifiers of thymic selection and central tolerance in type 1 diabetes. *Front Immunol*. (2022) 13. doi: 10.3389/fimmu.2022.889856

16. Ivashkiv LB. PTPN22 in autoimmunity: different cell and different way. *Immunity*. (2013) 39:91–3. doi: 10.1016/j.immuni.2013.07.007

17. Tizaoui K, Terrazzino S, Cargnin S, Lee KH, Gauckler P, Li H, et al. The role of PTPN22 in the pathogenesis of autoimmune diseases: A comprehensive review. *Semin Arthritis Rheum*. (2021) 51:513–22. doi: 10.1016/j.semarthrit.2021.03.004

18. Bottini N, Peterson EJ. Tyrosine phosphatase PTPN22: multifunctional regulator of immune signaling, development, and disease. *Annu Rev Immunol*. (2014) 32:83–119. doi: 10.1146/annurev-immunol-032713-120249

19. Zhang J, Zahir N, Jiang Q, Miliotis H, Heyraud S, Meng X, et al. The autoimmune disease–associated PTPN22 variant promotes calpain-mediated Lyp/Pep degradation associated with lymphocyte and dendritic cell hyperresponsiveness. *Nat Genet*. (2011) 43:902–9. doi: 10.1038/ng.904

20. Hamerman JA, Pottle J, Ni M, He Y, Zhang Z-Y, Buckner JH. Negative regulation of TLRsignaling in myeloid cells—implications for autoimmunediseases. *Immunol Rev*. (2016) 269:212–27. doi: 10.1111/imr.2016.269.issue-1

21. Wallis AM, Wallace EC, Hostager BS, Yi Z, Houtman JCD, Bishop GA. TRAF3 enhances TCR signaling by regulating the inhibitors Csk and PTPN22. *Sci Rep*. (2017) 7:2081. doi: 10.1038/s41598-017-02280-4

22. Wang Y, Shaked I, Stanford SM, Zhou W, Curtsinger JM, Mikulski Z, et al. The autoimmunity-associated gene PTPN22 potentiates toll-like receptor-driven, type 1 interferon-dependent immunity. *Immunity*. (2013) 39:111–22. doi: 10.1016/j.immuni.2013.06.013

23. Menard L, Saadoun D, Isnardi I, Ng Y-S, Meyers G, Massad C, et al. The PTPN22 allele encoding an R620W variant interferes with the removal of developing autoreactive B cells in humans. *J Clin Invest*. (2011) 121:3635–44. doi: 10.1172/JCI45790

24. Rieck M, Arechiga A, Onengut-Gumuscu S, Greenbaum C, Concannon P, Buckner JH. Genetic variation in PTPN22 corresponds to altered function of T and B lymphocytes. *J Immunol*. (2007) 179:4704–10. doi: 10.4049/jimmunol.179.7.4704

25. Vang T, Congia M, Macis MD, Musumeci L, Orru V, Zavattari P, et al. Autoimmune-associated lymphoid tyrosine phosphatase is a gain-of-function variant. *Nat Genet*. (2005) 37:1317–9. doi: 10.1038/ng1673

26. Bufalo NatássiaE, Dos Santos RB, Rocha AngélicaG, Teodoro L, Romaldini JoãoH, Ward LS. Polymorphisms of the genes CTLA4, PTPN22, CD40, and PPARG and their roles in Graves' disease: susceptibility and clinical features. *Endocrine*. (2020) 71:104–12. doi: 10.1007/s12020-020-02337-x

27. Kavvoura FK, Akamizu T, Awata T, Ban Y, Chistiakov DA, Frydecka I, et al. Cytotoxic T-lymphocyte associated antigen 4 gene polymorphisms and autoimmune thyroid disease: A meta-analysis. *J Clin Endocrinol Metab*. (2007) 92:3162–70. doi: 10.1210/jc.2007-0147

28. Ni J, Qiu L-J, Zhang M, Wen P-F, Ye X-R, Liang Y, et al. CTLA-4 CT60 (rs3087243) polymorphism and autoimmune thyroid diseases susceptibility: a comprehensive meta-analysis. *Endocrine Res*. (2014) 39:180–8. doi: 10.3109/07435800.2013.879167

29. Pawlak-Adamska E, Frydecka I, Bolanowski M, Tomkiewicz A, Jonkisz A, Karabon L, et al. CD28/CTLA-4/ICOS haplotypes confers susceptibility to Graves' disease and modulates clinical phenotype of disease. *Endocrine*. (2016) 55:186–99. doi: 10.1007/s12020-016-1096-1

30. Mitsuiki N, Schwab C, Grimbacher B. What did we learn from CTLA-4 insufficiency on the human immune system? *Immunol Rev*. (2019) 287:33–49. doi: 10.1111/imr.12721

31. Pazderska A, Oftedal BE, Napier CM, Ainsworth HF, Husebye ES, Cordell HJ, et al. A variant in the BACH2 gene is associated with susceptibility to autoimmune Addison's disease in humans. *J Clin Endocrinol Metab*. (2016) 101:3865–9. doi: 10.1210/jc.2016-2368

32. Onuma H, Kawamura R, Tabara Y, Yamashita M, Ohashi J, Kawasaki E, et al. Variants in the BACH2 and CLEC16A gene might be associated with susceptibility to insulin-triggered type 1 diabetes. *J Diabetes Investig*. (2019) 10:1447–53. doi: 10.1111/jdi.13057

33. Fichna M, Żurawek M, Słomiński B, Sumińska M, Czarnywojtek A, Rozwadowska N, et al. Polymorphism in BACH2 gene is a marker of polyglandular autoimmunity. *Endocrine*. (2021) 74:72–9. doi: 10.1007/s12020-021-02743-9

34. Fichna M, Małecki PP, Żurawek M, Furman K, Gębarski B, Fichna P, et al. Genetic variants and risk of endocrine autoimmunity in relatives of patients with Addison's disease. *Endocr Connect*. (2023) 12(6):e230008. doi: 10.1530/EC-23-0008

35. Cooper JD, Smyth DJ, Smiles AM, Plagnol V, Walker NM, Allen JE, et al. Meta-analysis of genome-wide association study data identifies additional type 1 diabetes risk loci. *Nat Genet*. (2008) 40:1399–401. doi: 10.1038/ng.249

36. Karim KA, John P, Bhatti A, Zia A, Shahid G, Akhtar P, et al. Association of 32 type 1 diabetes risk loci in Pakistani patients. *Diabetes Res Clin Pract*. (2015) 108:137–42. doi: 10.1016/j.diabres.2015.01.022

37. Dieter C, Lemos NatáliaE, Dorfman LE, Duarte GCK, Assmann TaísS, Crispim D. The rs11755527 polymorphism in the BACH2 gene and type 1 diabetes mellitus: case control study in a Brazilian population. *Arch Endocrinol Metab*. (2020) 64:138–43. doi: 10.20945/2359-3997000000214

38. Liu W, Wang Hai–Ning, Gu Zhao–Hui, Yang Shao–Ying, Ye Xiao–Ping, Pan Chun–Ming, et al. Identification of BACH2 as a susceptibility gene for Graves' disease in the Chinese Han population based on a three-stage genome-wide association study. *Hum Genet*. (2014) 133:661–71. doi: 10.1007/s00439-013-1404-2

39. Robertson CC, Inshaw JRJ, Onengut-Gumuscu S, Chen W-M, Santa Cruz DF, Yang H, et al. Fine-mapping, trans-ancestral and genomic analyses identify causal variants, cells, genes and drug targets for type 1 diabetes. *Nat Genet*. (2021) 53:962–71. doi: 10.1038/s41588-021-00880-5

40. Marquez A, Martin J. Genetic overlap between type 1 diabetes and other autoimmune diseases. *Semin Immunopathol*. (2022) 44:81–97. doi: 10.1007/s00281-021-00885-6

41. Cooper JD, Simmonds MJ, Walker NM, Burren O, Brand OJ, Guo H, et al. Seven newly identified loci for autoimmune thyroid disease. *Hum Mol Genet*. (2012) 21:5202–8. doi: 10.1093/hmg/dds357

42. Dendrou CA, Plagnol V, Fung E, Yang JHM, Downes K, Cooper JD, et al. Cell-specific protein phenotypes for the autoimmune locus IL2RA using a genotype-selectable human bioresource. *Nat Genet*. (2009) 41:1011–5. doi: 10.1038/ng.434

43. Garg G, Tyler JR, Yang JHM, Cutler AJ, Downes K, Pekalski M, et al. Type 1 diabetes-associated IL2RA variation lowers IL-2 signaling and contributes to diminished CD4+CD25+ Regulatory T cell function. *J Immunol*. (2012) 188:4644–53. doi: 10.4049/jimmunol.1100272

44. Cerosaletti K, Schneider A, Schwedhelm K, Frank I, Tatum M, Wei S, et al. Multiple autoimmune-associated variants confer decreased IL-2R signaling in CD4+CD25hi T cells of type 1 diabetic and multiple sclerosis patients. *PloS One*. (2013) 8(12):e83811. doi: 10.1371/journal.pone.0083811

45. De Luca F, Shoenfeld Y. The microbiome in autoimmune diseases. *Clin Exp Immunol*. (2019) 195:74–85. doi: 10.1111/cei.13158

46. Katsarou A, Gudbjörnsdottir S, Rawshani A, Dabelea D, Bonifacio E, Anderson BJ, et al. Type 1 diabetes mellitus. *Nat Rev Dis Primers*. (2017) 3:17016. doi: 10.1038/nrdp.2017.16

47. Pugliese A, Miceli D. The insulin gene in diabetes. *Diabetes/Metabolism Res Rev*. (2002) 18:13–25. doi: 10.1002/dmrr.v18:1

48. Barratt BJ, Payne F, Lowe CE, Hermann R, Healy BC, Harold D, et al. Remapping the insulin gene/IDDM2 locus in type 1 diabetes. *Diabetes*. (2004) 53:1884–9. doi: 10.2337/diabetes.53.7.1884

49. Catignani KG, German MS, Rutter WJ. The minisatellite in the diabetes susceptibility locus IDDM2 regulates insulin transcription. *Nat Genet*. (1995) 9:293–8. doi: 10.1038/ng0395-293

50. Vafiadis P, Bennett ST, Todd JA, Nadeau J, Grabs R, Goodyer CG, et al. Insulin expression in human thymus is modulated by INS VNTR alleles at the IDDM2 locus. *Nat Genet*. (1997) 15:289–92. doi: 10.1038/ng0397-289

51. Ahmed S, Bennett ST, Huxtable SJ, Todd JA, Matthews DR, Gough SCL. INS VNTR allelic variation and dynamic insulin secretion in healthy adult non-diabetic Caucasian subjects. *Diabetic Med*. (1999) 16:910–7. doi: 10.1046/j.1464-5491.1999.00169.x

52. Bennett ST, Lucassen AM, Gough SCL, Powell EE, Undlien DE, Pritchard LE, et al. Susceptibility to human type 1 diabetes at IDDM2 is determined by tandem repeat variation at the insulin gene minisatellite locus. *Nat Genet*. (1995) 9:284–92. doi: 10.1038/ng0395-284

53. Bennett ST, Wilson AJ, Cucca F, Nerup Jørn, Pociot F, Mckinney PA, et al. IDDM2-VNTR-encoded susceptibility to type 1 diabetes: dominant protection and parental transmission of alleles of the insulin gene-linked minisatellite locus. *J Autoimmun*. (1996) 9:415–21. doi: 10.1006/jaut.1996.0057

54. Bennett ST, Wilson AJ, Esposito L, Bouzekri N, Undlien DE, Cucca F, et al. Insulin VNTR allele-specific effect in type 1 diabetes depends on identity of untransmitted paternal allele. *Nat Genet*. (1997) 17:350–2. doi: 10.1038/ng1197-350

55. Alami CA, Polychronakos C. Insulin expression levels in the thymus modulate insulin-specific autoreactive T-cell tolerance: the mechanism by which the IDDM2 locus may predispose to diabetes. *Diabetes*. (2002) 51:1383–90. doi: 10.2337/diabetes.51.5.1383

56. Walter M, Albert E, Conrad M, Keller E, Hummel M, Ferber K, et al. IDDM2/insulin VNTR modifies risk conferred by IDDM1/HLA for development of Type 1 diabetes and associated autoimmunity. *Diabetologia*. (2003) 46:712–20. doi: 10.1007/s00125-003-1082-z

57. Marín-Sánchez A, Álvarez-Sierra D, González O, Lucas-Martin A, Sellés-Sánchez A, Rudilla F, et al. Regulation of TSHR expression in the thyroid and thymus may contribute to TSHR tolerance failure in graves' Disease patients via two distinct mechanisms. *Front Immunol*. (2019) 10. doi: 10.3389/fimmu.2019.01695

58. Prabhakar BS, Bahn RS, Smith TJ. Current perspective on the pathogenesis of graves' Disease and ophthalmopathy. *Endocrine Rev*. (2003) 24:802–35. doi: 10.1210/er.2002-0020

59. Stefan M, Faustino LC. Genetics of thyroid-stimulating hormone receptor—Relevance for autoimmune thyroid disease. *Front Endocrinol*. (2017) 8. doi: 10.3389/fendo.2017.00057

60. Stefan M, Wei C, Lombardi A, Li CW, Concepcion ES, Inabnet WB, et al. Genetic–epigenetic dysregulation of thymic TSH receptor gene expression triggers thyroid autoimmunity. *Proc Natl Acad Sci*. (2014) 111:12562–7. doi: 10.1073/pnas.1408821111

61. Struja T, Fehlberg H, Kutz A, Guebelin L, Degen C, Mueller B, et al. Can we predict relapse in Graves' disease? Results from a systematic review and meta-analysis. *Eur J Endocrinol*. (2017) 176:87–97. doi: 10.1530/EJE-16-0725

62. Rapoport B, Aliesky HA, Chen C-R, Mclachlan SM. Evidence that TSH receptor A-subunit multimers, not monomers, drive antibody affinity maturation in Graves' Disease. *J Clin Endocrinol Metab*. (2015) 100:E871–5. doi: 10.1210/jc.2015-1528

63. Colobran R, Armengol MDP, Faner R, Gärtner M, Tykocinski L-O, Lucas A, et al. Association of an SNP with intrathymic transcription of TSHR and Graves' disease: a role for defective thymic tolerance. *Hum Mol Genet*. (2011) 20:3415–23. doi: 10.1093/hmg/ddr247

64. Brand OJ, Barrett JC, Simmonds MJ, Newby PR, Mccabe CJ, Bruce CK, et al. Association of the thyroid stimulating hormone receptor gene (TSHR) with Graves' disease. *Hum Mol Genet*. (2009) 18:1704–13. doi: 10.1093/hmg/ddp087

65. Chu Y-D, Yeh C-T. The molecular function and clinical role of thyroid stimulating hormone receptor in cancer cells. *Cells*. (2020) 9(7):1730. doi: 10.3390/cells9071730

66. Costagliola S, Khoo D, Vassart G. Production of bioactive amino-terminal domain of the thyrotropin receptor via insertion in the plasma membrane by a glycosylphosphatidylinositol anchor. *FEBS Lett*. (1998) 436:427–33. doi: 10.1016/S0014-5793(98)01177-6

67. Davies T, Marians R, Latif R. The TSH receptor reveals itself. *J Clin Invest*. (2002) 110:161–4. doi: 10.1172/JCI0216234

68. Rapoport B, Mclachlan SM. TSH receptor cleavage into subunits and shedding of the A-subunit; A molecular and clinical perspective. *Endocr Rev*. (2016) 37:114–34. doi: 10.1210/er.2015-1098

69. Tanaka K, Chazenbalk GD, Mclachlan SM, Rapoport B. Subunit structure of thyrotropin receptors expressed on the cell surface. *J Biol Chem*. (1999) 274:33979–84. doi: 10.1074/jbc.274.48.33979

70. Ploski R, Szymaski K, Bednarczuk T. The genetic basis of Graves' Disease. *Curr Genomics*. (2011) 12:542–63. doi: 10.2174/138920211798120772

71. Kleinau G, Neumann S, Gruters A, Krude H, Biebermann H. Novel insights on thyroid-stimulating hormone receptor signal transduction. *Endocr Rev*. (2013) 34:691–724. doi: 10.1210/er.2012-1072

72. Mizutori Y, Chen C-R, Latrofa F, Mclachlan SM, Rapoport B. Evidence that shed thyrotropin receptor A subunits drive affinity maturation of autoantibodies causing Graves' disease. *J Clin Endocrinol Metab*. (2009) 94:927–35. doi: 10.1210/jc.2008-2134

73. Boguslawska J, Godlewska M, Gajda E, Piekielko-Witkowska A. Cellular and molecular basis of thyroid autoimmunity. *Eur Thyroid J*. (2022) 11(1):e210024. doi: 10.1530/ETJ-21-0024

74. Lee HJ, Stefan-Lifshitz M, Li CW, Tomer Y. Genetics and epigenetics of autoimmune thyroid diseases: Translational implications. *Best Pract Res Clin Endocrinol Metab*. (2023) 37:101661. doi: 10.1016/j.beem.2022.101661

75. Stefan M, Jacobson EM, Huber AK, Greenberg DA, Li CW, Skrabanek L, et al. Novel variant of thyroglobulin promoter triggers thyroid autoimmunity through an epigenetic interferon α-modulated mechanism. *J Biol Chem*. (2011) 286:31168–79. doi: 10.1074/jbc.M111.247510

76. Chu X, Pan C-M, Zhao S-X, Liang J, Gao G-Q, Zhang X-M, et al. A genome-wide association study identifies two new risk loci for Graves' disease. *Nat Genet*. (2011) 43:897–901. doi: 10.1038/ng.898

77. Dechairo BM, Zabaneh D, Collins J, Brand O, Dawson GJ, Green AP, et al. Association of the TSHR gene with Graves' disease: the first disease s*pecific locus*. *Eur J Hum Genet*. (2005) 13:1223–30. doi: 10.1038/sj.ejhg.5201485

78. Płoski Rafał, Brand OJ, Jurecka-Lubieniecka B, Franaszczyk M, Kula D, Krajewski Paweł, et al. Thyroid stimulating hormone receptor (TSHR) intron 1 variants are major risk factors for Graves' disease in three European Caucasian cohorts. *PloS One*. (2010) 5:e15512. doi: 10.1371/journal.pone.0015512

79. Pujol-Borrell R, Gimenez-Barcons M, Marin-Sanchez A, Colobran R. Genetics of graves' Disease: special focus on the role of TSHR gene. *Horm Metab Res*. (2015) 47:753–66. doi: 10.1055/s-0035-1559646

80. Hiratani H, Bowden DW, Ikegami S, Shirasawa S, Shimizu A, Iwatani Y, et al. Multiple SNPs in intron 7 of thyrotropin receptor are associated with Graves' disease. *J Clin Endocrinol Metab*. (2005) 90:2898–903. doi: 10.1210/jc.2004-2148

81. Zaletel K, Gaberscek S. Hashimoto's thyroiditis: from genes to the disease. *Curr Genomics*. (2011) 12:576–88. doi: 10.2174/138920211798120763

82. Ragusa F, Fallahi P, Elia G, Gonnella D, Paparo SR, Giusti C, et al. Hashimotos' thyroiditis: Epidemiology, pathogenesis, clinic and therapy. *Best Pract Res Clin Endocrinol Metab*. (2019) 33(6):101367. doi: 10.1016/j.beem.2019.101367

83. Ris-Stalpers C, Bikker H. Genetics and phenomics of hypothyroidism and goiter due to TPO mutations. *Mol Cell Endocrinol*. (2010) 322:38–43. doi: 10.1016/j.mce.2010.02.008

84. Mohssen M, Radhi S, Fadel-Al-Jumaili E, Abdulhasan A-HM, Tariq A. TPO gene rs2071400 polymorphisms as an independent risk factor for hypothyroidism in Iraqi patients. *Biomedicine*. (2023) 43:775–8. doi: 10.51248/.v43i02.2701

85. Tomari S, Watanabe M, Inoue N, Mizuma T, Yamanaka C, Hidaka Y, et al. The polymorphisms in the thyroid peroxidase gene were associated with the development of autoimmune thyroid disease and the serum levels of anti-thyroid peroxidase antibody. *Endocrine J*. (2017) 64:1025–32. doi: 10.1507/endocrj.EJ17-0191

86. Al-Mofarji ST, Jasim HM, Mohammed SB. Association between TPO gene polymorphisms with susceptibility to hyperthyroidism. *Biomedicine*. (2024) 43:1744–9. doi: 10.51248/.v43i6.3499

87. Mizuma T, Watanabe M, Inoue N, Arakawa Y, Tomari S, Hidaka Y, et al. Association of the polymorphisms in the gene encoding thyroglobulin with the development and prognosis of autoimmune thyroid disease. *Autoimmunity*. (2017) 50:386–92. doi: 10.1080/08916934.2017.1344971

88. Al-Mofarji ST, Jasim HM, Mohammed SB, Al-Samerriae AY. TPO gene expression in relation with promoter SNPs in Iraqi patients with hyperthyroidism. *Al-Rafidain J Med Sci*. (2023) 5:S100–105. doi: 10.54133/ajms.v5i1S.313

89. Khoshi A, Sirghani A, Ghazisaeedi M, Zarei Mahmudabadi A, Azimian A. Association between TPO Asn698Thr and Thr725Pro gene polymorphisms and serum anti-TPO levels in Iranian patients with subclinical hypothyroidism. *Hormones*. (2017) 16:75–83. doi: 10.14310/horm.2002.1721

90. Balmiki N, Bankura B, Guria S, Das TK, Pattanayak AK, Sinha A, et al. Genetic analysis of thyroid peroxidase (TPO) gene in patients whose hypothyroidism was found in adulthood in West Bengal, India. *Endocrine J*. (2014) 61:289–96. doi: 10.1507/endocrj.EJ13-0237

91. Czarnocka B, Eschler DC, Godlewska M, Tomer Y. "Chapter 44 - Thyroid Autoantibodies: Thyroid Peroxidase and Thyroglobulin Antibodies". In: Shoenfeld Y, Meroni PL, Gershwin ME, editors. *Autoantibodies*. (2014). p. 365–73. doi: 10.1016/B978-0-444-56378-1.00044-7

92. Le SN, Porebski BT, Mccoey J, Fodor J, Riley B, Godlewska M, et al. Modelling of thyroid peroxidase reveals insights into its enzyme function and autoantigenicity. *PloS One*. (2015) 10:e0142615. doi: 10.1371/journal.pone.0142615

93. Mclachlan SM, Rapoport B. Autoimmune response to the thyroid in humans: thyroid peroxidase–the common autoantigenic denominator. *Int Rev Immunol*. (2000) 19:587–618. doi: 10.3109/08830180009088514

94. Finke R, Seto P, Ruf J, Carayon P, Rapoport B. Determination at the molecular level of a B-cell epitope on thyroid peroxidase likely to be associated with autoimmune thyroid disease. *J Clin Endocrinol Metab*. (1991) 73:919–21. doi: 10.1210/jcem-73-4-919

95. Kim MiJ, Oh SoW, Youn H, Na J, Kang KW, Park DoJ, et al. Thyroid-related protein expression in the human thymus. *Int J Endocrinol*. (2017) 2017:1–10. doi: 10.1155/2017/8159892

96. Mclachlan SM, Rapoport B. Breaking tolerance to thyroid antigens: changing concepts in thyroid autoimmunity. *Endocrine Rev*. (2014) 35:59–105. doi: 10.1210/er.2013-1055

97. Misharin AV, Nagayama Y, Aliesky HA, Rapoport B, Mclachlan SM. Studies in mice deficient for the autoimmune regulator (Aire) and transgenic for the thyrotropin receptor reveal a role for aire in tolerance for thyroid autoantigens. *Endocrinology*. (2009) 150:2948–56. doi: 10.1210/en.2008-1690

98. Lahooti H, Edirimanne S, Walsh JP, Delbridge L, Hibbert E, Wall J. Single nucleotide polymorphism 1623 A/G (rs180195) in the promoter of the Thyroglobulin gene is associated with autoimmune thyroid disease but not with thyroid ophthalmopathy. *Clin Ophthalmol*. (2017) 11:1337–45. doi: 10.2147/OPTH.S136070

99. Collins JE, Heward JM, Carr-Smith J, Daykin J, Franklyn JA, Gough SCL. Association of a rare thyroglobulin gene microsatellite variant with autoimmune thyroid disease. *J Clin Endocrinol Metab*. (2003) 88:5039–42. doi: 10.1210/jc.2003-030093

100. Lo MS, Towne M, Vannoy GE, Brownstein CA, Lane AA, Chatila TA, et al. Monogenic Hashimoto thyroiditis associated with a variant in the thyroglobulin (TG) gene. *J Autoimmun*. (2018) 86:116–9. doi: 10.1016/j.jaut.2017.09.003

101. Weetman AP. An update on the pathogenesis of Hashimoto's thyroiditis. *J Endocrinological Invest*. (2020) 44:883–90. doi: 10.1007/s40618-020-01477-1

102. Latrofa F, Fiore E, Rago T, Antonangeli L, Montanelli L, Ricci D, et al. Iodine contributes to thyroid autoimmunity in humans by unmasking a cryptic epitope on thyroglobulin. *J Clin Endocrinol Metab*. (2013) 98:E1768–74. doi: 10.1210/jc.2013-2912

103. Arase N, Arase H. Cellular misfolded proteins rescued from degradation by MHC class II molecules are possible targets for autoimmune diseases. *J Biochem*. (2015) 158:367–72. doi: 10.1093/jb/mvv093

104. Barkoff MS, Kocherginsky M, Anselmo Joa˜O, Weiss RE, Refetoff S. Autoimmunity in patients with resistance to thyroid hormone. *J Clin Endocrinol Metab*. (2010) 95:3189–93. doi: 10.1210/jc.2009-2179

105. Ohba K, Sasaki S, Misawa NH, Matsushita A, Kuroda Go, Sakai Y, et al. Clinical outcomes of 34 patients with resistance to thyroid hormone beta: a twenty-year experience in Japan. *Endocrine J*. (2022) 69:179–88. doi: 10.1507/endocrj.EJ21-0390

106. Kühnen P, Turan S, Fröhler S, Güran Tülay, Abali S, Biebermann H, et al. Identification of PENDRIN (SLC26A4) mutations in patients with congenital hypothyroidism and "apparent" thyroid dysgenesis. *J Clin Endocrinol Metab*. (2014) 99:E169–76. doi: 10.1210/jc.2013-2619

107. Wemeau J-L, Kopp P. Pendred syndrome. *Best Pract Res Clin Endocrinol Metab*. (2017) 31:213–24. doi: 10.1016/j.beem.2017.04.011

108. Peter K. Mutations in the Pendred Syndrome (PDS/SLC26A) gene: an increasingly complex phenotypic spectrum from goiter to thyroid hypoplasia. *J Clin Endocrinol Metab*. (2014) 99:67–9. doi: 10.1210/jc.2013-4319

109. Vaidya B, Coffey R, Coyle B, Trembath R, San Lazaro C, Reardon W, et al. Concurrence of Pendred syndrome, autoimmune thyroiditis, and simple goiter in one family. *J Clin Endocrinol Metab*. (1999) 84:2736–8. doi: 10.1210/jcem.84.8.5903

110. Kong YM, Brown NK, Morris GP, Flynn JC. The essential role of circulating thyroglobulin in maintaining dominance of natural regulatory T cell function to prevent autoimmune thyroiditis. *Hormone Metab Res*. (2015) 47:711–20. doi: 10.1055/s-0035-1548872

111. Carayanniotis G. The cryptic self in thyroid autoimmunity: the paradigm of thyroglobulin. *Autoimmunity*. (2009) 36:423–8. doi: 10.1080/08916930310001602975

112. Napier C, Pearce SHS. Autoimmune Addison's disease. *Presse Med*. (2012) 41:e626-35. doi: 10.1016/j.lpm.2012.09.010

113. Dawoodji A, Chen J-L, Shepherd D, Dalin F, Tarlton A, Alimohammadi M, et al. High frequency of cytolytic 21-hydroxylase-specific CD8+ T cells in autoimmune Addison's disease patients. *J Immunol*. (2014) 193:2118–26. doi: 10.4049/jimmunol.1400056

114. Hellesen A, Aslaksen S, Breivik L, Røyrvik EC, Bruserud Øyvind, Edvardsen K, et al. 21-hydroxylase-specific CD8+ T cells in autoimmune Addison's disease are restricted by HLA-A2 and HLA-C7 molecules. *Front Immunol*. (2021) 12:742848. doi: 10.3389/fimmu.2021.742848

115. Song H, Fang F, Tomasson G, Arnberg Fk, Mataix-Cols D, Fernández de la Cruz L, et al. Association of stress-related disorders with subsequent autoimmune disease. *JAMA*. (2018) 319:2388–400. doi: 10.1001/jama.2018.7028

116. Pignatelli D, Carvalho BL, Palmeiro A, Barros A, Guerreiro SG, Macut D. The complexities in genotyping of congenital adrenal hyperplasia: 21-hydroxylase deficiency. *Front Endocrinol*. (2019) 10. doi: 10.3389/fendo.2019.00432

117. Asghari Kollahi N, Rohani F, Baghbani-Arani F, Shojaei A. Complex alleles of CYP21A2 are the most frequent causes of congenital adrenal hyperplasia in Iranian population. *Iranian J Pediatr*. (2019) 29(6):e91994. doi: 10.5812/ijp.91994

118. Carrozza C, Foca L, De Paolis E, Concolino P. Genes and pseudogenes: complexity of the RCCX locus and disease. *Front Endocrinol (Lausanne)*. (2021) 12:709758. doi: 10.3389/fendo.2021.709758

119. Brønstad I, Skinningsrud B, Bratland E, Løvas K, Undlien D, Husebye ES, et al. CYP21A2 polymorphisms in patients with autoimmune Addison's disease, and linkage disequilibrium to HLA risk alleles. *Eur J Endocrinol*. (2014) 171:743–50. doi: 10.1530/EJE-14-0432

120. *Strongest gene expression correlations in blood: HLA-C [Effect size: -0.319672, p-value(-log10): 3.3008076937936703], HLA-DRB1 [Effect size: -0.555033, p-value(-log10): 3.1042471621597683*. Ensembl.org.

121. Mavridou M, Mitchell A, Allinson K, Lane L, Pearce S. HLA-DRB1*0404 is associated with the deletion of the 21-hydroxylase pseudogene in AAD patients. In: *Society for Endocrinology BES 2022*. Endocrine Abstracts, Harrogate, United Kingdom (2022).

122. Lundtoft C, Eriksson D, Bianchi M, Aranda-Guillén M, Landegren N, Rantapää-Dahlqvist S, et al. Relation between HLA and copy number variation of steroid 21-hydroxylase in a Swedish cohort of patients with autoimmune Addison's disease. *Eur J Endocrinol*. (2023) 189:235–41. doi: 10.1093/ejendo/lvad102

123. Peterson P, Partanen J, Aavik E, Salmi H, Pelkonen R, Krohn KJE. Steroid 2 1 -hydroxylase gene polymorphsm in Addison's disease patients. *Tissue Antigens*. (1995) 46:63–7. doi: 10.1111/j.1399-0039.1995.tb02478.x

124. Bando H, Iguchi G, Okimura Y, Odake Y, Yoshida K, Matsumoto R, et al. A novel thymoma-associated autoimmune disease: Anti-PIT-1 antibody syndrome. *Sci Rep*. (2017) 7:43060. doi: 10.1038/srep43060

125. Kanie K, Bando H, Iguchi G, Muguruma K, Matsumoto R, Hidaka-Takeno R, et al. Pathogenesis of anti–PIT-1 antibody syndrome: PIT-1 presentation by HLA class I on anterior pituitary cells. *J Endocrine Soc*. (2019) 3:1969–78. doi: 10.1210/js.2019-00243

126. Pfaffle R, Kim C, Otten B, Wit J-M, Eiholzer U, Heimann G, et al. Pit-1:Clinical aspects. *Horm Res*. (1996) 45:25–8. doi: 10.1159/000184824

127. Yamamoto M, Iguchi G, Bando H, Kanie K, Hidaka-Takeno R, Fukuoka H, et al. Autoimmune pituitary disease: new concepts with clinical implications. *Endocrine Rev*. (2020) 41:261–72. doi: 10.1210/endrev/bnz003

128. Yamamoto M, Bando H. A new insight into GH regulation and its disturbance from nutrition and autoimmune perspectives. *Endocrine J*. (2023) 70:867–74. doi: 10.1507/endocrj.EJ23-0264

129. Bando H, Iguchi G, Fukuoka H, Yamamoto M, Hidaka-Takeno R, Okimura Y, et al. Involvement of PIT-1-reactive cytotoxic T lymphocytes in anti-PIT-1 antibody syndrome. *J Clin Endocrinol Metab*. (2014) 99:E1744–9. doi: 10.1210/jc.2014-1769

130. Pujol-Borrell R, Álvarez-Sierra D, Jaraquemada D, Marín-Sánchez A, Colobran R. Central tolerance mechanisms to TSHR in Graves' Disease: contributions to understand the genetic association. *Horm Metab Res*. (2018) 50:863–70. doi: 10.1055/a-0755-7927

131. Le Fourn V, Ferrand M, Franc J-L. Endoproteolytic cleavage of human thyroperoxidase: role of the propeptide in the protein folding process. *J Biol Chem*. (2005) 280:4568–77. doi: 10.1074/jbc.M408042200

frontiers | Frontiers in Immunology

TYPE Case Report
PUBLISHED 09 May 2025
DOI 10.3389/fimmu.2025.1563629

Check for updates

OPEN ACCESS

EDITED BY
Anette S. B. Wolff,
University of Bergen, Norway

REVIEWED BY
Otilia Marginean,
Victor Babes University of Medicine and Pharmacy, Romania
Akash Batta,
Dayanand Medical College and Hospital, India
Zhe Zhao,
Peking University Third Hospital, China

*CORRESPONDENCE
Hui Chen
chenhui@lzu.edu.cn

RECEIVED 20 January 2025
ACCEPTED 21 March 2025
PUBLISHED 09 May 2025

CITATION
Yao Z, Chen H, Hu X, Ge D, Xu X and Xu D (2025) Delayed diagnosis of the full triad autoimmune polyendocrine syndrome type 2 with adrenal crisis: a case report and literature review. *Front. Immunol.* 16:1563629. doi: 10.3389/fimmu.2025.1563629

COPYRIGHT
© 2025 Yao, Chen, Hu, Ge, Xu and Xu. This is an open-access article distributed under the terms of the Creative Commons Attribution License (CC BY). The use, distribution or reproduction in other forums is permitted, provided the original author(s) and the copyright owner(s) are credited and that the original publication in this journal is cited, in accordance with accepted academic practice. No use, distribution or reproduction is permitted which does not comply with these terms.

Delayed diagnosis of the full triad autoimmune polyendocrine syndrome type 2 with adrenal crisis: a case report and literature review

Zihong Yao [1,2], Hui Chen [2*], Xuejian Hu [2], Dan Ge [2], Xiangyu Xu [2] and Danxia Xu [2]

[1]The Second Clinical Medical College, Lanzhou University, Lanzhou, Gansu, China, [2]Department of Endocrinology and Metabolism, Lanzhou University Second Hospital, Lanzhou, Gansu, China

Background: Autoimmune polyendocrine syndrome type 2 (APS-2) is a rare disorder characterized by autoimmune damage to multiple endocrine glands and typically involves primary adrenal insufficiency (PAI), autoimmune thyroid disease (AITD), and type 1 diabetes mellitus (T1DM). Clinical presentations that feature the full triad alongside adrenal crisis (AC) are rare, with only four such cases reported globally. While AC is the most life-threatening acute complication of APS-2, its pathogenesis is complex and incompletely understood. While there are multiple potential triggers, the role of exogenous substances such as traditional Chinese medicine [TCM] has not been systematically examined.

Case presentation: A 69-year-old female was hospitalized with a 9-year history of increasing fatigue, which had recently worsened due to high fever, anorexia, and vomiting lasting 2 days. She has previously been diagnosed with T1DM (nine years prior) and AITD (five years prior). Four years earlier, she underwent thymoma resection. Three years before admission, she self-administered an unknown TCM remedy that coincided with increased fatigue and mucocutaneous hyperpigmentation. On admission, she was in hypovolemic shock and severe hyponatremia (118.0 mmol/L). Laboratory tests revealed low basal cortisol (2.38 μg/dL) and markedly elevated adrenocorticotropic hormone (>1250 pg/mL). An adrenocorticotropic hormone stimulation test confirmed non-responsive adrenal function, indicating PAI. Together with her medical history and positive antibody profile, APS-2 with AC was diagnosed. She responded well to high-dose intravenous glucocorticoid therapy, sodium supplementation, and symptomatic management. Although persistent hyponatremia recurred following discharge, it resolved following fludrocortisone acetate supplementation, and her condition remained stable at the last follow-up.

Conclusion: We report the fifth case of full-triad APS-2 with AC and document a 9-year diagnostic delay due to non-specific symptoms with asynchronous multi-glandular involvement. Thyroxine replacement therapy and potential TCM-induced changes may have aggravated cortisol metabolism and immune imbalances, hastening adrenal failure. Clinicians should implement stepwise organ-function monitoring in patients with any single-gland autoimmune

disease, maintain vigilance for exogenous medication use, and implement multidisciplinary management strategies to mitigate the risk of AC. This case provides critical insights into both the pathogenesis and clinical management of APS-2.

KEYWORDS

autoimmune polyendocrine syndrome type 2, adrenal insufficiency, adrenal crisis, hypothyroidism, diabetes mellitus

1 Introduction

Autoimmune polyendocrine syndrome type 2 (APS-2) is a rare disorder characterized by progressive multi-glandular dysfunction, classically involving primary adrenal insufficiency (PAI), autoimmune thyroid disease (AITD), and type 1 diabetes mellitus (T1DM) (1). The full triad of APS-2 is exceptionally rare in clinical practice, and cases progressing to adrenal crisis (AC) are especially challenging; only four such cases have been previously reported worldwide (2–5). Although AC represents the most severe acute complication of APS-2, its pathogenesis remains poorly understood. Recognized triggers include infections, surgery, and medications (6, 7), but systematic research into multifactorial mechanisms, especially the potential adrenal toxic effects of exogenous agents such as traditional Chinese medicine (TCM), is lacking. Importantly, cases of delayed diagnosis, exceeding 60% in APS-2, are closely linked to disease heterogeneity, non-specific clinical manifestations, and limited clinician awareness, factors that exacerbate AC risk (8–10). Early diagnosis is critical for APS-2 patients, as it enables timely initiation of hormone replacement therapy to prevent life-threatening complications like AC and significantly reduces irreversible organ damage and mortality linked to delayed intervention. Enhancing clinician awareness of the disease's heterogeneous presentations and implementing standardized screening protocols are key strategies to improve outcomes.

This report presents the fifth global case of full-triad APS-2 complicated by AC, emphasizing important clinical insights gained through a years-long diagnostic delay. This patient's disease progression highlights a temporal association between TCM exposure and PAI deterioration, providing direct clinical evidence for multifactorial AC pathogenesis. Three critical knowledge gaps are highlighted: (1) limited recognition of the heterogeneous presentation of APS-2 by non-endocrinologists; (2) insufficient attention to exogenous factors such as TCM in clinical practice; and (3) the need for systematic monitoring of adrenal cortex function in APS-2 patients to optimize replacement therapy. These findings offer valuable guidance for clinical management strategies and future research into TCM-induced adrenal toxicity.

2 Case presentation

A 69-year-old female was admitted to the endocrinology department in May 2023 due to progressive fatigue over nine years, acutely worsened by high fever, anorexia, and vomiting for two days. Her clinical history illustrates a typical progression of multiglandular failure. Nine years prior, she developed fatigue, poor appetite, dry mouth, polydipsia, and polyuria. Laboratory tests revealed elevated fasting blood glucose (FBG) of 22.0 mmol/L, positive insulin autoantibody (IAA), and anti-glutamic acid decarboxylase antibody (Anti-GAD antibody), confirming T1DM. Insulin therapy partially improved her symptoms. Five years prior, her fatigue worsened, associated with thyroid dysfunction: reduced free triiodothyronine (FT3) and free thyroxine (FT4), elevated thyroid-stimulating hormone (TSH), positive anti-thyroglobulin antibody (TGAb), and anti-thyroid peroxidase antibody (TPOAb). Diffuse thyroid lesions on ultrasound confirmed AITD with primary hypothyroidism, and levothyroxine replacement was initiated. Four years earlier, she developed bilateral ptosis and generalized myasthenia. Repetitive nerve stimulation indicated low-frequency decrement, neostigmine test was positive, and chest CT revealed an anterior mediastinal mass. Postoperative

Abbreviations: AC, Adrenal crisis; ACTH, Adrenocorticotropic hormone; ADH, Antidiuretic hormone; AIDs, Autoimmune disease; AITD, Autoimmune thyroid disease; ANA, Antinuclear antibodies; Anti-GAD, Anti-glutamic acid decarboxylase antibody; APS, Autoimmune Polyendocrine Syndrome; APS-1, Autoimmune Polyglandular Syndrome type 1; APS-2, Autoimmune Polyglandular Syndrome type 2; CKD, Chronic kidney disease; COR, Cortisol; CRH, Corticotropin-releasing hormone; DKA, Diabetic ketoacidosis; FBG, Fasting blood glucose; FT3, Free triiodothyronine; FT4, Free thyroxine; GD, Graves' disease; GRs, Glucocorticoid receptors; HPA, Hypothalamic-pituitary-adrenal; IAA, Insulin autoantibody; ICPis, Immune checkpoint inhibitors; LT4, Levothyroxine; MG, Myasthenia gravis; MHC, Major histocompatibility complex; PAI, Primary adrenal insufficiency; PRA, Plasma Renin Activity; RAA, Renin-angiotensin-aldosterone; SAI, Secondary adrenal insufficiency; SIADH, Syndrome of inappropriate antidiuretic hormone secretion; T1DM, Type 1 diabetes mellitus; TCM, Traditional Chinese medicine; TGAb, Thyroglobulin antibody; TPOAb, Thyroid peroxidase antibody; TRAb, Thyroid-stimulating hormone receptor antibody; TRs, Thyroid hormone receptors; TSH, Thyroid-stimulating hormone; TTS, Takotsubo syndrome; UK, United Kingdom; USA, United States of America; 11β-HSD2, 11β-hydroxysteroid dehydrogenase type 2; 21-OHAb, 21-hydroxylase antibody.

pathology confirmed thymoma (type B1). Perioperative glucocorticoids and pyridostigmine bromide were briefly used but discontinued post-discharge. No tumor recurrence was observed during outpatient follow-up. Three years prior, self-administration of an unspecified TCM worsened fatigue and caused patchy pigmentation on the tongue, later progressing to generalized mucocutaneous hyperpigmentation. Two days before admission, she experienced abrupt fatigue exacerbation, high fever, severe anorexia, as well as frequent nausea and vomiting, with a recent 4 kg weight loss. She had a 5-year history of orthostatic hypotension (blood pressure: 101/70 → 70/50 → 50/40 mmHg). No significant family history, postpartum hemorrhage, tuberculosis, or chronic kidney disease was reported.

On admission, the patient appeared lethargic, cachectic, with dry skin, sunken eyes, cold extremities, and extensive hyperpigmentation predominantly affecting non-sun-exposed areas, including the cheeks, nasolabial folds, tongue, palms, soles, elbows, and buttocks (Figure 1). Vital signs showed a blood pressure of 75/47 mmHg, heart rate of 140 bpm, BMI of 21.3 kg/m^2, and temperature of 39.0°C. Laboratory tests revealed severe hyponatremia (118.0 mmol/L), hypochloremia (87.1 mmol/L), elevated FBG (20.5 mmol/L), HbA1c (9.2%), and urine ketones (2 +). Markers of cardiac stress were elevated, including NT-proBNP (22,863.00 pg/mL) and hs-cTnT (33.05 ng/L). IAA, GAD antibody, and ANA were positive. Complement components (C3, C4), serum creatinine, eGFR, and urine protein levels were normal. Thyroid ultrasound revealed bilateral hyperechoic nodules (C-TIRADS 3) with diffuse parenchymal changes.

Given her chronic fatigue, orthostatic hypotension, acute-onset nausea and vomiting, anorexia, mucocutaneous hyperpigmentation, and hypovolemic shock, adrenal function tests were performed. Laboratory findings revealed a low cortisol level with markedly elevated ACTH. An ACTH stimulation test confirmed adrenal insufficiency, with a 60-minute cortisol level of 1.8 μg/dL, well below the stimulation threshold. Adrenal CT revealed normal morphology without masses or calcification. Electrocardiography, pituitary hormone levels, and pituitary CT were unremarkable. Echocardiography indicated normal systolic function with a left ventricular ejection fraction of 63%.

The final diagnoses included AC, APS-2, PAI, AITD (on thyroid replacement), T1DM, diabetic ketoacidosis (DKA), acute heart failure, severe hyponatremia, and hypochloremia. Immediate management included intravenous hydrocortisone (100 mg Q8h), saline resuscitation, 10% sodium chloride infusion, insulin therapy, and cardiac support. Within 24 hours, her blood pressure improved to 106/63 mmHg, and gastrointestinal symptoms were resolved. Hyponatremia was corrected to 136.8 mmol/L, and urine ketones became negative within 72 hours. Intravenous hydrocortisone was gradually tapered and transitioned to oral prednisone. At discharge, the patient's electrolytes had normalized, hyperpigmentation had significantly decreased, and symptoms such as fatigue and anorexia had resolved.

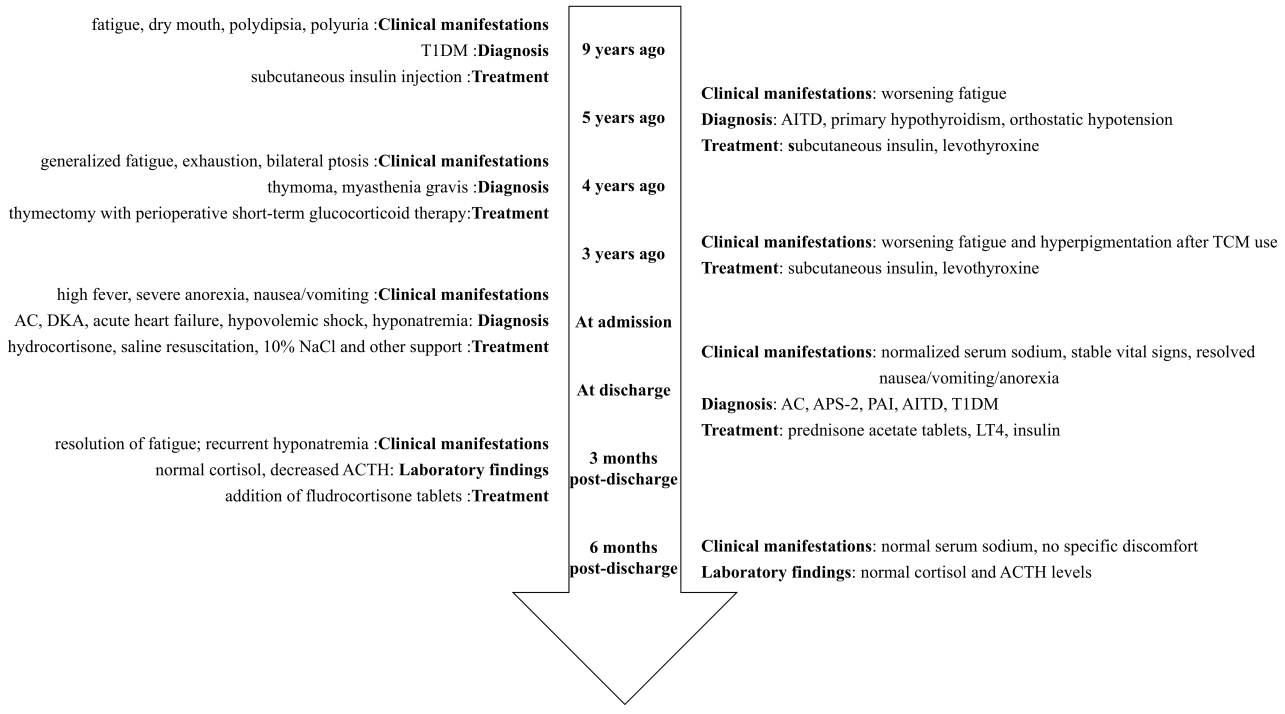

FIGURE 1
Timeline flowchart of disease progression and interventions. T1DM, Type 1 diabetes mellitus; AC, Adrenal crisis; DKA, Diabetic ketoacidosis; ACTH, Adrenocorticotropic hormone; AITD, Autoimmune thyroid disease; TCM, Traditional Chinese medicine; APS-2, Autoimmune polyendocrine syndrome type 2; PAI, Primary adrenal insufficiency.

During follow-up, fatigue and gastrointestinal symptoms fully resolved, and skin pigmentation almost completely cleared. Persistent mild hyponatremia prompted the initiation of fludrocortisone acetate (0.05 mg/day) to address suspected adrenal zona glomerulosa dysfunction. At the final follow-up, laboratory and clinical parameters remained normal, with no further episodes of decompensation (Figures 1–4; Table 1).

3 Discussion

3.1 Characteristics of APS-2

Autoimmune polyendocrine syndrome (APS) encompasses a group of autoimmune disorders (AIDs) involving two or more endocrine glands or non-endocrine organs. It is characterized by organ-specific lymphocytic infiltration and progressive functional failure mediated by circulating autoantibodies (1). APS is classified into three major subtypes based on genetic patterns and clinical features: APS-1 (associated with *AIRE* gene mutations), APS-2, and X-linked immune dysregulation syndrome. APS-2, also known as Schmidt syndrome and first described in 1926, is the most common subtype. It primarily affects the adrenal glands, thyroid, and pancreas, and it may coexist with non-endocrine AIDs such as myasthenia gravis (MG) (11). APS-2 is a polygenic disorder, involving multiple genetic loci and environmental factors, leading to significant heterogeneity in organ-specific damage. Major histocompatibility complex (*MHC*) genes on chromosome 6 are implicated in its pathology (12). Epidemiological studies estimate the prevalence of APS-2 at approximately 1/20,000, with a female-to-male ratio of 1.8–4.0:1 and peak onset occurring between 20 and 40 years of age (5). Notably, the full triad of adrenal, thyroid, and pancreatic involvement is extremely rare, with only four cases previously reported that progressed to AC. The present case represents the fifth reported instance of the full APS-2 triad complicated by AC. The patient's prolonged diagnostic journey highlights the clinical challenges posed by the asynchronous progression of multi-glandular involvement, nonspecific symptoms, and insufficient clinical awareness.

3.2 Cascade mechanisms from single-gland damage to APS-2

This patient's progressive disease offers a unique perspective into the pathophysiological mechanisms underlying the transformation from single-gland AID to full APS-2, involving the following key processes.

3.2.1 Genetic susceptibility

APS-2 develops in individuals with polygenic susceptibility strongly associated with specific HLA haplotypes (e.g., *HLA-DR3/DR4*). These genes may disrupt antigen presentation or immune tolerance mechanisms, increasing susceptibility to multi-organ

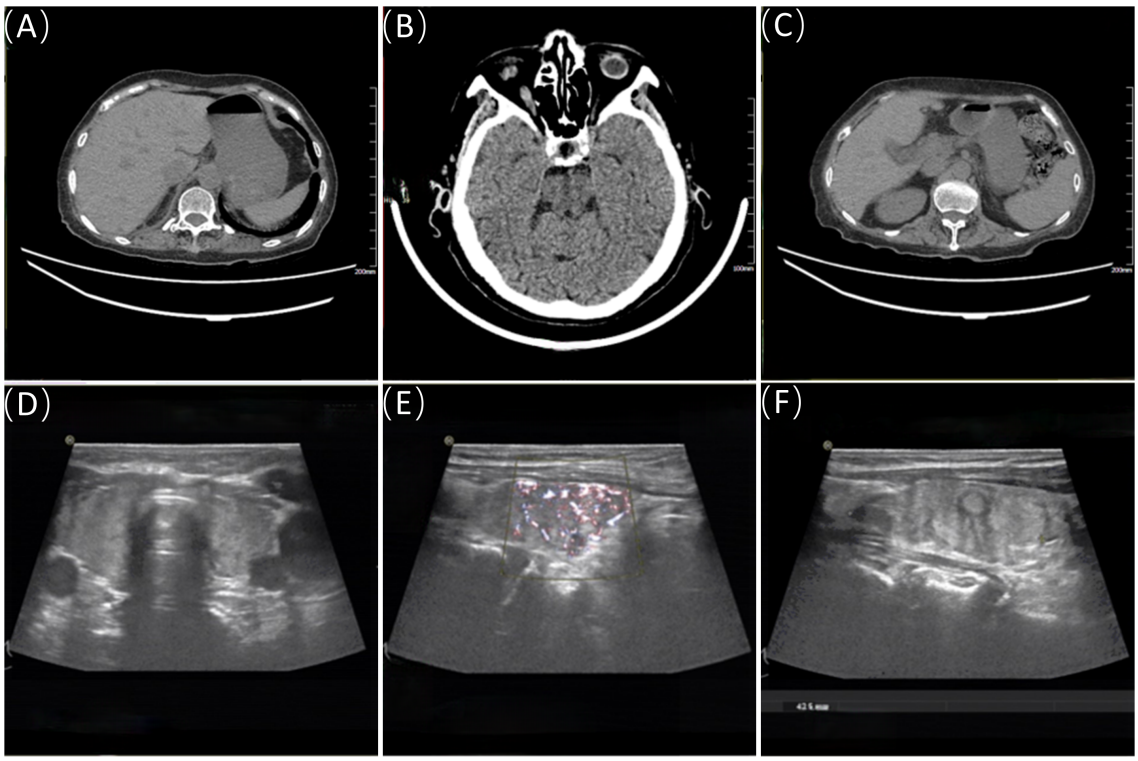

FIGURE 2
Adrenal CT, pituitary CT, and thyroid ultrasound. **(A, C)** show the CT images of the right and left adrenal glands, respectively; **(B)** displays the pituitary CT image. **(D–F)** are ultrasound images of the thyroid.

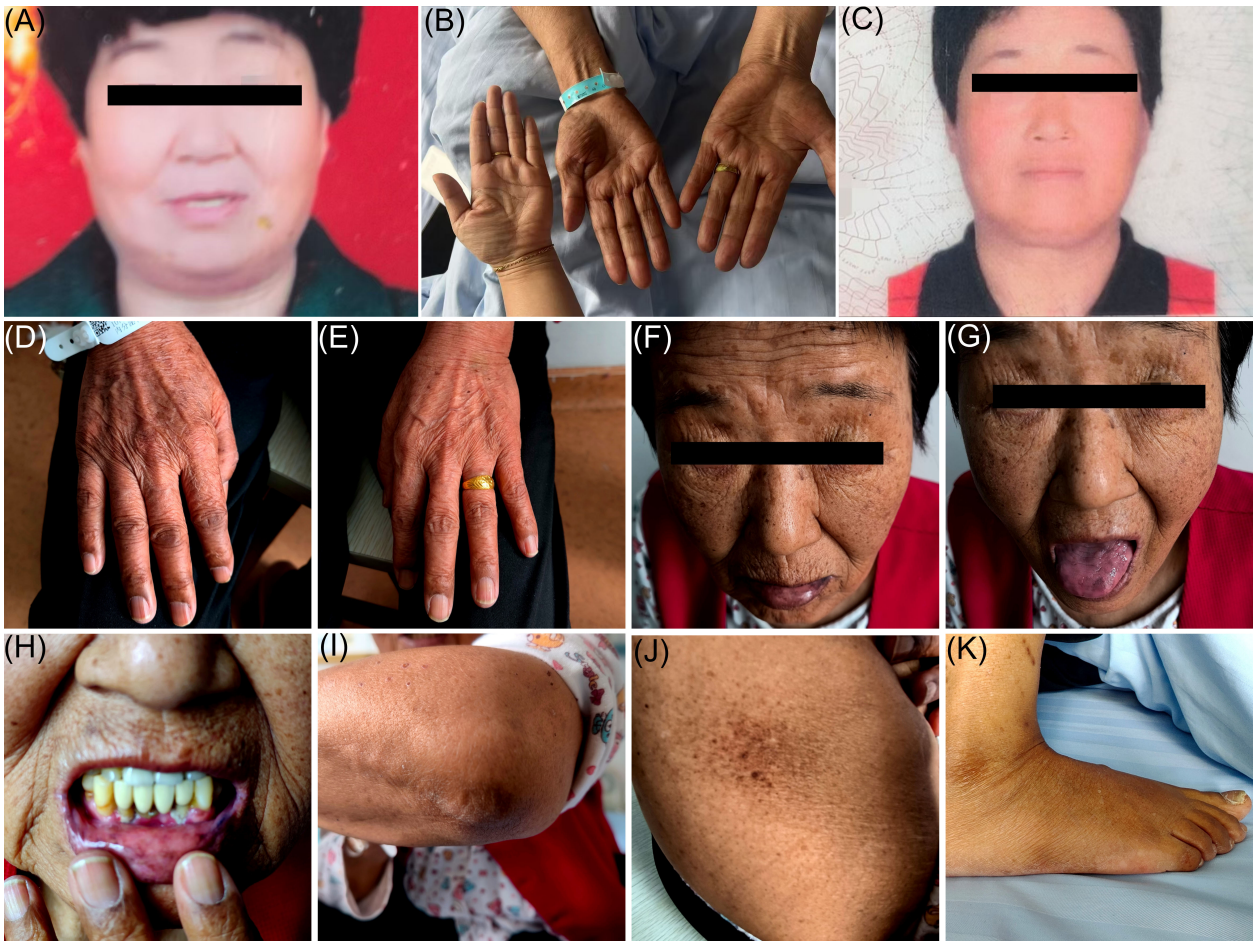

FIGURE 3
Body part images at different stages. **(A)** shows a facial image of the patient before illness onset; **(B)** shows an image of the patient's hand palm color and, for comparison, the treating physician's hand palm color at the time of admission; **(C)** shows a facial image of the patient after treatment; **(D–K)** show images of the patient's skin pigmentation on the back of the hands, face (lips, tongue, gums), elbows, buttocks, and feet, at the time of admission.

autoimmunity (13, 14). For instance, *HLA-DQ* and *HLA-DR* alleles may predispose to abnormal immune responses targeting thyroid, pancreatic β-cell, or adrenal cortical antigens. Polymorphisms in immune regulatory genes, such as *CTLA-4* (rs3087243) and *PTPN22* (rs2476601), can also impair T-cell receptor signaling and regulatory T-cell (Treg) function, exacerbating autoimmune progression (14). These genetic variations create a permissive microenvironment for cross-reactive immune responses against organ-specific antigens such as thyroglobulin, insulin, and 21-hydroxylase (15). Although genetic testing was not performed in this patient, the coexistence of thymoma and multiglandular involvement suggests the possible presence of *HLA-DR3/DR4* haplotypes or other immune regulatory gene variants.

Notably, the progression of PAI in this patient was unrelated to treatments for thymoma-associated MG. First, thymoma resection occurred prior to the onset of hyponatremia. Second, perioperative glucocorticoids were only briefly administered, with no prolonged immunosuppressants or cholinesterase inhibitors post-surgery being provided. Thus, the association between APS-2 and thymoma likely reflects shared autoimmune susceptibility rather than iatrogenic effects.

3.2.2 Immune dysregulation

The central mechanism of APS-2 involves a progressive breakdown of immune tolerance. A reduction in Treg numbers (decreased CD4+CD25+FoxP3+ cell proportions) and impaired Treg function (reduced IL-10/TGF-β secretion) lead to uncontrolled activation and proliferation of autoreactive T cells (16). For example, autoreactive T cells in PAI target 21-hydroxylase, while similar Th1/Th17-polarized responses may extend via chemokine networks to thyroid follicular cells and pancreatic β cells, triggering Graves' disease or T1DM (14, 17). In this case, thymectomy, critical for T-cell development, may have permitted the escape of autoreactive T-cells, and the absence of postoperative immunosuppression potentially accelerated the cascade-like autoimmune process.

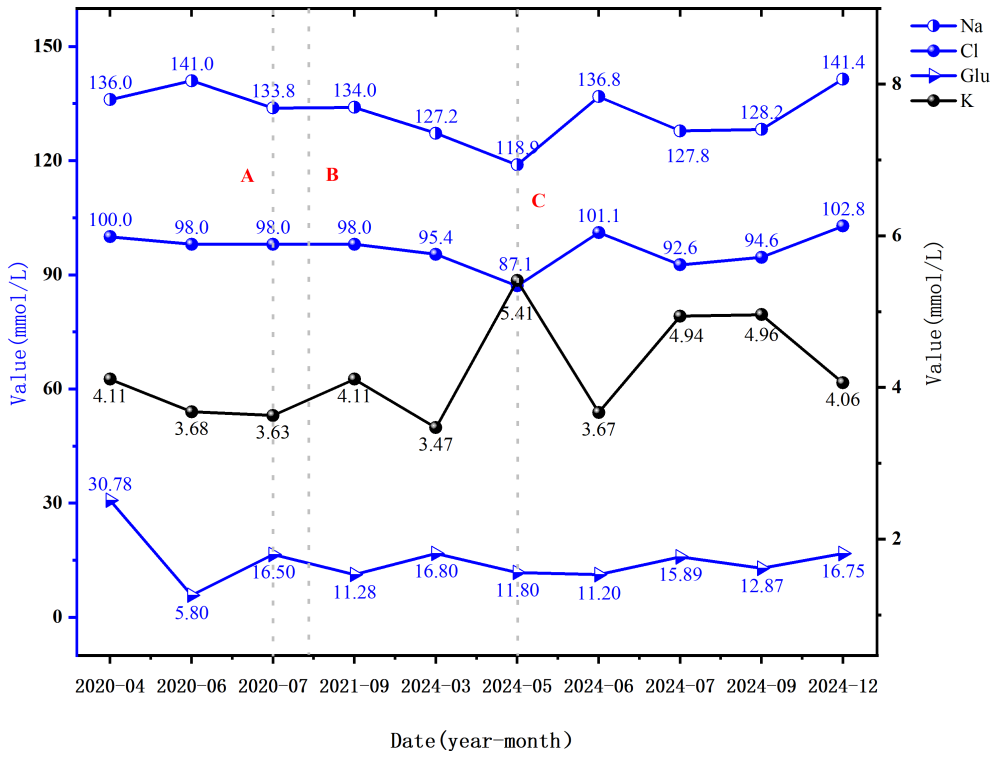

FIGURE 4
Blood glucose and electrolyte levels at various time points. Dashed line A represents the time of the first onset of hyponatremia; Dashed line B indicates the time of the first onset of skin and mucosal hyperpigmentation; Dashed line C marks the time of the first onset of hypochloremia (i.e., the time of the current admission). Abbreviations: Na, Sodium (135-145 mmol/L); Cl, Chloride (99-110 mmol/L); K, Potassium (3.5-5.5 mmol/L); Glu, Fasting glucose (3.90-6.10 mmol/L).

3.2.3 Antigen spread and molecular mimicry

Single-gland autoimmune damage can lead to multi-organ involvement through epitope spreading. For example, thyroid follicular destruction releases intracellular antigens such as thyroglobulin, which are captured by dendritic cells and cross-presented in lymph nodes, activating T-cell clones that subsequently target adrenal or pancreatic tissues (18). Environmental triggers (e.g., enteroviruses) may also disrupt immune tolerance via molecular mimicry (19). For instance, the PEVKEK sequence in Coxsackievirus B4 2C protein shares homology with the GAD65 antigen, potentially initiating cross-reactive immune responses against pancreatic islets (20). Similarly, *Mycobacterium avium* MAP3865c protein shares epitopes with pancreatic zinc transporter 8 (ZnT8) (21). The acute exacerbation of PAI symptoms after exposure to TCM in this case suggests that exogenous agents might promote antigen spreading via similar mechanisms.

3.2.4 Cumulative effects of autoantibodies

Autoantibodies associated with single-gland AID may predict the risk of subsequent multi-gland involvement. For example, patients with 21-hydroxylase antibody (21-OHAb)-positive PAI have approximately a 50% risk of developing additional endocrine autoimmune disorders, suggesting that antibodies may contribute to tissue damage via complement activation or antibody-dependent cellular cytotoxicity (13). Notably, certain antibodies (e.g., anti-interferon-α) may also compromise innate immunity, creating a vicious cycle of infection and autoimmunity (22). In this patient, the progressive expansion of autoantibodies (IAA → Anti-GAD → TPOAb/TGAb) illustrates this cumulative autoimmune damage. Importantly, the patient's ANA positivity—which are commonly associated with systemic lupus erythematosus, Sjögren's syndrome, and systemic sclerosis—warrants regular monitoring of ANA titers and prompt evaluation for symptoms such as facial rash, recurrent oral ulcers, severe alopecia, polyarthralgia, dry mouth or eyes, frothy urine, or unexplained fever (23, 24).

Based on these mechanisms, we propose a structured monitoring approach for patients with single-gland AID (25, 26): 1) initial comprehensive screening for relevant autoantibodies (e.g., 21-OHAb, TPOAb, GAD65Ab); 2) biannual or annual evaluation of target organ function (morning cortisol, thyroid function, oral glucose tolerance test); and 3) prompt assessment for new glandular involvement when nonspecific symptoms (e.g., fatigue, weight loss) arise.

3.3 Diagnosis and differential diagnosis of APS-2

The patient presented with chronic fatigue, hyponatremia, orthostatic hypotension, and mucocutaneous hyperpigmentation.

10.3389/fimmu.2025.1563629

TABLE 1 Patient laboratory and hormonal test results.

Analyte	Result	Reference interval	Unit
Fasting Blood Glucose	20.5 ↑	3.9~6.1	mmol/L
Glycated Hemoglobin	9.2% ↑	4.0~6.0	%
Fasting Insulin	0.54 ↓	3.00~25.00	mIU/L
Fasting C-Peptide	0.17 ↓	0.48~5.05	ng/mL
2-Hour Postprandial Insulin	55.71 ↑	3.00~25.00	mIU/L
2-Hour Postprandial C-Peptide	0.12 ↓	0.48~5.05	ng/mL
Insulin Autoantibody	16.40	0.00~20.00	IU/mL
Anti-Glutamic Acid Decarboxylase Antibody	102.00 ↑	0.00~30.00	IU/mL
Antinuclear Antibody	Positive	Negative	–
Anti-double stranded DNA antibody	Negative	Negative	–
Complement component 3	1.2	0.7~1.4	g/L
Complement component 3	0.25	0.10~0.40	g/L
Serum Creatinine	56	41~81	μmolL
pH Value	7.34↓	7.35~7.45	–
Base Excess	-4.8 ↓	-3.0~3.0	mmol/L
Urine Glucose	Positive(1+)	Negative	–
Urine Ketone Bodies	Positive (2+)	Negative	–
24-Hour Urine Sodium Excretion	358 ↑	130-260	mmol/L
Urine Protein	Negative	Negative	–
Luteinizing Hormone	21.23	15.90~54.00	mIU/mL
Follicle-Stimulating Hormone	44.67	23.00~116.30	mIU/mL
Growth Hormone	8.37 ↑	0.00~5.00	ng/mL
Prolactin	80.78 ↑	1.80~20.30	ng/mL
Insulin-like Growth Factor-1	16.90 ↓	31.00~323.00	ng/mL
Parathyroid Hormone	14.00	11.00~67.00	pg/mL
White Blood Cell Count	9.8 ↑	3.5-9.5	$\times10^9$/L
C-Reactive Protein	10.59 ↑	<10.00	mg/L
N-terminal pro-B-type Natriuretic Peptide	22863.00 ↑	≤125.00	pg/mL
High-Sensitivity Troponin T	33.05 ↑	≤14.00	ng/L
Adrenocorticotropic hormone_ at admission	>1250.00 ↑	5.00~46.00	pg/mL
Cortisol_ at admission	2.38 ↓	5.00~25.00	μg/dL
Cortisol, 60 min after cosyntropin (1 μg)	1.8 ↓	>18.0	μg/dL
Adrenocorticotropic hormone_ at discharge	1237.00↑	5.00~46.00	pg/mL
Cortisol_ at discharge	1.62↓	5.00~25.00	μg/dL
Adrenocorticotropic hormone_ 1-month post-discharge	589.00↑	5.00~46.00	pg/mL
Cortisol_ 1-month post-discharge	1.62↓	5.00~25.00	μg/dL
Adrenocorticotropic hormone_ 3 months post-discharge	55.30↑	5.00~46.00	pg/mL
Cortisol_ 3 months post-discharge	5.06	5.00~25.00	μg/dL
Adrenocorticotropic hormone_ 6 months post-discharge	19.90	5.00~46.00	pg/mL
Cortisol_6 months post-discharge	5.16	5.00~25.00	μg/dL

"-" means that the corresponding indicator has no unit.
"↑" means higher than the reference range and "↓" means lower than the reference range.

Prominent clinical features in admission included nausea, vomiting, severe anorexia, and hypovolemic shock. Laboratory findings indicated low cortisol and markedly elevated ACTH, consistent with PAI (27). Differential diagnoses were systematically considered and ultimately excluded: 1) Secondary adrenal insufficiency (SAI): Elevated ACTH levels and a normal pituitary CT effectively ruled out SAI (28); 2) Chronic kidney disease (CKD)-related electrolyte disturbances: Normal serum creatinine, eGFR, and absence of proteinuria excluded CKD as a cause of hyponatremia (29); 3) Myxedema: Though the patient had a history of primary hypothyroidism, stable TSH levels under adequate levothyroxine replacement therapy excluded thyroid-related etiology. Hypothyroidism-associated hyponatremia typically involves antidiuretic hormone (ADH) dysregulation and impaired free water excretion, whereas this patient exhibited hyponatremia with elevated urinary sodium excretion inconsistent with renal water retention mechanisms (30); 4) Gastrointestinal disorders: Normal gastrointestinal imaging and absence of endoscopic evidence excluded these diagnoses (31); 5) Malignancy/paraneoplastic syndrome: No unexplained fever, acute weight loss (4 kg loss correlated with acute decompensation), normal tumor markers (CEA, CA199), and absence of masses on thoracic/abdominal CT (prior thymoma resection without recurrence) ruled out this possibility (32); 6) Syndrome of inappropriate antidiuretic hormone secretion (SIADH): SIADH typically presents with euvolemic or mildly hypervolemic hyponatremia with normal cortisol/ACTH levels (33). The presence of severe hyponatremia with elevated urinary sodium and hypovolemia supported renal sodium wasting characteristic of PAI (34). The ACTH stimulation test further confirmed primary adrenal cortex dysfunction.

Following confirmation of PAI, etiological evaluation was conducted. Major causes of PAI include tuberculosis, autoimmune disorders, infections, tumors, and medications. This patient had no history of tuberculosis, systemic fungal infections, or HIV. Adrenal CT revealed no structural abnormalities, excluding

adrenalectomy, hemorrhage, tumors, infiltration, congenital adrenal hyperplasia, or infectious adrenalitis (35, 36). The absence of long-term use of adrenal enzyme inhibitors (e.g., ketoconazole) ruled out drug-induced PAI (36). Adrenoleukodystrophy, typically affecting prepubertal males, was unlikely given the patient's adult-onset presentation. The patient's clinical history of MG and multiple autoimmune antibodies strongly suggested immune dysregulation, supporting autoimmune PAI (35). APS-2 diagnostic criteria require the coexistence of at least two endocrine AIDs (AITD, PAI, T1DM) with corresponding autoantibodies (5). This patient met these criteria based on her sequential diagnoses of T1DM, AITD, and autoimmune PAI. Although adrenal-specific antibodies were not tested, the patient's autoimmune background and thorough exclusion of alternative causes confirmed APS-2.

Diagnostic challenges in this case included: 1) Nonspecific symptoms and overlapping clinical conditions: Chronic fatigue and anorexia were attributed initially to concurrent conditions such as MG-related muscle weakness, AITD-induced metabolic slowdown, and catabolic changes from DKA. The insidious onset and nonspecific nature of PAI, compounded by limited clinician awareness, contributed to delays in the recognition of key indicators such as hyponatremia, hyperpigmentation, and orthostatic hypotension. 2) Complex pathophysiology of hyponatremia: Persistent hyponatremia necessitated a differentiation between hypothyroidism and DKA. In hypothyroidism, hyponatremia arises from impaired water excretion, abnormal ADH secretion, aquaporin dysregulation, and reduced cardiac output (37–40). DKA-related hyponatremia results primarily from dehydration and osmotic diuresis (41, 42). Conversely, in PAI, hyponatremia results from combined aldosterone and cortisol deficiencies, leading to sodium wasting, water retention, and dysregulated ADH secretion (43, 44). Although treatment with 10% sodium chloride temporarily normalized serum sodium levels during hospitalization, persistent hyponatremia post-discharge indicated involvement of the adrenal zona glomerulosa. This dynamic course highlights the importance of a careful evaluation of the multifactorial nature of hyponatremia in polyendocrine disorders to avoid misdiagnosis.

3.4 Diagnosis and differential diagnosis of AC

AC represents the most severe manifestation of PAI, occurring in patients with APS-2 when cortisol production becomes inadequate or cortisol requirements increase due to acute stressors such as infection, surgery, excessive sweating, vomiting, or inadequate glucocorticoid treatment (6). Without prompt glucocorticoid replacement, AC rapidly becomes life-threatening, with an annual incidence of 6%–8% (6). AC is diagnosed when a patient with PAI experiences acute deterioration with at least two of the following symptoms or signs: hypotension, acute abdominal pain, nausea/vomiting, altered mental status, fatigue, fever, or biochemical abnormalities such as hyponatremia, hyperkalemia, or hypoglycemia, necessitating immediate intravenous glucocorticoid administration (6). This patient presented with an acute exacerbation of fatigue, nausea/vomiting, severe hyponatremia, reduced insulin requirements, and evidence of hypovolemic shock. Intravenous sodium hydrocortisone succinate (100 mg Q8h) was promptly initiated. This led to a rapid clinical improvement within 24 hours, including resolution of fatigue, improved appetite, and normalization of vital signs, confirming the diagnosis of AC.

A critical differential diagnosis to consider is stress-induced cardiomyopathy (Takotsubo syndrome, TTS, characterized by transient, reversible left ventricular dysfunction often triggered by intense emotional or physical stress such as emotional trauma, surgery, or acute illness. The pathophysiology of TTS involves excessive catecholamine release, causing microvascular dysfunction and myocardial stunning (45). Under normal conditions, cortisol mitigates catecholamine-induced endothelial damage by suppressing inflammatory cytokines (e.g., IL-6, TNF-α) and modulating the hypothalamic-pituitary-adrenal (HPA) axis to prevent sympathetic hyperactivation. In cortisol states of cortisol deficiency such as PAI, compensatory sympathetic hyperactivation and catecholamine excess (46, 47), combined with uncontrolled inflammation and increased β-receptor sensitivity amplify cardiotoxicity (48–50), resulting in microvascular spasms, calcium overload, oxidative stress, and excitation-contraction uncoupling (51–54). In patients with PAI, TTS can manifest as acute left heart failure, cardiogenic shock, or refractory arrhythmias (e.g., torsades de pointes), with echocardiography showing characteristic regional wall motion abnormalities. A previously reported case described TTS with cardiogenic shock in a patient with PAI following corticotropin-releasing hormone (CRH) testing, highlighting iatrogenic stress as a potential trigger (55). Chronic under-treatment with glucocorticoids increases TTS risk during periods of infection or surgery (56, 57).

Although the patient described in this report presented initially with features suggestive of acute left heart failure and cardiogenic shock, initial electrocardiography and echocardiography revealed no abnormalities, precluding the need for further serial cardiac ultrasound monitoring. Nonetheless, clinicians should remain vigilant for TTS in AC patients presenting with acute cardiac symptoms or unexpected cardiac deterioration during glucocorticoid therapy or stress events. Optimizing glucocorticoid dosing reduces catecholamine-related toxicity risk, while prompt echocardiography facilitated the early detection of TTS (57).

3.5 Multiple mechanisms inducing AC

In contrast with previously reported APS-2 cases, this patient's AC involved multifactorial triggers, including thyroid hormone replacement therapy, DKA, acute heart failure, and potential TCM-induced adrenal toxicity. This case highlights the cumulative effects of levothyroxine replacement and TCM exposure in accelerating the progression of PAI.

The regulatory effects of thyroxine on adrenal cortical function may involve four mechanisms: 1) Accelerated cortisol clearance:

Levothyroxine increases basal metabolic rate and induces hepatic cytochrome P450 enzymes (e.g., CYP3A4), enhancing cortisol hydroxylation and conjugation, thereby accelerating conversion to inactive metabolites such as cortisone (58, 59). Additionally, thyroid hormones may modulate 11β-hydroxysteroid dehydrogenase activity, influencing cortisol-cortisone interconversion (60, 61). 2) HPA axis dysregulation: Short-term levothyroxine therapy enhances CRH/ACTH secretion to stimulate cortisol production. However, chronic treatment may suppress TSH via negative feedback, potentially reducing adrenal reserve function (58, 62, 63). 3) Receptor-level cross-regulation: Co-expression of thyroid hormone receptors (TRs) and glucocorticoid receptors (GRs) can lead to receptor cross-talk. Low cortisol levels observed in AITD patients may stem from TR-mediated upregulation of GR sensitivity, accelerating cortisol catabolism (64–66). 4) Direct inhibition of steroid synthesis: Animal studies indicate that exogenous thyroxine downregulates steroidogenic acute regulatory protein (StAR) and cholesterol side-chain cleavage enzyme (CYP11A1) in adrenal cortical cells, impairing critical steps in cortisol synthesis and reducing adrenal responsiveness to ACTH (62, 67–69). Clinicians should therefore suspect PAI in hypothyroid patients who present with persistent fatigue despite adequate thyroid replacement therapy (26). Further research is needed to clarify how thyroxine differentially affects cortisol metabolism across various pathological states (62, 65, 70).

Additionally, this case provides clinical evidence, through a clear temporal association, that TCM exposure may accelerate APS-2 progression. Potential mechanisms include: 1) Mineralocorticoid-like effects: Glycyrrhizin derivatives inhibit 11β-hydroxysteroid dehydrogenase type 2 (11β-HSD2), leading to abnormal renal cortisol accumulation, mimicking mineralocorticoid activity, and subsequently suppressing the renin-angiotensin-aldosterone (RAA) system (71–74). Chronic exposure may lead to zona fasciculata atrophy and compensatory ACTH elevation (75, 76). 2) Disruption of glucocorticoid metabolism: Components such as tanshinone IIA and triptolide induce CYP3A4 expression by activating nuclear receptors (e.g., PXR) and epigenetic modifications (e.g., H3K4me2 methylation), thus accelerating glucocorticoid metabolism (77–80). Although specific TCM components responsible for the observed clinical deterioration in this case remain unidentified, the clear temporal correlation between TCM use and the clinical manifestations (e.g., worsening fatigue, hyperpigmentation) supports a causal relationship between TCM exposure and progression from subclinical to overt PAI. Clinicians should thoroughly assess the use of herbal products and dietary supplements in APS-2 patients and avoid prolonged administration of agents potentially disruptive to the adrenal axis- without robust pharmacological evidence (81).

3.6 Treatment strategies, prognosis, and limitations

Physiologic-dose hormone replacement remains the cornerstone of APS-2 management. Given the interconnected nature of endocrine gland dysfunction, treatment necessitates coordinated and timely dose adjustments (26). In this case, electrolyte and metabolic abnormalities were effectively corrected with adequate hormonal combination therapy. At the last follow-up, laboratory parameters including serum sodium (141.4 mmol/L), potassium (4.06 mmol/L), basal cortisol (5.72 μg/dL), and ACTH (19.9 pg/mL) had normalized, accompanied by a complete resolution of fatigue and anorexia. A comprehensive three-tier management strategy was implemented, emphasizing patient education: 1) Daily monitoring of blood glucose, blood pressure, and symptom diaries; 2) Stress response measures, such as doubling glucocorticoid doses during infection or/trauma; 3) Emergency preparedness, including carrying an emergency card detailing the patient's diagnosis and medication regimen.

Study limitations: The presented case focused primarily on evaluating cortisol deficiency during hospitalization. The absence of serum potassium abnormalities led to an incomplete assessment of the RAA system, highlighting the importance of a systematic evaluation of this axis in PAI patients, even when potassium levels are found to be normal. Emerging evidence indicates that approximately 35% of autoimmune PAI patients maintain normal serum potassium during early zona glomerulosa dysfunction. Additionally, laboratory constraints precluded testing for anti-adrenal cortex antibodies and acetylcholine receptor antibodies. Despite these limitations, systematic clinical evaluation effectively excluded common secondary PAI causes, including infections, metabolic causes, or iatrogenic factors. Furthermore, this case highlights that negative 21-OHAb results do not fully exclude autoimmune PAI, particularly in patients with advanced disease or coexisting autoimmune conditions, where antibody-negative rates can reach 30% (82). Comprehensive diagnosis in antibody-negative cases should integrate dynamic antibody monitoring, adrenal function assessments, and genetic testing to prevent missed diagnoses of autoimmune PAI (83).

3.7 Clinical features and literature analysis of APS-2 complicated by AC

AC is a leading cause of mortality among APS-2 patients, yet it remains poorly characterized. To improve clinical understanding, we analyzed previously reported APS-2 cases complicated by AC. A systematic literature review was conducted in PubMed (up to June 2024) using the search terms: *("Polyendocrinopathies, Autoimmune"[Mesh] OR "autoimmune polyendocrine syndrome type 2 [Title/Abstract]") AND ("Adrenal Insufficiency"[MeSH] OR "Addison Disease"[MeSH] OR "Adrenal Crisis"[Title/Abstract])*. Case reports and series meeting APS-2 diagnostic criteria with confirmed AC events were included, yielding 18 patients (Table 2).

3.7.1 Case characteristics

Demographics and Geographic Distribution: Females predominated (15/18, 83.3%; male-to-female ratio 1:5). The age of onset ranged widely (4–74 years; mean 35.5 ± 22.5 years), with the highest proportion (44.4%) aged >40 years. Geographically, China (22.2%) and the U.S. (16.7%) contributed the most cases.

Initial Clinical Encounters and Diagnostic Delays: 46.7% (7/15) of patients initially presented to emergency departments, while only

TABLE 2 Overview of published cases involving APS-2 complicated by AC.

Author	Gender	Age (y)	Disease Composition	Initial Disease	Clinical Presentation	Trigger	Time[a] (days)	Auto-Ab	Hyponatremia	Hyperkalemia	Hypovolemic Shock	Treatment	Prognosis
Nelson (2)	Female	11	T1DM +AITD+PAI	T1DM	weakness, anorexia, vomiting, fever	-	2920	TGAb (+) 21-OHAb (+)	Yes	Yes	Yes	prednisolone + LT4 + fludrocortisone + insulin	growth retardation
Murray (84)	Female	26	AITD+PAI	T1DM	lethargy, vomiting, nausea, hypoglycemia	LT4-therapy	150	TPOAb (+) 21-OHAb (+)	Yes	Yes	Yes	glucocorticoids+ fludrocortisone +LT4	clinical stability
Mazul-Sunko (85)	Female	43	AITD+PAI	PAI	weakness, vomiting, fatigue	Surgery	0	TPOAb (+) 21-OHAb (+)	No	No	Yes	hydrocortisone + LT4	clinical stability
Tsang (3)	Female	42	T1DM +AITD+PAI	AITD	weakness, nausea, vomiting	Infection	1275	TPOAb (+) TGAb (+)	Yes	Yes	Yes	hydrocortisone + LT4+ insulin	clinical stability
Ghanny (86)	Male	6	T1DM +PAI	T1DM	lethargy, vomiting, hyperpigmentation	-	2005	21-OHAb (+)	Yes	-	-	hydrocortisone + fludrocortisone + insulin	clinical stability
Chang (87)	Male	4	T1DM +PAI	T1DM	hypoglycemia, hyperpigmentation	-	180	–	Yes	No	Yes	hydrocortisone + fludrocortisone + insulin	clinical stability
Vallianou (88)	Female	74	AITD+PAI	AITD	fatigue, nausea, vomiting, hyperpigmentation	LT4-therapy	5	TPOAb (+) TGAb (+) 21-OHAb (+)	Yes	Yes	Yes	adrenal steroid hormone+ LT4	–
Bain (89)	Female	57	AITD+PAI	AITD	weight and appetite loss, vomiting, hyperpigmentation	Infection	3285	TPOAb (+) TGAb (+) 21-OHAb (+)	Yes	No	Yes	hydrocortisone + fludrocortisone + LT4	clinical stability
Gürkan (90)	Female	36	AITD+PAI	–	nausea, vomiting, appetite loss	Shock	0	TPOAb (+) TGAb (+)	Yes	Yes	Yes	methyl prednisolone + fludrocortisone	clinical stability
Wang (91)	Female	38	AITD+PAI	AITD	hyperpigmentation, appetite loss, nausea	-	850	TPOAb (+) TGAb (+)	Yes	Yes	Yes	hydrocortisone + fludrocortisone + LT4	clinical stability
Schulz (92)	Male	15	AITD+PAI	GD	weight loss, nausea, vomiting, hyperpigmentation	-	180	TPOAb (+) TRAb (+) 21-OHAb (+)	Yes	No	Yes	hydrocortisone + fludrocortisone + carbimazole	clinical stability
Yanachkova (93)	Female	41	AITD+PAI	AITD	hyperpigmentation	Pregnancy	5840	–	Yes	Yes	-	prednisolone + fludrocortisone + LT4	clinical stability
Wiśniewski (94)	Female	78	AITD+PAI	AITD	diarrhea, vomiting, weakness, fatigue	-	-	TPOAb (+) TGAb (+)	Yes	No	Yes	hydrocortisone + fludrocortisone + LT4	clinical stability

(Continued)

10.3389/fimmu.2025.1563629

TABLE 2 Continued

Author	Gender	Age (y)	Disease Composition	Initial Disease	Clinical Presentation	Trigger	Time[a] (days)	Auto-Ab	Hyponatremia	Hyperkalemia	Hypovolemic Shock	Treatment	Prognosis
Lassoued (95)	Female	28	AITD+PAI	AITD	fever, palpitation, vomiting, weight loss	Thyroid Crisis	0	TPOAb (+) TGAb (+)	Yes	Yes	Yes	hydrocortisone + LT4	clinical stability
Lantz (4)	Female	21	T1DM +AITD+PAI	–	nausea, vomiting, weakness	Infection	-	–	Yes	Yes	Yes	LT4+insulin +hydrocortisone + fludrocortisone	clinical stability
Bonataki (96)	Female	11	AITD+PAI	PAI	hyperpigmentation, vomiting, weight loss, fatigue, weakness	–	2190	TPOAb (+), TGAb (+) 21-OHAb (+)	Yes	Yes	Yes	hydrocortisone + fludrocortisone	clinical stability
Spagnolo (97)	Female	55	AITD+PAI	AITD	weight loss, nausea, vomiting, palpitation	ICPis	10	TPOAb (+) TGAb (+)	Yes	Yes	Yes	hydrocortisone + fludrocortisone + LT4	clinical stability
Pan (5)	Female	60	T1DM +AITD+PAI	AITD	weight loss, nausea, vomiting, weakness	ICPis	150	TPOAb (+) TGAb (+)	Yes	Yes	No	hydrocortisone+ LT4+ insulin	occasional hypoglycemia
This case	Female	69	T1DM +AITD+PAI	T1DM	Fatigue, appetite loss, weight loss, nausea, vomiting, weakness, hyperpigmentation	LT4 therapy +DKA+ AHF +TCM	3285	TPOAb (+), TGAb (+) IAA (+), ANA (+) GAD65Ab (+)	Yes	No	Yes	prednisolone + fludrocortisone + LT4+insulin	clinical stability

Time[a] (days), days ever since the initial disease to the diagnosis of APS-2; AC, Adrenal crisis; ICPis, immune checkpoint inhibitors; T1DM, type 1 diabetes mellitus; PAI, autoimmune adrenal insufficiency; AITD, autoimmune thyroid disease; TPOAb, thyroid peroxidase antibody; TGAb, thyroglobulin antibody; TRAb, thyroid-stimulating hormone receptor antibody; 21-OHAb, 21-hydroxylase antibody; IAA, insulin autoantibody; ANA, antinuclear antibody; GAD65Ab, anti-glutamic acid decarboxylase 65 antibody; LT4, levothyroxine; DKA, Diabetic ketoacidosis; AHF, Acute heart failure; TCM, traditional Chinese medicine; USA, United States of America; UK, United Kingdom. "-" means not mentioned in the article.

10.3389/fimmu.2025.1563629

13.3% (2/15) sought care at endocrinology clinics, likely reflecting the acute nature of AC, typically manifesting with hypovolemic shock (93.8%). The median time from first disease onset to APS-2 diagnosis was 180 days (range: 0–5840 days). In the presented case, the patient experienced a markedly prolonged diagnostic delay of 3,285 days, far exceeding the median, underscoring the need for a heightened awareness and systematic adrenal function evaluations in patients presenting with persistent fatigue, hyponatremia, and orthostatic hypotension, particularly in the presence of concurrent T1DM or AITD.

3.7.2 Crisis triggers and disease patterns

Triggers: Specific precipitating factors were identified in 61.1% (11/18) of AC cases, most commonly these included infections (27.3%), levothyroxine replacement (18.2%), and immune checkpoint inhibitors (18.2%). Our case uniquely highlights AC triggered by multiple concurrent factors, including levothyroxine replacement, DKA, acute heart failure, and TCM exposure, suggesting that cumulative stressors may elevate the risk of adrenal decompensation (26).

Disease Combinations: All patients exhibited PAI, 88.9% had AITD, and 38.9% had T1DM. The most common disease combination was AITD+PAI (66.7%), whereas the complete triad (T1DM+AITD+PAI) accounted for only 22.2% of reported cases. Our study contributes the fifth globally reported case of full-triad APS-2 complicated by AC, further expanding the spectrum of clinical disease manifestations. Initial presentations included AITD (55.6%, 10/18), T1DM (22.2%, 4/18), and PAI (11.1%, 2/18), with only one case exhibiting simultaneous onset of all three conditions.

3.7.3 Biochemical features

Hyponatremia occurred in 94.4% (17/18) of cases and hyperkalemia in 70.6% (12/17). In our case, chronic anorexia and vomiting likely masked significant potassium elevation, highlighting the importance of evaluating nutritional status when interpreting electrolyte abnormalities to avoid misdiagnosis.

3.8 Early identification and long-term management.

Autoimmune PAI typically develops insidiously, with immune dysregulation typically preceding overt PAI by several years. The natural disease progression includes five-stages and can be dynamically assessed using the ACTH stimulation test (98, 99). This test evaluates baseline cortisol, ACTH, upright renin, aldosterone, and cortisol responses at 60 minutes post-ACTH administration. These parameters establish diagnostic stages as follows: Stage 0 (normal adrenal function), Stage I (elevated renin with normal/low aldosterone, indicating early adrenal cortical dysfunction), Stage II (markedly elevated renin, reduced aldosterone, and abnormal cortisol response), Stage III (elevated ACTH with normal/low cortisol), and Stage IV (significant ACTH elevation, low cortisol, and classic PAI symptoms). Typically, zona glomerulosa dysfunction (aldosterone production) precedes impairment of the zona fasciculata and reticularis (cortisol synthesis) due to local cortisol protection. For patients positive for 21-OHAb, periodic ACTH stimulation tests combined with RAA monitoring are recommended, enabling the timely initiation of hormone replacement therapy at subclinical stages (Stage I) to delay overt PAI.

Long-term APS-2 management requires multidisciplinary collaboration and structured follow-up. Annual screening should encompass thyroid function (TSH, FT4, TPOAb, TGAb), adrenal function (morning cortisol, ACTH, 21-OHAb), gonadal function (FSH/estradiol in females, testosterone in males), and glucose metabolism (HbA_1c, C-peptide) (26, 100). Pregnancy necessitates more intensive monitoring of thyroid, glucose, and adrenal parameters (100–104). Screening for non-endocrine autoimmune complications such as pernicious anemia, autoimmune gastritis, and celiac disease, should include complete blood count, gastric parietal cell antibodies, intrinsic factor antibodies, and tissue transglutaminase antibodies (100–102). Asymptomatic antibody-positive individuals should undergo evaluations every 3–6-months, and regular screening is also advised for first-degree relatives (26). Clinicians should systematically document symptoms such as fatigue, weight changes, hyperpigmentation, thyroid enlargement, and vitiligo as part of a comprehensive assessment (101–103, 105).

Emerging diagnostic tools include combined antibody panels (e.g., IL-17/IL-22 autoantibodies alongside GAD65, 21-OHAb, TPOAb) (106), genetic risk profiling (e.g., HLA-DR3/DR4 haplotypes such as DRB1*0404) (107, 108), innovative functional assays (e.g., low-dose ACTH stimulation with dynamic renin activity) (109, 110), and omics technologies (e.g., metabolomics/proteomics to identify early metabolic abnormalities) (111). Current, APS-2 diagnosis remains primarily clinical and antibody-based. Future research efforts should focus on developing dynamic predictive models integrating antibody profiles, adrenal function, and genetic risk data, alongside AI-assisted diagnostic algorithms employing immunometabolic biomarkers for early detection and intervention.

4 Conclusion

This study reports the fifth case of full triad APS-2 complicated by AC. The multifactorial triggers of AC and prolonged diagnostic delay highlight key clinical challenges in managing APS-2: 1) nonspecific clinical presentations and asynchronous multiglandular involvement contributing to diagnostic delays; 2) the complexity of differentiating electrolyte disturbances such as hyponatremia, necessitating dynamic hormonal evaluations; and 3) the potential contribution of exogenous factors (e.g., TCM) in exacerbating adrenal insufficiency by disrupting cortisol metabolism and immune homeostasis. Consequently, we recommend: 1) stepwise monitoring though antibody screening and regular target organ function assessments in patients with

single-gland autoimmune diseases; 2) vigilance for cortisol-ACTH axis dynamics during thyroid hormone replacement therapy; 3) cautious use of TCM to avoid potential adrenal toxicity; and 4) multidisciplinary management, including structured glucocorticoid adjustment during stress events for patients with an elevated risk for AC.

Study limitations include incomplete RAA axis evaluation and unavailability of specific antibody testing. Future research should integrate genetic and metabolomic information to refine predictive models, better understand TCM-related adrenal toxicity, and optimize early precision-based interventions. In summary, this case not only expands the clinical spectrum of APS-2 but also highlights the need for increased awareness by clinicians, systematic follow-up, and targeted preventive strategies to improve patient outcomes.

Data availability statement

The original contributions presented in the study are included in the article/supplementary material. Further inquiries can be directed to the corresponding author.

Ethics statement

Written informed consent was obtained from the individual(s) for the publication of any potentially identifiable images or data included in this article. Written informed consent was obtained from the participant/patient(s) for the publication of this case report.

Author contributions

ZY: Conceptualization, Data curation, Formal analysis, Investigation, Methodology, Software, Visualization, Writing – original draft. DX: Conceptualization, Data curation, Investigation, Software, Writing – original draft. XH: Conceptualization, Methodology, Supervision, Validation, Writing – review & editing. DG: Formal analysis, Methodology, Validation, Software, Writing – review & editing. XX: Formal analysis, Methodology, Investigation, Software, Writing – review & editing. HC: Conceptualization, Data curation, Formal analysis, Funding acquisition, Investigation, Methodology, Resources, Supervision, Writing – review & editing.

Funding

The author(s) declare that financial support was received for the research and/or publication of this article. This study was supported by the National Natural Science Foundation project of China (C031002), Gansu Provincial Science Foundation of China (21JR7RA416, 25JRRA597) and Lanzhou University Second Hospital's "Cuiying Technology Innovation" Program (CY2018-ZD02).

Acknowledgments

We thank all the participants for their contribution to this study.

Conflict of interest

The authors declare that the research was conducted in the absence of any commercial or financial relationships that could be construed as a potential conflict of interest.

Generative AI statement

The author(s) declare that no Generative AI was used in the creation of this manuscript.

Publisher's note

All claims expressed in this article are solely those of the authors and do not necessarily represent those of their affiliated organizations, or those of the publisher, the editors and the reviewers. Any product that may be evaluated in this article, or claim that may be made by its manufacturer, is not guaranteed or endorsed by the publisher.

References

1. Husebye ES, Anderson MS, Kämpe O. Autoimmune polyendocrine syndromes. *N Engl J Med*. (2018) 378:1132–41. doi: 10.1056/NEJMra1713301

2. Nelson RP, Traisman HS, Deddish RB, Green OC. Schmidt's syndrome in a child with diabetes mellitus. *Diabetes Care*. (1978) 1:37–9. doi: 10.2337/diacare.1.1.37

3. Tsang CC, Ko GT, Wong KK, Chan HS, Yu AW. Autoimmune polyendocrinopathy type ii in a Chinese patient. *Hong Kong Med J*. (2006) 12:385–7. Available online at: https://pubmed.ncbi.nlm.nih.gov/17028360.

4. Lantz R, Naboulsi W, Yu S, Al-Samkari M. Management of adrenal deficiency and shock in a patient with polyglandular autoimmune syndrome type ii. *Cureus*. (2023) 15: e41440. doi: 10.7759/cureus.41440

5. Pan Q, Li P. Challenges in autoimmune polyendocrine syndrome type 2 with the full triad induced by anti-programmed cell death 1: A case report and review of the literature. *Front Immunol*. (2024) 15:1366335. doi: 10.3389/fimmu.2024.1366335

6. Rushworth RL, Torpy DJ, Falhammar H. Adrenal crises in older patients. *Lancet Diabetes Endocrinol*. (2020) 8:628–39. doi: 10.1016/s2213-8587(20)30122-4

7. Husebye ES, Pearce SH, Krone NP, Kämpe O. Adrenal insufficiency. *Lancet*. (2021) 397:613–29. doi: 10.1016/s0140-6736(21)00136-7

8. Park E, Kim MS, Noh ES, Lee JE, Kim SJ, Kwon YS, et al. Multiple endocrine neoplasia type 2 and autoimmune polyendocrine syndromes (Type 1 diabetes mellitus and graves' Disease) in a 16-year-old male with kabuki syndrome. *Endocr J*. (2022) 69:1211–6. doi: 10.1507/endocrj.EJ22-0084

9. Gonciarz M, Krogulecki M, Brodowska-Kania D, Cierniak S, Kamiński G. Delay in diagnosis of autoimmune polyendocrine syndrome type 2 as a consequence of misinterpretation of gastrointestinal symptoms. *Case Rep Gastrointest Med*. (2022) 2022:6623020. doi: 10.1155/2022/6623020

10. Dieli-Crimi R, Núñez C, Estrada L, López-Palacios N. an autoimmune polyglandular syndrome complicated with celiac disease and autoimmune hepatitis. *Ann Hepatol*. (2016) 15:588–91. doi: 10.5604/16652681.1203162

11. Vazquez SE, Ferré EM, Scheel DW, Sunshine S, Miao B, Mandel-Brehm C, et al. Identification of novel, clinically correlated autoantigens in the monogenic autoimmune syndrome aps1 by proteome-wide phip-seq. *Elife*. (2020) 9:e55053. doi: 10.7554/eLife.55053

12. Ariolli A, Agolini E, Mazza T, Petrizzelli F, Petrini S, D'Oria V, et al. The putative role of tim-3 variants in polyendocrine autoimmunity: insights from a wes investigation. *Int J Mol Sci*. (2024) 25:10994. doi: 10.3390/ijms252010994

13. Cutolo M. Autoimmune polyendocrine syndromes. *Autoimmun Rev*. (2014) 13:85–9. doi: 10.1016/j.autrev.2013.07.006

14. Dittmar M, Kahaly GJ. Genetics of the autoimmune polyglandular syndrome type 3 variant. *Thyroid*. (2010) 20:737–43. doi: 10.1089/thy.2010.1639

15. Wrońska K, Hałasa M, Szczuko M. The role of the immune system in the course of hashimoto's thyroiditis: the current state of knowledge. *Int J Mol Sci*. (2024) 25:6883. doi: 10.3390/ijms25136883

16. Shikama N, Nusspaumer G, Holländer GA. Clearing the aire: on the pathophysiological basis of the autoimmune polyendocrinopathy syndrome type-1. *Endocrinol Metab Clin North Am*. (2009) 38:273–88,vii. doi: 10.1016/j.ecl.2009.01.011

17. Das D, Akhtar S, Kurra S, Gupta S, Sharma A. Emerging role of immune cell network in autoimmune skin disorders: an update on pemphigus, vitiligo and psoriasis. *Cytokine Growth Factor Rev*. (2019) 45:35–44. doi: 10.1016/j.cytogfr.2019.01.001

18. Büyükçelik M, Keskin M, Keskin Ö, Bay A, Kılıç BD, Kor Y, et al. Autoimmune polyglandular syndrome type 3c with ectodermal dysplasia, immune deficiency and hemolytic-uremic syndrome. *J Clin Res Pediatr Endocrinol*. (2014) 6:47–50. doi: 10.4274/Jcrpe.1128

19. Ellis RJ, Varela-Calvino R, Tree TI, Peakman M. Hla class ii molecules on haplotypes associated with type 1 diabetes exhibit similar patterns of binding affinities for coxsackievirus P2c peptides. *Immunology*. (2005) 116:337–46. doi: 10.1111/j.1365-2567.2005.02233.x

20. Marttila J, Juhela S, Vaarala O, Hyöty H, Roivainen M, Hinkkanen A, et al. Responses of coxsackievirus B4-specific T-cell lines to 2c protein-characterization of epitopes with special reference to the gad65 homology region. *Virology*. (2001) 284:131–41. doi: 10.1006/viro.2001.0917

21. Masala S, Zedda MA, Cossu D, Ripoli C, Palermo M, Sechi LA. Zinc transporter 8 and map3865c homologous epitopes are recognized at T1d onset in sardinian children. *PloS One*. (2013) 8:e63371. doi: 10.1371/journal.pone.0063371

22. Celmeli F, Kocabas A, Isik IA, Parlak M, Kisand K, Ceylaner S, et al. Unexplained cyanosis caused by hepatopulmonary syndrome in a girl with apeced syndrome. *J Pediatr Endocrinol Metab*. (2017) 30:365–9. doi: 10.1515/jpem-2016-0276

23. Pisetsky DS, Lipsky PE. New insights into the role of antinuclear antibodies in systemic lupus erythematosus. *Nat Rev Rheumatol*. (2020) 16:565–79. doi: 10.1038/s41584-020-0480-7

24. Bossuyt X. Dfs70 autoantibodies: clinical utility in antinuclear antibody testing. *Clin Chem*. (2024) 70:374–81. doi: 10.1093/clinchem/hvad181

25. Norasyikin AW, Rozita M, Mohd Johan MJ, Suehazlyn Z. Autoimmune polyglandular syndrome presenting with jaundice and thrombocytopenia. *Med Princ Pract*. (2014) 23:387–9. doi: 10.1159/000357645

26. Kahaly GJ, Frommer L. Autoimmune polyglandular diseases. *Best Pract Res Clin Endocrinol Metab*. (2019) 33:101344. doi: 10.1016/j.beem.2019.101344

27. Bornstein SR, Allolio B, Arlt W, Barthel A, Don-Wauchope A, Hammer GD, et al. Diagnosis and treatment of primary adrenal insufficiency: an endocrine society clinical practice guideline. *J Clin Endocrinol Metab*. (2016) 101:364–89. doi: 10.1210/jc.2015-1710

28. De Silva SDN, Aravinthan M, Katulanda P. Glucocorticoid-induced adrenal insufficiency: an uncommon cause of hypercalcaemia. *Endocrinol Diabetes Metab Case Rep*. (2022) 2022:21–0177. doi: 10.1530/edm-21-0177

29. Jia W, Yu R, Wang L, Zhu D, Guo L, Weng J, et al. Prevalence of chronic kidney disease among chinese adults with diabetes: A nationwide population-based cross-sectional study. *Lancet Reg Health West Pac*. (2025) 55:101463. doi: 10.1016/j.lanwpc.2024.101463

30. Cao Y, Zhu HJ, Zheng HY, Li J. Myxedema. *Lancet Diabetes Endocrinol*. (2014) 2:600. doi: 10.1016/s2213-8587(14)70063-4

31. Alshardan A, Saeed MK, Alotaibi SD, Alashjaee AM, Salih N, Marzouk R. Harbor seal whiskers optimization algorithm with deep learning-based medical imaging analysis for gastrointestinal cancer detection. *Health Inf Sci Syst*. (2024) 12:35. doi: 10.1007/s13755-024-00294-7

32. Melanis K, Stefanou MI, Kitsos DK, Athanasaki A, Theodorou A, Koropouli E, et al. Paraneoplastic neurological syndromes as initial presentation of tumors: an eight-year single-center experience. *J Clin Med*. (2024) 13:824. doi: 10.3390/jcm13030824

33. Poch E, Molina A, Piñeiro G. Syndrome of inappropriate antidiuretic hormone secretion. *Med Clin (Barc)*. (2022) 159:139–46. doi: 10.1016/j.medcli.2022.02.015

34. Zlosa M, Grubišić B, Švitek L, Sabadi D, Canecki-Varžić S, Mihaljević I, et al. Implications of dysnatremia and endocrine disturbances in covid-19 patients. *Int J Mol Sci*. (2024) 25:9856. doi: 10.3390/ijms25189856

35. Gunna S, Singh M, Pandey R, Marak RSK, Aggarwal A, Mohanta B, et al. Etiology, clinical characteristics and mortality among Indian patients with addison's disease. *Endocr Connect*. (2023) 12:e220439. doi: 10.1530/ec-22-0439

36. Mofokeng TRP, Ndlovu KCZ, Beshyah SA, Ross IL. Tiered healthcare in South Africa exposes deficiencies in management and more patients with infectious etiology of primary adrenal insufficiency. *PloS One*. (2020) 15:e0241845. doi: 10.1371/journal.pone.0241845

37. Chen J. Is there a causal relationship between hypothyroidism and hyponatremia? *Ther Adv Endocrinol Metab*. (2023) 14:20420188231180983. doi: 10.1177/20420188231180983

38. Schrier RW. Vasopressin and aquaporin 2 in clinical disorders of water homeostasis. *Semin Nephrol*. (2008) 28:289–96. doi: 10.1016/j.semnephrol.2008.03.009

39. Schrier RW. Molecular mechanisms of clinical concentrating and diluting disorders. *Prog Brain Res*. (2008) 170:539–50. doi: 10.1016/s0079-6123(08)00441-x

40. Liamis G, Filippatos TD, Liontos A, Elisaf MS. Management of endocrine disease: hypothyroidism-associated hyponatremia: mechanisms, implications and treatment. *Eur J Endocrinol*. (2017) 176:R15–r20. doi: 10.1530/eje-16-0493

41. Spasovski G. Hyponatraemia-treatment standard 2024. *Nephrol Dial Transplant*. (2024) 39:1583–92. doi: 10.1093/ndt/gfae162

42. Trachtman H. Cell volume regulation: A review of cerebral adaptive mechanisms and implications for clinical treatment of osmolal disturbances: ii. *Pediatr Nephrol*. (1992) 6:104–12. doi: 10.1007/bf00856852

43. Fofi C, Maresca B, Altieri S, Menè P, Festuccia F. Renal involvement in adrenal insufficiency (Addison disease): can we always recognize it? *Intern Emerg Med*. (2020) 15:23–31. doi: 10.1007/s11739-019-02209-x

44. Kamoi K, Tamura T, Tanaka K, Ishibashi M, Yamaji T. Hyponatremia and osmoregulation of thirst and vasopressin secretion in patients with adrenal insufficiency. *J Clin Endocrinol Metab*. (1993) 77:1584–8. doi: 10.1210/jcem.77.6.8263145

45. Ghazal RM, Almutlaq KO, Mohammed Rahim O, Elesely RA. Pericardiocentesis, a stress-relieving procedure causing a paradoxical effect: A case report on stress-induced takotsubo cardiomyopathy. *Cureus*. (2025) 17:e77773. doi: 10.7759/cureus.77773

46. O'Rorke J, Butler G, Chandra R. Takotsubo cardiomyopathy in a 66-year-old woman: A case of stress-induced cardiomyopathy mimicking acute coronary syndrome in the presence of cardiovascular risk factors. *Cureus*. (2025) 17:e76909. doi: 10.7759/cureus.76909

47. López-Trejo FI, Cedillo-Urbina MR, Maldonado-Tenesaca AP, Rivera-Guerrero JC, Andrade-Cuellar EN. Hyponatraemia-induced takotsubo syndrome secondary to idiopathic syndrome of inappropriate antidiuretic hormone: A case report. *Eur Heart J Case Rep*. (2025) 9:ytaf006. doi: 10.1093/ehjcr/ytaf006

48. Kuang J, Jia Z, Chong TK, Chen J, Liu K, Wang X, et al. Sacubitril/valsartan attenuates inflammation and myocardial fibrosis in takotsubo-like cardiomyopathy. *J Mol Cell Cardiol*. (2025) 200:24–39. doi: 10.1016/j.yjmcc.2025.01.003

49. Tian L, Liu B, Ren Y, Cui J, Pang Z. Proteomics of stress-induced cardiomyopathy: insights from differential expression, protein interaction networks, and functional pathway enrichment in an isoproterenol-induced ttc mouse model. *PeerJ*. (2025) 13:e18984. doi: 10.7717/peerj.18984

50. Arcari L, Camastra G, Ciolina F, Belmonte E, De Santis D, Danti M, et al. Cardiac magnetic resonance in patients with takotsubo syndrome: clinical correlates of T2 mapping. *Int J Cardiol*. (2025) 419:132716. doi: 10.1016/j.ijcard.2024.132716

51. Mohammed S, Maitra S. Extracorporeal membrane oxygenation in the management of takotsubo cardiomyopathy secondary to mitral valve replacement surgery: A case report. *Cureus*. (2024) 16:e71258. doi: 10.7759/cureus.71258

52. Batta A, Gupta AK, Singal G, Mohan B, Kumar S, Jaiswal B, et al. Autoimmune polyendocrine syndrome ii presenting paradoxically as takotsubo cardiomyopathy: A case report and reappraisal of pathophysiology. *Egypt Heart J*. (2022) 74:82. doi: 10.1186/s43044-022-00321-6

53. Baker JT, Cury R, Hernandez-Suarez DF. Myocarditis as a possible underlying cause for mid-ventricular takotsubo cardiomyopathy: A case report. *Cureus*. (2024) 16:e75813. doi: 10.7759/cureus.75813

54. Bader M, Mubarak M, Ali S, Hasan Z, Alsudairy N. A case of takotsubo cardiomyopathy in a 65-year-old woman triggered by emotional stress. *Cureus*. (2024) 16:e73533. doi: 10.7759/cureus.73533

55. Kabuto T, Kaneko S, Nomura S, Terashita S, Kitahori K, Ikeda M, et al. Delayed onset immune-related pituitary adrenal insufficiency induced by neoadjuvant nivolumab therapy for locally advanced lung cancer in the postoperative period: A case report. *Surg Case Rep*. (2025) 11:24–0044. doi: 10.70352/scrj.cr.24-0044

56. Jehangir M. Takotsubo cardiomyopathy after orthotopic liver transplantation. *Int J Cardiovasc Imaging*. (2025) Online ahead of print. doi: 10.1007/s10554-025-03350-9

57. Campean R, Hasun M, Stöllberger C, Bucher J, Finsterer J, Schnack C, et al. Takotsubo-like syndrome triggered by fludrocortisone overdose for addison's disease: A case report. *J Med Case Rep*. (2016) 10:281. doi: 10.1186/s13256-016-1074-5

58. Bilginer MC, Tam AA, Faki S, Bestepe N, Dellal FD, Ozdemir D, et al. Evaluation of adrenal reserve in patients with differentiated thyroid cancer receiving thyroid hormone suppression therapy- case-control comparative study. *Endocr Res*. (2023) 48:9–15. doi: 10.1080/07435800.2022.2158338

59. Jansen HI, van Herwaarden AE, Huijgen HJ, Vervloet MG, Hillebrand JJ, Boelen A, et al. Lower accuracy of testosterone, cortisol, and free T4 measurements using automated immunoassays in people undergoing hemodialysis. *Clin Chem Lab Med*. (2023) 61:1436–45. doi: 10.1515/cclm-2022-1133

60. Bazyka DA, Bruslova KM, Liashenko LO, Pushkareva TI, Tsvyetkova NM, Galkina SG, et al. Drivers of hyperferremia in children living on radiologically contaminated territories after the chnpp accident in Ukraine. *Probl Radiac Med Radiobiol*. (2023) 28:239–53. doi: 10.33145/2304-8336-2023-28-239-253

61. Peterson SH, Ackerman JT, Holser RR, McDonald BI, Costa DP, Crocker DE. Mercury bioaccumulation and cortisol interact to influence endocrine and immune biomarkers in a free-ranging marine mammal. *Environ Sci Technol*. (2023) 57:5678–92. doi: 10.1021/acs.est.2c08974

62. Seejore K, Giannoudi M, Osborn D, Lynch JM, Al-Qaissi A, Dunwoodie E, et al. Characterisation of the onset and severity of adrenal and thyroid dysfunction associated with ctla4-related hypophysitis. *Eur J Endocrinol*. (2021) 186:83–93. doi: 10.1530/eje-21-0760

63. Graca GM, Aguiar LR, De Lacerda L. New diagnostic approach to central hypothyroidism after traumatic brain injury in children and adolescents. *Eur Thyroid J*. (2025) 14. doi: 10.1530/etj-24-0184

64. Patalong-Wójcik M, Golara A, Sokołowska A, Zając K, Kozłowski M, Krzyścin M, et al. Associations of hormonal and metabolic parameters with bone mineralization in young adult females. *Nutrients*. (2023) 15. doi: 10.3390/nu15112482

65. Chen K, Chen L, Dai J, Ye H. Mafld in patients with cushing's disease is negatively associated with low free thyroxine levels rather than with cortisol or tsh levels. *Int J Endocrinol*. (2023) 2023:6637396. doi: 10.1155/2023/6637396

66. Yu P, Yuan H, Chen H, Li X. Thyroid function spectrum in cushing's syndrome. *BMC Endocr Disord*. (2024) 24:80. doi: 10.1186/s12902-024-01614-4

67. Godoi FGA, Dias MA, Guerreiro ADS, Branco GS, Montagner CC, Moreira RG, et al. Physiological responses on the reproductive, metabolism and stress endpoints of astyanax lacustris females (Teleostei: characiformes) after diclofenac and ibuprofen exposure. *Comp Biochem Physiol C Toxicol Pharmacol*. (2024) 278:109846. doi: 10.1016/j.cbpc.2024.109846

68. Jasim SA, Golgouneh S, Jaber MM, Indiaminov SI, Alsaikhan F, Hammid AT, et al. Effects of short-term exposure to the heavy metal, nickel chloride (Nicl(2)) on gill histology and osmoregulation components of the gray mullet, mugil cephalus. *Comp Biochem Physiol C Toxicol Pharmacol*. (2022) 258:109361. doi: 10.1016/j.cbpc.2022.109361

69. Liu T, Rossiter JP, Houlden RL, Awad S. Sparsely granulated corticotroph pituitary macroadenoma presenting with pituitary apoplexy resulting in remission of hypercortisolism. *AACE Clin Case Rep*. (2022) 8:166–70. doi: 10.1016/j.aace.2022.04.003

70. Marino A, Albanese I, Larose S, Fantus IG. Combined central hypothyroidism and adrenal insufficiency associated with retinoic acid therapy for cutaneous T-cell lymphoma. *AACE Clin Case Rep*. (2022) 8:251–4. doi: 10.1016/j.aace.2022.08.004

71. Quaschning T, Ruschitzka F, Niggli B, Lunt CM, Shaw S, Christ M, et al. Influence of aldosterone vs. Endothelin receptor antagonism on renovascular function in liquorice-induced hypertension. *Nephrol Dial Transplant*. (2001) 16:2146–51. doi: 10.1093/ndt/16.11.2146

72. Russo S, Mastropasqua M, Mosetti MA, Persegani C, Paggi A. Low doses of liquorice can induce hypertension encephalopathy. *Am J Nephrol*. (2000) 20:145–8. doi: 10.1159/000013572

73. Kerstens MN, Guillaume CP, Wolthers BG, Dullaart RP. Gas chromatographic-mass spectrometric analysis of urinary glycyrrhetinic acid: an aid in diagnosing liquorice abuse. *J Intern Med*. (1999) 246:539–47. doi: 10.1046/j.1365-2796.1999.00551.x

74. Armanini D, Lewicka S, Pratesi C, Scali M, Zennaro MC, Zovato S, et al. Further studies on the mechanism of the mineralocorticoid action of licorice in humans. *J Endocrinol Invest*. (1996) 19:624–9. doi: 10.1007/bf03349029

75. Kraus SD. Glycyrrhizin-induced inhibition of the pituitary-adrenal stress response. *J Exp Med*. (1958) 108:325–8. doi: 10.1084/jem.108.3.325

76. Hanafusa J, Mune T, Tanahashi T, Isomura Y, Suwa T, Isaji M, et al. Altered corticosteroid metabolism differentially affects pituitary corticotropin response. *Am J Physiol Endocrinol Metab*. (2002) 282:E466–73. doi: 10.1152/ajpendo.00065.2001

77. He H, Nie YL, Li JF, Meng XG, Yang WH, Chen YL, et al. Developmental regulation of cyp3a4 and cyp3a7 in chinese han population. *Drug Metab Pharmacokinet*. (2016) 31:433–44. doi: 10.1016/j.dmpk.2016.08.008

78. Yu C, Ye S, Sun H, Liu Y, Gao L, Shen C, et al. Pxr-mediated transcriptional activation of cyp3a4 by cryptotanshinone and tanshinone iia. *Chem Biol Interact*. (2009) 177:58–64. doi: 10.1016/j.cbi.2008.08.013

79. Xu Y, Zhang YF, Chen XY, Zhong DF. Cyp3a4 inducer and inhibitor strongly affect the pharmacokinetics of triptolide and its derivative in rats. *Acta Pharmacol Sin*. (2018) 39:1386–92. doi: 10.1038/aps.2017.170

80. Zhang W, Guo J, Wang D, Ren S, Hua H, Morikawa T, et al. Effect of cyp3a inducer/inhibitor on pharmacokinetics of five alkaloids in evodiae fructus. *Chem Biol Interact*. (2020) 327:109146. doi: 10.1016/j.cbi.2020.109146

81. Lv C, Huang L. Xenobiotic receptors in mediating the effect of sepsis on drug metabolism. *Acta Pharm Sin B*. (2020) 10:33–41. doi: 10.1016/j.apsb.2019.12.003

82. Falorni A, Nikoshkov A, Laureti S, Grenbäck E, Hulting AL, Casucci G, et al. High diagnostic accuracy for idiopathic addison's disease with a sensitive radiobinding assay for autoantibodies against recombinant human 21-hydroxylase. *J Clin Endocrinol Metab*. (1995) 80:2752–5. doi: 10.1210/jcem.80.9.7673419

83. Betterle C, Volpato M, Rees Smith B, Furmaniak J, Chen S, Zanchetta R, et al. Ii. Adrenal cortex and steroid 21-hydroxylase autoantibodies in children with organ-specific autoimmune diseases: markers of high progression to clinical addison's disease. *J Clin Endocrinol Metab*. (1997) 82:939–42. doi: 10.1210/jcem.82.3.3849

84. Murray JS, Jayarajasingh R, Perros P. Lesson of the week: deterioration of symptoms after start of thyroid hormone replacement. *Bmj*. (2001) 323:332–3. doi: 10.1136/bmj.323.7308.332

85. Mazul-Sunko B, Resetic J, Solter M, Ivanec Z. Postoperative adrenal crisis in a patient with schmidt syndrome (Autoimmune polyglandular endocrinopathy type ii). *Eur J Anaesthesiol*. (2004) 21:416–7. doi: 10.1017/s0265021504235116

86. Ghanny S, Wallerstein R, Chartoff A, Post J, Aisenberg J, Auyeung V. Six year old with autoimmune polyglandular syndrome: can genetics tell us the story? *J Pediatr Endocrinol Metab*. (2010) 23:725–8. doi: 10.1515/jpem.2010.23.7.725

87. Chang JT, Chen YY, Chiu PC. 21-hydroxylase autoantibody-negative addison's disease in a 5-year-old boy with adrenal crisis and type 1 diabetes mellitus. *J Pediatr Endocrinol Metab*. (2010) 23:1201–5. doi: 10.1515/jpem.2010.189

88. Vallianou N, Gounari P, Skourtis A. A case of autoimmune polyglandular syndrome type ii presenting with adrenal crisis. *Hippokratia*. (2013) 17:191. Available online at: https://www.endocrine-abstracts.org/ea/0029/ea0029p386.

89. Bain A, Stewart M, Mwamure P, Nirmalaraj K. Addison's disease in a patient with hypothyroidism: autoimmune polyglandular syndrome type 2. *BMJ Case Rep*. (2015) 2015:bcr2015210506. doi: 10.1136/bcr-2015-210506

90. Gürkan E, Çetinarslan B, Güzelmansur İ, Kocabaş B. Latent polyglandular autoimmune syndrome type 2 case diagnosed during a shock manifestation. *Gynecol Endocrinol*. (2016) 32:521–3. doi: 10.3109/09513590.2015.1137096

91. Wang X, Ping F, Qi C, Xiao X. Delayed diagnosis with autoimmune polyglandular syndrome type 2 causing acute adrenal crisis: A case report. *Med (Baltimore)*. (2016) 95:e5062. doi: 10.1097/md.0000000000005062

92. Schulz L, Hammer E. Autoimmune polyglandular syndrome type ii with co-manifestation of addison's and graves' Disease in a 15-year-old boy: case report and literature review. *J Pediatr Endocrinol Metab*. (2020) 33:575–8. doi: 10.1515/jpem-2019-0506

93. Yanachkova V, Chaveeva P, Staynova R, Milcheva R. Autoimmune polyglandular syndrome type 2 and pregnancy. *Folia Med (Plovdiv)*. (2020) 62:408–11. doi: 10.3897/folmed.62.e48580

94. Wiśniewski OW, Matuszak P, Kasprzak A, Łącka K. Severe hyponatremia as the first sign of late-onset schmidt's syndrome: A case report. *Caspian J Intern Med*. (2021) 12:S392–s6. doi: 10.22088/cjim.12.0.392

95. Lassoued N, Alaya W, Rebai S, Arfa S, Zantour B, Habib Sfar M. Acute adrenal crisis precipitated by thyroid storm in a patient with undiagnosed autoimmune polyglandular syndrome type 2. *Endocrinol Diabetes Metab Case Rep*. (2023) 2023:21–0152. doi: 10.1530/edm-21-0152

96. Bonataki M, Dikaiakou E, Anastasopoulou P, Fakiolas S, Kafetzi M, Vlachopapadopoulou EA. An 11-year-old girl with autoimmune polyglandular syndrome (Aps) type 2: A case report and review of literature. *J Pediatr Endocrinol Metab*. (2023) 36:508–12. doi: 10.1515/jpem-2022-0619

97. Spagnolo CC, Campo I, Campennì A, Cardile D, Cannavò S, Silvestris N, et al. Challenges and pitfalls in the management of endocrine toxicities from immune checkpoint inhibitors: A case presentation of synchronous thyrotoxicosis and primary adrenal insufficiency in a melanoma patient. *Hormones (Athens)*. (2024) 23:759–64. doi: 10.1007/s42000-024-00535-0

98. Betterle C, Presotto F, Furmaniak J. Epidemiology, pathogenesis, and diagnosis of addison's disease in adults. *J Endocrinol Invest*. (2019) 42:1407–33. doi: 10.1007/s40618-019-01079-6

99. Manso J, Pezzani R, Scarpa R, Gallo N, Betterle C. The natural history of autoimmune addison's disease with a non-classical presentation: A case report and review of literature. *Clin Chem Lab Med*. (2018) 56:896–900. doi: 10.1515/cclm-2017-1108

100. Dittmar M, Kahaly GJ. Polyglandular autoimmune syndromes: immunogenetics and long-term follow-up. *J Clin Endocrinol Metab*. (2003) 88:2983–92. doi: 10.1210/jc.2002-021845

101. Garelli S, Dalla Costa M, Sabbadin C, Barollo S, Rubin B, Scarpa R, et al. Autoimmune polyendocrine syndrome type 1: an italian survey on 158 patients. *J Endocrinol Invest*. (2021) 44:2493–510. doi: 10.1007/s40618-021-01585-6

102. Van den Driessche A, Eenkhoorn V, Van Gaal L, De Block C. Type 1 diabetes and autoimmune polyglandular syndrome: A clinical review. *Neth J Med*. (2009) 67:376–87. Available online at: https://pubmed.ncbi.nlm.nih.gov/17028360.

103. Reato G, Morlin L, Chen S, Furmaniak J, Smith BR, Masiero S, et al. Premature ovarian failure in patients with autoimmune addison's disease: clinical, genetic, and immunological evaluation. *J Clin Endocrinol Metab*. (2011) 96:E1255–61. doi: 10.1210/jc.2011-0414

104. Laakso S, Holopainen E, Betterle C, Saari V, Vogt E, Schmitt MM, et al. Pregnancy outcome in women with apeced (Aps-1): A multicenter study on 43 females with 83 pregnancies. *J Clin Endocrinol Metab*. (2022) 107:e528–e37. doi: 10.1210/clinem/dgab705

105. Humbert L, Proust-Lemoine E, Dubucquoi S, Kemp EH, Saugier-Veber P, Fabien N, et al. Lessons from prospective longitudinal follow-up of a french apeced cohort. *J Clin Endocrinol Metab*. (2025) 110:e757–e73. doi: 10.1210/clinem/dgae211

106. Perniola R, Fierabracci A, Falorni A. Autoimmune addison's disease as part of the autoimmune polyglandular syndrome type 1: historical overview and current evidence. *Front Immunol*. (2021) 12:606860. doi: 10.3389/fimmu.2021.606860

107. Gunjur A, Klein O, Kee D, Cebon J. Anti-programmed cell death protein 1 (Anti-pd1) immunotherapy induced autoimmune polyendocrine syndrome type ii (Aps-2): A case report and review of the literature. *J Immunother Cancer*. (2019) 7:241. doi: 10.1186/s40425-019-0713-y

108. Robles DT, Fain PR, Gottlieb PA, Eisenbarth GS. The genetics of autoimmune polyendocrine syndrome type ii. *Endocrinol Metab Clin North Am*. (2002) 31:353–68, vi-vii. doi: 10.1016/s0889-8529(01)00015-9

109. Betterle C, Coco G, Zanchetta R. Adrenal cortex autoantibodies in subjects with normal adrenal function. *Best Pract Res Clin Endocrinol Metab*. (2005) 19:85–99. doi: 10.1016/j.beem.2004.11.008

110. Kubo H, Tsurutani Y, Inoue K, Watanabe K, Yamazaki Y, Sunouchi T, et al. Characteristics of aldosterone-producing adenomas in patients without plasma renin activity suppression. *PloS One*. (2022) 17:e0267732. doi: 10.1371/journal.pone.0267732

111. Pallayova M, Breznoscakova D. The altered circadian pattern of basal insulin requirements - an early marker of autoimmune polyendocrine syndromes in type 1 diabetes mellitus. *Endocr Regul*. (2020) 54:126–32. doi: 10.2478/enr-2020-0015

frontiers | Frontiers in Immunology

TYPE Original Research
PUBLISHED 15 May 2025
DOI 10.3389/fimmu.2025.1500866

Check for updates

OPEN ACCESS

EDITED BY
Alessandro Antonelli,
University of Pisa, Italy

REVIEWED BY
Ninfa Ramírez Durán,
Autonomus University of the State of Mexico Medicine Faculty, Mexico
Marlena Godlewska,
Centrum Medyczne Kształcenia Podyplomowego, Poland
Manuel Rojas,
University of California, Davis, United States

*CORRESPONDENCE
Yajuan Xu
cnzzzsl@163.com

RECEIVED 11 February 2025
ACCEPTED 15 April 2025
PUBLISHED 15 May 2025

CITATION
Zhang C, Xu Y, Zhang M, Li J, Sun Z, Wang Y and Lin P (2025) An exploratory study on the metagenomic and proteomic characterization of hypothyroidism in the first half of pregnancy and correlation with Th1/Th2 balance.
Front. Immunol. 16:1500866.
doi: 10.3389/fimmu.2025.1500866

COPYRIGHT
© 2025 Zhang, Xu, Zhang, Li, Sun, Wang and Lin. This is an open-access article distributed under the terms of the Creative Commons Attribution License (CC BY). The use, distribution or reproduction in other forums is permitted, provided the original author(s) and the copyright owner(s) are credited and that the original publication in this journal is cited, in accordance with accepted academic practice. No use, distribution or reproduction is permitted which does not comply with these terms.

An exploratory study on the metagenomic and proteomic characterization of hypothyroidism in the first half of pregnancy and correlation with Th1/Th2 balance

Chenchen Zhang, Yajuan Xu*, Miao Zhang, Jingjing Li, Zongzong Sun, Yixin Wang and Pengkun Lin

Department of Obstetrics and Gynecology, Third Affiliated Hospital of Zhengzhou University, Zhengzhou, China

Objective: To explore the gut microbiota and proteomic characteristics of hypothyroidism in the first half of pregnancy (referred to as hypothyroidism in the first half of pregnancy) and its association with Th (T helper cells, Th)1/Th2 balance using metagenomics combined with proteomics.

Methods: Stool and blood samples were collected from 20 hypothyroid (hypothyroidism group) and normal pregnant women (normal group) in the first half of pregnancy. Flora and proteomic characteristics were analyzed using metagenomics sequencing and 4D-DIA proteomics. Th1 and Th2 cells were quantified, and cytokine levels were measured using cellular micro-bead arra. The enzyme-linked immunosorbent test (ELISA) was utilized to assess differential proteins.

Results: (1) Metagenomic sequencing revealed distinct microbial profiles: The β-diversity of gut microbiota was diminished in the hypothyroidism group ($p < 0.05$). LEfSe analysis identified *Phocaeicola vulgatus* and *Bacteroides fragilis* enriched in the hypothyroidism group ($p<0.05$), and Kyoto Encyclopedia of Genes and Genomes(KEGG) analysis showed significant enrichment in pathways related to peptidoglycan biosynthesis and glycerol ester metabolism.(2) Proteomic analysis demonstrated downregulation of Diacylglycerol Kinase Kappa (DGKK) and P05109|S10A8(S10A8) proteins in the hypothyroidism group, with marked enrichment in the KEGG pathways for

vascular smooth muscle contraction and phosphatidylinositol signaling. (3) ELISA validation confirmed that the proteins DGKK and S10A8 were downregulated in pregnant women in the hypothyroidism group.

Conclusion: Increased *P. vulgatus* and *B. fragilis*, decreased DGKK and S10A8 proteins, and a left shift in the Th1/Th2 balance in patients with hypothyroidism in the first half of pregnancy may be associated with the development of the disease.

KEYWORDS

first half of pregnancy, hypothyroidism, metagenomics sequencing, proteomics, gut microbiota

1 Background

Hypothyroidism in pregnancy is a common endocrine disorder (1). Moreover, it increases the risk of adverse pregnancy outcomes such as miscarriage, gestational hypertension, and fetal malformations (2). We generally define the gestational age of less than 20 weeks as the first half of pregnancy (3). Notably, maternal and fetal demand for thyroid hormones increases during pregnancy, and the fetus is unable to synthesize thyroid hormones before 20 weeks of gestation (2). Therefore, hypothyroidism in the first half of pregnancy has a profound effect on fetal growth and development (2).The gut microbiota is recognized as the second-largest gene pool in humans. It provides essential metabolites and hormones, prevents invasion by pathogenic microorganisms, and is closely related to immune system disorders (4, 5). The gut microbiota affects thyroid homeostasis through multiple mechanisms and plays a role in the development of hypothyroidism during pregnancy (6, 7). Our group previously demonstrated that gut microbiota disorders exist in patients with hypothyroidism during the first half of pregnancy through 16SrRNA gene sequencing (8–10). Serum proteomics in women with hypothyroidism during the first half of pregnancy is underexplored, with few studies addressing this period. Metagenomics enables species-level annotation and analysis of gut microbial genes, functions, and metabolic pathways, revealing their biological significance. Proteomic methods screen for biomarkers and investigate disease pathogenesis.

In the first half of pregnancy, the Th1/Th2 balance shifts from Th2 to Th1 dominance by late pregnancy (11). Th1/Th2 imbalances, influenced by gut microbiota disorders, regulate inflammatory cytokine secretion and contribute to immune dysfunction, potentially altering inflammatory protein expression and impacting autoimmune disease development (12–14). Despite limited research, this study examines gut microbiota and proteomic characteristics in hypothyroid pregnant women, analyzing changes and associations with Th1/Th2 balance using metagenomic and proteomic approaches.

2 Materials and methods

2.1 Research objectives

From July to August 2024, pregnant women receiving regular perinatal care were selected at the Third Affiliated Hospital of Zhengzhou University's outpatient obstetrics clinic. Twenty women in their first trimester with hypothyroidism who met the inclusion criteria comprised the hypothyroidism group, and 20 with normal pregnancies formed the normal group.

Inclusion Criteria: 1) thyroid function during pregnancy in accordance with the 2022 Guidelines for the Management of Thyroid Disease Prevention and Control in Pregnancy and Childbirth (1) and the reference range of hypothyroidism in pregnancy (TSH >4.0 mIU/L and FT4 <12 mIU/L) established by the Department of Laboratory of the Third Affiliated Hospital of Zhengzhou University. 2) The week of pregnancy was less than 20 weeks.

Exclusion criteria: 1) age below 18 or above 35 years; 2) pregnancy with complications; 3) use of artificial insemination or assisted reproductive technology; 4) multiple pregnancies (twins or more); 5) severe anxiety or depression; 6) history of circulatory, digestive, or other medical conditions, or past gastrointestinal surgery; 7) chronic use of antibiotics or medications regulating gut microbiota; 8) current use of anti-thyroid or thyroid replacement medications; 9) presence of liver disease, malignant tumors, or other severe systemic conditions; 10) ongoing infection or history of chronic inflammation and autoimmune diseases.

Ethics Statement: This study was approved by the Medical Ethics Committee of the Third Affiliated Hospital of Zhengzhou University, China. All enrolled members voluntarily participated and signed the informed consent forms.

2.2 Stool and blood sample collection and storage

All patients had their feces collected within 24 hours following the diagnosis of hypothyroidism in pregnancy. Prior to sample collection,

they were instructed to ensure that the feces did not contact the bedpan, were free from urine contamination, and were collected from the mid-feces using a sterile spoon. The collected samples were then placed in sterile 2.0 mL tubes, transported to the laboratory within 2 hours, and stored at -80°C until further processing.

Blood samples were simultaneously collected, with all pregnant women fasting for 8–12 hours beforehand. Two 5 mL blood specimens were drawn from the elbow vein using a sterile syringe needle, deposited into Ethylenediaminetetraacetic acid (EDTA) and sodium heparin anticoagulation tubes, and immediately refrigerated at 4°C. The blood samples in EDTA tubes were centrifuged at 4°C, 2000 rpm for 10 minutes within 2 hours of collection. Subsequently, the upper serum layer was aspirated with a sterile pasteurized pipette and stored in a freezing tube at -80°C.

2.3 Data collection

Data on age, body mass index (BMI), gestational week, and serum-free T4 (FT4), thyroid-stimulating hormone (TSH), fasting glucose (GLU), hemoglobin (HGB), and hypersensitive C-reactive protein (hs-CRP) levels were collected from all pregnant women at enrollment.

2.4 Cytokine detection

Interleukin (IL)-2, IL-6, IL-10, and tumor necrosis factor-α(TNF-α) levels were measured using a Human Cytokine Kit (China Jiangxi Sage Biotechnology Co.) based on flow fluorescence technology. The kit contains microspheres encapsulating antibodies specific to IL-2, IL-6, IL-10, and TNF-α. The capture microsphere mixture is mixed with 25 μL of serum, and then the mixture is incubated with 25 μL of fluorescently labeled detection antibody for 2.5 h at 20-25°C under dark conditions. The beads were washed and resuspended in PBS, the samples were analyzed using flow cytometry, and the data were recorded. The samples were analyzed, and data were recorded using a flow cytometer (BD FACSC cantoII, USA) and corresponding software (BD FACSDiva Software, version 8.0.2) (15, 16).

2.5 Flow cytometry

Th1 and Th2 cells were quantified using intracellular cytokine staining after peripheral blood collection from pregnant women in sodium heparin anticoagulated tubes. 200ul of anticoagulated whole blood was added to each flow-through tube separately, and the dissolved stimulants (phorbol myristate acetate (50ng/mL), ionomycin (1mg/mL), and brefeldin A (10 mg/mL) were added to the flow-through tubes, and the tubes were incubated for 4 hours at 37°C in 5% CO2. followed by the addition of APC-CY7-CD3 (0.2mg/ml) and FITC-CD4 (0.2mg/ml) antibodies for cell surface labeling. Cells were incubated for 20 minutes in a light-proof environment, erythrocyte lysate was added, and the cells were incubated for 25 minutes. Cells were centrifuged at 500 g at 4°C, the supernatant was discarded, and a fixed membrane-breaking solution (Preparation of 1× Perm/Wash Buffer: The 10× Perm/Wash Buffer was diluted with deionized distilled water (ddH2O) at a volumetric ratio of 1:9 to achieve the desired 1× working concentration.) was added. Following a 30-minute incubation in darkness, cells were stained with PE-IFN-γ (0.2mg/ml) and PE-CY7-IL-4 (0.2mg/ml) antibodies for 30 minutes. After washing, cells were resuspended in phosphate buffer (PBS 2 ml) and analyzed via flow cytometry using FlowJo software (Tree Star, Ashland, OR, USA, version10.8.1). All antibodies were sourced from BD Biosciences (Franklin Lakes, NJ, USA).

Th1 and Th2 Cell Gating Strategy:The gating strategy was implemented following compensation controls. Initial lymphocyte population identification was performed based on cellular characteristics, utilizing forward scatter (FSC) and side scatter (SSC) parameters plotted on the x-axis and y-axis, respectively (Figure 1A). Subsequent to this primary gating, single-cell populations were isolated through the exclusion of doublets, achieved by plotting forward scatter height (FSC-H) against forward scatter area (FSC-A) on the y-axis and x-axis, respectively (Figure 1B). CD4+ T cell populations were then specifically gated using APC-CY7 and FITC fluorescence parameters on the x-axis and y-axis (Figure 1C). The percentage contents of Th1 and Th2 cells, represented by CD3+CD4+IFN-γ+ for Th1 cells and CD3+CD4+IL-4+ for Th2 cells, were displayed with IFN-γ and IL-4 as the abscissa and SSC as the ordinate, respectively (Figures 1D, E). All cellular proportions and corresponding graphical representations were systematically recorded, with data analysis performed using FlowJo software (Tree Star, Ashland, OR, USA, version10.8.1).

2.6 Metagenomics sequencing and data analysis

Total DNA was extracted from 0.20 g of fecal specimens using the MagPure Stool DNA KF Kit B (cat. no.MD511, Magen, China). To minimize the interference of host sequences in DNA extraction and subsequent analysis, the Bowtie2 software (version 2.4.4, https://github.com/BenLangmead/bowtie2) (17) was employed during the extraction process to remove sequences aligned to the host genome, thereby reducing the impact on microbial analysis. 1 μg of genomic DNA was then sheared ultrasonically using a Covaris instrument to produce 300 bp fragments for sequencing on the DNBSEQ platform (BGI, Shenzhen, China) using cPAS. The resultant fasta format sequences underwent quality control and assembly with Fastp and MEGAHIT software (version 1.1.2, https://github.com/voutcn/megahit) (18), respectively. Gene sets were annotated to the KEGG database (https://www.genome.jp/kegg/) via Diamond software (version 2.0.13, https://github.com/bbuchfink/diamond) (19). Non-redundant gene sets were clustered using CD-HIT (version 4.8.1, https://github.com/weizhongli/cdhit) (20) and compared to the NR database (https://ftp.ncbi.nlm.nih.gov/blast/db/FASTA/) using BLAST (version 2.2.28, http://

blast.ncbi.nlm.nih.gov/Blast.cgi) (21) Statistical analysis was performed using the Wilcoxon rank-sum test and LDA.

2.7 Proteomics analysis and data processing

Mass spectrometry data from 40 samples were collected using a TimsTOF Pro instrument in the data-independent acquisition (DIA) mode. The experimental procedure was as follows: protein extraction and enrichment were performed using a C18 column. After enrichment and quality control, 20 μg of peptides from each sample were combined and eluted using a Shimadzu LC-20AB liquid phase system. Liquid phase separation was performed with a 5 μm 20 cmx180 μm Gemini C18 column for high pH and a 5 μm 4.6x250 mm Gemini C18 column for RP separation to acquire DDA mode data. The DDA data were analyzed, and spectral libraries were generated using MaxQuant's Andromeda engine (https://www.maxquant.org/). Following corrections to the DIA data, the SWATH-MS target-decoy model was employed to derive quantitative significance. Differential analysis utilizing the MSstats package from the Bioconductor repository (version 4.14.2 https://bioconductor.org/packages/MSstats/) identified proteins with differences >1.2 and $p < 0.05$ as significant. Functional analyses were then conducted on these proteins.

2.8 Enzyme-linked immunosorbent assay

Sixteen pregnant women with hypothyroidism ≤20 weeks' gestation and 16 normal pregnant women were selected as the validation cohort, and blood samples from this cohort were collected and stored using the same procedure. After thawing the samples at room temperature, selected differentially expressed proteins were verified by sandwich enzyme immunoassay. Human DGKK (DGKK) ELISA kit (Item No. EK10756) produced by Signalway Antibody (USA) was used as the DGKK indicator, and the human S10 calcium-binding protein A8 (S10A8) indicator was verified by the human S100 calcium-binding protein A8 (S100A8) enzyme-linked (22) immunosorbent assay kit (Item No. E-EL-H1289) produced by Wuhan Eliretech Biotechnology Co., Ltd. Plasma was diluted within the linear range of each assay following the manufacturer's recommendations. Absorbance (OD) was measured at 450 nm using a Biotek EPOCH microplate spectrophotometer. Standard curves were plotted, and protein concentrations were calculated using ELISACALC software.

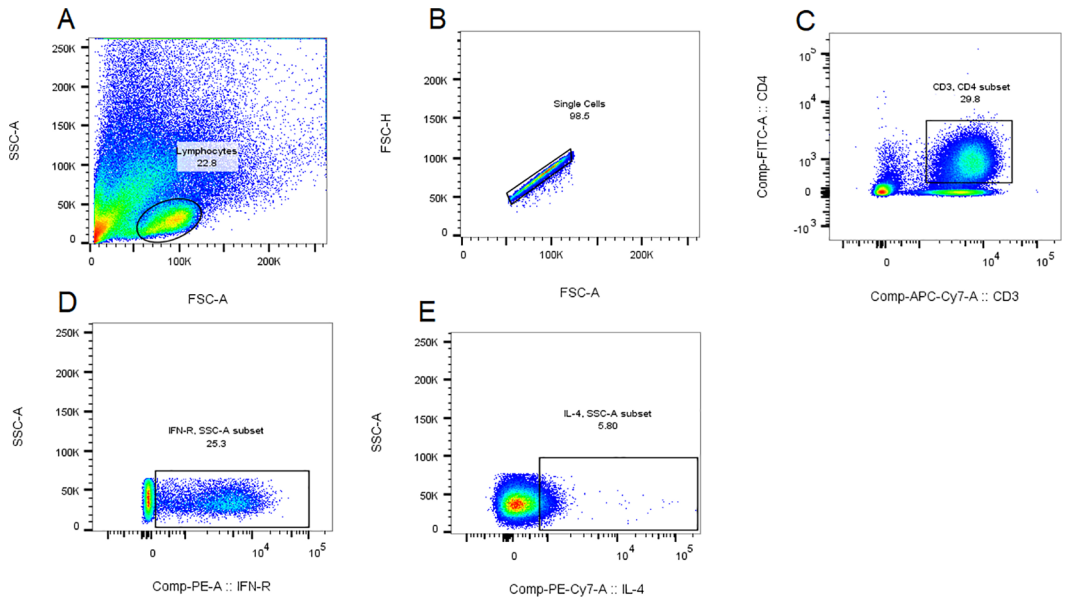

FIGURE 1
Th1 and Th2 cell gating strategy. The gating strategy was implemented following compensation controls. Initial lymphocyte population identification was performed based on cellular characteristics, utilizing forward scatter (FSC) and side scatter (SSC) parameters plotted on the x-axis and y-axis, respectively **(A)**. Subsequent to this primary gating, single-cell populations were isolated through the exclusion of doublets, achieved by plotting forward scatter height (FSC-H) against forward scatter area (FSC-A) on the y-axis and x-axis, respectively **(B)**. CD4+ T cell populations were then specifically gated using APC-CY7 and FITC fluorescence parameters on the x-axis and y-axis **(C)**. For quantitative analysis of T helper cell subsets, Th1 and Th2 cell populations were identified through the detection of intracellular cytokines, with IFN-γ and IL-4 expression plotted against SSC on the y-axis and x-axis, respectively, representing the proportions of CD3+CD4+IFN-γ+ Th1 cells and CD3+CD4+IL-4+ Th2 cells **(D, E)**. All cellular proportions and corresponding graphical representations were systematically recorded, with data analysis performed using FlowJo software (Tree Star, Ashland, OR, USA, version10.8.1).

2.9 Statistical analysis

All statistical analyses of the metagenomic and proteomic sequencing data were performed using R (version 3.4.1). The SPSS 26.0 software (IBM Corp. Released 2019.IBM SPSS Statistics for Windows, version 26.0. Armonk, NY: IBM Corp) was used for statistical analysis. Normally distributed measures were described using mean ± standard deviation, t-tests were used for comparisons between groups, medians and quartiles are used to describe non-normally distributed measures, and comparisons between groups were performed using the Wilcoxon rank sum test. Correlation analysis was performed using Spearman's analysis, and statistical significance was set at $P < 0.05$.

3 Results

3.1 Comparison of basic data between the hypothyroid and normal groups

Twenty pregnant women with hypothyroidism and 20 in the normal group during early pregnancy were studied. Table 1 shows no significant differences in age, BMI, gestational week, GLU, or HGB between groups ($p > 0.05$).

3.2 Macro gene-based analysis of differential gut microbiota composition and its functional enrichment

Analysis of gut microorganism α-diversity showed a significant difference in the chao1 index between the two groups ($p < 0.05$) (Figure 2A). β-diversity, assessed by Bray-Curtis distance, also differed (Figure 2B). Principal Component Analysis (PCA) and Principal Co-ordinates Analysis (PCoA) analyses indicated significant differences in species composition (Figure 2C), linking dysbiosis in the gut microbiota to the hypothyroidism group. Dominant species in the hypothyroid group included *P. vulgatus* and *B. fragilis* (Figures 2D, E). LEfSe analysis identified 27 distinct taxa between groups; *Bacteroidales*, *Bacteroides*, and *B. fragilis* were enriched in the hypothyroid group, while Clostridia prevailed in the normal group. Furthermore, *B. fragilis*, *B. ovatus*, and *B. uniformis* were more abundant in the hypothyroid group, in contrast to *Lachnospira* and *Faecalibacterium prausnitzii*, which were less prevalent (Figures 2F, G). KEGG gene pathway analysis revealed active metabolism in carbohydrate, amino acid, glycan biosynthesis, and metabolism (Figure 3A). Differential KEGG function analysis annotated genes and their pathways, showing enrichment in peptidoglycan biosynthesis and glycerolipid metabolism in the hypothyroid group (Figure 3B).

3.3 Serum proteomics sequencing and differential protein function analysis

Orthogonal partial least squares analysis (OPLS-DA) was used to analyze the data from the hypothyroidism and normal groups, demonstrating a statistically significant difference between the two groups (Figure 4A). Using 4D-DIA proteomic sequencing, 2196 proteins were screened; 69 proteins were upregulated and 37 downregulated in the hypothyroid group versus the normal group (Figure 4B). STAMP analysis indicated significant downregulation of DGKK and S10A8 in the hypothyroid group, both crucial for inflammation and immune response (Figure 4C). KEGG pathway analysis revealed significant enrichment in the vascular smooth muscle contraction and phosphatidylinositol signaling pathways ($p < 0.05$) (Figure 4D).

3.4 ELISA validation of DGKK and S10A8 expression

Serum levels of DGKK and S10A8 in pregnant women with hypothyroidism (Group H) and normal pregnant women (Group C) during pregnancy were determined using ELISA, and as shown in Figure 5, serum DGKK and S10A8 were significantly downregulated in the hypothyroidism group compared with the normal group ($p < 0.05$).

3.5 Comparison of serologic indices between the hypothyroid and normal groups

Peripheral blood Th1 and Th2 cells were detected in both groups of pregnant women using flow cytometry, and as shown

TABLE 1 Comparison of clinical data between the hypothyroid and normal groups.

	Hypothyroidism group (n=20)	Normal group (n=20)	P-value
age	31.85 ± 4.19	30.90 ± 4.17	0.478
BMI (kg/m^2)	23.59 ± 3.39	22.41 ± 3.33	0.277
gestation week (week)	15.50 (11.25,16.75)	12.00 (10.25,16.00)	0.429
GLU (g/L)	4.59 ± 0.32	4.67 ± 0.42	0.533
HGB (g/L)	118.30 ± 10.14	117.01 ± 29.10	0.853

p-value less than 0.05 was statistically significant.

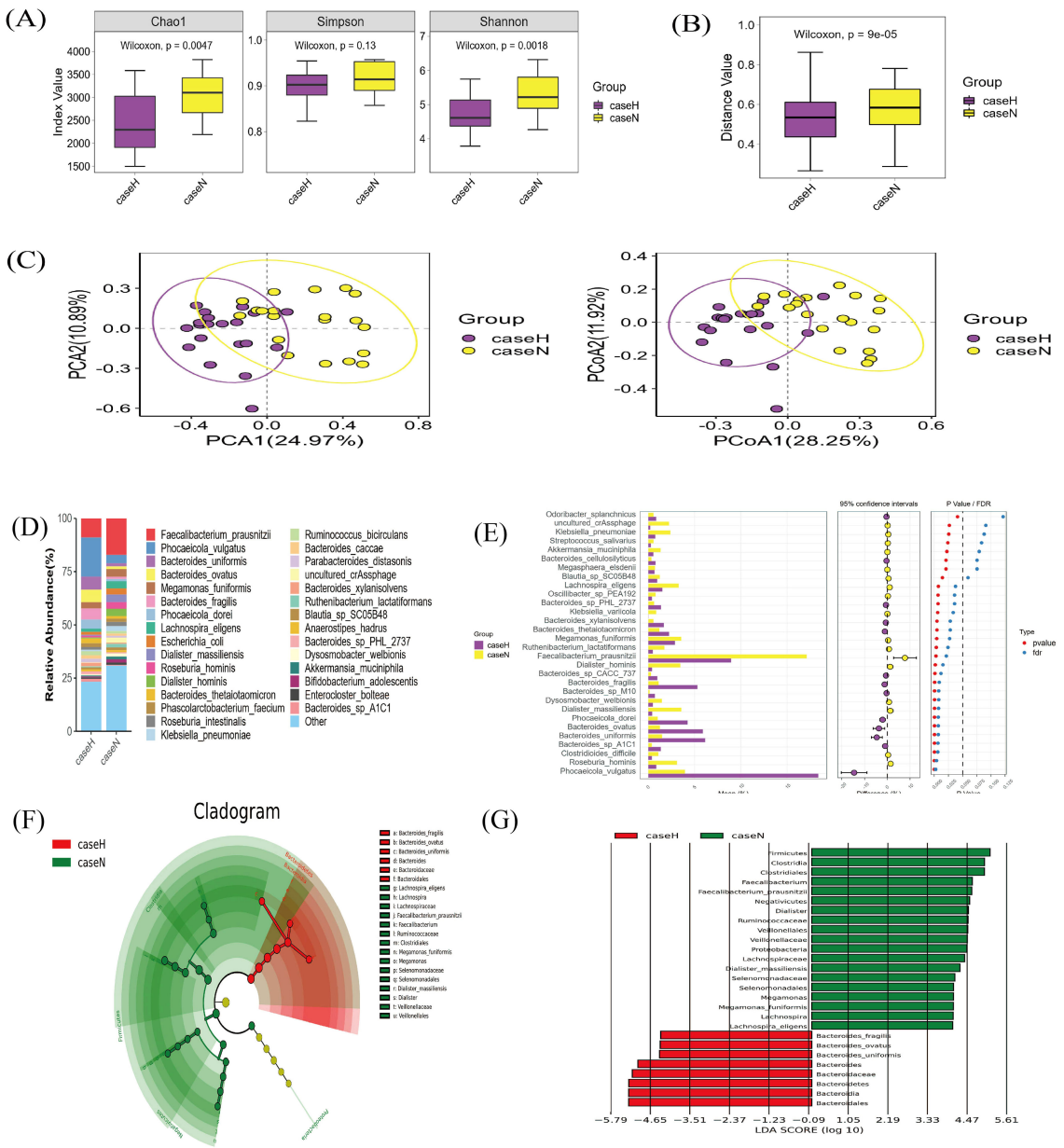

FIGURE 2
Metagenomic sequencing for species diversity and compositional analysis. **(A)** Alpha diversity analysis: A higher Chao1 index indicates a greater number of species. $p < 0.05$ indicates statistical significance. **(B)** β-diversity analysis: Based on the β-diversity shown by Bray-Curtis distance analysis; $p < 0.05$ indicates statistical significance. **(C)** PCA and PCoA plot: PCA1 and PCA2 explained 24.97% and 10.89% of the variance; respectively. 28.25% of the variance, as explained by PCoA1 and 11.92% by PCoA2, respectively. **(D)** Stacked plot of species abundance in the gut microbiota at the species level: Horizontal coordinates represent groupings, and vertical coordinates represent the relative abundance of species. The bar color indicates species classification, and longer lengths indicate higher relative abundances. **(E)** STAMP analysis of the top 30 differentially abundant species between the hypothyroid and normal groups: P-values result from statistical tests and FDR is the false discovery rate, the corrected p-value; points to the left of the dotted line ($p < 0.05$) denote significant differences. **(F)** LEfSe circular evolutionary branching diagram: This plot identifies the species in both sample groups that best explain the differences between the groups. The inner circle is at a high taxonomic level, and the outer circle is at a low taxonomic level. Each dot represents a specific species classification, with dot size indicating high relative abundance. **(G)** Histogram of LEfSe LDA distribution: This analysis suggests the extent of its influence on intergroup differences. Vertical coordinates represent taxonomic units with differences, and horizontal coordinates represent LDA values. The image shows only classifications with LDA values greater than a set threshold (typically two).

in Figure 6, where lymphocytes expressing both CD3 and CD4 were gated as CD4+ T cells. We quantified Th1 and Th2 cells by measuring IFN-γ and IL-4 expression levels. The cytokine levels were determined using the cell microbead array method. As presented in Online Resource 1(Table 2), TSH, hs-CRP, IL-2, IL-6, TNF-α, Th1, and Th1/Th2 levels in the hypothyroidism group were significantly higher than those in the normal group, while FT4 and Th2 levels were lower than those in the normal group; the difference between the two groups was statistically significant ($p < 0.05$), while that between the two groups in terms of IL-10 was not.

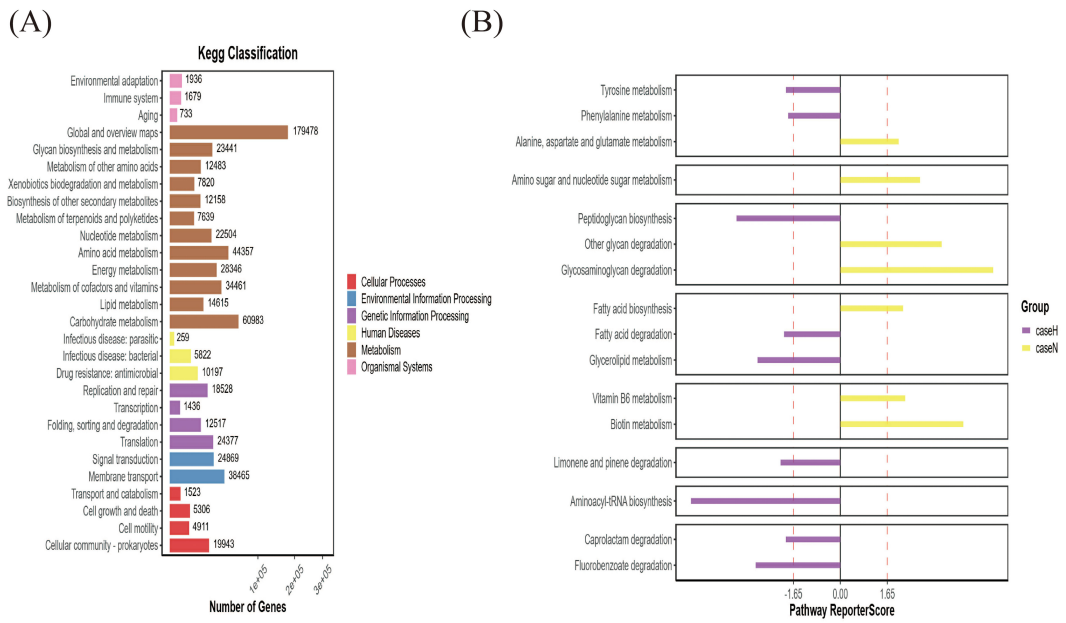

FIGURE 3
Gene function analysis of gut microbiota. **(A)** Histogram of functional gene statistics. The horizontal axis represents the number of genes, the vertical axis denotes the functional classifications, and the color corresponds to these classifications. The length of the bars reflects the quantity of genes, and a legend on the right side categorizes the primary functional classification for each secondary level. **(B)** Functional KEGG-pathway enrichment map. The horizontal axis displays the Reporter score values, the vertical axis lists the pathways, and the color denotes the subgroup of the enrichment. The diagram only includes functional classifications that exceed a predefined Reporter score threshold.

3.6 Correlation of dominant strains with screening proteins and serologic indices in the hypothyroid group

Spearman's correlation analysis showed that *P. vulgatus* and *B. fragilis* were significantly positively correlated with Th1/Th2 and positively correlated with IL-2 (Figure 7A). DGKK and S10A8 proteins were negatively correlated with Th1/Th2 ratios (Figure 7A). *P. vulgatus* was negatively correlated with S10A8, and *B. fragilis* was negatively correlated with DGKK (Figure 7B).

4 Discussion

Recent years have seen a yearly increase in the incidence of hypothyroidism during pregnancy (1). In the first trimester, the fetus relies primarily on maternal thyroid hormones until the 20th week (2). Notably, the impact of hypothyroidism, including miscarriage, intensifies in the early stages of pregnancy (2). However, the pathogenesis of hypothyroidism and its screening markers in this period remain unclear. Thus, this study employed metagenomic and proteomic approaches to explore their relationship and identify potential hypothyroidism biomarkers in early pregnancy.

This study demonstrated no differences between the hypothyroidism and normal groups in terms of age, BMI, or other general conditions during pregnancy. Metagenomic sequencing results showed that the relative abundances of *P. vulgatus* and *B. fragilis* were higher in the hypothyroidism group, and the outer membrane vesicles of anaplastic bacilli cells were enriched in proteases and peptidoglycans (23, 24). Thus, *P. vulgatus* is potentially pathogenic (25). Moreover, secreted serine and cysteine proteases can induce intestinal inflammation by decreasing trans-epithelial electrical resistance and intestinal mucosal epithelial permeability and allowing innate immune cells such as neutrophils to enter the intestines and destroy the intestinal barrier (26). *B. fragilis* produces enterotoxin and the *B. fragilis* toxin, which activates the IL-17 immune cascade in the intestinal epithelium through nuclear factor kappa-B (NF-κB) and signal transducer and activator of transcription 3 (STAT3) pathways, fostering a pro-inflammatory environment that results in intestinal inflammation (27). Therefore, we hypothesized that both strains contribute to "leaky gut" by exacerbating this inflammation (28), which diminishes the intestinal mucosa's production and secretion of β-glucuronidase and sulfate lyase, obstructing thyroid hormones' re-entry into the enterohepatic circulation (29), and prompting an autoimmune response in the thyroid gland (7, 30), leading to hypothyroidism.

In this study, KEGG enrichment analysis revealed significant enrichment of peptidoglycan biosynthesis and glycerol ester metabolism pathways in the hypothyroid group. We hypothesized that *P. vulgatus* and *B. fragilis* contribute to hypothyroidism during early pregnancy due to: (1) an increase in β-N-acetylaminoglucosidase, enhancing peptidoglycan production by catalyzing acetylamino glucose removal from peptidoglycan fragments (31, 32). This stimulates the Nucleotide Binding Oligomerization Domain

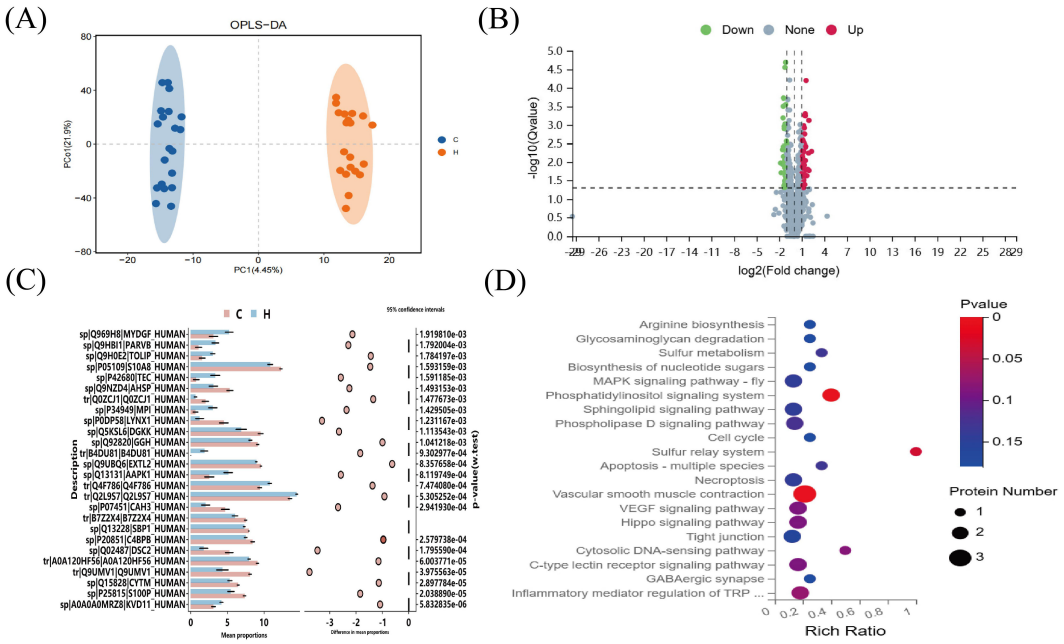

FIGURE 4
4D-DIA proteomic analysis. **(A)** OPLS-DA Score Chart **(B)** Differential Protein Volcano Plot. The x-axis represents protein differential folds (expressed as log2), while the y-axis shows the corresponding -log10 (Q-value). A Q-value < 0.05 and Fold Change > 1.2 were criteria used to identify significant differential proteins by default. Red points in the graph denote significantly up-regulated proteins, green points indicate significantly down-regulated proteins, and gray points represent proteins with no significant changes. **(C)** SATMP Analysis Plot, displaying the first 26 differentially significant proteins at $p < 0.05$. **(D)** Differential Protein KEGG-Pathway Enrichment Bubble Plot. The x-axis shows the enrichment ratio, the y-axis labels the KEGG Pathway, and the bubble size reflects the number of proteins annotated to a specific KEGG Pathway. The color gradient indicates the enrichment significance value (p<0.05 denotes statistical significance), with deeper reds signifying smaller significance values.

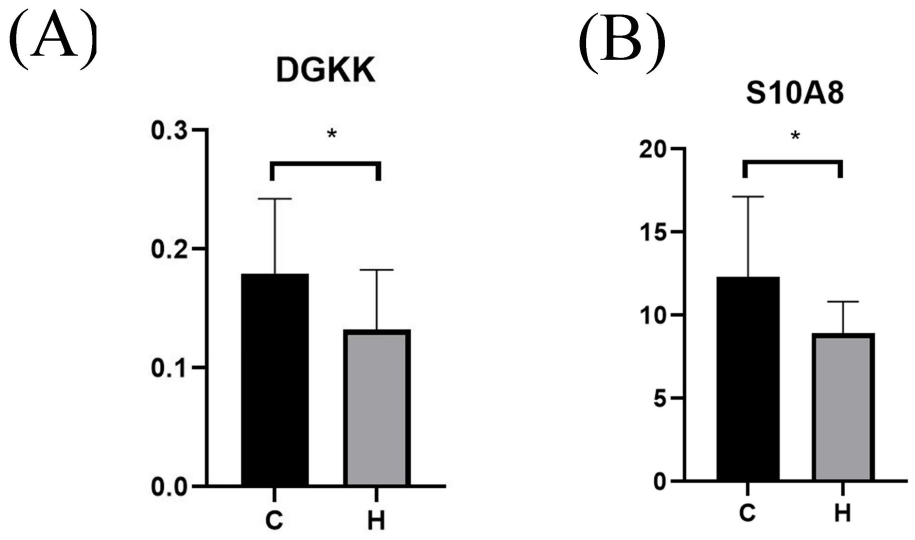

FIGURE 5
ELISA validation of serum protein level box plots for different populations. Serum levels of DGKK (Figure 4A) and S10A8 (Figure 4B) in the hypothyroid and normal groups. $p < 0.05$ indicates a statistically significant difference. Group H represents the hypothyroidism group in the first half of pregnancy. Group C represents the normal control group during the same period. * represents P < 0.05.

10.3389/fimmu.2025.1500866

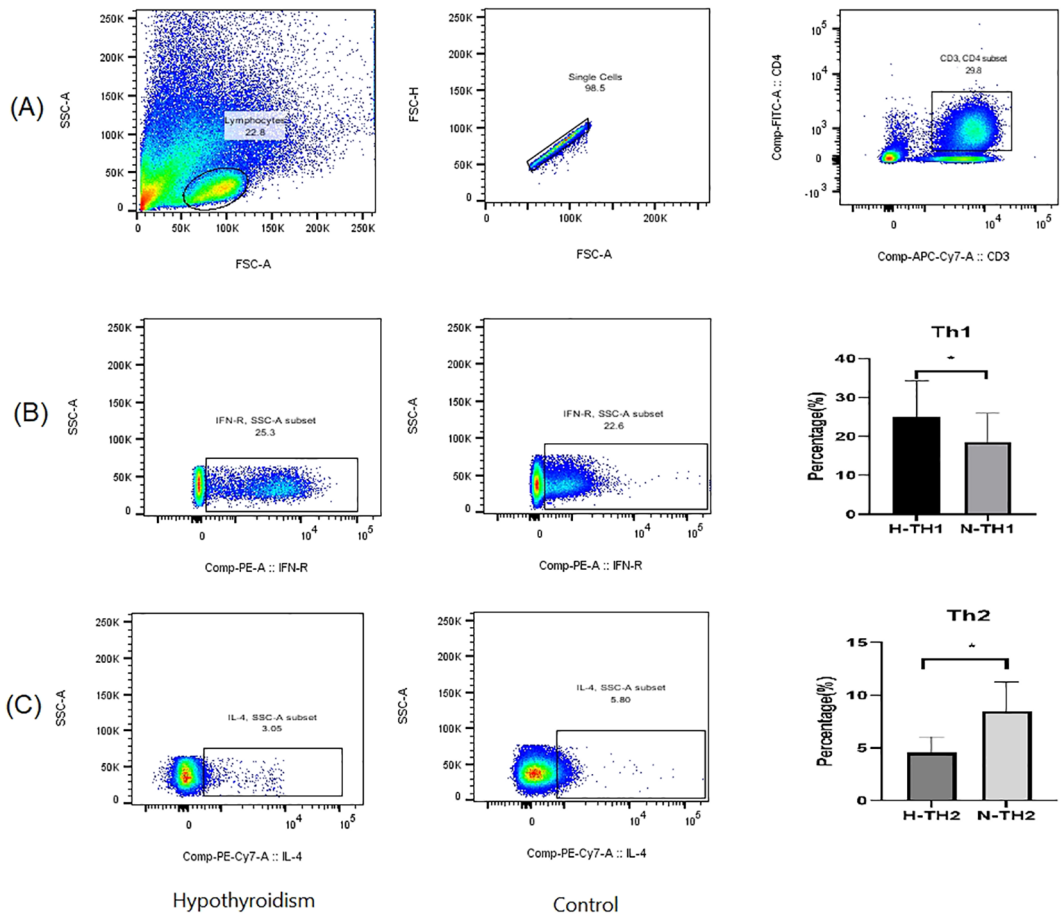

FIGURE 6
Detection of Th1 and Th2 cells using flow cytometry. **(A)** Flow cytometry gating strategy; **(B)** Percentage of Th1 cells; **(C)** Percentage of Th2 cells. $p < 0.05$ indicates statistical significance. * represents P < 0.05.

Containing 1 (NOD1) receptor, triggering the receptor interacting protein kinase 2 (RIP2) kinase and activating the NF-κB pathway (25, 33), which induces an autoimmune response in the thyroid (34); (2) elevated Short-chain fatty acids (SCFA) production resulting from increased mucus-degrading enzymes from *Mycobacterium avium* and intestinal mucus cleavage (35). Furthermore, the AMPK pathway activation increases lysophosphatidic acid production in glycerol ester metabolism, which, via the G Protein-Coupled Receptors

TABLE 2 Comparison of serologic data between the hypothyroid and normal groups.

	Hypothyroidism group (n=20)	Normal Group (n=20)	P−value
TSH (mIU/L)	5.28 (4.64, 6.66)	1.50 (1.26, 2.41)	<0.026*
FT4(mIU/L)	14.1 (11.7, 17.18)	16.45(14.80, 18.95)	0.009*
hsCRP	4.01 (3.16, 6.08)	1.52 (0.57, 3.75)	0.001*
IL-2	0.63 (0.10, 5.09)	0.06 (0.00, 0.47)	0.007*
IL-10	1.06 (0.74, 7.51)	0.98 (0.71, 1.42)	0.355
IL-6	2.64 (1.85, 12.79)	1.44 (1.21, 2.38)	0.038*
TNF-α	1.37 (0.39, 10.04)	0.74 (0.05, 1.13)	0.023*
Th1	24.92 ± 9.38	18.61 ± 7.34	0.023*
TH2	4.55 ± 1.51	8.48 ± 2.77	<0.001*
Th1/Th2	6.02 ± 3.12	2.25 ± 0.87	<0.001*

p-value less than 0.05 was statistically significant.
* represents P < 0.05.

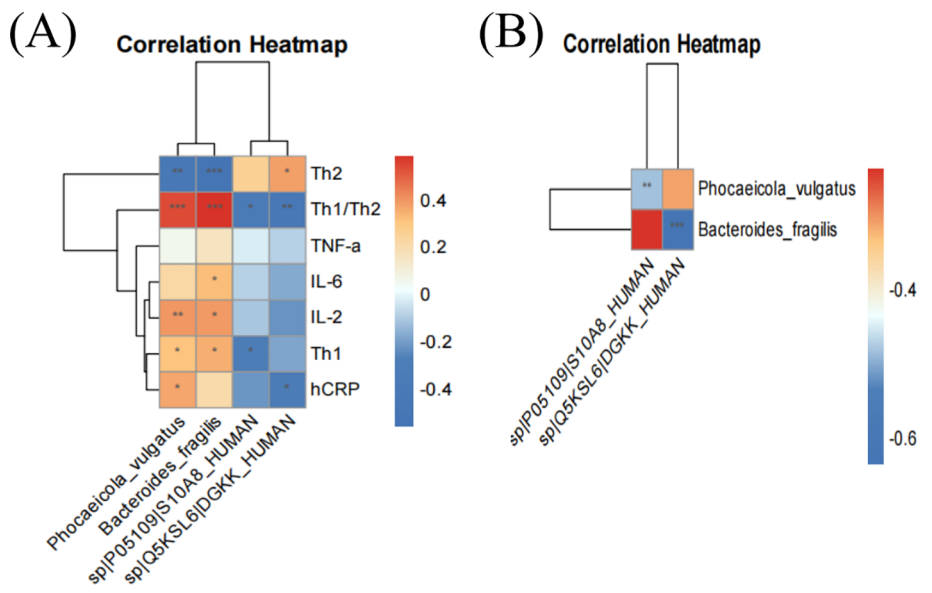

FIGURE 7
Correlation heatmap of dominant strains with clinical indicators and significantly down-regulated proteins. Red and blue represent positive and negative correlations, respectively. * implies $p < 0.05$, ** implies $p < 0.01$, and *** implies $p < 0.001$.

(GPCR) pathway, activates the NF-κB pathway (36, 37), escalating pro-inflammatory mediators like TNF-α and IL-6, leading to thyroid autoimmunity and hormonal disruptions.

The proteomic results of this study showed that DGKK and S10A8 were significantly down-regulated in patients with hypothyroidism in the first half of pregnancy. ELISA validation showed that DGKK and S10A8 were significantly down-regulated in patients with hypothyroidism in the first half of pregnancy. The down-regulation of DGKK affects the protein kinase C pathway and reduces the H2O2 production (38). H2O2 is synthesized by dual oxidase (DUOX) and participates in the catalysis of iodide by thyroid peroxidase (TPO) (39, 40). As an essential molecule for iodine binding and thyroid hormone synthesis, a decrease in H2O2 levels affects iodine binding in thyroid cells and the synthesis and secretion of thyroid hormones (41). Downregulation of S10A8 inhibits NADPH oxidase and reduces the production of H2O2 (42–44). S10A8 also affects Adenosine triphosphate (ATP) production, regulates Ca2+ reduction, influences phosphatidylinositol (PI) and H2O2 production (45), and is involved in the development of hypothyroidism during the first half of pregnancy.

Enrichment analysis of differential protein KEGG pathways in this study showed that phosphatidylinositol signaling and smooth vascular muscle contraction pathways were significantly enriched. Therefore, we hypothesized that the downregulation of DGKK and S10A8 is involved in the development of hypothyroidism in the first half of pregnancy, which may (1) reduce Diacylglycerol (DAG) phosphorylation and inhibit phosphatidic acid production by the protein kinase C pathway by downregulation of DGKK (46), which reduces PI in the phosphatidylinositol signaling pathway (45) and in turn affects inositol-dependent thyroid stimulating hormone (TSH) signaling (47), resulting in altered TSH synthesis and secretion and leading to hypothyroidism (48) (2). S10A8 downregulation affects ATP and Ca2+, not only vascular smooth muscle contraction (49, 50), but also regulates thyroglobulin (thyroid hormone precursor) synthesis and secretion in thyroid cells (51), promoting the onset of hypothyroidism.

Flow cytometry results indicated an increase in Th1 cells and a decrease in Th2 cells in pregnant women with hypothyroidism compared to the normal group, with a Th1/Th2 balance shift toward Th1. Additionally, hs-CRP, IL-2, IL-6 and TNF-α levels were elevated in the hypothyroidism group, suggesting an inflammatory response in these patients during the first half of pregnancy, aligning with previous studies (12). When the Th1/Th2 ratio is elevated, Th1 dominates the immune response, which not only promotes the increased release of IL-2, IL-6, TNF-α (52, 53), but also affects autoimmunity and stimulates the synthesis and release of chemotactic immunity factors from thyroid cells, thereby expanding autoimmune feedback (54–56) and accelerating the Fas-mediated apoptosis of thyroid cells (54). This promotes thyroid damage and induces hypothyroidism (52).

The correlation analysis indicated that *P. vulgatus* and *B. fragilis* significantly correlate with Th1/Th2 ratios, showing positive associations with IL-2, DGKK, and S10A8, yet negative associations with Th1/Th2. *P. vulgatus* negatively correlates with S10A8, while *B. fragilis* negatively correlates with IL-2 and DGKK, suggesting distinct bacterial-protein interactions. These interactions are believed to contribute to hypothyroidism by altering Th1/Th2 balance and cytokine profiles through several mechanisms: (1) increased *B. fragilis* may enhance protease release, acting as virulence factors to disrupt the intestinal barrier and degrade extracellular DGKK (46) and S10A8; (2) upregulation of *Bacteroides* may modulate transcription factors, increasing Th1 and decreasing Th2 cells, thereby shifting the Th1/Th2 balance and impacting pro-inflammatory cytokine release (57); (3)

downregulation of S10A8 impairs myeloid-derived suppressor cells (MDSC) via the Toll-like receptor 4 (TLR4) pathway (58, 59), thus hindering T cell-mediated immunity and disrupting Th1/Th2 balance (60, 61). These pathways potentially elevate Th1/Th2 ratios, exacerbate thyroid damage, and induce hypothyroidism.

Our study has limitations. The small sample size, influenced by regional dietary and lifestyle habits may have impacted our results. Secondly, due to limitations in sample size, our power analysis reveals that the current study achieves approximately 70% statistical power for detecting large effect sizes. Thus, further research with a larger sample and diverse histological approaches is necessary to investigate hypothyroidism's onset during early pregnancy.

In summary, we examined the altered gut microbiota and proteomic characteristics in patients with early pregnancy hypothyroidism and investigated their association with Th1/Th2 cells using macro proteomics. This was an exploratory study. Our findings suggest that increased *P. vulgatus* and *B. fragilis*, decreased DGKK and S10A8 proteins, and a left shift in the Th1/Th2 balance in patients with hypothyroidism in the first half of pregnancy may be associated with the development of the disease. This study offers novel insights into early pregnancy hypothyroidism pathogenesis and potential biomarker identification.

Data availability statement

Metagenomics and mass spectrometry proteomics data have been deposited in the ProteomeXchange Consortium (https://proteomecentral.proteomexchange.org) with dataset identifier PXD055369. Other data were deposited in Figshare database ((https://figshare.com), dataset DOI is 10.6084/m9.figshare.26879455.

Ethics statement

The studies involving humans were approved by Ethics Committee of the Third Affiliated Hospital of Zhengzhou University. The studies were conducted in accordance with the local legislation and institutional requirements. The participants provided their written informed consent to participate in this study. The animal study was approved by the Medical Ethics Committee of the Third Affiliated Hospital of Zhengzhou University, China. The study was conducted in accordance with the local legislation and institutional requirements. Written informed consent was obtained from the individual(s) for the publication of any potentially identifiable images or data included in this article.

Author contributions

CZ: Writing – original draft, Writing – review & editing. YX: Writing – original draft, Writing – review & editing. MZ: Writing – review & editing, Formal analysis, Methodology. JL: Writing – review & editing, Data curation, Formal analysis, Methodology, Visualization. ZS: Writing – review & editing, Formal analysis, Methodology, Validation, Visualization. YW: Writing – review & editing, Data curation, Methodology, Software. PL: Data curation, Methodology, Software, Writing – review & editing.

Funding

The author(s) declare that financial support was received for the research and/or publication of this article. This work was supported by Henan Science and Technology Department (Item NO.222102310668).

Acknowledgments

We sincerely acknowledge the Third Affiliated Hospital of Zhengzhou University for the help we received, and we sincerely appreciated the pregnant women who volunteered to participate in this study.

Conflict of interest

The authors declare that the research was conducted in the absence of any commercial or financial relationships that could be construed as a potential conflict of interest.

Generative AI statement

The author(s) declare that no Generative AI was used in the creation of this manuscript.

Publisher's note

All claims expressed in this article are solely those of the authors and do not necessarily represent those of their affiliated organizations, or those of the publisher, the editors and the reviewers. Any product that may be evaluated in this article, or claim that may be made by its manufacturer, is not guaranteed or endorsed by the publisher.

Supplementary material

The Supplementary Material for this article can be found online at: https://www.frontiersin.org/articles/10.3389/fimmu.2025.1500866/full#supplementary-material

References

1. Writting Committee for Guidelines for Prevention and Management of Thyroid Diseases During Pregnancy and Perinatal Period Chinese Society of Endocrinology and Chinese Medical Association, Women's Health Care Branch of Chinese Preventive Medicine Association. Guidelines for prevention and management of thyroid diseases during pregnancy and perinatal period. *Chin J Endocrinol Metab*. (2022) 38:539–51. doi: 10.3760/cma.j.cn311282-20220416-00234

2. Lee SY, Pearce EN. Assessment and treatment of thyroid disorders in pregnancy and the postpartum period. *Nat Rev Endocrinol*. (2022) 18:158–71. doi: 10.1038/s41574-021-00604-z

3. Kuspanova M, Gaiday A, Dzhardemaliyeva N, Tuganbayev M, Gorobeiko M, Dinets A, et al. Biochemical markers for prediction of the first half pregnancy losses: a review. *Rev Bras Ginecol Obstet*. (2024) 46:e–rbgo72. doi: 10.61622/rbgo/2024rbgo72

4. Lynch SV, Pedersen O. The Human Intestinal Microbiome in Health and Disease. *N Engl J Med*. (2016) 375:2369–79. doi: 10.1056/NEJMra1600266

5. Clemente JC, Ursell LK, Parfrey LW, Knight R. The impact of the gut microbiota on human health: an integrative view. *Cell*. (2012) 148:1258–70. doi: 10.1016/j.cell.2012.01.035

6. Wu R, An J, Ding T, Xue H, Li X, Wang C. Pos0396 the level of peripheral regulatory t cells is associated with the changes of intestinal microbiota in patients with rheumatoid arthritis ann rheum dis. *Ann Rheum Dis*. (2021) 2:80. doi: 10.1136/annrheumdis-2021-eular.2783

7. Jiang W, Lu G, Gao D, Lv Z, Li D. The relationships between the gut microbiota and its metabolites with thyroid diseases. *Front Endocrinol (Lausanne)*. (2022) 13:943408. doi: 10.3389/fendo.2022.943408

8. Wang B, Xu Y, Zhang M, Zhang J, Hou X, Li J, et al. Oral and intestinal microbial features in pregnant women with hypothyroidism and their correlations with pregnancy outcomes. *Am J Physiol-Endoc M*. (2020) 11:319. doi: 10.1152/ajpendo.00234.2020

9. Cai Y, Xu Y, Ban Y, Li J, Sun Z, Zhang M, et al. Plasma Lipid Profile and Intestinal Microflora in Pregnancy Women With Hypothyroidism and Their Correlation With Pregnancy Outcomes. *Front Endocrinol (Lausanne)*. (2021) 12:792536. doi: 10.3389/fendo.2021.792536

10. Wu B, Xu Y, Ban Y, Zhang M, Sun Z, Cai Y, et al. Correlation between the intestinal microflora and peripheral blood Th1/Th2 balance in hypothyroidism during the first half of pregnancy. *Front Cell Infect Microbiol*. (2023) 13:1159238. doi: 10.3389/fcimb.2023.1159238

11. Challis JR, Lockwood CJ, Myatt L, Norman JE, Strauss JF, Petraglia F. Inflammation and pregnancy. *Reprod Sci*. (2009) 1:16. doi: 10.1177/1933719108329095

12. Salvi V, Gianello V, Tiberio L, Sozzani S, Bosisio D. Cytokine Targeting by miRNAs in Autoimmune Diseases. *Front Immunol*. (2019) 10:15. doi: 10.3389/fimmu.2019.00015

13. Zhu X, Zhu J. CD4 T Helper Cell Subsets and Related Human Immunological Disorders. *Int J Mol Sci*. (2020) 21:8011. doi: 10.3390/ijms21218011

14. Kageyama T, Matsuo T, Kurakake R, Sano T. Relationship between T cells and microbiota in health and disease. *Prog Mol Biol Transl Sci*. (2020) 171:95–129. doi: 10.1016/bs.pmbts.2020.03.007

15. Morgan E, Varro R, Sepulveda H, Ember JA, Apgar J, Wilson J, et al. Cytometric bead array: a multiplexed assay platform with applications in various areas of biology. *Clin Immunol*. (2004) 2:110. doi: 10.1016/j.clim.2003.11.017

16. Rimac V, Bojanić I, Gojčeta K, Golubić Ćepulić B. Evaluation of the BD Stem Cell Enumeration Kit on the BD FACSCanto II flow cytometer using bd facscanto clinical and bd facsdiva software. *Int J Lab Hematol*. (2021) 1:43. doi: 10.1111/ijlh.13315

17. Langmead B, Salzberg SL. Fast gapped-read alignment with Bowtie 2. *Nat Methods*. (2012) 9:357–9. doi: 10.1038/nmeth.1923

18. Li D, Liu CM, Luo R, Sadakane K, Lam TW. MEGAHIT: an ultra-fast single-node solution for large and complex metagenomics assembly via succinct de Bruijn graph. *Bioinformatics*. (2015) 31:1674–6. doi: 10.1093/bioinformatics/btv033

19. Gautam A, Felderhoff H, Bağci C, Huson DH. Using AnnoTree to Get More Assignments, Faster, in DIAMOND+MEGAN Microbiome Analysis. *mSystems*. (2022) 7:e0140821. doi: 10.1128/msystems.01408-21

20. Kondratenko Y, Korobeynikov A, Lapidus A. CDSnake: Snakemake pipeline for retrieval of annotated OTUs from paired-end reads using CD-HIT utilities. *BMC Bioinf*. (2020) 21:303. doi: 10.1186/s12859-020-03591-6

21. Schmid S, Jeevannavar A, Julian TR, Tamminen M. Portable BLAST-like algorithm library and its implementations for command line, Python and R. *PLoS One*. (2023) 18:e0289693. doi: 10.1371/journal.pone.0289693

22. Hou Z, Sun A, Li Y, Song X, Liu S, Hu X, et al. What Are the Reliable Plasma Biomarkers for Mild Cognitive Impairment? A Clinical 4D Proteomics Study and Validation. *Mediat Inflamm*. (2024) 2024:7709277. doi: 10.1155/2024/7709277

23. Elhenawy W, Debelyy MO, Feldman MF. Preferential packing of acidic glycosidases and proteases into Bacteroides outer membrane vesicles. *mBio*. (2014) 5:e00909–e914. doi: 10.1128/mBio.00909-14

24. Gilmore WJ, Johnston EL, Bitto NJ, Zavan L, O'Brien-Simpson N, Hill AF, et al. Bacteroides fragilis outer membrane vesicles preferentially activate innate immune receptors compared to their parent bacteria. *Front Immunol*. (2022) 13:970725. doi: 10.3389/fimmu.2022.970725

25. Onderdonk AB, Franklin ML, Cisneros RL. Production of experimental ulcerative colitis in gnotobiotic guinea pigs with simplified microflora. *Infect Immun*. (1981) 32:225–31. doi: 10.1128/iai.32.1.225-231.1981

26. Mills RH, Dulai PS, Vázquez-Baeza Y, Sauceda C, Daniel N, Gerner RR, et al. Multi-omics analyses of the ulcerative colitis gut microbiome link Bacteroides vulgatus proteases with disease severity. *Nat Microbiol*. (2022) 1:7. doi: 10.1038/s41564-021-01050-3

27. Wong SH, Yu J. Gut microbiota in colorectal cancer: mechanisms of action and clinical applications. *Nat Rev Gastroenterol Hepatol*. (2019) 16:690–704. doi: 10.1038/s41575-019-0209-8

28. Niewiem M, Grzybowska-Chlebowczyk U. Intestinal Barrier Permeability in Allergic Diseases. *Nutrients*. (2022) 14:1893. doi: 10.3390/nu14091893

29. Fenneman AC, Bruinstroop E, Nieuwdorp M, van der Spek AH, Boelen A. A Comprehensive Review of Thyroid Hormone Metabolism in the Gut and Its Clinical Implications. *Thyroid*. (2023) 33:32–44. doi: 10.1089/thy.2022.0491

30. Su X, Zhao Y, Li Y, Ma S, Wang Z. Gut dysbiosis is associated with primary hypothyroidism with interaction on gut-thyroid axis. *Clin Sci (Lond)*. (2020) 134:1521–35. doi: 10.1042/CS20200475

31. Nihira T, Suzuki E, Kitaoka M, Nishimoto M, Ohtsubo K, Nakai H. Discovery of β-1,4-D-mannosyl-N-acetyl-D-glucosamine phosphorylase involved in the metabolism of N-glycans. *J Biol Chem*. (2013) 288:27366–74. doi: 10.1074/jbc.M113.469080

32. Su H, Sheng X, Liu Y. Insights into the catalytic mechanism of N-acetylglucosaminidase glycoside hydrolase from Bacillus subtilis: a QM/MM study. *Org Biomol Chem*. (2016) 14:3432–42. doi: 10.1039/c6ob00320f

33. Cañas MA, Fábrega MJ, Giménez R, Badia J, Baldomà L. Outer Membrane Vesicles From Probiotic and Commensal Escherichia coli Activate NOD1-Mediated Immune Responses in Intestinal Epithelial Cells. *Front Microbiol*. (2018) 9:498. doi: 10.3389/fmicb.2018.00498

34. Lu Y, Xing C, Zhang C, Lv X, Liu G, Chen F, et al. Promotion of IL–17/NF–κB signaling in autoimmune thyroid diseases. *Exp Ther Med*. (2023) 25:51. doi: 10.3892/etm.2022.11750

35. Di Vincenzo F, Del Gaudio A, Petito V, Lopetuso LR, Scaldaferri F. Gut microbiota, intestinal permeability, and systemic inflammation: a narrative review. *Intern Emerg Med*. (2024) 19:275–93. doi: 10.1007/s11739-023-03374-w

36. Liu H, Nie C, Hu X, Li J. Highland barley β-glucan supplementation attenuated hepatic lipid accumulation in Western diet-induced non-alcoholic fatty liver disease mice by modulating gut microbiota. *Food Funct*. (2024) 15:1250–64. doi: 10.1039/d3fo03386d

37. Prentki M, Madiraju SR. Glycerolipid metabolism and signaling in health and disease. *Endocr Rev*. (2008) 29:647–76. doi: 10.1210/er.2008-0007

38. Chauhan-Puri AK, Lee KH, Magoski NS. Hydrogen peroxide and phosphoinositide metabolites synergistically regulate a cation current to influence neuroendocrine cell bursting. *J Physiol*. (2021) 599:5281–300. doi: 10.1113/JP282302

39. Nakagawa Y, Rüstow B, Rabe H, Kunze D, Waku K. The *de novo* synthesis of molecular species of phosphatidylinositol from endogenously labeled CDP diacylglycerol in alveolar macrophage microsomes. *Arch Biochem Biophys*. (1989) 268:559–66. doi: 10.1016/0003-9861(89)90323-8

40. Marique L, Van Regemorter V, Gérard AC, Craps J, Senou M, Marbaix E, et al. The expression of dual oxidase, thyroid peroxidase, and caveolin-1 differs according to the type of immune response (TH1/TH2) involved in thyroid autoimmune disorders. *J Clin Endocr Metab*. (2014) 99:1722–32. doi: 10.1210/jc.2013-3469

41. Köhrle J. Selenium, Iodine and Iron-Essential Trace Elements for Thyroid Hormone Synthesis and Metabolism. *Int J Mol Sci*. (2023) 24:3393. doi: 10.3390/ijms24043393

42. Berthier S, Nguyen MV, Baillet A, Hograindleur MA, Paclet MH, Polack B, et al. Molecular interface of S100A8 with cytochrome b558 and NADPH oxidase activation. *PLoS One*. (2012) 7:e40277. doi: 10.1371/journal.pone.0040277

43. Kerkhoff C, Nacken W, Benedyk M, Dagher MC, Sopalla C, Doussiere J. The arachidonic acid-binding protein S100A8/A9 promotes NADPH oxidase activation by interaction with p67phox and Rac-2. *FASEB J*. (2005) 19:467–9. doi: 10.1096/fj.04-2377fje

44. Alves JV, da Costa RM, Awata WMC, Bruder-Nascimento A, Singh S, Tostes RC, et al. NADPH oxidase 4-derived hydrogen peroxide counterbalances testosterone-induced endothelial dysfunction and migration. *Am J Physiol-Endoc M*. (2024) 6:327. doi: 10.1152/ajpendo.00365.2023

45. Godlewska M, Banga PJ. Thyroid peroxidase as a dual active site enzyme: Focus on biosynthesis, hormonogenesis and thyroid disorders of autoimmunity and cancer. *Biochimie*. (2019) 160:34–45. doi: 10.1016/j.biochi.2019.02.003

46. Tu GW, Zhang Y, Ma JF, Hou JY, Hao GW, Su Y, et al. Extracellular vesicles derived from CD4+ T cells carry DGKK to promote sepsis-induced lung injury by regulating oxidative stress and inflammation. *Cell Mol Biol Lett*. (2023) 2:28. doi: 10.1186/s11658-023-00435-y

47. Grasberger H, Van Sande J, Hag-Dahood Mahameed A, Tenenbaum-Rakover Y, Refetoff S. A familial thyrotropin (TSH) receptor mutation provides *in vivo* evidence that the inositol phosphates/Ca2+ cascade mediates TSH action on thyroid hormone synthesis. *J Clin Endocrinol Metab*. (2007) 92:2816–20. doi: 10.1210/jc.2007-0366

48. Fallahi P, Ferrari SM, Elia G, Ragusa F, Paparo SR, Caruso C, et al. Myo-inositol in autoimmune thyroiditis, and hypothyroidism. *Rev Endocr Metab Dis*. (2018) 19:349–54. doi: 10.1007/s11154-018-9477-9

49. Muñoz-Castañeda J, Garcia-Saez R, Lopez-Baltanas R, Romero A, Ortiz M, Ureña J, et al. 1610 FGF23-mediated hypertension via augmented calcium entry in vascular smooth muscle cells. *Nephrol Dial Transpl*. (2024) 39. doi: 10.1093/ndt/gfae069.190

50. Batbaatar MA, Kinoshita T, Ikeda S, Nishi K, Iwasaki H, Ganbaatar N, et al. Nardilysin in vascular smooth muscle cells controls blood pressure via the regulation of calcium dynamics. *Biochem Bioph Res Co*. (2024) 712-713:149961. doi: 10.1016/j.bbrc.2024.149961

51. Törnquist K, Sukumaran P, Kemppainen K, Löf C, Viitanen T. Canonical transient receptor potential channel 2 (TRPC2): old name-new games. Importance in regulating of rat thyroid cell physiology. *Pflugers Arch*. (2014) 466:2025–34. doi: 10.1007/s00424-014-1509-z

52. Guo Y, Zynat J, Xing S, Xin L, Li S, Mammat N, et al. Immunological changes of T helper cells in flow cytometer-sorted CD4+ T cells from patients with Hashimoto's thyroiditis. *Exp Ther Med*. (2018) 15:3596–602. doi: 10.3892/etm.2018.5825

53. Ferrari SM, Paparo SR, Ragusa F, Elia G, Mazzi V, Patrizio A, et al. Chemokines in thyroid autoimmunity. *Best Pract Res Clin Endocrinol Metab*. (2023) 37:101773. doi: 10.1016/j.beem.2023.101773

54. Fountoulakis S, Vartholomatos G, Kolaitis N, Frillingos S, Philippou G, Tsatsoulis A. Differential expression of Fas system apoptotic molecules in peripheral lymphocytes from patients with Graves' disease and Hashimoto's thyroiditis. *Eur J Endocrinol*. (2008) 158:853–9. doi: 10.1530/EJE-08-0092

55. Antonelli A, Ferrari SM, Corrado A, Di Domenicantonio A, Fallahi P. Autoimmune thyroid disorders. *Autoimmun Rev*. (2015) 14:174–80. doi: 10.1016/j.autrev.2014.10.016

56. Ragusa F, Fallahi P, Elia G, Gonnella D, Paparo SR, Giusti C, et al. Hashimotos' thyroiditis: Epidemiology, pathogenesis, clinic and therapy. *Best Pract Res Clin Endocrinol Metab*. (2019) 33:101367. doi: 10.1016/j.beem.2019.101367

57. Li K, Hao Z, Du J, Gao Y, Yang S, Zhou Y. Bacteroides thetaiotaomicron relieves colon inflammation by activating aryl hydrocarbon receptor and modulating $CD4^+$T cell homeostasis. *Int Immunopharmacol*. (2021) 90:107183. doi: 10.1016/j.intimp.2020.107183

58. Deguchi A, Yamamoto T, Shibata N, Maru Y. S100A8 may govern hyper-inflammation in severe COVID-19. *FASEB J*. (2021) 35:e21798. doi: 10.1096/fj.202101013

59. von Wulffen M, Luehrmann V, Robeck S, Russo A, Fischer-Riepe L, van den Bosch M, et al. S100A8/A9-alarmin promotes local myeloid-derived suppressor cell activation restricting severe autoimmune arthritis. *Cell Rep*. (2023) 7:42. doi: 10.1016/j.celrep.2023.113006

60. Esparvarinha M, Madadi S, Aslanian-Kalkhoran L, Nickho H, Dolati S, Pia H, et al. Dominant immune cells in pregnancy and pregnancy complications: T helper cells (TH1/TH2, TH17/Treg cells), NK cells, MDSCs, and the immune checkpoints. *Cell Biol Int*. (2023) 2:47. doi: 10.1002/cbin.11955

61. Qi J, Zhou X, Bai Z, Lu Z, Zhu X, Liu J, et al. FcγRIIIA activation-mediated up-regulation of glycolysis alters MDSCs modulation in CD4+ T cell subsets of Sjögren syndrome. *Cell Death Dis*. (2023) 1:14. doi: 10.1038/s41419-023-05631-4

frontiers | Frontiers in Immunology

TYPE Original Research
PUBLISHED 18 August 2025
DOI 10.3389/fimmu.2025.1635712

Check for updates

OPEN ACCESS

EDITED BY
Alessandro Antonelli,
University of Pisa, Italy

REVIEWED BY
Collynn F. Woeller,
University of Rochester Medical Center, United States
Chaokui Wang,
Chongqing Eye Institute, China
Ruili Wei,
Shanghai Changzheng Hospital, China

*CORRESPONDENCE
Jie Shen
sjiesy@smu.edu.cn
Thomas Efferth
efferth@uni-mainz.de
Yi Wang
wangyieye@126.com

†These authors have contributed equally to this work

RECEIVED 26 May 2025
ACCEPTED 28 July 2025
PUBLISHED 18 August 2025

CITATION
Hai Y, Ma Q, Liu Z, Li D, Huang A, Zhu Y, Yongbo D, Song C, Yu G, Fang S, Liu L, Wang Y, Efferth T and Shen J (2025) Oxidative stress-related biomarkers in thyroid eye disease: evidence from bioinformatics analysis and experimental validation. *Front. Immunol.* 16:1635712. doi: 10.3389/fimmu.2025.1635712

COPYRIGHT
© 2025 Hai, Ma, Liu, Li, Huang, Zhu, Yongbo, Song, Yu, Fang, Liu, Wang, Efferth and Shen. This is an open-access article distributed under the terms of the Creative Commons Attribution License (CC BY). The use, distribution or reproduction in other forums is permitted, provided the original author(s) and the copyright owner(s) are credited and that the original publication in this journal is cited, in accordance with accepted academic practice. No use, distribution or reproduction is permitted which does not comply with these terms.

Oxidative stress-related biomarkers in thyroid eye disease: evidence from bioinformatics analysis and experimental validation

Yuanping Hai[1,2†], Qintao Ma[1†], Zhitao Liu[3†], Dongxiao Li[2], Anqi Huang[1], Yan Zhu[1], Duan Yongbo[4], Cheng Song[1], Genfeng Yu[1], Sijie Fang[5], Lan Liu[1], Yi Wang[6,7*], Thomas Efferth[2*] and Jie Shen[1*]

[1]Department of Endocrinology and Metabolism, The Eighth Affiliated Hospital of Southern Medical University (The First People's Hospital of Shunde Foshan), Foshan, Guangdong, China, [2]Department of Pharmaceutical Biology, Institute of Pharmaceutical and Biomedical Sciences, Johannes Gutenberg University, Mainz, Germany, [3]Department of Orthopedics, People's Hospital of Ningxiang City, Hunan University of Chinese Medicine, Changsha, China, [4]Department of Ophthalmopathy, The Eighth Affiliated Hospital of Southern Medical University (The First People's Hospital of Shunde Foshan), Foshan, China, [5]Department of Ophthalmology, Shanghai Ninth People's Hospital, Shanghai Jiao Tong University School of Medicine, Shanghai, China, [6]Department of Ophthalmology, Peking University Third Hospital, Beijing, China, [7]Beijing Key Laboratory of Restoration of Damaged Ocular Nerve, Peking University Third Hospital, Beijing, China

Background: Oxidative stress is a key contributor to the pathogenesis of the autoimmune condition thyroid eye disease (TED). However, its precise molecular mechanisms and reliable biomarkers remain unclear. Bioinformatics enables the identification of differentially expressed genes through transcriptomic analysis. However, distinguishing truly relevant findings from false discoveries remains challenging. Immunohistochemistry helps address this limitation by validating protein expression levels, revealing local immune responses, and linking microscopic tissue changes to clinical manifestations.

Methods: Oxidative stress-related differentially expressed genes (OS-DEGs) were identified. Gene Ontology (GO) and Kyoto Encyclopedia of Genes and Genomes (KEGG) pathway analyses were performed to explore their biological functions and pathways. Machine learning methods, including LASSO regression and random forest, were used to select key diagnostic genes. Receiver operating characteristic curves assessed their diagnostic performance. A nomogram model was constructed using logistic regression based on selected oxidative stress-related core genes. Single-gene gene set enrichment analysis evaluated the diagnostic potential and functional relevance of these core genes. Expression of three key genes/proteins repeatedly highlighted in multi-omics TED studies was confirmed in 22 orbital tissues by immunohistochemistry with quantitative analysis using automated image tools minimizing operator bias.

Results: Fifty-three OS-DEGs were selected. GO and KEGG enrichment analyses revealed significant involvement of OS-DEGs in cellular responses to oxidative stress, ROS metabolism, and mitochondrial dysfunction, highlighting the role of oxidative damage in TED. Five diagnostic genes (*AKT1, APEX1, FOS, MCL1*, and *ANGPTL7*) were identified through machine learning approaches (LASSO regression and random forest), demonstrating strong diagnostic potential with

a combined model achieving an area under the curve (AUC) of 0.931. The nomogram model developed using the selected genes showed good predictive performance for TED risk assessment. Immunohistochemical validation confirmed significant upregulation of FOS, MCL1, and ANGPTL7 in TED *versus* controls.

Conclusions: To the best of our knowledge, this study is the first to identify three oxidative stress-related genes/proteins as potential biomarkers for TED through bioinformatic analysis of multi-omics data followed by immunohistochemical validation, providing new insights into their roles in the pathogenesis of the disease. These biomarkers could aid in early screening and risk assessment for TED.

KEYWORDS

ANGPTL7, artificial intelligence, biomarkers, FOS, immunohistochemistry, MCL1, oxidative stress, thyroid eye disease

1 Introduction

Thyroid eye disease (TED) is a chronic autoimmune orbital disorder associated with thyroid dysfunction, characterized by inflammation, tissue remodeling, and fibrosis (1–4). Its pathogenesis involves disruption of immune tolerance, leading to infiltration of immune cells — such as macrophages and lymphocytes — into orbital tissues and the release of inflammatory mediators (5–8). As key effector cells, orbital fibroblasts (OFs) differentiate into myofibroblasts or adipocytes under inflammatory stimuli, promoting fibrosis or fat expansion and contributing to proptosis (7, 9, 10). Activated OFs also produce glycosaminoglycans and cytokines, further aggravating orbital inflammation and tissue remodeling (1, 7, 8, 11).

In recent years, oxidative stress has garnered increasing attention for its critical role in TED progression (6, 12–16). Oxidative stress refers to an imbalance between the production and elimination of reactive oxygen species (ROS), which promotes OF proliferation and induces the expression of the 72 kDa heat shock protein, further increasing ROS levels and exacerbating oxidative stress (1, 6). Oxidative stress-related molecules, including superoxide dismutase, superoxide anion, malondialdehyde, hydrogen peroxide, and glutathione reductase are significantly elevated in OFs from TED patients compared to healthy controls (6, 14). ROS are natural byproducts of cellular metabolism and play essential roles in maintaining cellular homeostasis and signaling. However, excessive ROS levels or deficiencies in antioxidant defense mechanisms lead to oxidative damage to proteins, lipids, membranes, and nucleic acids, ultimately resulting in mitochondrial dysfunction and loss of enzymatic activity (12, 13, 15, 16). Several studies have confirmed increased oxidative damage markers in blood, urine, and tear samples from TED patients (13). Blood samples from TED patients show elevated levels of hydrogen peroxide and lipid hydroperoxides along with increased activity of antioxidant enzymes such as superoxide dismutase and catalase, whereas glutathione peroxidase and glutathione reductase activities are reduced (12, 13). Furthermore, ROS promote OFs proliferation, glycosaminoglycan secretion, and the release of pro-inflammatory cytokines and various inflammatory mediators, thereby aggravating TED pathogenesis (1). Therefore, elucidating the oxidative stress mechanisms underlying TED could provide new insights into disease management and therapeutic strategies.

Redox signaling pathways play key roles in TED progression by upregulating potent inflammatory cytokines such as interleukin (IL)-1β, IL-6, and transforming growth factor (TGF)-β, thereby promoting inflammation, adipogenesis, and fibrosis (13). In addition, oxidative stress induced by smoking is one of the most significant risk factors for TED, whereas antioxidant interventions such as selenium supplementation may help mitigate disease progression (15, 16). Several *in vitro* studies demonstrated that bioactive components from traditional Chinese medicine may have therapeutic potential by suppressing oxidative stress in OFs (1, 13). Although the pathogenic role of oxidative stress in TED is widely recognized, its precise molecular mechanisms remain unclear.

Abbreviations: AKT1, AKT serine/threonine kinase 1; ANGPTL7, Angiopoietin-like; AP-1, Activator Protein-1; APEX1, apurinic/apyrimidinic endonuclease 1; AUC, Area under the curve; BP, Biological processes; CC, Cellular components; DCA, Decision curve analysis; DE-OSRGs, Oxidative stress-related differentially expressed genes; DEGs, Differentially expressed genes; DSGs, Diagnostic signature genes; FOS, c-Fos, Fos proto-oncogene, AP-1 transcription factor subunit; GEO, Gene Expression Omnibus; GO, Gene Ontology; GSEA, Gene Set Enrichment Analysis; IL-1β, Interleukin-1β; KEGG, Kyoto Encyclopedia of Genes and Genomes; logFC, Log fold change; MCL1, Myeloid Cell Leukemia-1; MF, Molecular functions; MsigDB, Molecular Signatures Database; OFs, Orbital fibroblasts; OS-DEGs, Oxidative stress-related differential genes; OSRGs, Oxidative stress-related genes; RF, Random forest; ROC, Receiver operating characteristic; ROS, Reactive oxygen species; TED, Thyroid eye disease; TGF-β, Transforming growth factor-β.

Recent advances in bioinformatics and genomic technologies have enabled the identification of differentially expressed genes and signaling pathways through transcriptomic analysis (3–5, 17, 18). However, the association between oxidative stress and TED has not been systematically explored using these methods. Although bioinformatic tools are effective for discovering disease-related targets, they are limited by false positives and lack experimental confirmation. To address this, we used immunohistochemistry to validate the identified targets, providing protein-level evidence and reflecting local immune activity linked to TED pathology (5, 9). Previous immunohistochemical studies have contributed to elucidating TED pathogenesis but often depended on operator-based assessments (9, 10). In contrast, our study utilized a validated and fully automated software platform to conduct quantitative analysis, thereby enhancing the objectivity and reproducibility of the results (5, 9).

We employed transcriptomic sequencing and bioinformatics analysis to identify five core oxidative stress-related genes (*AKT1, APEX1, FOS, MCL1, and ANGPTL7*) associated with TED. Subsequently, a literature review and analysis of original data from these publications revealed that *FOS, MCL1*, and *ANGPTL7* were identified in TED-related multi-omics studies (3–5, 19–23), including single-cell RNA sequencing (21) and our previously published transcriptomic (3), bioinformatic analyses (4), and high-throughput proteomic analyses (5). Furthermore, immunohistochemical validation was performed to confirm the expression of FOS, MCL1, and ANGPTL7 at the protein level, aiming to elucidate the oxidative stress mechanisms underlying the pathogenesis of TED and to provide a theoretical basis for precision diagnosis and treatment.

2 Methods

2.1 Patients and samples

This study was conducted in accordance with the principles outlined in the Declaration of Helsinki and was approved by the Institutional Review Board of Shunde Hospital, Southern Medical University (Ethics approval No. KYLS20240815). Written informed consent was obtained from all participants prior to their inclusion in the study.

A total of 22 orbital tissue samples were collected from 22 individuals at the Department of Ophthalmology, Shunde Hospital, Southern Medical University (Foshan, China). Of these, 12 TED samples — comprising six from patients with clinically active and severe TED, and six from those with inactive and mild TED — were obtained during urgent decompression or rehabilitative orbital decompression surgeries. The remaining 10 specimens were harvested during blepharoplasty procedures from individuals without any history of autoimmune, orbital, or thyroid disorders. Immediately after surgical excision, tissues were snap-frozen in liquid nitrogen and stored at −80 °C. Prior to immunohistochemical analysis, all samples were processed using the formalin-fixed, paraffin-embedded technique.

2.2 Collection of public transcriptomic data and oxidative stress-related differential gene identification

We extracted a total of 458 oxidative stress-related genes (OSRGs) from the Gene Ontology (GO) knowledgebase (http://geneontology.org/). The GSE58331 dataset was obtained from the Gene Expression Omnibus (GEO) database (http://www.ncbi.nlm.nih.gov/geo), comprising 27 orbital tissue samples from TED patients and 22 samples from healthy individuals. Probe annotation files from the corresponding platforms were utilized to map probes to gene symbols. Differentially expressed genes (DEGs) in retro-orbital tissues of TED patients and healthy controls were identified using the "limma" package, with the threshold set at $p < 0.05$ and $|\text{fold change (FC)}| > 0.3$. The identified DEGs were then intersected with oxidative stress-related genes to obtain oxidative stress-related differential genes (OS-DEGs).

2.3 Enrichment analyses of OS-DEGs

We utilized the clusterProfiler package in R to perform GO and Kyoto Encyclopedia of Genes and Genomes (KEGG) pathway enrichment analyses on OS-DEGs, aiming to explore their biological functions and significance. A threshold of $p < 0.05$ was set for statistical significance. Additionally, the enrichment results were visually represented using bubble plots and bar charts.

2.4 Screening oxidative stress-related core genes in TED

This study employed LASSO regression and random forest (RF) machine learning algorithms to identify key oxidative stress-related genes in TED. LASSO regression, a widely used dimension reduction method, excels in high-dimensional data analysis by incorporating regularization to enhance predictive accuracy. A 10-fold cross-validation was performed using the "glmnet" package in R, optimizing the model through a tuning penalty parameter. Additionally, we applied RF, a supervised learning algorithm based on decision trees, to further refine the selection of hub genes. Feature importance was assessed using the Mean Decrease Gini Index, which quantifies the contribution of each variable to classification performance. The intersection of genes identified by both methods was considered as the oxidative stress-related core gene set. The expression levels of these core genes between groups were visualized using boxplots. Furthermore, to evaluate their diagnostic potential, we generated receiver operating characteristic (ROC) curves and used the "pROC" package in R to

calculate the area under the curve (AUC), providing a quantitative measure of diagnostic efficiency.

2.5 Development of an oxidative stress-related nomogram for TED

We utilized the "rms" package in R to develop a nomogram model based on the selected oxidative stress-related core genes. The total score generated by the model exhibited a positive correlation with the risk of TED occurrence. The nomogram included "points", representing the individual scores of each candidate gene, and "total points", which reflected the cumulative gene scores. The probability of TED occurrence for an individual was estimated by mapping the total score to the corresponding risk level. To assess the predictive performance of the model, we conducted calibration curve analysis, decision curve analysis (DCA), and clinical impact evaluation, ensuring its accuracy and clinical applicability.

2.6 Gene set enrichment analysis for single genes

In this study, gene set enrichment analysis (GSEA) was performed to functionally annotate samples with varying expression levels of target genes. Samples were first stratified into high-expression and low-expression groups based on the median expression level of the target gene. The clusterProfiler package was utilized for the GSEA analysis, using the c5.go.Hs.symbols.gmt gene set file to identify biological processes significantly associated with the expression of the target gene. The log fold change (logFC) values between the two groups were calculated, and pathways with a p-value < 0.05 were considered significantly enriched. Finally, for each target gene, the top five significantly upregulated pathways were selected and visualized through enrichment plots, providing deeper insights into the underlying biological mechanisms.

2.7 Immunohistochemical procedure

Tissue sections were deparaffinized using an environmentally friendly dewaxing solution for 30 min and rehydrated in anhydrous ethanol for 15 min. Epitope retrieval was performed in 20× Tris-EDTA buffer (pH 8.0) using a microwave oven for 30 minutes. Non-specific background staining was blocked with 3% hydrogen peroxide and a protein blocking reagent for 25 and 30 min, respectively. The sections were then incubated overnight at 4 °C with the following primary antibodies and dilutions: FOS (1:300; Servicebio, Cat# GB11069), MCL1 (1:200; Servicebio, Cat# GB11696), and ANGPTL7 (1:300; Proteintech, Cat# 10396-1-AP). Signal amplification was carried out using HRP-conjugated secondary antibodies corresponding to the species of the primary antibodies, followed by incubation at room temperature for 50 min. Chromogen detection was performed using freshly prepared DAB solution. Hematoxylin was used for counterstaining, and tissue sections were dehydrated through a graded ethanol series (75%, 85%, 100%), each for 5 minutes. Finally, slides were cleared in xylene for 5 min and sealed with mounting medium.

2.8 Quantitative analysis of immunostaining

The immunostained slides were scanned using the Panoramic scanner (3DHISTECH Ltd., Budapest, Hungary) and subsequently analyzed with DensitoQuant software through the Panoramic Viewer platform. Positive signals were detected via automated color deconvolution, which differentiated pixel intensity levels — brown indicating positive immunoreactivity and blue serving as a negative counterstain. The proportion of positive cells was determined by dividing the number of positively stained cells by the total cell count across six separately annotated regions of orbital tissue (5, 9).

For each immunostained slide, six representative areas were selected separately from the orbital connective tissue and orbital adipose tissue (Supplementary Figure S1) as our previously studied (5, 9). All sections stained with the same antibody were analyzed under uniform parameter settings in the DensitoQuant software. The extent of positive staining was quantified based on the software's built-in algorithm. The average value across the six annotated regions was calculated to represent the protein expression level for each tissue type. Consistent application of analysis parameters across all samples ensured reproducibility and allowed for fast, automated, and operator-independent quantification. Statistical analyses were conducted using the Statistical Package for the Social Sciences. Independent t-tests were employed to compare differences between two groups. A *p*-value less than 0.05 was regarded as statistically significant. Data visualization and graph generation were carried out using Prism software.

3 Results

3.1 Demographic and clinical data

Demographic and clinical data are presented in Table 1.

3.2 Identification of oxidative stress-related DEGs associated with TED

To identify oxidative stress-related differentially expressed genes (DE-OSRGs) in TED, we first screened for DEGs using the threshold $\log2|FC| > 0.3$ and *p*-value < 0.05 as our previously studied (4), identifying a total of 1,631 DEGs. The volcano plot (Figure 1A) presents the overall distribution of these DEGs, highlighting significantly upregulated and downregulated genes between TED and control samples. Next, we intersected the identified DEGs with a predefined set of 458 OSRGs, resulting in

10.3389/fimmu.2025.1635712

TABLE 1 Demographic and clinical data.

Indicators	Active GO (n=6)	Inactive GO (n=6)	Control (n=10)
Age (year)	54 ± 5.3	33.2 ± 6.2	35.8 ± 15.3
Gender, female *N* (%)	3 (50)	6 (100)	7 (70)
CAS (point)	3.7 ± 0.5	0.3 ± 0.5	N/A
Duration (year)	0.6 ± 0.2	5.0 ± 3.1	N/A
Orbital irradiation ratio *N* (%)	0 (0)	0 (0)	N/A
Smoker	1 (17)	0 (0)	N/A
Drinker	0 (0)	0 (0)	N/A
Severe *N* (%)	6 (100)	0 (0)	N/A
Mild *N* (%)	0 (0)	6 (100)	N/A
Steroid therapy *N* (%)	6 (100)	6 (100)	N/A

Data are shown as mean ± standard deviation. CAS, clinical activity score; N, number; N/A, not available; Duration, duration of orbital disease.

53 DE-OSRGs. The Venn diagram (Figure 1B) illustrates this intersection process, showing the overlap between the oxidative stress-related gene set and the identified DEGs. To further explore the expression patterns of these 53 DE-OSRGs, we generated a heatmap (Figure 1C), which clearly differentiates TED and control groups based on gene expression profiles. This analysis helped identify potential oxidative stress-related biomarkers that may play a key role in TED pathogenesis.

3.3 Enrichment analysis of DE-OSRGs

To explore the potential biological functions and pathways associated with DE-OSRGs in TED, we conducted GO and KEGG pathway enrichment analyses. The GO enrichment analysis (Figure 2A) revealed the functional involvement of DE-OSRGs across biological processes (BP), cellular components (CC), and molecular functions (MF). In the BP category, genes were significantly enriched in cellular responses to oxidative stress, reactive oxygen species, and hydrogen peroxide, reinforcing the central role of oxidative stress in TED pathophysiology. In the CC category, enrichment in mitochondrial outer membrane, organelle outer membrane, and membrane microdomains highlights the critical role of mitochondria in TED progression and its potential association with oxidative damage. In the MF category, genes were significantly associated with antioxidant activity, peroxidase activity, and oxidoreductase activity (acting on NAD(P)H, quinones, or peroxides), suggesting that oxidative stress regulation and free radical scavenging mechanisms may be pivotal in TED development.

In the KEGG pathway analysis (Figure 2B), DE-OSRGs were significantly enriched in pathways such as chemical carcinogenesis—ROS, Toll-like receptor signaling, and the AGE-RAGE signaling pathway. These findings indicate a strong association between oxidative stress and inflammatory responses, metabolic dysregulation, and disease progression in TED. Additionally, the enrichment of pathways related to fluid shear stress and atherosclerosis as well as lipid metabolism and atherosclerosis suggests that vascular dysfunction and oxidative stress-induced endothelial damage may play a crucial role in TED pathogenesis.

3.4 Identification of five diagnostic OS-DEGs for TED

To identify key oxidative stress-related differentially expressed genes (OS-DEGs) for TED, we applied LASSO regression and random forest (RF) algorithms to screen significant genes that could effectively distinguish TED patients from healthy individuals (Figures 3A–D). The genes identified by these two machine learning methods were then intersected, yielding five diagnostic signature genes (DSGs), including *AKT1*, *APEX1*, *FOS*, *MCL1*, and *ANGPTL7* for further

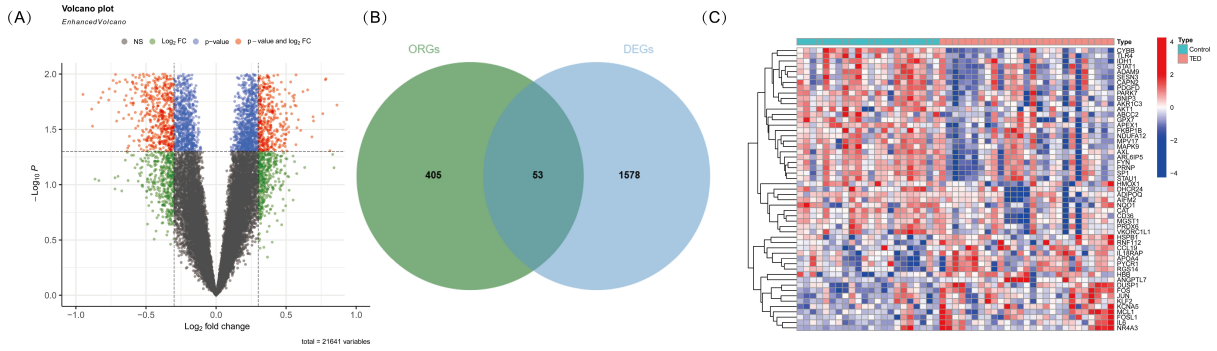

FIGURE 1
(A) Volcano plot illustrating differentially expressed genes (DEGs) in TED and control samples. The x-axis represents the log2 fold change, while the y-axis represents the -log10 *p*-value. Genes with significant upregulation (red). **(B)** Venn diagram showing the intersection of DEGs with oxidative stress-related genes. The overlapping region represents oxidative stress-related differentially expressed genes (DE-OSRGs). **(C)** Heatmap displaying the expression patterns of DE-OSRGs in TED and control samples. Each column represents an individual sample, while each row represents a gene. The color scale indicates relative expression levels, with red representing high expression and blue representing low expression.

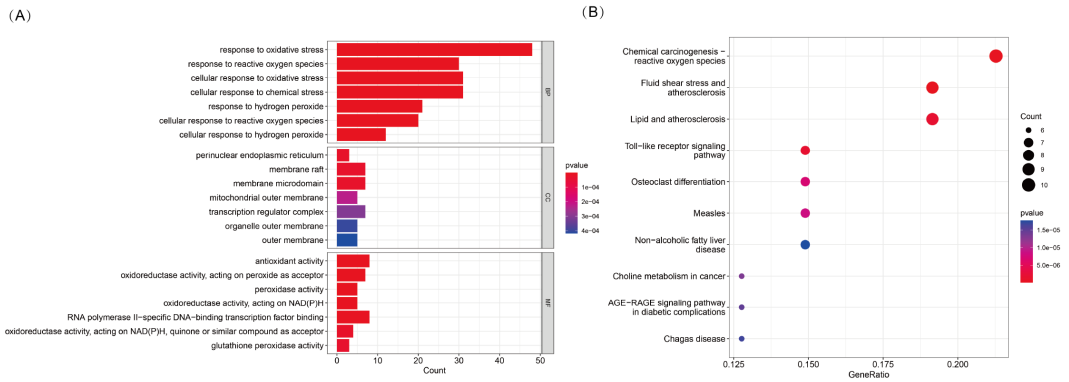

FIGURE 2
(A) KEGG pathway enrichment analysis of 53 DE-OSRGs, displayed as a bar plot. **(B)** GO enrichment analysis of 53 DE-OSRGs, visualized using a bubble plot, covering biological processes (BP), cellular components (CC), and molecular functions (MF).

analysis (Figures 4A, B). To assess the ability of these individual genes to differentiate TED from normal samples, ROC curves were constructed. The AUC values for each gene were as follows: *AKT1* (AUC = 0.813), *APEX1* (AUC = 0.816), *FOS* (AUC = 0.801), *MCL1* (AUC = 0.687), and *ANGPTL7* (AUC = 0.811), demonstrating their potential as diagnostic biomarkers for TED (Figure 4C). Furthermore, a diagnostic model incorporating these five DSGs was constructed and evaluated using ROC analysis, achieving an AUC of

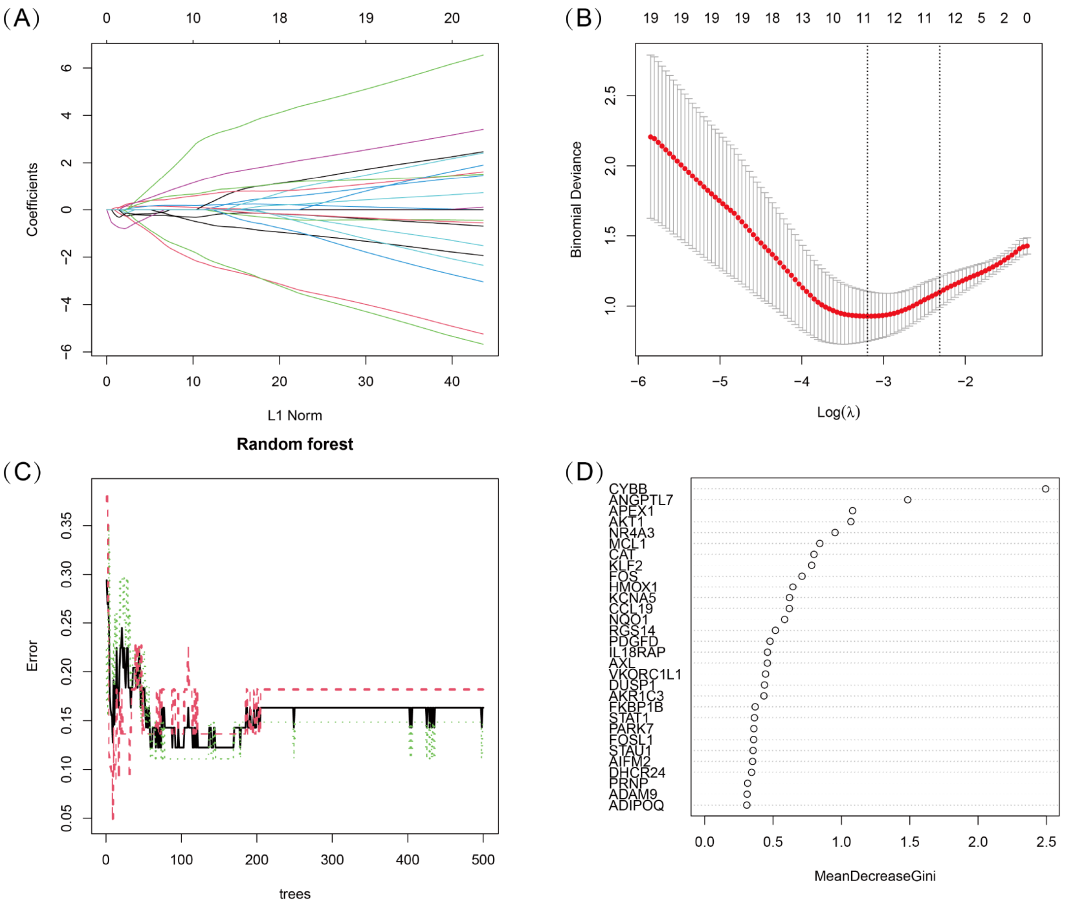

FIGURE 3
(A, B) LASSO logistic regression with 10-fold cross-validation was used to optimize the penalized parameter and identify key oxidative stress-related diagnostic genes for TED. **(C, D)** Random Forest (RF) algorithm was applied to evaluate the importance of oxidative stress-related candidate genes. Genes were ranked based on their Mean Decrease Gini Index, and the model's error rate was analyzed.

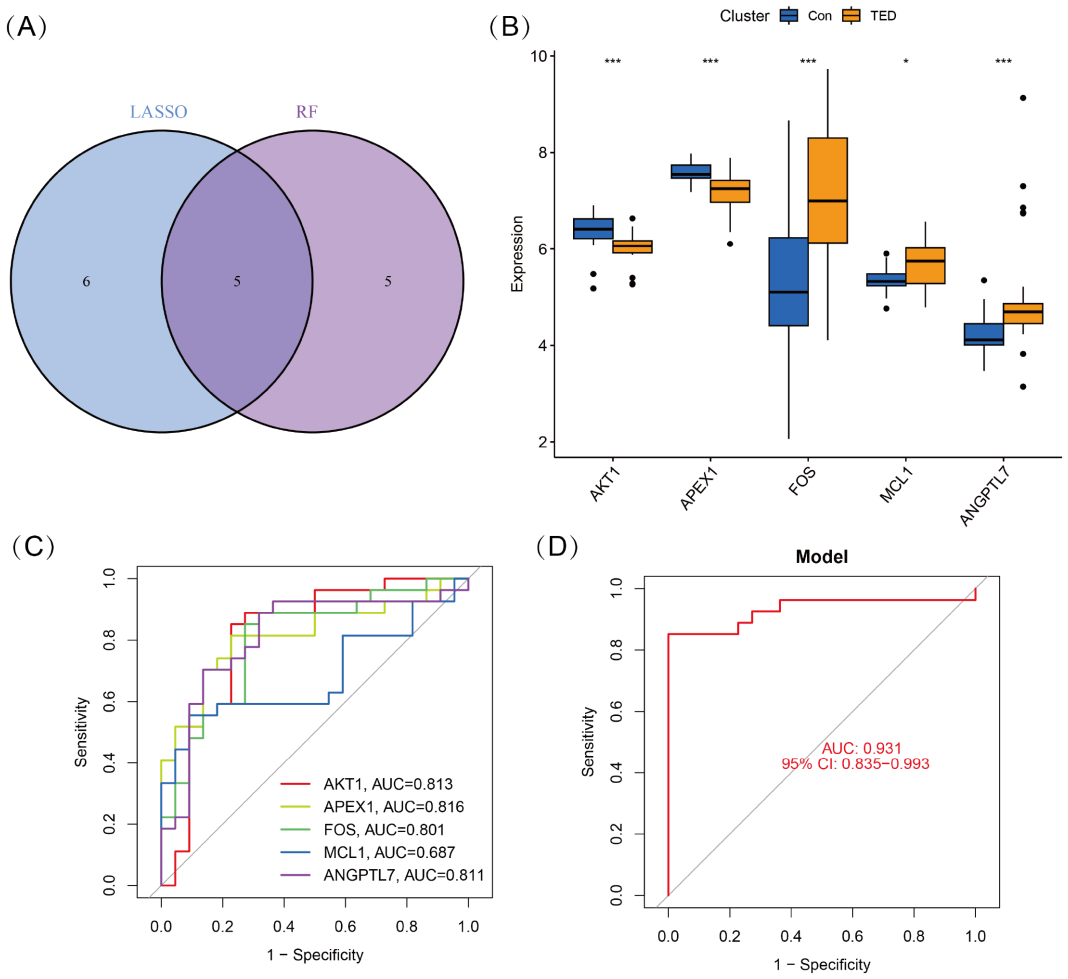

FIGURE 4
(A) Five DSGs were identified as oxidative stress-related diagnostic genes through the intersection of genes selected by LASSO and RF algorithms. **(B)** Boxplots displaying the expression levels of the five identified DSGs in TED and control groups. The expression differences between the two groups were statistically significant ($p < 0.05$), indicating their potential role in TED pathogenesis. **(C)** Receiver operating characteristic (ROC) curves for each DSG, illustrating their diagnostic performance. **(D)** The combined diagnostic model incorporating all five DSGs achieved an AUC of 0.931 (95% CI: 0.835–0.993), demonstrating its high predictive accuracy for distinguishing TED from control samples. Statistical significance: *P < 0.05; ***P < 0.001.

0.931 (95% CI: 0.835–0.993), indicating excellent diagnostic performance (Figure 4D). These findings suggest that these five oxidative stress-related genes could serve as potential biomarkers for TED diagnosis and provide insights into the role of oxidative stress in TED pathogenesis.

3.5 Construction of the nomogram model

We developed a nomogram model for five DSGs using logistic regression (Figure 5A). The predictive performance of the model was evaluated using calibration curves, which demonstrated a small deviation between the predicted and actual risk of TED (Figure 5B). As shown in Figure 5C, the results suggest that the nomogram model may assist in clinical decision-making by providing an individualized risk assessment for TED patients. Additionally, a clinical impact curve (Figure 5D) was generated based on DCA. The "number high risk" curve, representing individuals classified as high risk, closely aligns with the "number high risk with event" curve, indicating that the nomogram model has reasonable predictive accuracy and may be useful for risk stratification in TED.

3.6 Single-gene GSEA analysis of *MCL1*, *FOS*, and *ANGPTL7*

Single-gene GSEA analysis revealed that three oxidative stress-related genes, *viz.*, *MCL1*, *FOS*, and *ANGPTL7*, were significantly associated with multiple biological processes in TED (Figures 6A–C). *MCL1* was primarily enriched in RNA metabolism and regulatory processes, including establishment of RNA localization (GOBP_ESTABLISHMENT_OF_RNA_LOCALIZATION), regulation of RNA splicing (GOBP_REGULATION_OF_RNA_SPLICING), and RNA localization (GOBP_RNA_LOCALIZATION). Additionally, it was enriched in nuclear speck formation (GOCC_NUCLEAR_SPECK) and SMAD binding

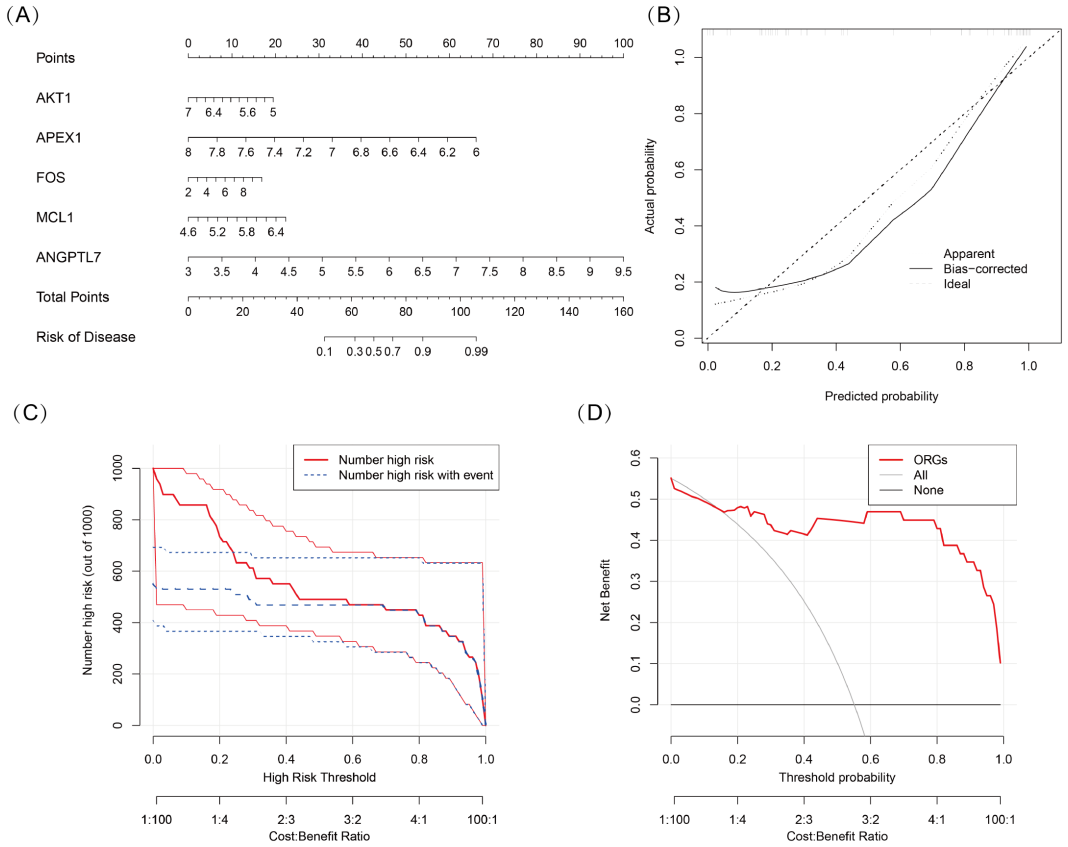

FIGURE 5
(A) Nomogram model based on five oxidative stress-related DSGs (AKT1, APEX1, FOS, MCL1, and ANGPTL7) for predicting the occurrence of TED. Each gene is assigned a score, and the total score corresponds to the predicted TED risk. **(B)** Calibration curve assessing the predictive accuracy of the nomogram model. The curve shows a close alignment between the predicted and actual TED risk, indicating good model reliability. **(C)** Clinical impact curve evaluating the potential impact of the model in a clinical setting. The "number high risk" curve closely follows the "number high risk with event" curve, suggesting that the model effectively identifies high-risk TED patients. **(D)** Decision curve analysis (DCA) demonstrating the clinical utility of the nomogram model. The net benefit curves suggest that the model may be useful for guiding clinical decision-making.

(GOMF_SMAD_BINDING), suggesting that *MCL1* plays a crucial role in RNA metabolism and gene expression regulation and may influence TED pathogenesis via the TGF-β/SMAD-mediated inflammation and fibrosis pathway.

FOS was significantly enriched in epithelial development and muscle function-related processes, including epidermis development (GOBP_EPIDERMIS_DEVELOPMENT), keratinocyte differentiation (GOBP_KERATINOCYTE_DIFFERENTIATION), muscle contraction (GOBP_MUSCLE_CONTRACTION), and muscle tissue development (GOBP_MUSCLE_TISSUE_DEVELOPMENT). These results suggest that *FOS* may play a pivotal role in eyelid barrier repair, fibroblast activation, and extraocular muscle remodeling, potentially contributing to extraocular muscle hypertrophy and motility dysfunction in TED.

ANGPTL7 was predominantly enriched in keratinization, ion channel function, and signaling receptor regulation-related processes, including keratinization (GOBP_KERATINIZATION), ion channel complex formation (GOCC_ION_CHANNEL_COMPLEX), and monatomic cation channel activity (GOMF_MONOATOMIC_CATION_CHANNEL_ACTIVITY). Additionally, it was associated with passive transmembrane transporter activity (GOMF_PASSIVE_TRANSMEMBRANE_TRANSPORTER_ACTIVITY) and signaling receptor regulator activity (GOMF_SIGNALING_RECEPTOR_REGULATOR_ACTIVITY). These findings indicate that *ANGPTL7* may be involved in orbital barrier function, intercellular communication, and inflammation signaling regulation, ultimately contributing to inflammation and fibrosis progression in TED.

3.7 FOS, MCL1, and ANGPTL7 are upregulated in orbital tissues of TED patients

Quantitative immunohistochemical analysis revealed that the expression levels of FOS ($P < 0.001$), MCL1 ($P = 0.003$), and ANGPTL7 ($P = 0.011$) were significantly higher in the orbital connective tissues of TED patients compared to controls (Figure 7, Table 2). Further subgroup analysis showed that FOS expression was significantly elevated in active TED compared to inactive TED ($p = 0.030$), whereas MCL1 and ANGPTL7 levels were

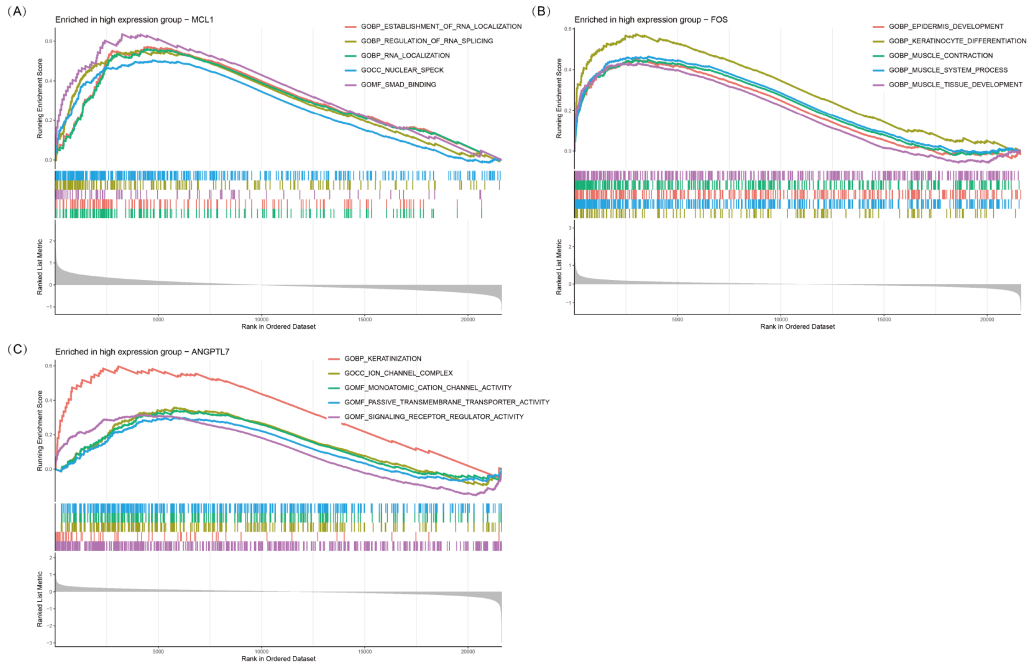

FIGURE 6
GSEA plots of GO terms enriched in the high-expression groups of *MCL1* **(A)**, *FOS* **(B)**, and *ANGPTL7* **(C)**. The top five significantly enriched GO pathways ($p < 0.05$) associated with high expression of each gene are shown.

similarly increased in both TED subgroups without statistically significant difference. In contrast, significant differences were not observed in the staining of orbital adipose tissues (Table 2).

4 Discussion

To the best of our knowledge, this study systematically explored for the first time the role of oxidative stress-related biomarkers in TED through transcriptomic sequencing, bioinformatics analysis, and immunohistochemical validation. The results highlight the significant role of oxidative stress-related molecules in the pathogenesis of TED and identify three key diagnostic oxidative stress-related genes (FOS, MCL1, and ANGPTL7) as potential biomarkers. These genes exhibited strong diagnostic capabilities, with a combined predictive model achieving an AUC of 0.931, indicating good discriminatory ability between TED patients and healthy controls. Notably, immunohistochemistry confirmed elevated expression levels of the three oxidative stress-related proteins (FOS, MCL1, and ANGPTL7) in orbital tissues from TED patients compared to healthy controls, suggesting their potential involvement in disease pathogenesis.

Further GO and KEGG enrichment analyses revealed potential molecular mechanisms underlying oxidative stress in the development of TED. GO analysis showed that DE-OSRGs were significantly enriched in cellular responses to oxidative stress, ROS metabolism, and mitochondrial dysfunction, emphasizing the role of mitochondrial oxidative damage in TED progression. KEGG analysis revealed that DE-OSRGs are involved in oxidative stress-related signaling pathways, including the Toll-like receptor pathway, AGE-RAGE signaling, and chemical carcinogenesis-ROS pathways, all of which are known to be associated with chronic inflammation and tissue remodeling. Additionally, the enrichment of DE-OSRGs in pathways related to vascular dysfunction and atherosclerosis suggests that endothelial oxidative stress may play a role in the orbital tissue remodeling and progression of TED.

FOS (c-Fos) is an immediate early gene that encodes the transcription factor c-Fos, which plays a crucial role in cell proliferation, differentiation, and survival. Fos can form an Activator Protein-1 (AP-1) complex with Jun family proteins to regulate the expression of specific genes (24). FOS is significantly upregulated in the extraocular muscles of TED patients, with RNA levels significantly higher than in healthy controls (22) and a transcriptomic and our bioinformatics analyses also revealed that FOS expression is elevated in TED (12, 23). In addition, the single-cell RNA sequencing study revealed increased expression of FOS in TED, primarily produced by lipofibroblasts with pro-adipogenic roles, which are involved in inflammation and oxidative stress (21). Our study further confirmed through immunohistochemistry that FOS protein expression is markedly elevated in TED patients. Furthermore, FOS was significantly upregulated in active TED tissues relative to inactive TED, with a statistically significant difference between the two groups.

In other disease models, FOS promotes oxidative stress, inflammation, and fibrosis through the AP-1 signaling pathway. For instance, in cardiac tissue, FOS induces ROS generation and myocardial fibrosis, and inhibiting FOS can significantly reduce inflammation (25). Furthermore, FOS is critically involved in Gli1

10.3389/fimmu.2025.1635712

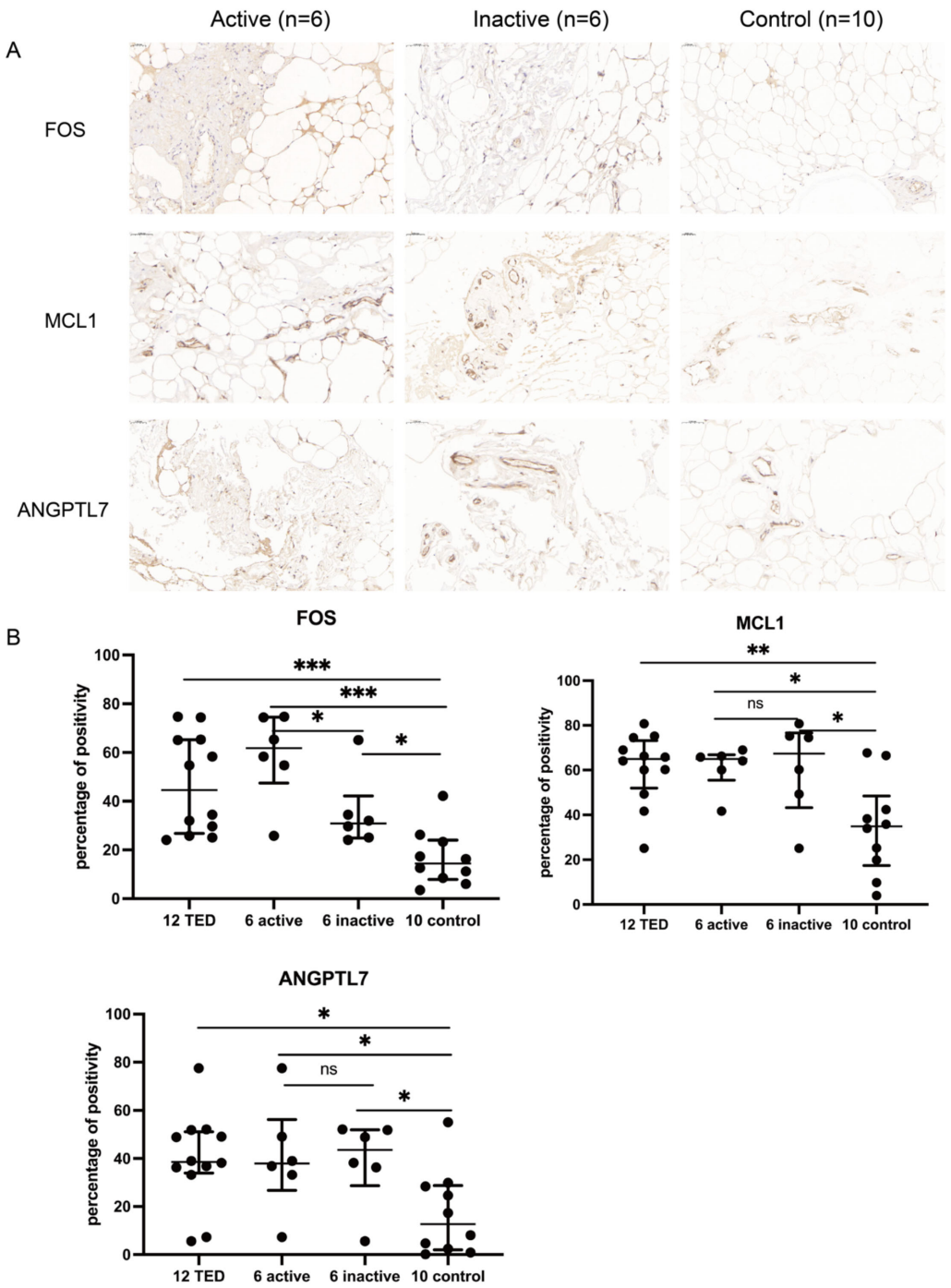

FIGURE 7
(A) Immunohistochemistry staining results of FOS, MCL1, and ANGPTL7 in the orbital connective/adipose tissue of patients with active (n=6) or inactive TED (n=6) and controls (n=10). Compared with normal controls, staining of FOS, MCL1, and ANGPTL7 was markedly increased in orbital tissues from TED patients. Notably, subgroup analysis showed significantly higher FOS expression in active TED compared to inactive TED, while no differential expression of MCL1 or ANGPTL7 was observed between the two TED subgroups. Bars represent 0.050 mm. **(B)** Percent positivity of FOS, MCL1, and ANGPTL7 in different orbital connective tissues from active TED (n=6), inactive TED (n=6), and control patients (n=10). Compared to controls, the percent positivity of FOS, MCL1, and ANGPTL7 was significantly higher in orbital connective tissues from patients with TED. FOS exhibited a high, moderate, and low percent positivity in the orbital tissues of active TED, inactive TED, and control groups, respectively. In contrast, MCL1 and ANGPTL7 showed similarly high expression in both active and inactive TED groups, with no significant difference between them, but both were significantly elevated compared to controls. *$p < 0.05$, **$p < 0.01$, ***$p < 0.001$; ns, not significant.

10.3389/fimmu.2025.1635712

TABLE 2 Statistical analysis of immunohistochemical staining of orbital connective tissue and orbital adipose tissue collected from patients with TED and control subjects.

Molecules	TED (n=12)	Control (n=10)	*p1*	Active TED (n=6)	Inactive TED (n=6)	*p2*	*p3*	*p4*
Orbital connective tissue								
FOS	47.6 ± 21.0	16.7± 11.5	*<0.001*	60.1 ± 18.9	35.1 ± 15.2	*<0.001*	*0.030*	*0.016*
MCL1	61.0 ± 15.7	34.4 ± 21.2	*0.003*	61.2 ± 10.0	60.8 ± 21.0	*0.012*	*0.974*	*0.029*
ANGPTL7	39.7 ± 19.5	17.1 ± 17.6	*0.011*	40.5 ± 22.9	38.8 ± 17.6	*0.037*	*0.889*	*0.032*
Orbital adipose tissue								
FOS	22.4 ± 20.8	14.6 ± 15.3	*0.342*	29.1 ± 27.6	15.6 ± 9.0	*0.195*	*0.298*	*0.875*
MCL1	32.9 ± 10.6	21.4 ± 17.3	*0.071*	33.0 ± 14.9	32.7 ± 5.1	*0.193*	*0.962*	*0.079*
ANGPTL7	18.0 ± 10.7	12.2 ± 10.0	*0.201*	14.7 ± 8.4	21.3 ± 12.4	*0.606*	*0.306*	*0.126*

Data are presented as mean ± standard deviation. Significance values: *P1*, TED vs control; *P2*, active TED vs control; *P3*, active vs inactive TED; *P4*, inactive TED vs control.

depletion-induced oxidative stress and apoptosis (26). Elevated expression of FOS aggravates oxidative damage and promotes cell death, thereby contributing to the progression of intervertebral disc degeneration. Notably, targeting FOS inhibition may serve as a potential therapeutic strategy to mitigate disc degeneration (26).

GSEA analysis indicates that FOS is primarily enriched in processes related to epithelial development and muscle function, suggesting that it may play a key role in eyelid barrier repair, fibroblast activation, and extraocular muscle remodeling, which are closely related to extraocular muscle hypertrophy and functional abnormalities in TED. A previous study demonstrated that members of the FOS family undergo transient upregulation in human skeletal muscle following exercise, indicating their pivotal role in modulating muscle-specific gene expression, promoting remodeling, and contributing to adaptation processes (27). Furthermore, reanalysis of the original data from our previous high-throughput proteomics study on TED indicated that FOS is engaged in numerous molecular pathways and participates in diverse biological processes (5). This further supports the idea that FOS might promote pathological remodeling of TED extraocular muscles through oxidative stress and inflammation regulation mechanisms.

MCL1 (Myeloid Cell Leukemia-1), a member of the BCL-2 family, primarily functions to inhibit apoptosis, maintain mitochondrial homeostasis, and regulate oxidative stress. It influences cell survival and adaptability by regulating ROS production, mitochondrial autophagy, and long-chain fatty acid oxidation (28–30). Multi-omics analyses, including single-cell RNA sequencing (21) and transcriptomic (20, 23), demonstrated upregulation of MCL1 in TED orbital tissues, a finding validated by immunohistochemistry. Importantly, the single-cell RNA sequencing study revealed increased expression of MCL1 in TED, primarily produced by lipofibroblasts and T cells, which may be involved in inflammation and oxidative stress (21).

MCL1 plays a critical role in maintaining mitochondrial function and energy metabolism balance (28–30). In the oxidative stress environment related to TED, MCL1 may influence OFs survival and adaptability by regulating mitochondrial function and ROS balance. Our GSEA analysis indicates that MCL1 is mainly enriched in RNA metabolism and SMAD signaling pathways, suggesting that it may impact TED's pathological progression through TGF-β/SMAD-mediated inflammation and fibrosis. This finding aligns with previous studies, where TGF-β signaling promotes fibroblast activation and drives TED-related orbital fibrosis (1, 7, 9, 10). Alternative splicing of MCL1 has been shown in the literature to generate isoforms with distinct functions, influencing the balance between apoptosis and cell survival (31), which may be closely related to oxidative stress-associated splicing abnormalities in TED. Although there is currently no direct experimental evidence demonstrating its interaction with SMAD proteins, given its anti-apoptotic properties and the pivotal role of the TGF-β/SMAD signaling pathway in TED fibrosis, it is speculated that MCL1 may promote inflammation and fibrosis progression by affecting fibroblast survival or modulating TGF-β/SMAD-driven transcriptional programs. Therefore, MCL1 may play an important role in maintaining mitochondrial homeostasis, regulating ROS, inflammation and fibrosis signaling, and could be further investigated as a potential target for oxidative stress regulation in TED.

ANGPTL7 (Angiopoietin-like 7) is a member of the angiopoietin-like protein family and plays a key role in angiogenesis, metabolic regulation, and inflammation (32). ANGPTL7 is highly expressed in ocular tissues (such as the trabecular meshwork), and is primarily involved in intraocular pressure regulation, extracellular matrix remodeling, and is closely associated with glaucoma, inflammation, and oxidative stress (33–35). ANGPTL7 is significantly upregulated in TNF-α-induced human umbilical vein endothelial cells and mediates TNF-α-induced oxidative stress, with its inhibition reducing ROS levels, increasing NO and eNOS expression, inhibiting NF-κB activation, and enhancing the Nrf-2/HO-1 antioxidant pathway, thereby alleviating oxidative stress damage (34). Additionally, in a glaucoma model, ANGPTL7 promotes oxidative stress and mitochondrial dysfunction, while inhibiting its expression can alleviate oxidative damage (35).

Analysis of original transcriptomic and bioinformatics data demonstrates a significant upregulation of ANGPTL7 in the orbital tissue and or orbital fibroblasts of TED patients (19, 23).

Consistently, our immunohistochemical investigation confirmed that ANGPTL7 protein expression is markedly increased in TED orbital connective tissues. The GSEA results show that ANGPTL7 is mainly enriched in processes related to keratinization, ion transport, and receptor signaling regulation, suggesting its potential role in orbital barrier function, inflammation modulation, and intercellular communication, which ultimately influences the inflammation and fibrosis progression in TED. ANGPTL7 has been reported to be associated with keratinization, as evidenced by its expression in corneal tissues and its role in preserving ocular surface integrity (36). Therefore, ANGPTL7 may play a key role in the orbital tissue remodeling and oxidative stress process related to TED and warrants further investigation into its specific regulatory mechanisms and potential therapeutic value.

In addition, although no direct interactions among FOS, MCL1, and ANGPTL7 have been reported in the current literature, all three molecules are critically involved in the regulation of oxidative stress. FOS promotes oxidative stress and induces ROS generation through the AP-1 signaling pathway (24–26), MCL1 regulates mitochondrial function and ROS balance (28–30), and ANGPTL7 promotes oxidative stress, mitochondrial dysfunction, and increased ROS levels (32–35). Given their respective roles in ROS production and mitochondrial dysfunction, it is plausible that these molecules may functionally interact in the oxidative stress-driven pathogenesis of TED. Further mechanistic studies are needed to elucidate their potential crosstalk.

The clinical significance and potential therapeutic value of these findings are noteworthy. Previous studies have demonstrated the pivotal role of oxidative stress in TED, leading to the consideration of antioxidant therapies as potential interventions (12, 13, 15, 16). For example, selenium supplementation has been shown to alleviate TED symptoms and reduce oxidative damage (1, 2, 13). The three diagnostic oxidative stress-related proteins identified in this study could serve as potential targets for precision treatment. Furthermore, the nomogram model developed in this study shows strong predictive capability in clinical assessments, suggesting that integrating these biomarkers into clinical detection could aid in early screening and risk stratification, and dynamic monitoring of treatment responses in TED patients. For the secreted protein ANGPTL7, its level in peripheral blood or tear fluid can be investigated to evaluate potential correlations with inflammation or disease severity in TED. In contrast, for the nuclear protein FOS and the intracellular protein MCL1, their roles in the oxidative processes of TED can be elucidated through further cellular experiments.

However, this study has several limitations. Firstly, the analysis is based on transcriptomic data, which does not comprehensively capture the effects of epigenetic modifications and post-transcriptional regulation on oxidative stress mechanisms in TED. As miRNA-mediated post-transcriptional regulation, DNA methylation, and histone modifications play important roles in inflammatory and autoimmune diseases, future studies could further explore how these mechanisms influence the expression and function of oxidative stress-related biomarkers in TED. Secondly, although immunohistochemical validation was performed, further functional studies (e.g., gene knockdown or overexpression in orbital fibroblasts) are required to clarify their specific roles in the oxidative stress–related progression of TED. Additionally, the dataset used in this study was derived from a relatively small cohort, and future studies with larger, multi-center cohorts are required to validate the reliability of these findings and further assess their clinical applicability.

In conclusion, this study identified three oxidative stress-related proteins (FOS, MCL1, and ANGPTL7) as potential biomarkers for TED and explored their roles in its pathogenesis. Bioinformatics analysis and immunohistochemical validation demonstrated involvement of these genes in oxidative stress pathways and may contribute to TED progression. The nomogram model demonstrated strong diagnostic potential, suggesting its value for early screening and risk assessment in TED. Further research is needed to validate these findings and assess their clinical applicability.

Data availability statement

Publicly available datasets were analyzed in this study. This data can be found here: http://www.ncbi.nlm.nih.gov/geo/, accession number GSE58331.

Ethics statement

The studies involving humans were approved by Shunde Hospital, Southern Medical University, Foshan Shunde First People's Hospital (Ethics Approval No. KYLS20240815). The studies were conducted in accordance with the local legislation and institutional requirements. The participants provided their written informed consent to participate in this study.

Author contributions

YH: Writing – original draft, Writing – review & editing. QM: Writing – review & editing, Writing – original draft. ZL: Writing – review & editing. DL: Writing – review & editing. AH: Writing – review & editing. YZ: Writing – review & editing. DY: Writing – review & editing. CS: Writing – review & editing. GY: Writing – review & editing. SF: Writing – review & editing. LL: Writing – review & editing. YW: Writing – review & editing. TE: Writing – review & editing. JS: Writing – review & editing.

Funding

The author(s) declare that financial support was received for the research and/or publication of this article. This research was funded by the National Natural Science Foundation of China (82400917, 82170800), Guangdong Basic and Applied Basic Research Foundation (2024A1515012893), Hunan University of Chinese

Medicine-Hospital Collaborative Research Grant Program (2024XYLH249), the Natural Science Foundation of Changsha (kq2208498), and the Hunan Provincial Natural Science Foundation of China (25JJ81107).

Acknowledgments

We are deeply grateful to Rosenbaum JT and their teams for their generous support with orbital tissue collection and sample coordination from TED patients and healthy individuals.

Conflict of interest

The authors declare that the research was conducted in the absence of any commercial or financial relationships that could be construed as a potential conflict of interest.

The author(s) declared that they were an editorial board member of Frontiers, at the time of submission. This had no impact on the peer review process and the final decision.

Generative AI statement

The author(s) declare that no Generative AI was used in the creation of this manuscript.

Publisher's note

All claims expressed in this article are solely those of the authors and do not necessarily represent those of their affiliated organizations, or those of the publisher, the editors and the reviewers. Any product that may be evaluated in this article, or claim that may be made by its manufacturer, is not guaranteed or endorsed by the publisher.

Supplementary material

The Supplementary Material for this article can be found online at: https://www.frontiersin.org/articles/10.3389/fimmu.2025.1635712/full#supplementary-material

References

1. Lee ACH, Kahaly GJ. Pathophysiology of thyroid-associated orbitopathy. *Best Pract Res Clin Endocrinol Metab*. (2023) 37:101620. doi: 10.1016/j.beem.2022.101620

2. Bartalena L, Kahaly GJ, Baldeschi L, Dayan CM, Eckstein A, Marcocci C, et al. The 2021 European Group on Graves' orbitopathy (EUGOGO) clinical practice guidelines for the medical management of Graves' orbitopathy. *Eur J Endocrinol*. (2021) 185:G43–67. doi: 10.1530/EJE-21-0479

3. Ma Q, Hai Y, Duan Y, Yu G, Song C, Huang S, et al. Inflammatory profiling and immune cell infiltration in dysthyroid optic neuropathy: insights from bulk RNA sequencing. *Front Immunol*. (2025) 16:1550694. doi: 10.3389/fimmu.2025.1550694

4. Ma Q, Hai Y, Shen J. Signatures of six autophagy-related genes as diagnostic markers of thyroid-associated ophthalmopathy and their correlation with immune infiltration. *Immun Inflammation Dis*. (2024) 12:e70093. doi: 10.1002/iid3.70093

5. Hai Y, Ma Q, Fang S, Bahramimehr F, Song C, Duan Y, et al. High-throughput proteomics and immunohistochemistry of orbital connective tissue in graves' Orbitopathy. *J Clin Endocrinol Metab*. (2025). doi: 10.1210/clinem/dgaf299

6. Hai YP, Lee ACH, Chen K, Kahaly GJ. Traditional Chinese medicine in thyroid-associated orbitopathy. *J Endocrinol Invest*. (2023) 46:1103–13. doi: 10.1007/s40618-023-02024-4

7. Dik WA, Virakul S, van Steensel L. Current perspectives on the role of orbital fibroblasts in the pathogenesis of Graves' ophthalmopathy. *Exp Eye Res*. (2016) 142:83–91. doi: 10.1016/j.exer.2015.02.007

8. Bahn RS. Graves' ophthalmopathy. *N Engl J Med*. (2010) 362:726–38. doi: 10.1056/NEJMra0905750

9. Hai YP, Saeed MEM, Ponto KA, Elflein HM, Lee ACH, Fang S, et al. A multicenter, single-blind, case-control, immunohistochemical study of orbital tissue in thyroid eye disease. *Thyroid*. (2022) 32:1547–58. doi: 10.1089/thy.2022.0173

10. Hai YP, Lee ACH, Frommer L, Diana T, Kahaly GJ. Immunohistochemical analysis of human orbital tissue in Graves' orbitopathy. *J Endocrinol Invest*. (2020) 43:123–37. doi: 10.1007/s40618-019-01116-4

11. Smith TJ, Hegedus L. Graves' Disease. *N Engl J Med*. (2016) 375:1552–65. doi: 10.1056/NEJMra1510030

12. Ma C, Li H, Lu S, Li X. Thyroid-associated ophthalmopathy: the role of oxidative stress. *Front Endocrinol (Lausanne)*. (2024) 15:1400869. doi: 10.3389/fendo.2024.1400869

13. Buonfiglio F, Ponto KA, Pfeiffer N, Kahaly GJ, Gericke A. Redox mechanisms in autoimmune thyroid eye disease. *Autoimmun Rev*. (2024) 23:103534. doi: 10.1016/j.autrev.2024.103534

14. Hou TY, Wu SB, Kau HC, Tsai CC. The role of oxidative stress and therapeutic potential of antioxidants in graves' Ophthalmopathy. *Biomedicines*. (2021) 9:1871. doi: 10.3390/biomedicines9121871

15. Lanzolla G, Marcocci C, Marino M. Antioxidant therapy in graves' Orbitopathy. *Front Endocrinol (Lausanne)*. (2020) 11:608733. doi: 10.3389/fendo.2020.608733

16. Lanzolla G, Marcocci C, Marino M. Oxidative stress in graves disease and graves orbitopathy. *Eur Thyroid J*. (2020) 9:40–50. doi: 10.1159/000509615

17. Zhang H, Zhou Y, Yu B, Deng Y, Wang Y, Fang S, et al. Multi-omics approaches to discover biomarkers of thyroid eye disease: A systematic review. *Int J Biol Sci*. (2024) 20:6038–55. doi: 10.7150/ijbs.103977

18. Marino M, Rotondo Dottore G, Menconi F, Comi S, Cosentino G, Rocchi R, et al. Role of genetics and epigenetics in Graves' orbitopathy. *Eur Thyroid J*. (2024) 13:e240179. doi: 10.1530/ETJ-24-0179

19. He S, Nie H, Yin X, Zhong Z. Identification of key extracellular proteins as the potential biomarkers in thyroid eye disease. *PloS One*. (2025) 20:e0322415. doi: 10.1371/journal.pone.0322415

20. Wang Y, Liu Y, Cai J, Zong T, Zhang Z, Xie T, et al. Differentially expressed genes in orbital adipose/connective tissue of thyroid-associated orbitopathy. *PeerJ*. (2023) 11:e16569. doi: 10.7717/peerj.16569

21. Li Z, Wang M, Tan J, Zhu L, Zeng P, Chen X, et al. Single-cell RNA sequencing depicts the local cell landscape in thyroid-associated ophthalmopathy. *Cell Rep Med*. (2022) 3:100699. doi: 10.1016/j.xcrm.2022.100699

22. Romero-Kusabara IL, Filho JV, Scalissi NM, Melo KC, Demartino G, Longui CA, et al. Distinct inflammatory gene expression in extraocular muscle and fat from patients with Graves' orbitopathy. *Eur J Endocrinol*. (2017) 176:481–8. doi: 10.1530/EJE-16-0945

23. Yang S, Wang X, Xiao W, Xu Z, Ye H, Sha X, et al. Dihydroartemisinin exerts antifibrotic and anti-inflammatory effects in graves' Ophthalmopathy by targeting orbital fibroblasts. *Front Endocrinol (Lausanne)*. (2022) 13:891922. doi: 10.3389/fendo.2022.891922

24. Yao H, Wu Y, Zhong Y, Huang C, Guo Z, Jin Y, et al. Role of c-Fos in DNA damage repair. *J Cell Physiol*. (2024) 239:e31216. doi: 10.1002/jcp.31216

25. Palomer X, Roman-Azcona MS, Pizarro-Delgado J, Planavila A, Villarroya F, Valenzuela-Alcaraz B, et al. SIRT3-mediated inhibition of FOS through histone H3 deacetylation prevents cardiac fibrosis and inflammation. *Signal Transduct Target Ther*. (2020) 5:14. doi: 10.1038/s41392-020-0114-1

26. Liu L, Zhang Y, Fu J, Ai X, Long D, Leng X, et al. Gli1 depletion induces oxidative stress and apoptosis of nucleus pulposus cells via Fos in intervertebral disc degeneration. *J Orthop Translat*. (2023) 40:116–31. doi: 10.1016/j.jot.2023.05.008

27. Puntschart A, Wey E, Jostarndt K, Vogt M, Wittwer M, Widmer HR, et al. Expression of fos and jun genes in human skeletal muscle after exercise. *Am J Physiol*. (1998) 274:C129–37. doi: 10.1152/ajpcell.1998.274.1.C129

28. Wright T, Turnis ME, Grace CR, Li X, Brakefield LA, Wang YD, et al. Anti-apoptotic MCL-1 promotes long-chain fatty acid oxidation through interaction with ACSL1. *Mol Cell*. (2024) 84:1338–1353 e8. doi: 10.1016/j.molcel.2024.02.035

29. Vier J, Hacker G, Kirschnek S. Contribution of A1 to macrophage survival in cooperation with MCL-1 and BCL-X(L) in a murine cell model of myeloid differentiation. *Cell Death Dis*. (2024) 15:677. doi: 10.1038/s41419-024-07064-z

30. Sancho M, Leiva D, Lucendo E, Orzaez M. Understanding MCL1: from cellular function and regulation to pharmacological inhibition. *FEBS J*. (2022) 289:6209–34. doi: 10.1111/febs.16136

31. Tyson-Capper A, Gautrey H. Regulation of Mcl-1 alternative splicing by hnRNP F, H1 and K in breast cancer cells. *RNA Biol*. (2018) 15:1448–57. doi: 10.1080/15476286.2018.1551692

32. Brown SF, Nguyen H, Mzyk P, De Ieso ML, Unser AM, Brown I, et al. ANGPTL7 and its role in IOP and glaucoma. *Invest Ophthalmol Vis Sci*. (2024) 65:22. doi: 10.1167/iovs.65.3.22

33. Praveen K, Patel GC, Gurski L, Ayer AH, Persaud T, Still MD, et al. ANGPTL7, a therapeutic target for increased intraocular pressure and glaucoma. *Commun Biol*. (2022) 5:1051. doi: 10.1038/s42003-022-03932-6

34. Li J, Liang T, Wang Y, Gan Y, Kou Z, Zhang Y, et al. Angiopoietin-like protein 7 mediates TNF-alpha-induced adhesion and oxidative stress in human umbilical vein epithelial cell. *Gen Physiol Biophys*. (2020) 39:285–92. doi: 10.4149/gpb_2019062

35. Cao T, Wang J, Wu Y, Wang L, Zhang H. Antiglaucoma potential of beta-glucogallin is mediated by modulating mitochondrial responses in experimentally induced glaucoma. *Neuroimmunomodulation*. (2020) 27:142–51. doi: 10.1159/000512992

36. Toyono T, Usui T, Yokoo S, Taketani Y, Nakagawa S, Kuroda M, et al. Angiopoietin-like 7 is an anti-angiogenic protein required to prevent vascularization of the cornea. *PloS One*. (2015) 10:e0116838. doi: 10.1371/journal.pone.0116838

frontiers | Frontiers in Immunology

TYPE Original Research
PUBLISHED 02 September 2025
DOI 10.3389/fimmu.2025.1605739

Check for updates

OPEN ACCESS

EDITED BY
Alessandro Antonelli,
University of Pisa, Italy

REVIEWED BY
Priyanka Choudhury,
Medical College of Wisconsin, United States
Manuel Rojas,
University of California, Davis, United States

*CORRESPONDENCE
Guoxi Jin
jinguoxi@bbmu.edu.cn

RECEIVED 03 April 2025
ACCEPTED 12 August 2025
PUBLISHED 02 September 2025

CITATION
Zhang L, Zhou X, Cheng T, Wang Q, Pei X, Yu L and Jin G (2025) Dysregulated tryptophan metabolism: driving T cell subsets and PI3K-Akt pathway alterations in Hashimoto's thyroiditis. *Front. Immunol.* 16:1605739. doi: 10.3389/fimmu.2025.1605739

COPYRIGHT
© 2025 Zhang, Zhou, Cheng, Wang, Pei, Yu and Jin. This is an open-access article distributed under the terms of the Creative Commons Attribution License (CC BY). The use, distribution or reproduction in other forums is permitted, provided the original author(s) and the copyright owner(s) are credited and that the original publication in this journal is cited, in accordance with accepted academic practice. No use, distribution or reproduction is permitted which does not comply with these terms.

Dysregulated tryptophan metabolism: driving T cell subsets and PI3K-Akt pathway alterations in Hashimoto's thyroiditis

Lijian Zhang, Xinrui Zhou, Tingwei Cheng, Qiong Wang, Xiaoyan Pei, Lei Yu and Guoxi Jin*

Department of Endocrinology, The First Affiliated Hospital of Bengbu Medical University, Bengbu, Anhui, China

Purpose: This study explored the role of tryptophan (Trp) metabolism in Hashimoto's thyroiditis (HT) pathogenesis using clinical samples and animal models, given the unclear mechanisms and limited treatments of HT.
Methods: Clinically, serum Trp, lactic acid, and alanine levels in 10 HT patients and 10 healthy controls were measured by ELISA. In animal experiments, female C57BL/6 mice were divided into Con, HT, HT+T (Trp supplemented), and HT+I (Trp metabolism inhibitor IDO1/TDO-IN-4 treated) groups. After inducing autoimmune thyroiditis, various tests were conducted, including ELISA for inflammation factors, HE staining for thyroid pathology, flow cytometry for T cell subsets, RNA-seq for gene expression, Western Blotting for PI3K-Akt pathway proteins, and CIBERSORT for immune cell analysis.
Results: HT patients had significantly lower serum Trp levels. The HT group showed thyroid damage and increased inflammation factors. Trp supplementation alleviated thyroid damage and reduced inflammation factors, while the inhibitor worsened them. Trp also regulated T cell subsets and immune cell environment. RNA-seq and Western Blotting indicated Trp's impact on immune response and PI3K-Akt pathway.
Conclusion: Trp metabolism abnormality is associated with HT. Trp supplementation can alleviate HT progression by regulating T cell function and the PI3K-Akt pathway, while inhibiting Trp metabolism exacerbates it. This suggests Trp metabolism's potential as a therapeutic target for HT.

KEYWORDS

tryptophan metabolism, Hashimoto's thyroiditis, T cell subsets, PI3K-Akt signaling pathway, immune

Highlights

This study demonstrates significantly decreased serum Trp levels in HT patients, suggesting an association between Trp metabolic abnormalities and HT pathogenesis. By showing Trp's impact on inflammation, T cell subsets, and the PI3K-Akt pathway in animal models, it uncovers a novel mechanistic link. These findings highlight Trp supplementation as a potential therapeutic strategy to mitigate HT progression, offering a new avenue for managing this common endocrine disorder. The mechanistic insights into Trp's immunomodulatory effects advance understanding of HT and may inform future treatments targeting metabolic pathways in autoimmune endocrine diseases.

1 Introduction

The treatment of HT currently relies primarily on levothyroxine replacement therapy. However, even after thyroid function is controlled, patients may still experience persistent extrathyroidal symptoms, such as constipation, diarrhea, edema, anxiety, and hair loss (1, 2). Although studies have confirmed that both cellular and humoral immunity are involved in HT, the specific mechanisms remain to be further clarified. A comprehensive approach using diverse research methods is needed to conduct in-depth exploration and analysis of the immune mechanisms of HT (3).

To explore the potential impact of amino acid metabolism abnormalities in HT, we used metabolomics to analyze serum samples from HT patients and healthy individuals. We identified Trp, lactic acid, and alanine as differential metabolites for further study. Trp, an essential amino acid, is metabolized through three main pathways: the kynurenine (Kyn) pathway, the 5-hydroxytryptamine (5-HT) pathway, and the indole-3-pyruvate (I3P) pathway (4–6). The Kyn pathway, accounting for 95% of Trp metabolism, occurs in immune and epithelial cells and is initiated by Indoleamine 2,3-dioxygenase (IDO) or Tryptophan 2,3-dioxygenase (TDO) (6). In this metabolic pathway, IDO1 initiates the conversion of Trp to Kyn, which acts as an Aryl Hydrocarbon Receptor (AhR) ligand; activated AhR translocates to the nucleus and up-regulates IDO1 in dendritic cells (DCs), establishing an IDO1–Kyn–AhR positive-feedback loop. This loop confers DCs with an immunosuppressive phenotype that drives regulatory T cells (Tregs) differentiation, suppresses effector T cells, and maintains self-tolerance (5, 7). A Study reports that HT patients exhibit fewer IDO^+ plasmacytoid dendritic cells (pDCs), elevated serum Trp, a reduced Kyn/Trp ratio, and heightened *in vitro* IFN-α responses (8). These data implicate Trp-metabolic imbalance in HT pathogenesis via immune-homeostasis disruption; dissecting this mechanism may inform new diagnostics and therapeutics.

In HT patients, the helper T cells (Th)/Tregs balance is markedly skewed toward Th1, Th2, and Th17 subsets (9, 10). Within $CD4^+$ T cells, AhR is absent in Th1 and Th2, high in Th17, and low in Tregs (11). The Kyn pathway bidirectionally regulates the Th17/Tregs balance via AhR-dependent mechanisms, inhibiting Th17 polarization and promoting Tregs differentiation (12–14), positioning it as a potential therapeutic target in HT.

Collectively, Trp metabolism appears to modulate the balance of Th-cell subsets and thereby participate in the pathogenesis of HT. Although the precise mechanisms operating in HT remain incompletely elucidated, significant advances in understanding Trp metabolism have already been achieved in other disorders—including COVID-19, glioma, and inflammation-induced depression—where it has demonstrated promising clinical translational potential (6). Consequently, investigating the interplay between Trp metabolism and HT is scientifically imperative and may open new avenues for immune-metabolic reprogramming–based targeted therapies.

2 Materials and methods

2.1 Patient population

Ten female HT patients and ten healthy women (25–65 years) were recruited from the Endocrinology Outpatient Clinic of the First Affiliated Hospital of Bengbu Medical University between June and December 2023.

Inclusion criteria:

- HT patients: ① Positive serum TPOAb (>60 IU/mL) or TgAb (>60 IU/mL); ② Thyroid ultrasound revealing heterogeneous parenchymal texture, with or without hypoechoic areas or thyroid nodules.
- Control group: ① Normal thyroid function and thyroid autoantibodies; ② No thyroid diseases or autoimmune diseases; ③ Absence of infectious disease and normal hepatic, renal, glycemic, and lipid profiles.

Exclusion criteria:

- Use of medications affecting thyroid function or presence of other thyroid disorders;
- Coexisting autoimmune disease or malignancy;
- current treatment with immunosuppressive or glucocorticoid agents;
- active infection, inflammation, recent trauma, or other causes.

After confirming eligibility, we obtained written informed consent and collected peripheral blood for serum isolation. Demographic and clinical data were extracted from medical records, anonymized, and stored under secure identifiers to safeguard participant privacy.

2.2 Experimental animals

Female C57BL/6 mice (6–8 weeks old) were purchased from GemPharmatech Co., Ltd. (Nanjing, China).

2.3 Reagents and instruments

Main reagents and instruments are in Supplementary Materials.

2.4 Animal model

The establishment of the HT mice model in this study was performed as described in the reference (PMID: 34124070) (15).

Female C57BL/6 mice (6–8 weeks old) were used to establish the model. After 1-week adaptive feeding, they were randomly divided into 4 groups (n=10 per group):

- Control (Con) group: From the second week onward, the mice received 0.05% NaCl as drinking water. On the same week, they were given multiple subcutaneous injections of PBS at the dorsal, abdominal, and cervical regions, and daily intraperitoneal PBS injections were initiated and continued until the end of the experiment. Two weeks later, multi-site subcutaneous PBS injections were repeated.
- HT model (HT) group: Beginning in the second week, the mice received 0.05% NaI as drinking water and were administered the first series of subcutaneous injections of porcine thyroglobulin (200 μg per mouse) emulsified in complete Freund's adjuvant (CFA) at multiple sites on the dorsal, abdominal, and cervical regions. Concurrently, daily intraperitoneal injections of PBS were initiated and maintained until the end of the experiment. Two weeks later, a second set of subcutaneous injections of porcine thyroglobulin (200 μg per mouse) emulsified in incomplete Freund's adjuvant (IFA) was given at multiple sites.
- HT + Trp (HT+T) group: The regimen was identical to that of the HT group, except that the daily intraperitoneal injection was replaced with 20 mg/kg Trp (dissolved in PBS).
- HT + Kyn-pathway inhibitor (HT+I) group: The regimen was identical to that of the HT group, except that the daily intraperitoneal PBS injection was replaced with 20 mg/kg of the Kyn-pathway inhibitor (IDO1/TDO-IN-4) administered every other day. IDO1/TDO-IN-4 is a potent dual inhibitor of both IDO1 and TDO and therefore functions as an effective Kyn-pathway inhibitor (16). A stock solution of 20 mg/ml was prepared in DMSO and diluted ten-fold with 20% (w/v) SBE-β-CD in normal saline immediately before use.

Four weeks after the final immunization challenge, the mice were euthanized, and serum, thyroid glands, and spleens were collected for subsequent analyses.

2.5 Experimental assays

2.5.1 ELISA

Serum concentrations of Trp, lactic acid, and alanine in human samples were quantified with commercially available kits. Mouse serum levels of TPOAb, TgAb, IL-17, and Trp were likewise determined using standardized ELISA kits.

2.5.2 HE staining

Thyroid specimens were fixed in 4% paraformaldehyde, processed through graded ethanol, embedded in paraffin, sectioned at 4 μm, and stained with hematoxylin and eosin for histopathological evaluation.

2.5.3 Flow cytometry

Splenic lymphocytes were isolated and surface-stained for CD4 and CD25, followed by intracellular staining for IL-4, IFN-γ, and IL-17A using fluorochrome-conjugated antibodies. Data were acquired on a flow cytometer and analyzed to quantify the expression profiles of the indicated markers.

2.5.4 RNA-seq

Total RNA sequencing was performed by Biomarker Technologies Co., Ltd. (Beijing, China). RNA quality assessment, library construction, library quality control, and Illumina sequencing were executed according to the company's standardized pipelines. Raw reads were uploaded to the BMKCloud platform (www.biocloud.net) for adapter/quality trimming, alignment to the reference genome, transcript quantification, and differential expression analysis, ensuring a comprehensive and reproducible data interpretation.

2.5.5 Western blot

Frozen thyroid tissues stored at −80°C were lysed in RIPA buffer containing protease and phosphatase inhibitors. Protein concentrations were determined by BCA assay, and 30 μg of total protein per sample was separated by SDS-PAGE and transferred to PVDF membranes. After blocking, membranes were probed overnight at 4°C with primary antibodies against mTOR, p-mTOR (Ser2448), PI3K, p-PI3K (Tyr607), Akt, and p-Akt (Ser473). GAPDH was used as the loading control. HRP-conjugated secondary antibodies were applied, and signals were detected by enhanced chemiluminescence. Band intensities were quantified to assess the effect of Trp metabolism on PI3K-Akt pathway activity.

2.6 Immune cell landscape analysis

Immune-cell composition in tissue samples was determined with the CIBERSORT algorithm implemented in R. The signature gene matrix (LM22) was obtained from the original publication (PMID 25822800) (17). The CIBERSORT R package was installed and run to extract immune cell proportion data and perform visualization. The Wilcoxon rank-sum test was used to compare the immune cell proportions under different conditions. $P<0.05$ was considered statistically significant. After running the CIBERSORT R package, estimated immune-cell proportions were extracted and visualized. Between-group differences were evaluated by the Wilcoxon rank-sum test; $P < 0.05$ was considered statistically significant.

10.3389/fimmu.2025.1605739

TABLE 1 Clinical characteristics of patients with hashimoto's thyroiditis (HT group) and healthy individuals (HC group).

Clinical variable	HC (n=10)	HT (n=10)	*P*
Age (year)	45.00 ± 9.83	49.60 ± 9.97	0.313
TT3 (nmol/L)	1.73 ± 0.35	2.55 ± 4.01	0.532
TT4 (nmol/L)	98.37 ± 11.57	66.41 ± 30.07	0.009*
FT3 (pmol/L)	5.09 ± 0.37	4.20 ± 0.87	0.008*
FT4 (pmol/L)	15.70 ± 1.47	12.66 ± 3.56	0.023*
TPOAb (U/mL)	47.90 (41.08, 55.75)	> 1300.00 (548.2, > 1300.00)	< 0.001*
TgAb (U/mL)	15.90 (<15.00, 19.30)	235.30 (93.48, > 500.00)	0.002*
TSH (mIU/L)	2.92 (2.14, 4.34)	4.66 (2.62, 34.02)	0.162
urine iodine (ug/L)	135.70 ± 71.66	198 ± 105.01	0.139
Duration of disease (year)	–	6.65 (0, 11.33)	–
Medication status			
- Stable levothyroxine ≥ 6 wk	–	6 (60%)	–
- Treatment-naïve newly diagnosed	–	3 (30%)	–
- ≥4-wk wash-out	–	1 (10%)	–

Normally distributed data are expressed as mean ± SD, and intergroup comparisons were performed using Student's t-test. Non-normally distributed data are presented as Mdn (Q1, Q3), and the Mann-Whitney U test was employed for intergroup comparisons, *indicating P<0.05.

2.7 Statistics analysis

All statistical analyses were performed with SPSS 21.0 (IBM Corp., Armonk, NY, USA). Normally distributed data are expressed as mean ± standard deviation (M ± SD) or mean ± standard error of the mean (M ± SEM); differences between two groups were evaluated by two-sample t-test, and those among multiple groups by one-way or multi-way ANOVA followed by appropriate *post-hoc* tests. Non-normally distributed data are presented as median and interquartile range [Mdn (Q1, Q3)] and analyzed with the Mann-Whitney U or Wilcoxon rank-sum test. Statistical significance was set at a two-tailed $P < 0.05$.

3 Result

3.1 Alterations of serum metabolites in patients with HT

The baseline demographic and clinical characteristics of the enrolled participants are summarized in Table 1. Serum samples from both groups were analyzed using the ELISA method, and the results are presented in Figure 1. ELISA quantification revealed significantly lower concentrations of serum Trp ($P < 0.0001$), lactate ($P < 0.01$), and alanine ($P < 0.001$) in the HT group compared with the healthy controls (HC group), with Trp exhibiting the greatest decrease (Figure 1).

3.2 Impact of Trp on inflammation in HT mice

Following model induction, thyroid tissues were collected and subjected to HE staining to observe the morphological structure of thyroid follicular cells and lymphocyte infiltration (Figure 2A). In the Con group, follicular cells were neatly arranged, follicles were round or oval, and staining was light red, with no inflammatory cell infiltration. In contrast, the HT group exhibited extensive follicular destruction, marked atrophy or loss of follicles, and dense perifollicular lymphocytic infiltrates. Trp supplementation (HT+T group) partially preserved follicular integrity and reduced inflammatory infiltrates compared with HT group. Conversely, blockade of the Kyn pathway (HT+I group) exacerbated follicular

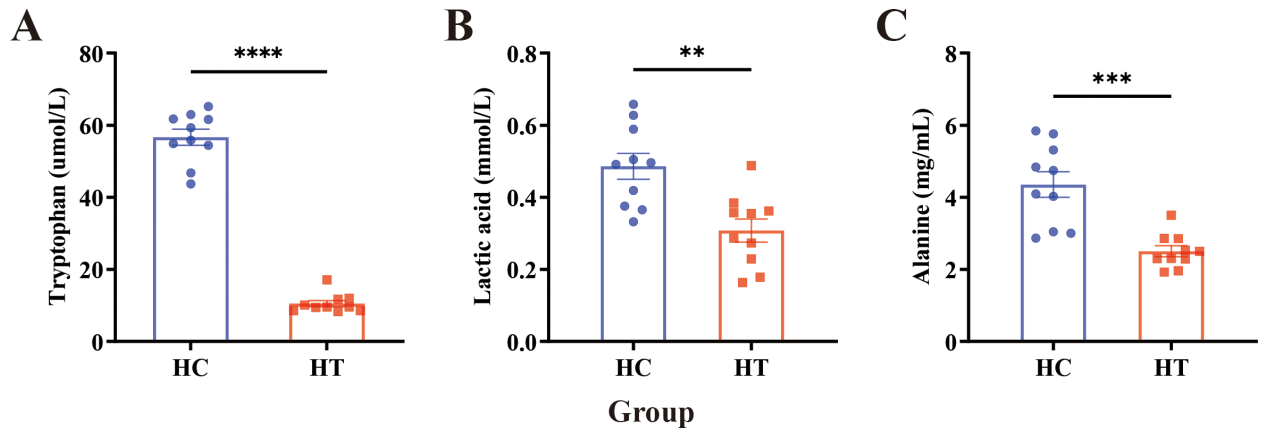

FIGURE 1
ELISA detection of serum metabolite levels in HT patients (HT) and healthy individuals (HC). **(A–C)** Serum concentrations of **(A)** tryptophan, **(B)** lactate, and **(C)** alanine in healthy controls and HT patients. Data are expressed as mean ± SEM; n = 10 per group. Statistical comparisons were performed using an unpaired two-tailed Student's t-test. Asterisks denote significant differences: **P<0.01, ***P<0.001, ****P<0.0001.

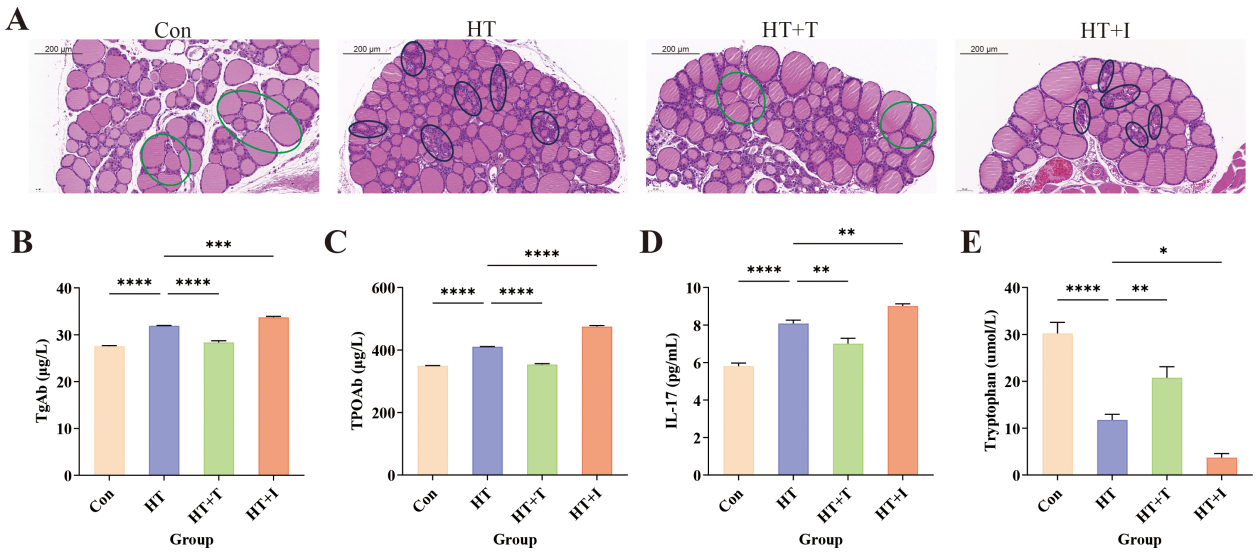

FIGURE 2
Effects of Trp on HT mice. **(A)** Representative HE-stained thyroid sections (original magnification, ×20) showing follicular architecture and lymphocytic infiltration; representative areas of inflammatory cell infiltration in the HT and HT+I groups are circled in black, while representative healthy regions in the Con and HT+T groups are circled in green. Three independent mice per group were analyzed. **(B–E)** Serum levels of **(B)** thyroglobulin antibody (TgAb), **(C)** thyroid peroxidase antibody (TPOAb), **(D)** interleukin-17 (IL-17), and **(E)** Trp determined by ELISA. For ELISA, three biologically independent samples were assayed in triplicate; data are presented as mean ± SEM. Statistical comparisons were performed using two-way ANOVA. Asterisks denote significant differences: *P<0.05, **P<0.01, ***P<0.001, ****P<0.0001.

atrophy and amplified lymphocytic infiltration beyond the severity observed in the HT group.

Serum levels of TgAb (Figure 2B), TPOAb (Figure 2C), and IL-17 (Figure 2D) were quantified by ELISA. Relative to Con group, HT group exhibited marked elevations of TgAb, TPOAb, and IL-17 (all $P < 0.0001$). Compared with the HT group, the levels of TgAb ($P<0.0001$), TPOAb ($P<0.0001$), and IL-17 ($P<0.01$) in the HT+T group were significantly decreased, while the levels of TgAb ($P<0.001$), TPOAb ($P<0.0001$), and IL-17 ($P<0.01$) in the HT+I group were significantly increased. These findings indicate that Trp mitigates HT-associated inflammation, whereas blockade of the Kyn pathway aggravates it, implicating this pathway in the suppression of thyroid autoimmunity.

Furthermore, the Trp levels in serum were quantified by ELISA (Figure 2E). Relative to the Con group, the Trp levels in the HT group were significantly decreased ($P<0.0001$). Compared with the HT group, the Trp levels in the HT+T group were significantly increased ($P<0.01$), and the Trp levels in the HT+I group were significantly decreased ($P<0.05$).

3.3 Impact of Trp on $CD4^+$ T cell subsets in HT mice

The proportion of $CD4^+$ T cell subpopulations in mouse spleens was measured using flow cytometry to explore the impact of Trp on immune cell function. Relative to the Con group, the proportions of Th1 (Figure 3A), Th2 (Figure 3B), and Th17 (Figure 3C) cells in the HT group were significantly increased (all $P < 0.00001$), while the proportion of $CD4^+CD25^+$ cells (Figure 3D) was significantly decreased ($P < 0.00001$). Compared with the HT group, Trp administration (HT+T group) reversed these changes, the proportions of Th1 ($P < 0.00001$), Th2 ($P < 0.00001$), and Th17 ($P < 0.0001$) cells were significantly decreased, and the proportion of CD4+CD25+ cells was significantly increased ($P < 0.0001$). In contrast, the proportions of Th1 ($P < 0.00001$), Th2 ($P < 0.00001$), and Th17 ($P < 0.0001$) in the HT+I group were significantly increased, and the proportion of CD4+CD25+ cells was significantly decreased ($P < 0.0001$). Although CD25 is also expressed by activated conventional T cells, $CD4^+CD25^+$ cells are highly enriched for $Foxp3^+$ Tregs and can therefore serve as a surrogate Treg population in the absence of intracellular Foxp3 staining (18).

3.4 Impact of Trp on the transcriptome of thyroid tissue in HT mice

To systematically evaluate the influence of Trp supplementation on the thyroid transcriptome of HT mice, bulk RNA-sequencing was conducted. Differential expression analysis ($|\log_2$ fold change$| \geq 2$ and FDR < 0.05) revealed that Trp supplementation profoundly remodeled the thyroid transcriptome (Figure 4A). Compared with the HT group, the HT+T group exhibited 880 differentially expressed genes (DEGs) (322 up-regulated, 558 down-regulated) and the HT+I group exhibited 290 DEGs (191 up-regulated, 99 down-regulated). In the comparison between HT+T and HT+I groups, the HT+I group displayed 1,024 DEGs relative to HT+T group (659 up-regulated, 365 down-regulated).

Gene Ontology (GO) enrichment analysis (Figure 4B) revealed significant differences in gene expression between the HT and HT +T groups, particularly in immune response, where more than 30

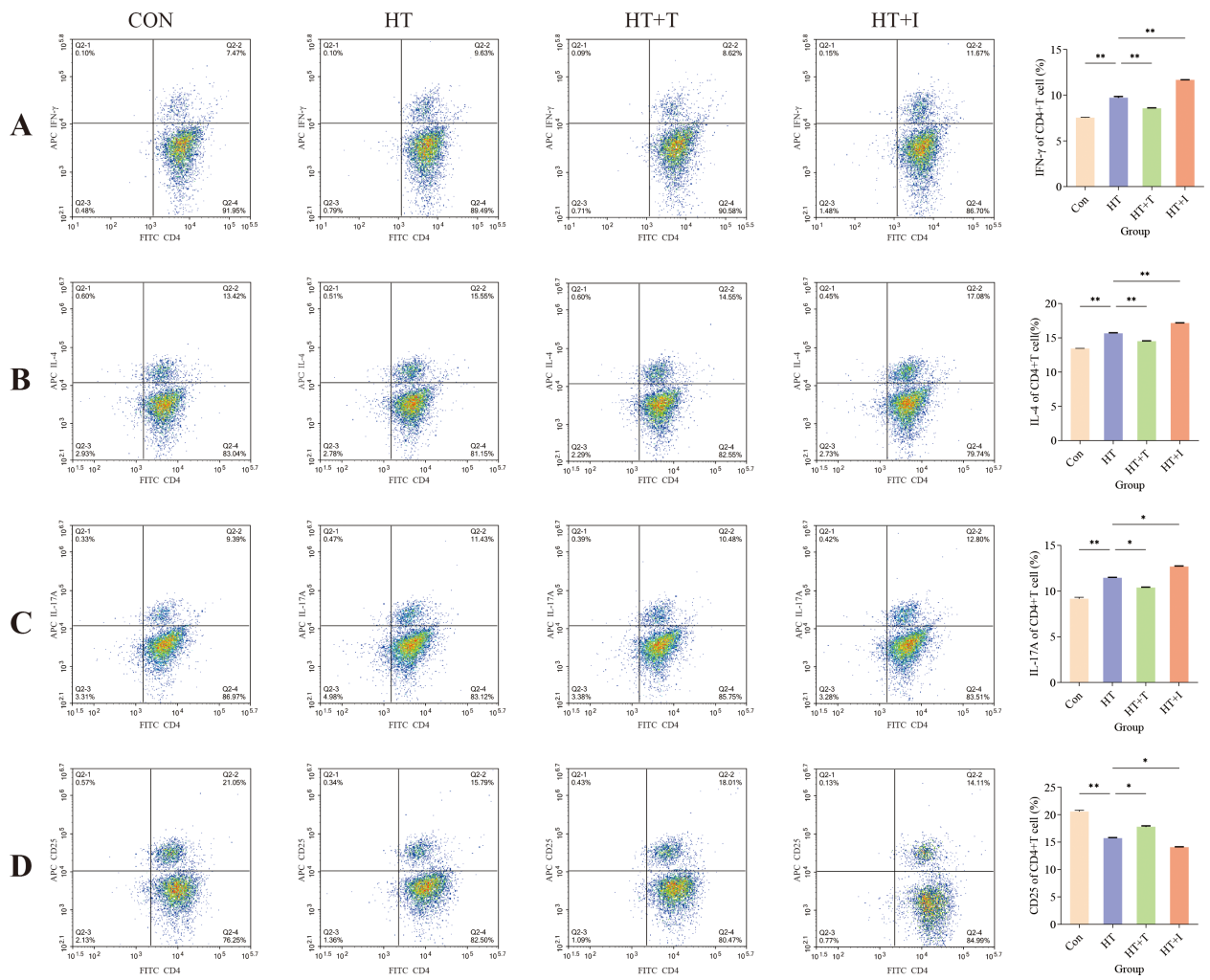

FIGURE 3
Flow cytometric analysis of splenic T cell subsets. **(A)** Percentage of IFN-γ$^+$CD4$^+$ (Th1) cells. **(B)** Percentage of IL-4$^+$CD4$^+$ (Th2) cells. **(C)** Percentage of IL-17A$^+$CD4$^+$ (Th17) cells. **(D)** Percentage of CD25$^+$CD4$^+$ cells. For each group, splenocytes from three biologically independent mice were stained and analyzed in triplicate. Data are presented as mean ± SEM. Comparisons among groups were performed using two-way ANOVA. Asterisks denote significant differences: * P<0.0001, ** P<0.00001.

genes were significantly enriched (q-value<0.01). Kyoto Encyclopedia of Genes and Genomes (KEGG) pathway analysis (Figure 4C) showed significant enrichment of the PI3K-Akt signaling pathway in both groups, with 23 DEGs involved (5.64% of total DEGs). Consistently, Gene Set Enrichment Analysis (GSEA) (Figure 4D) confirmed significant enrichment of immune response (NES = -1.782, P = 0.0013) and the PI3K–Akt signaling pathway (NES = -1.939, P = 0.0012).

Transcriptomic data were subjected to KEGG functional annotation, and pathways containing ≥10 DEGs were retained for comparative analysis. The intersection of such pathways across treatment groups is depicted in Figure 4E. The most prominently represented categories included hematopoietic cell lineage, Yersinia infection, Epstein-Barr virus infection, the Ras signaling pathway, and the PI3K-Akt signaling pathway, each exhibiting substantial enrichment of DEGs. Because the PI3K-Akt signaling pathway is pivotal in orchestrating immune cell maturation, differentiation, trafficking, and survival (19), it was selected for subsequent mechanistic investigation and experimental validation.

3.5 Effects of Trp the PI3K–Akt signaling pathway in HT mice

To determine whether Trp influences HT through the PI3K-Akt axis, the thyroid levels of key pathway proteins (mTOR, p-mTOR, PI3K, p-PI3K, Akt, and p-Akt) were quantified by western blotting (Figure 5A). Densitometric analysis with ImageJ revealed that total mTOR (Figure 5B), PI3K (Figure 5D), and Akt (Figure 5F) remained unchanged in both HT+T and HT+I groups relative to HT group (P > 0.05). In contrast, the expression levels of p-PI3K (Figure 5E) and p-Akt (Figure 5G) proteins were decreased in the HT+T group (P<0.05 and P<0.001, respectively), while there was no significant difference in the expression of p-mTOR (Figure 5C)

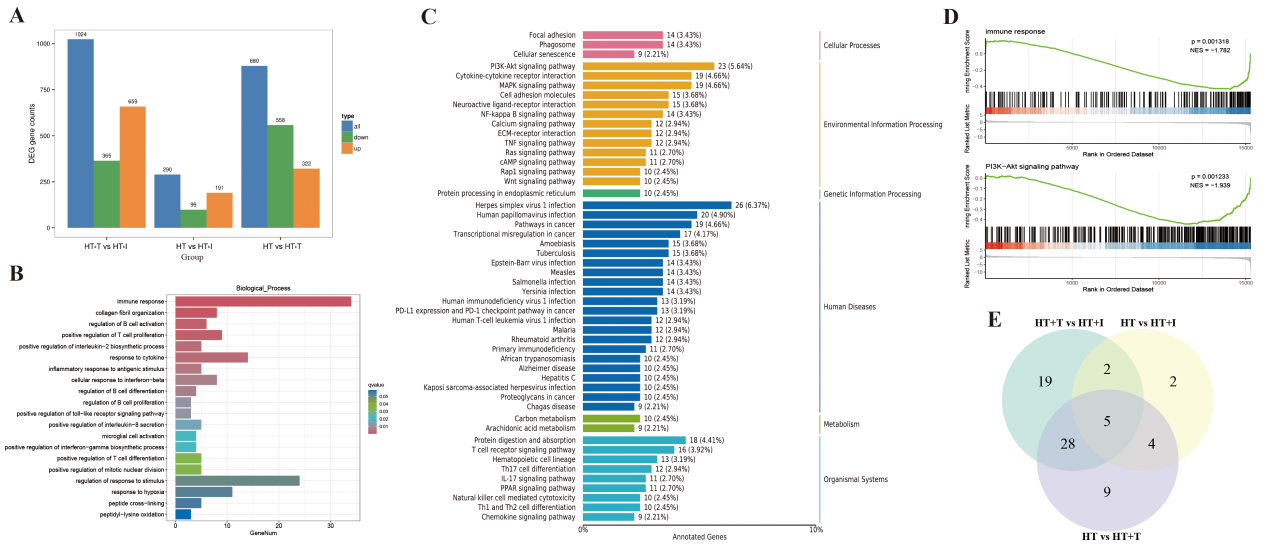

FIGURE 4
Transcriptional analysis of thyroid tissue from HT mice. Each group (HT, HT+T and HT+I) comprised three biologically independent samples. **(A)** Bar chart of DEGs. **(B)** GO biological process enrichment bar chart of DEGs between HT and HT+T groups. **(C)** KEGG pathway classification plot of DEGs between HT and HT+T groups. **(D)** GSEA analysis plot between HT and HT+T groups. **(E)** Venn diagram of intersecting genes.

protein (P>0.05). Conversely, the expression levels of p-mTOR (P<0.05) and p-Akt (P<0.01) proteins were increased in the HT+I group, and there was no significant difference in the expression of p-PI3K protein (P>0.05).

3.6 Trp modulates thyroidal immune cell infiltration in HT mice

To explore the regulatory effect of Trp on immune cells in the thyroid of HT mice, the CIBERSORT algorithm was used to analyze the RNA-seq dataset of thyroid tissue to characterize the composition of immune cell subpopulations (Figure 6A). Comparison of immune cell distribution between the HT and HT +T groups revealed significant differences (Figure 6B). Relative to HT group, HT + T group significantly reduced the abundance of $CD8^+$ T cells ($P < 0.05$) and, to a lesser extent, resting memory $CD4^+$ T cells ($P < 0.05$), with $CD8^+$ T cells exhibiting the greatest fold change.

4 Discussion

4.1 The relationship between HT and Trp metabolism

Trp catabolism is increasingly recognized as a pivotal contributor to autoimmune pathogenesis. A convergent finding across multiple studies is an elevated serum Kyn/Trp ratio in patients with diverse autoimmune diseases (ADs) and in corresponding animal models, a parameter that correlates with disease activity and supports its utility as a biomarker (20–25). Building on these observations, our study further investigated the changes in serum metabolite levels in HT patients through clinical sample analysis. Consistent with previous reports, circulating Trp concentrations were markedly reduced in HT patients (Figure 1A). In the HT animal model, we found that Trp supplementation could alleviate the progression of HT, while treatment with IDO1/TDO-IN-4 worsened it (Figure 2). Collectively, these data implicate dysregulated Trp metabolism in HT pathogenesis and establish modulation of Trp availability as a rational therapeutic strategy for this disorder.

Figure 2E shows that, relative to the HT group, administration of IDO1/TDO-IN-4 produced a paradoxical decrease in serum Trp. In theory, inhibition of the rate-limiting enzymes IDO1 and TDO should reduce Trp flux through the Kyn pathway and thereby elevate circulating Trp. The unexpected decline can be reconciled by two non-mutually exclusive explanations: (i) the inhibitor failed to achieve an effective concentration or activity *in vivo*, or (ii) the blocked Trp was diverted to alternative Trp metabolic branches rather than the Kyn pathway. A recent study in a murine depression model supports the latter possibility. The TDO inhibitor paeoniflorin increased hepatic 5-HT/Trp ratios while decreasing Kyn/Trp ratios, indicating that TDO blockade diverts Trp away from the Kyn pathway and toward 5-HT synthesis (26). This unexpected finding indicates that the *in vivo* effects of IDO/TDO inhibition on the global Trp metabolic network are more intricate than current theoretical frameworks suggest, and a comprehensive elucidation of the underlying molecular mechanisms and metabolic fluxes is urgently warranted in future investigations.

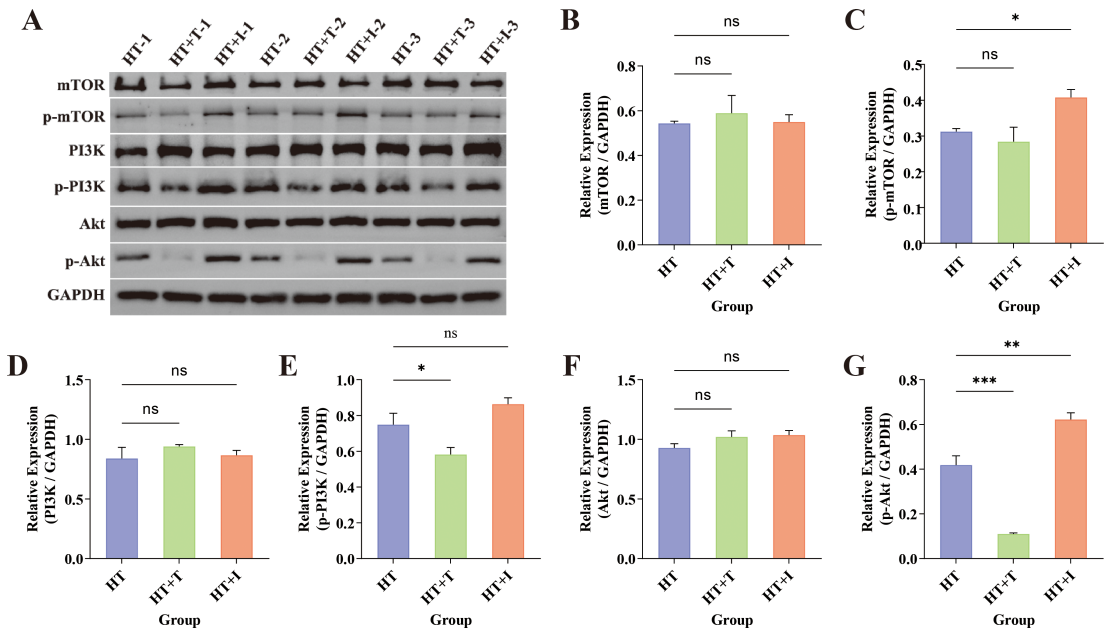

FIGURE 5
Western Blot analysis of thyroid tissue from HT mice. **(A)** Representative immunoblots for mTOR (~250–289 kDa), p-mTOR (~289 kDa), PI3K (~126 kDa), p-PI3K (~80 kDa), Akt (~60 kDa), and p-Akt (~60 kDa) across the three experimental groups (n = 3 biologically independent samples per group). GAPDH served as the loading control. **(B–G)** Quantification of relative protein expression normalized to GAPDH for **(B)** mTOR, **(C)** p-mTOR, **(D)** PI3K, **(E)** p-PI3K, **(F)** Akt, and **(G)** p-Akt. Data are presented as mean ± SEM. Inter-group comparisons were performed using one-way ANOVA. ns, not significant; *P<0.05; **P<0.01; ***P<0.001.

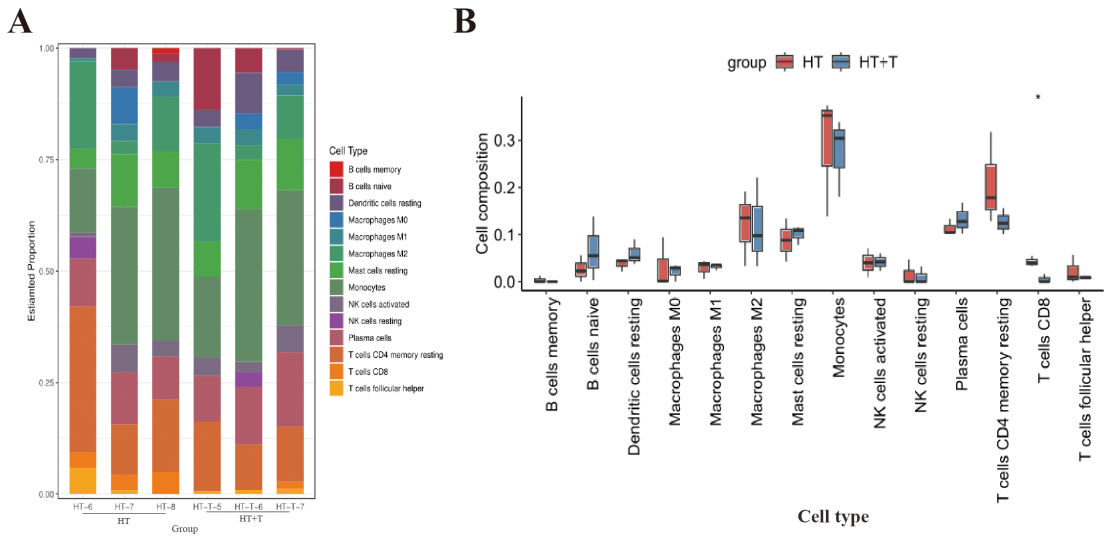

FIGURE 6
Immune cell landscape in thyroid tissue of HT versus HT+T mice. **(A)** Relative abundances of 22 immune cell subsets estimated by CIBERSORT based on bulk RNA-seq profiles (n = 3 per group). **(B)** Comparative analysis of immune cell proportions between HT and HT+T groups. Data are shown as box-and-whisker plots (median ± interquartile range). Statistical significance was determined by the two-tailed Wilcoxon rank-sum test; *P<0.05.

4.2 Effects of Trp metabolism on T cell subsets

Lymphocytic infiltration constitutes the hallmark histopathological feature of HT (27). Nevertheless, the precise mechanisms underlying its action in HT remain to be fully elucidated. In HT, the infiltrate is composed predominantly of T lymphocytes, whose sustained targeting of thyroid follicular cells results in parenchymal destruction, progressive fibrosis, and, ultimately, glandular atrophy with attendant hypothyroidism (28). Given the immunoregulatory potency of Trp metabolites (29, 30), we hypothesized that altered Trp catabolism may mechanistically link metabolic dysregulation to immune cell-mediated thyroid injury.

Trp degradation products critically modulate immune cell function. DCs, as key antigen-presenting cells, can modulate the activation and differentiation of various Th subsets by sensing environmental signals (31). In an inflammatory setting, increased IDO1 expression in DCs promotes Tregs differentiation, suppresses effector T cell activity, and enhances the Kyn pathway, which breaks down Trp into Kyn (32). Kyn binds to and activates the AhR, a transcription factor involved in regulating immune cell differentiation and function. AhR activation up-regulates its own expression and increases IDO1 expression in DCs, forming a positive feedback loop (IDO1-Kyn-AhR) that enhances the immunosuppressive capacity of DCs (33, 34). Trp metabolism also regulates immune responses through AhR-independent pathways. The breakdown of Trp can influence the metabolism of immune cells by activating GCN2 kinase and other pathways. This indirectly regulates the activity of the mTOR pathway, thereby limiting T cell proliferation (30). Notably, this metabolic-immune crosstalk may simultaneously reshape the distribution of immune cells in both the peripheral circulation and the target tissue.

Previous study utilizing transcription-factor profiling of peripheral-blood mononuclear cells (PBMCs) have demonstrated that the homeostatic balance among Th1/Tregs, Th2/Tregs, and Th17/Tregs subsets is disrupted in HT patients, manifesting as a predominance of Th1, Th2, and Th17 cell populations (9). Meta-analyses of newly diagnosed autoimmune thyroiditis cohorts and corresponding animal models further converge on an elevated Th17/Tregs ratio as a cardinal immunological signature of the disease (35–38). Consistent with these observations, flow-cytometric quantification of splenic $CD4^+$ T cell subsets in our murine model revealed that Trp partially restored the Th/Tregs balance (Figure 3). Collectively, these suggest that Trp may improve the immune microenvironment by modulating peripheral $CD4^+$ T cell subset homeostasis.

To characterize the immune landscape of thyroid tissue, we applied the CIBERSORT algorithm, which deconvolves bulk RNA-seq data into the relative abundance of 22 distinct immune cell subsets and has become a widely accepted tool for quantifying tissue-infiltrating leukocytes in immune-mediated diseases (17). CIBERSORT analysis demonstrated that Trp markedly decreased the relative abundance of $CD8^+$ T cells and resting memory $CD4^+$ T cells in the thyroid of HT mice, with $CD8^+$ T cells showing the most pronounced decrease (Figure 6).

$CD8^+$ T cells are potent drivers of autoimmunity; they inflict tissue injury through direct cytotoxicity and pro-inflammatory cytokine release (39). In HT, the activation and expansion of $CD8^+$ T cells can exacerbate the immune response, triggering an attack on thyroid tissue (3). Moreover, both TPOAb and TgAb antigens are recognized by $CD8^+$ T cells and participate in thyroid tissue destruction (40). With respect to the interplay between tryptophan metabolism and $CD8^+$ T cells, studies have demonstrated that tryptophan insufficiency activates GCN2 kinase, which in turn suppresses mTORC1 signaling. This triggers an energetic reprogramming of $CD8^+$ T cells—most notably a marked reduction in glycolysis—that ultimately impedes their clonal expansion and acquisition of effector functions (41). The results suggest that Trp could contribute to the pathogenesis of HT through its regulation of $CD8^+$ T cell infiltration and function within the thyroid. Overall, Trp may attenuate HT progression via a dual mechanism: rebalancing peripheral T cell subsets while simultaneously restraining tissue-infiltrating lymphocytes.

4.3 Trp metabolism and the PI3K-Akt signaling pathway

HT, a prevalent autoimmune endocrine disorder, involves aberrant regulation of multiple signaling pathways (42, 43). Here, transcriptomic profiling of murine thyroid tissue showed that Trp exerts its therapeutic effects in HT chiefly by modulating immune-related biological processes (Figure 4B). According to the KEGG pathway enrichment analysis, the PI3K-Akt signaling pathway showed significant enrichment in the environmental information processing category (Figure 4C).

During T cell development, the PI3K-Akt signaling pathway is implicated in the β-selection checkpoint, facilitating the progression of T cells from $CD4^-CD8^-$ to $CD4^+CD8^+$ by supporting cell survival, proliferation, and metabolic processes (44). Inhibitors of this pathway can selectively suppress the activation and proliferation of Tregs while having a relatively smaller impact on other $CD4^+$ T cells (45). Studies have shown that blocking PI3Kγ or PI3Kδ in $CD8^+$ T cells alone can enhance their anti-tumor properties (46). The PI3K-Akt signaling pathway is also strongly linked to the development of thyroid diseases. Existing studies have shown that long-term iodine deficiency or excessive iodine intake may contribute to the onset and progression of HT by altering the DNA methylation levels of the PRKAA2 and ITGA6 genes within the PI3K-Akt signaling pathway (47). Similarly, Trp and its metabolites can inhibit inflammation through the PI3K-Akt signaling pathway (48).

Western blot analysis revealed no significant inter-group differences in total protein levels of mTOR, PI3K, or Akt following treatment with Trp or IDO1/TDO-IN-4 (Figure 5). In contrast, phosphorylation status was markedly altered. Relative to the HT group, phosphorylation of PI3K and Akt was significantly attenuated in the HT+T group, whereas phosphorylation of mTOR and Akt was markedly elevated in the HT+I group. These data indicate that Trp suppresses PI3K-Akt signaling via diminished PI3K and Akt phosphorylation, whereas IDO1/TDO-IN-4 activates the same pathway through increased mTOR and Akt phosphorylation.

Emerging evidence indicates that the Kyn-AhR axis exerts bidirectional control over Akt phosphorylation. In a murine model of autoimmune hepatitis, hepatic IDO1 activation accelerates the Kyn pathway, which via AhR signaling attenuates Th17 differentiation, expands Tregs, and suppresses Akt phosphorylation, ultimately ameliorating liver injury (49). These findings align with our observation that Trp-mediated IDO1 activation dampens PI3K-Akt signaling in HT. Conversely, in glioma, elevated TDO2-derived Kyn engages AhR to potentiate PI3K-Akt signaling and accelerate malignant cell proliferation (50, 51). This divergence likely stems from two factors. First, the experimental strategies differ: the former study enhanced Kyn production by activating IDO1, whereas the latter abolished Kyn synthesis by deleting TDO2; our approach employed the dual IDO1/TDO inhibitor IDO1/TDO-IN-4, which simultaneously targets both branches of the Kyn pathway. Second, cell-intrinsic differences dictate distinct AhR-downstream signaling networks, yielding opposing effects on Akt activity. Future studies should therefore utilize selective IDO1 or TDO2 inhibitors to dissect cell-type-specific modulation of the Akt pathway and to elucidate the underlying mechanistic distinctions.

4.4 Limitations and future directions

In summary, Trp metabolism may influence T cells via the PI3K-Akt signaling pathway and thereby participate in the initiation and progression of HT. These findings not only provide a new perspective on HT pathogenesis but also offer important clues for future immunomodulatory therapeutic strategies targeting HT.

Nevertheless, several limitations must be acknowledged. First, the limited sample size restricts the generalizability and reliability of the results. Second, the molecular intermediates that link specific Trp catabolites to discrete T cell subsets remain to be delineated. Third, the observation that serum Trp levels increase in the HT mouse model after treatment with IDO1/TDO-IN-4 remains incompletely explained, and the underlying mechanism requires further clarification. Finally, although altered Akt phosphorylation was documented, the causality of this event was not confirmed through pharmacological or genetic Akt blockade.

Future investigations should therefore (i) validate the immunomodulatory effects of Trp in larger, multi-center HT cohorts; (ii) integrate isotope-tracing metabolomics, single-cell transcriptomics, and conditional knockout models to dissect the Trp–immune cell regulatory circuitry; and (iii) employ selective Akt inhibitors to establish direct functional links. These efforts will be critical for translating mechanistic insights into therapeutic strategies that improve clinical outcomes and quality of life for patients with HT and related thyroid disorders.

Data availability statement

The data presented in the study are deposited in the NCBI SRA repository, accession number PRJNA1304611.

Ethics statement

The studies involving humans were approved by the Ethics Committee of the First Affiliated Hospital of Bengbu Medical University. The studies were conducted in accordance with the local legislation and institutional requirements. The participants provided their written informed consent to participate in this study. The animal study was approved by the Ethics Committee of the Bengbu Medical University. The study was conducted in accordance with the local legislation and institutional requirements.

Author contributions

LZ: Visualization, Investigation, Validation, Data curation, Writing – review & editing, Writing – original draft, Formal analysis. XZ: Validation, Data curation, Writing – review & editing. TC: Data curation, Validation, Writing – review & editing. QW: Writing – review & editing, Supervision. XP: Writing – review & editing, Supervision. LY: Supervision, Writing – review & editing. GJ: Conceptualization, Methodology, Project administration, Writing – review & editing, Supervision, Resources, Funding acquisition.

Funding

The author(s) declare financial support was received for the research and/or publication of this article. This work was supported by the Bengbu Medical University Clinical Research Special Fund (2022byflc007) and the High-Level Scientific and Technological Innovation Team of the First Affiliated Hospital of Bengbu Medical University (BYYFY2022TD001).

Acknowledgments

We are deeply grateful to everyone who has contributed to the completion of this study.

Conflict of interest

The authors declare that the research was conducted in the absence of any commercial or financial relationships that could be construed as a potential conflict of interest.

Generative AI statement

The author(s) declare that no Generative AI was used in the creation of this manuscript.

Any alternative text (alt text) provided alongside figures in this article has been generated by Frontiers with the support of artificial intelligence and reasonable efforts have been made to ensure accuracy, including review by the authors wherever possible. If you identify any issues, please contact us.

Publisher's note

All claims expressed in this article are solely those of the authors and do not necessarily represent those of their affiliated organizations, or those of the publisher, the editors and the reviewers. Any product that may be evaluated in this article, or claim that may be made by its manufacturer, is not guaranteed or endorsed by the publisher.

Supplementary material

The Supplementary Material for this article can be found online at: https://www.frontiersin.org/articles/10.3389/fimmu.2025.1605739/full#supplementary-material

References

1. Hoff G, Bernklev T, Johnsen L, Reitsma L, Sina D, Lauzike A, et al. Thyroidectomy for euthyroid patients with hashimoto disease and persisting symptoms. *Ann Intern Med*. (2024) 177:101–3. doi: 10.7326/M23-1593

2. Li J, Huang Q, Sun S, Zhou K, Wang X, Pan K, et al. Thyroid antibodies in Hashimoto's thyroiditis patients are positively associated with inflammation and multiple symptoms. *Sci Rep*. (2024) 14:27902. doi: 10.1038/s41598-024-78938-7

3. Zheng H, Xu J, Chu Y, Jiang W, Yao W, Mo S, et al. A global regulatory network for dysregulated gene expression and abnormal metabolic signaling in immune cells in the microenvironment of graves' Disease and hashimoto's thyroiditis. *Front Immunol*. (2022) 13:879824. doi: 10.3389/fimmu.2022.879824

4. Xue C, Li G, Zheng Q, Gu X, Shi Q, Su Y, et al. Tryptophan metabolism in health and disease. *Cell Metab*. (2023) 35:1304–26. doi: 10.1016/j.cmet.2023.06.004

5. Seo SK, Kwon B. Immune regulation through tryptophan metabolism. *Exp Mol Med*. (2023) 55:1371–9. doi: 10.1038/s12276-023-01028-7

6. Chen X, Xu D, Yu J, Song XJ, Li X, Cui YL. Tryptophan metabolism disorder-triggered diseases, mechanisms, and therapeutic strategies: A scientometric review. *Nutrients*. (2024) 16:3380. doi: 10.3390/nu16193380

7. Stone TW, Williams RO. Modulation of T cells by tryptophan metabolites in the kynurenine pathway. *Trends Pharmacol Sci*. (2023) 44:442–56. doi: 10.1016/j.tips.2023.04.006

8. Leskela S, Rodriguez-Munoz A, de la Fuente H, Figueroa-Vega N, Bonay P, Martin P, et al. Plasmacytoid dendritic cells in patients with autoimmune thyroid disease. *J Clin Endocrinol Metab*. (2013) 98:2822–33. doi: 10.1210/jc.2013-1273

9. Safdari V, Alijani E, Nemati M, Jafarzadeh A. Imbalances in T cell-related transcription factors among patients with hashimoto's thyroiditis. *Sultan Qaboos Univ Med J*. (2017) 17:e174–e80. doi: 10.18295/squmj.2016.17.02.007

10. Luty J, Ruckemann-Dziurdzinska K, Witkowski JM, Bryl E. Immunological aspects of autoimmune thyroid disease - Complex interplay between cells and cytokines. *Cytokine*. (2019) 116:128–33. doi: 10.1016/j.cyto.2019.01.003

11. Veldhoen M, Hirota K, Westendorf AM, Buer J, Dumoutier L, Renauld JC, et al. The aryl hydrocarbon receptor links TH17-cell-mediated autoimmunity to environmental toxins. *Nature*. (2008) 453:106–9. doi: 10.1038/nature06881

12. Lozano-Ordaz V, Rodriguez-Miguez Y, Ortiz-Cabrera AE, Hernandez-Bazan S, Mata-Espinosa D, Barrios-Payan J, et al. Beneficial or detrimental activity of regulatory T cells, indoleamine 2,3-dioxygenase, and heme oxygenase-1 in the lungs is influenced by the level of virulence of Mycobacterium tuberculosis strain infection. *Front Cell Infect Microbiol*. (2023) 13:1105872. doi: 10.3389/fcimb.2023.1105872

13. Desvignes L, Ernst JD. Interferon-gamma-responsive nonhematopoietic cells regulate the immune response to Mycobacterium tuberculosis. *Immunity*. (2009) 31:974–85. doi: 10.1016/j.immuni.2009.10.007

14. Favre D, Mold J, Hunt PW, Kanwar B, Loke P, Seu L, et al. Tryptophan catabolism by indoleamine 2,3-dioxygenase 1 alters the balance of TH17 to regulatory T cells in HIV disease. *Sci Transl Med*. (2010) 2:32ra6. doi: 10.1126/scitranslmed.3000632

15. Jia X, Zhai T, Qu C, Ye J, Zhao J, Liu X, et al. Metformin reverses hashimoto's thyroiditis by regulating key immune events. *Front Cell Dev Biol*. (2021) 9:685522. doi: 10.3389/fcell.2021.685522

16. Zhang Y, Li Y, Chen X, Chen X, Chen C, Wang L, et al. Discovery of 1-(Hetero) aryl-beta-carboline derivatives as IDO1/TDO dual inhibitors with antidepressant activity. *J Med Chem*. (2022) 65:11214–28. doi: 10.1021/acs.jmedchem.2c00677

17. Newman AM, Liu CL, Green MR, Gentles AJ, Feng W, Xu Y, et al. Robust enumeration of cell subsets from tissue expression profiles. *Nat Methods*. (2015) 12:453–7. doi: 10.1038/nmeth.3337

18. Liu Z, Baines KJ, Niessen NM, Heer MK, Clark D, Bishop GA, et al. Characterizing Foxp3(+) and Foxp3(-) T cells in the homeostatic state and after allo-activation: resting CD4(+)Foxp3(+) Tregs have molecular characteristics of activated T cells. *Front Immunol*. (2024) 15:1292158. doi: 10.3389/fimmu.2024.1292158

19. Glaviano A, Foo ASC, Lam HY, Yap KCH, Jacot W, Jones RH, et al. PI3K/AKT/mTOR signaling transduction pathway and targeted therapies in cancer. *Mol Cancer*. (2023) 22:138. doi: 10.1186/s12943-023-01827-6

20. Eryavuz Onmaz D, Tezcan D, Yilmaz S, Onmaz M, Unlu A. Altered kynurenine pathway metabolism and association with disease activity in patients with systemic lupus. *Amino Acids*. (2023) 55:1937–47. doi: 10.1007/s00726-023-03353-7

21. Harris DMM, Szymczak S, Schuchardt S, Labrenz J, Tran F, Welz L, et al. Tryptophan degradation as a systems phenomenon in inflammation - an analysis across 13 chronic inflammatory diseases. *EBioMedicine*. (2024) 102:105056. doi: 10.1016/j.ebiom.2024.105056

22. Biernacki T, Sandi D, Bencsik K, Vecsei L. Kynurenines in the pathogenesis of multiple sclerosis: therapeutic perspectives. *Cells*. (2020) 9:1564. doi: 10.3390/cells9061564

23. Seymour BJ, Trent B, Allen BE, Berlinberg AJ, Tangchittsumran J, Jubair WK, et al. Microbiota-dependent indole production stimulates the development of collagen-induced arthritis in mice. *J Clin Invest*. (2023) 134:e167671. doi: 10.1172/JCI167671

24. Lanz TV, Williams SK, Stojic A, Iwantscheff S, Sonner JK, Grabitz C, et al. Tryptophan-2,3-Dioxygenase (TDO) deficiency is associated with subclinical neuroprotection in a mouse model of multiple sclerosis. *Sci Rep*. (2017) 7:41271. doi: 10.1038/srep41271

25. Murfitt SA, Zaccone P, Wang X, Acharjee A, Sawyer Y, Koulman A, et al. Metabolomics and lipidomics study of mouse models of type 1 diabetes highlights divergent metabolism in purine and tryptophan metabolism prior to disease onset. *J Proteome Res*. (2018) 17:946–60. doi: 10.1021/acs.jproteome.7b00489

26. Liang X, Su T, Wu P, Dai Y, Chen Y, Wang Q, et al. Identification of paeoniflorin from Paeonia lactiflora pall. As an inhibitor of tryptophan 2,3-dioxygenase and assessment of its pharmacological effects on depressive mice. *J Ethnopharmacol*. (2023) 317:116714. doi: 10.1016/j.jep.2023.116714

27. Chandanwale SS, Nair R, Gambhir A, Kaur S, Pandey A, Shetty A, et al. Cytomorphological spectrum of thyroiditis: A review of 110 cases. *J Thyroid Res*. (2018) 2018:5246516. doi: 10.1155/2018/5246516

28. Zhao Z, Gao Y, Pei X, Wang W, Zhang H. Causal role of immune cells in Hashimoto's thyroiditis: Mendelian randomization study. *Front Endocrinol (Lausanne)*. (2024) 15:1352616. doi: 10.3389/fendo.2024.1352616

29. Peyraud F, Guegan JP, Bodet D, Cousin S, Bessede A, Italiano A. Targeting tryptophan catabolism in cancer immunotherapy era: challenges and perspectives. *Front Immunol*. (2022) 13:807271. doi: 10.3389/fimmu.2022.807271

30. Correale J. Immunosuppressive amino-acid catabolizing enzymes in multiple sclerosis. *Front Immunol*. (2020) 11:600428. doi: 10.3389/fimmu.2020.600428

31. Yin X, Chen S, Eisenbarth SC. Dendritic cell regulation of T helper cells. *Annu Rev Immunol*. (2021) 39:759–90. doi: 10.1146/annurev-immunol-101819-025146

32. Meireson A, Devos M, Brochez L. IDO expression in cancer: different compartment, different functionality? *Front Immunol*. (2020) 11:531491. doi: 10.3389/fimmu.2020.531491

33. Quintana FJ, Sherr DH. Aryl hydrocarbon receptor control of adaptive immunity. *Pharmacol Rev*. (2013) 65:1148–61. doi: 10.1124/pr.113.007823

34. Esser C, Rannug A. The aryl hydrocarbon receptor in barrier organ physiology, immunology, and toxicology. *Pharmacol Rev*. (2015) 67:259–79. doi: 10.1124/pr.114.009001

35. Chen A, Huang L, Zhang L. Helper T cell 17 and regulatory T cell levels in peripheral blood of newly diagnosed patients with autoimmune thyroid disease: A meta-analysis. *Horm Metab Res*. (2023) 55:40–50. doi: 10.1055/a-2117-7652

36. Zhao N, Wang Z, Cui X, Wang S, Fan C, Li Y, et al. *In vivo* inhibition of microRNA-326 in a NOD.H-2(h4) mouse model of autoimmune thyroiditis. *Front Immunol*. (2021) 12:620916. doi: 10.3389/fimmu.2021.620916

37. Wang W, Zhang BT, Jiang QL, Zhao HQ, Xu Q, Zeng Y, et al. Leptin receptor antagonist attenuates experimental autoimmune thyroiditis in mice by regulating Treg/Th17 cell differentiation. *Front Endocrinol (Lausanne)*. (2022) 13:1042511. doi: 10.3389/fendo.2022.1042511

38. Cao Y, Jin X, Sun Y, Wen W. Therapeutic effect of mesenchymal stem cell on Hashimoto's thyroiditis in a rat model by modulating Th17/Treg cell balance. *Autoimmunity*. (2020) 53:35–45. doi: 10.1080/08916934.2019.1697689

39. Levescot A, Cerf-Bensussan N. Regulatory CD8(+) T cells suppress disease. *Science*. (2022) 376:243–4. doi: 10.1126/science.abp8243

40. Ehlers M, Thiel A, Bernecker C, Porwol D, Papewalis C, Willenberg HS, et al. Evidence of a combined cytotoxic thyroglobulin and thyroperoxidase epitope-specific cellular immunity in Hashimoto's thyroiditis. *J Clin Endocrinol Metab*. (2012) 97:1347–54. doi: 10.1210/jc.2011-2178

41. Fallarino F, Grohmann U, You S, McGrath BC, Cavener DR, Vacca C, et al. The combined effects of tryptophan starvation and tryptophan catabolites down-regulate T cell receptor zeta-chain and induce a regulatory phenotype in naive T cells. *J Immunol*. (2006) 176:6752–61. doi: 10.4049/jimmunol.176.11.6752

42. Subhi O, Schulten HJ, Bagatian N, Al-Dayini R, Karim S, Bakhashab S, et al. Genetic relationship between Hashimoto;s thyroiditis and papillary thyroid carcinoma with coexisting Hashimoto;s thyroiditis. *PloS One*. (2020) 15:e0234566. doi: 10.1371/journal.pone.0234566

43. Zhou Y, Shen H, Lan W, Shi Y, Yao Q, Wen W. Mechanism of Xiaoying Daotan decoction in treating Hashimoto's thyroiditis based on the Notch/Treg/Th17 pathway. *Ann Transl Med*. (2021) 9:1760. doi: 10.21037/atm-21-6253

44. Juntilla MM, Koretzky GA. Critical roles of the PI3K/Akt signaling pathway in T cell development. *Immunol Lett*. (2008) 116:104–10. doi: 10.1016/j.imlet.2007.12.008

45. Abu-Eid R, Samara RN, Ozbun L, Abdalla MY, Berzofsky JA, Friedman KM, et al. Selective inhibition of regulatory T cells by targeting the PI3K-Akt pathway. *Cancer Immunol Res*. (2014) 2:1080–9. doi: 10.1158/2326-6066.CIR-14-0095

46. Dwyer CJ, Arhontoulis DC, Rangel Rivera GO, Knochelmann HM, Smith AS, Wyatt MM, et al. Ex vivo blockade of PI3K gamma or delta signaling enhances the antitumor potency of adoptively transferred CD8(+) T cells. *Eur J Immunol*. (2020) 50:1386–99. doi: 10.1002/eji.201948455

47. Ren B, Wan S, Wu H, Qu M, Chen Y, Liu L, et al. Effect of different iodine levels on the DNA methylation of PRKAA2, ITGA6, THEM4 and PRL genes in PI3K-AKT signaling pathway and population-based validation from autoimmune thyroiditis patients. *Eur J Nutr*. (2022) 61:3571–83. doi: 10.1007/s00394-022-02907-x

48. Fang L, Chen H, Kong R, Que J. Endogenous tryptophan metabolite 5-Methoxytryptophan inhibits pulmonary fibrosis by downregulating the TGF-beta/SMAD3 and PI3K/AKT signaling pathway. *Life Sci*. (2020) 260:118399. doi: 10.1016/j.lfs.2020.118399

49. Xiao Y, Luo T, Duan C, Wang X, Yang Y, Li R, et al. Ethyl acetate extract from Herpetospermun cardigerum wall. Ameliorated concanavalin A-induced autoimmune hepatitis in mice by reprofiling gut microenvironment to modulate IDO1/KYN and PI3K/AKT/NF-kappaB pathways. *J Ethnopharmacol*. (2025) 345:119578. doi: 10.1016/j.jep.2025.119578

50. Zhong C, Peng L, Tao B, Yin S, Lyu L, Ding H, et al. TDO2 and tryptophan metabolites promote kynurenine/AhR signals to facilitate glioma progression and immunosuppression. *Am J Cancer Res*. (2022) 12:2558–75.

51. Ma W, Ye L, Zhong C, Li J, Ye F, Lv L, et al. Kynurenine produced by tryptophan 2,3-dioxygenase metabolism promotes glioma progression through an aryl hydrocarbon receptor-dependent signaling pathway. *Cell Biol Int*. (2022) 46:1577–87. doi: 10.1002/cbin.11833

Frontiers in Immunology

Explores novel approaches and diagnoses to treat immune disorders.

The official journal of the International Union of Immunological Societies (IUIS) and the most cited in its field, leading the way for research across basic, translational and clinical immunology.

Discover the latest Research Topics

See more →

Frontiers

Avenue du Tribunal-Fédéral 34
1005 Lausanne, Switzerland
frontiersin.org

Contact us

+41 (0)21 510 17 00
frontiersin.org/about/contact